E1.28:ONWI-360/v.1

ONWI-360(1)
LBL-11616
UC-70
Volume I

Lawrence Berkeley Laboratory
UNIVERSITY OF CALIFORNIA

EARTH SCIENCES DIVISION

ORIGINAL

COMPLETED
260

MIGRATION OF RADIONUCLIDES THROUGH SORBING MEDIA ANALYTICAL SOLUTIONS--II

T.H. Pigford, P.L. Chambré, M. Albert, M. Foglia,
M. Harada, F. Iwamoto, T. Kanki, D. Leung,
S. Masuda, S. Muraoka, and D. Ting

October 1980

Prepared for the U.S. Department of Energy under Contract W-7405-ENG-48

LEGAL NOTICE

This book was prepared as an account of work sponsored by an agency of the United States Government. Neither the United States Government nor any agency thereof, nor any of their employees, makes any warranty, express or implied, or assumes any legal liability or responsibility for the accuracy, completeness, or usefulness of any information, apparatus, product, or process disclosed, or represents that its use would not infringe privately owned rights. Reference herein to any specific commercial product, process, or service by trade name, trademark, manufacturer, or otherwise, does not necessarily constitute or imply its endorsement, recommendation, or favoring by the United States Government or any agency thereof. The views and opinions of authors expressed herein do not necessarily state or reflect those of the United States Government or any agency thereof.

Printed in the United States of America
Available from
National Technical Information Service
U.S. Department of Commerce
5285 Port Royal Road
Springfield, VA 22161
Price Code: A18

ONWI-360(1)
LBL-11616
UCB-NE-4003
UC-70
Volume I

MIGRATION OF RADIONUCLIDES THROUGH SORBING MEDIA
ANALYTICAL SOLUTIONS--II*

T. H. Pigford, P. L. Chambré, M. Albert, M. Foglia,
M. Harada, F. Iwamoto, T. Kanki, D. Leung, S. Masuda, S. Muraoka, and D. Ting

Earth Sciences Division, Lawrence Berkeley Laboratory
and
Department of Nuclear Engineering, University of California
Berkeley, California 94720

October 1980

---

*Prepared for the U. S. Department of Energy under contract W-7405-ENG-48 Administered by the Office of Nuclear Waste Isolation, Battelle Memorial Institute under MPO E511-05200.

I

The authors invite comments and would appreciate being notified of any errors in the report.

T. H. Pigford
Department of Nuclear Engineering
University of California
Berkeley, CA 94720

REPORT OUTLINE

MIGRATION OF RADIONUCLIDES THROUGH SORBING MEDIA, ANALYTICAL SOLUTIONS--II

1. Introduction and Summary
    - 1.1. Relation to the Previous Report
    - 1.2. One-Dimensional Equilibrium Transport
    - 1.3. One-Dimensional Nonequilibrium Transport
    - 1.4. One-Dimensional Flow with Transverse Dispersion
    - 1.5. Transport in Multi-Dimensional Flow
    - 1.6. Finite Element Analysis of Radionuclide Migration
2. One-dimensional Transport with Local Chemical Equilibrium
    - 2.1. General Solution of the One-Dimensional Equilibrium Transport Equation for an Infinite Medium
    - 2.2. Effect of Time Delay to Start of Leaching on the Transport of ^{226}Ra and Its Precursors
    - 2.3. Effect of Waste Geometry on Dissolution Rate and Radionuclide Transport
    - 2.4. One-Dimensional Transport Through Multi-Layer Media--Transport of the ^{237}Np Decay Chain Through a Neptunium-Sorbing Overpack
    - 2.5. Solubility-Limited Dissolution and Transport of a Radionuclide
        - 2.5.1. Introduction
        - 2.5.2. Analysis
        - 2.5.3. Solubility-Limited Transport of ^{239}Pu
    - 2.6. Transport with Equilibrium between Different Chemical Species
        - 2.6.1. Introduction
        - 2.6.2. Formulation
        - 2.6.3. Application of the General Solution
        - 2.6.4. Effects of Two Chemical Species of Neptunium on the Migration of $^{237}\text{Np} \rightarrow {}^{233}\text{U} \rightarrow {}^{229}\text{Th} \rightarrow {}^{225}\text{Ra}$

2.7. Maxima of Release Bands (D. K. Ting and P. L. Chambré)
  2.7.1. Introduction
  2.7.2. The Governing Equations and Initial Conditions
  2.7.3. The Boundary Conditions
  2.7.4. The General Solution to a Decaying Band Release
  2.7.5. Approximate Solution to a Decaying Band Release
  2.7.6. Extremum of the Solution for the First Member
  2.7.7. Extremum of the Solution for the Second Member
  2.7.8. Extremum of the Solution for the Third Member
  2.7.9. Example of the Utilization of the Method and Comparison with the Exact Solution
  2.7.10. Application of the Method: The Effects of Variations in Parameter Values on the Maximum Concentrations
2.8. Nomenclature
2.9. Literature References
3. One-dimensional Non-Equilibrium Transport
3.1. Nonequilibrium Sorption in Chromatographic Columns: Impulse Release (D. K. Ting and P. L. Chambré)
  3.1.1. Introduction
  3.1.2. The Governing Equations
  3.1.3. Analytical Solutions
  3.1.4. Characteristics of the Analytical Solutions
  3.1.5. Application to Sorption Experiments
3.2. Transport of Radionuclide Decay Chains with Nonequilibrium Reversible Reactions
  3.2.1. Analytical Solution of the Three-State Model
  3.2.2. Solutions for a Plane Source of Dissolving Nuclides at $z = 0$
  3.2.3. Nonequilibrium between Liquid and Solid; Transport Limited by Mass Transfer
  3.2.4. Non-Equilibrium Transport of ^{234}U

- 3.3. Two Chemical Species in Liquid, Nonequilibrium
  - 3.3.1. Mathematical Model
  - 3.3.2. Local Reaction Equilibrium
  - 3.3.3. Local Sorption Equilibrium, Nonequilibrium Reactions
  - 3.3.4. Nonequilibrium Sorption
  - 3.3.5. Two Species, Irreversible Reaction
  - 3.3.6. Two Species, Reversible Reactions, Nonequilibrium
- 3.4. Nomenclature
- 3.5. Literature References

4. Transport in a One-Dimensional Flow Field with Transverse Dispersion
- 4.1. Transport of Radionuclides Released from a Point Source
  - 4.1.1. The Transport Equation
  - 4.1.2. Initial and Boundary Conditions
  - 4.1.3. Source Terms and Release Modes
  - 4.1.4. Integrated Conservation Equation
  - 4.1.5. Concentrations for an Impulse Point-Source Release
  - 4.1.6. Concentrations for a General Point-Source Release at $x=y=z=0$
  - 4.1.7. Concentrations for a Step Release from a Point Source
  - 4.1.8. Concentrations for a Band Release from a Point Source
  - 4.1.9. First Nuclide in Chain, Step Release, No Axial Dispersion
  - 4.1.10. Application to Various Far-Field Boundary Conditions
  - 4.1.11. Comparison with the One-Dimensional Solutions for an Infinite Plane Source
  - 4.1.12. Application to the Transport of $^{234}U \rightarrow {}^{230}Th \rightarrow {}^{226}Ra \rightarrow$
  - 4.1.13. Longitudinal Dispersion Superimposed Upon Transverse Dispersion
- 4.2. Transport of Radionuclides Released from a Finite Plane Source (P. L. Chambré)
- 4.3. Comparison of Concentrations from an Array of Discrete Sources with Concentrations from an Infinite Plane Source
  - 4.3.1. Parameters Used
  - 4.3.2. Comparison for a Finite Plane Source and an Infinite Plane Source

4.3.3. Comparison for an Array of Point Sources and for an Infinite Plane Source
4.3.4. Effect of Longitudinal Dispersion on the Calculations of Transverse Dispersion
4.4. Literature References
5. Transport in Multi-Dimensional Flow (P. L. Chambré)
5.1. Formulation of Governing Equations
5.2. Two-Dimensional Potential (Darcy) Flow
5.3. Solution of the Two-Dimensional Transport Equation
5.4. Computation of the Time-Position Function in Two-Dimensional Flow Fields
5.5. Solution of the Three-Dimensional Transport Equation
5.6. Nuclide Transport in the Presence of Dispersion
5.7. Literature References
6. Finite-Element Analysis of Radionuclide Migration
Appendix A. The Semi-Equilibrium Transport Equation with Irreversible Mineralization
Appendix B. Nonrecursive General Solution of the One-Dimensional Equilibrium Transport Equation
Appendix C. The Superposition Equation for a Source with Time-Dependent Surface Area
Appendix D. The Computer Program MAX 1
Appendix E. Radioactive Transmutation of a Mineralized Species
Appendix F. Consistency of Point-Source and Plane-Source Solutions
Appendix G. Properties of Functions for the Three-Dimensional Transport Equation
Appendix H. Verification of the Three-dimensional Equation (5.5.45).

[redacted]

1. Introduction and Summary

The present report presents further analytical solutions, and the results of such solutions, for the migration of radionuclides in geologic media.

1.1. Relation to Our Previous Report

In an earlier report (H1) we have derived the basic transport equations which describe the space-dependent and time-dependent concentration of a radionuclide in groundwater as the radionuclide propagates by convection and dispersion through a geologic (porous) medium with sorption occurring between the solid and liquid. The equations are formulated for a radionuclide member of a radioactive decay chain of arbitrary length. Boundary conditions are derived which reflect the time-dependent dissolution rate of a particular radionuclide into groundwater where the waste is emplaced in a geologic repository.

Analytical solutions presented in our earlier report are for one-dimensional transport with local chemical and sorptive equilibrium. These solutions are presented both in a recursive form and also in a general explicit form. The explicit solution in the absence of dispersion is presented for a radionuclide in a decay chain of arbitrary length. Solutions are presented for migration in an infinite homogeneous porous medium as well as in layered porous media. Some numerical examples of the solutions are given for a three-member decay chain. The general solutions in this earlier report have been used extensively in developing some of the new analytical solutions presented here.

1.2. One-Dimensional Equilibrium Transport

In the present report we generalize the solutions for one-dimensional equilibrium transport in an infinite medium. The explicit solution for a radionuclide in a decay chain of arbitrary length, presented in our first report (H1) for no dispersion, is now extended to include dispersion (Sec. 2.1). These solutions are also extended to include the effect of possible irreversible mineralization of sorbed radionuclides.

These one-dimensional equilibrium solutions are used to calculate the space-dependent concentrations of the $^{234}U \rightarrow {}^{230}Th \rightarrow {}^{226}Ra \rightarrow$ decay chain, showing the effect of various delay times prior to the beginning of waste dissolution (Sec. 2.2).

Our previous analyses have assumed the dissolution of an infinite plane source of radionuclides, and the demonstrations have assumed either a constant fractional rate of dissolution of contained radionuclides or a constant rate of dissolution of the waste matrix. The latter assumption is equivalent to the dissolution of a semi-infinite slab source with a constant rate of penetration of the waste matrix due to corrosion. When the waste in the repository consists of an array of waste canisters of finite volume, such as spheres, cylinders, or cubes, a constant rate of penetration due to corrosion no longer results in a constant rate of dissolution of the waste matrix. In Section 2.3 the time-dependent dissolution rates for these canister geometries are developed for equivalent planar sources. A new superposition theorem for these time-dependent dissolution rates is developed (Appendix C). The effect of waste geometry on the migration features of the $^{234}U \rightarrow {}^{230}Th \rightarrow {}^{226}Ra \rightarrow$ decay chain is demonstrated (Sec. 2.2).

In Section 2.4 the solutions for one-dimensional equilibrium transport in multilayered media are applied to calculate the transport of ^{237}Np through a specially sorbing overpack surrounding the waste canister, followed by its transport into the surrounding geologic medium.

Our previous solutions have assumed that there is no solubility limit on the concentration of a radionuclide in the groundwater. In Sec. 2.5 we modify these equations to calculate the solubility-limited transport of a radionuclide with no precursors, assuming that the radionuclide is released from the waste when the waste matrix dissolves. The solution is applied to calculate the solubility-limited transport of ^{239}Pu in a geologic medium, assuming dissolution of waste canisters containing unreprocessed spent fuel and other canisters containing reprocessed high-level glass waste.

Our previous analyses have assumed that a given radionuclide exists in a single chemical state in the liquid and a single sorbed state on the solid. In Sec. 2.6 the possibility of several different chemical states of a radionuclide in the liquid and on the solid is considered, with the assumption of local chemical equilibrium. Possible examples of different chemical states are different oxidation states, complexes, and polymers. For a given radionuclide the sorptive properties may differ markedly for the different chemical species of that radionuclide. It is shown that with an appropriate definition of the transport parameters to include equilibrium constants, the present radionuclide transport solutions can be generalized to apply as well to radionuclide transport with multi-species equilibrium. The application of this new solution is demonstrated for the transport of ^{237}Np, with local equilibrium between two oxidation states, each with different assumed sorption constants.

In Section 2.7 we present a new and simple method for estimating the maximum concentration of a radionuclide predicted to occur at a given position, or at a given time, as the decay chain involving this radionuclide propagates through the geologic medium. This method saves considerable computer time in estimating the maximum concentration in that it does not require the determination of the entire nuclide concentration history. The method is applied to actinide chains present in high-level reprocessed wastes and in unreprocessed spent fuels.

1.3. One-Dimensional Nonequilibrium Transport

The present report extends the analytical solutions of one-dimensional transport to include the departure from local-chemical equilibrium. One instance, of possible importance for long-term migration in some geologic media and of likely importance in some laboratory and field experiments, is the transport of a dissolved radionuclide which has not reached sorption equilibrium with the adjacent solid. These non-equilibrium effects are important in deducing sorption mechanisms from laboratory and field data, and they may contribute to accelerated transport of some radionuclides.

In Sections 3.1 and 3.2 the transport equation is solved for the case of a single radionuclide which does not reach sorption equilibrium. The impulse release solution of Section 3.1 provides a valuable diagnostic tool to understand the migration features accompanying this kind of nonequilibrium. The solution is also used to deduce effective sorption rate constants from laboratory data reported in the literature. This analysis provides a useful tool for obtaining more information from such experiments and for designing more meaningful laboratory and field experiments on radionuclide sorption.

Another non-equilibrium phenomenon considered in this analyses is the possible nonequilibrium reversible mineralization of a portion of the sorbed radionuclides, which can alter both the magnitude and shape of the concentration profile of this radionuclide as it propagates through the geologic medium. The effects of non-equilibrium mass transfer between liquid and solid and nonequilibrium reversible mineralization reactions are included in a new analysis of non-equilibrium transport in a one-dimensional flow field,

[redacted]

applicable to a radionuclide in a multi-member decay chain. The analysis, with numerical examples for the $^{234}\mathrm{U} \rightarrow {}^{230}\mathrm{Th} \rightarrow {}^{226}\mathrm{Ra} \rightarrow$ decay chain, is presented in Section 3.3.

A third non-equilibrium phenomenon considered is the existence of two or more chemical species of a dissolved radionuclide, with these species related to each other by rate processes rather than by simple equilibria. New analytic solutions for these non-equilibrium effects are presented and are demonstrated by numerical examples in Section 3.4.

1.4. One-Dimensional Flow with Transverse Dispersion

In the one-dimensional solutions presented in our previous report dispersion has been assumed to occur only in the direction of the one-dimensional flow of groundwater. This is a proper condition for one-dimensional convective transport of radionuclides dissolved from an infinite plane source, because in that geometry the effects of transverse dispersion must cancel. However, before applying these results to discrete waste sources or to repository emplacements of finite size, the effects of transverse dispersion must be demonstrated.

In Section 4.1 new analytical solutions are presented for the space-time-dependent concentration of a radionuclide, in a decay chain of arbitrary length, for a time-dependent point source, with one-dimensional flow of groundwater and for local chemical equilibrium between the groundwater and the adjacent solid. The point-source solutions are demonstrated for the transport of radionuclides in the $^{234}\mathrm{U} \rightarrow {}^{230}\mathrm{Th} \rightarrow {}^{226}\mathrm{Ra} \rightarrow$ decay chain.

In Section 4.3 the three-dimensional concentration profiles for a finite plane source are compared with the concentration profiles predicted for an infinite plane source. This provides a useful guide as to the distances from a finite repository at which the infinite-plane-source solution is no longer a useful approximation. The point-source solution is used to calculate the three-dimensional concentration profiles for an array of point sources, simulating an array of waste canisters in a repository. These three-dimensional profiles are compared with those from the plane-source solution, demonstrating the distance from the discrete sources at which solutions from an equivalent plane source are valid approximations.

[redacted]

1.5. Multi-Dimensional Flow

Although the analytical solutions for one-dimensional groundwater flow are useful for establishing benchmarks for numerical solutions and for some long-term predictions of radionuclide transport, the full utilization of the power of analytical solutions for benchmark and predictive purposes does not obtain until solutions for radionuclide transport in two-dimensional and three-dimensional flow fields are developed. New solutions for multidimensional radionuclide transport, presented in Chapter 5, are now derived for the time-independent incompressible multidimensional flow of groundwater through porous media. Solutions are obtained in both the recursive as well as general explicit form for a radionuclide in a decay chain of arbitrary length, with local chemical equilibrium between the water and solid. These solutions provide a powerful tool for predicting radionuclide transport along a hydrologic flow field that has been established from field data and/or from hydrologic mapping.

1.6. Finite Element Analysis of Radionuclide Migration

As a departure from analytical solutions of the basic transport equations, a finite-element solution of the transport of radionuclides through porous media, with one-dimensional flow of groundwater, is presented in Chapter 6. The results are compared with those of our analytical solutions. The finite-element numerical technique can also be applied to multi-layered media. The finite-element analysis is an alternate approach to the solution of the basic transport equations. It compares favorably with the numerical solution of the partial differential equations as used in existing numerical codes.

Reference

H1. M. Harada, P. L. Chambre', M. Foglia, K. Higashi, F. Iwamoto, D. Leung, T. H. Pigford, D. Ting, "Migration of Radionuclides Through Sorbing Media: Analytical Solutions--I," LBL-10500, February 1980.

2.1 General Solution of the One-Dimensional Equilibrium Transport Equation

In our previous report (H1) we presented a general non-recursive solution of the one-dimensional transport equation without dispersion, generalized to radionuclide decay chains containing any number of members (see Eq. (4.127) of (H1)). For finite dispersion explicit solutions were presented for a radionuclide decay chain containing three members ((H1), Eq. (5.34)). A solution generalized to decay chains of arbitrary length was presented in the recursive form ((H1), Eq. (4.59)). Recursive solutions are useful in understanding and predicting the hydrologic transport of radionuclides. However, for extensive numerical caluculations a non-recursive solution is desirable.

We present here a generalized non-recursive solution of the one-dimensional transport equation with dispersion. The solution is written first in terms of a generalized source representing the time-space-dependent rate of dissolution of each individual radionuclide. It is then written more explicitly for the time-dependent dissolution rate at an equivalent plane source of dissolving waste material. The solution is presented in terms of newly defined functions $F^j_{r,m}(z,t)$. The generalized dispersion solutions are shown to reduce to the generalized dispersion-free solutions presented in our previous report (H1). The $F^j_{r,m}$ functions simplified for the dispersion-free case are also given.

2.1.1 Summary of the theoretical development

In our previous report (ref. (H1), Sect. 2.3.4) we developed the basic differential equation for the one-dimensional transport of radionuclide i and its precursor i-1, in the more general case of non-equilibrium between species dissolved in the groundwater and sorbed on the adjacent solid. Here we assume local chemical equilibrium between a species in the liquid and that species sorbed on the solid. However, it is possible to include in the present solution the effect of a possible irreversible mineralization of the sorbed species into a different chemical species which remains on the solid and which contributes no longer to the transport process. The first-order rate constant for this mineralization reaction is included in the present formulation.

The differential equation to be solved, derived in Appendix A, is:

$$\hat{L}_i N_i = \lambda_{i-1} K_{i-1} N_{i-1} + \phi_i'''(z,t), \text{ for } -\infty<z<\infty,\ t>0 \qquad (2.1.1)$$

where the operator $\hat{L}_i$ is defined as:

$$\hat{L}_i = -D\frac{\partial^2}{\partial z^2} + v\frac{\partial}{\partial z} + K_i\frac{\partial}{\partial t} + \eta_i K_i \tag{2.1.2}$$

and where:

$N_i(z,t)$ = concentration of isotope i in groundwater, at distance z and time t, atoms/m^3_{water}.

$\phi_i'''(z,t)$ = general source term of radionuclide i in water phase, atoms/(yr) (m^3_{water}).

D = coefficient of axial dispersion (m^2/yr), assumed to be the same for all the isotopes in a radioactive decay chain

$$K_i = \text{retardation coefficient} = 1 + \frac{1-\varepsilon}{\varepsilon} K_{D,i}\ , \tag{2.1.3}$$

v = water velocity, m/yr, in the z direction. We assume, through section 2.4, that v is strictly positive

λ_i = decay constant, 1/yr

$K_{D,i}$ = sorption equilibrium constant =

$$\frac{\text{concentration of nuclide i adsorbed in the solid}}{\text{concentration of nuclide i in the liquid}}$$

ε = porosity,

$$\eta_i = \lambda_i + \frac{1-\varepsilon}{\varepsilon}\ \frac{\vec{k}_i K_{D,i}}{K_i} \tag{2.1.4}$$

$\vec{k}_i$ = first order reaction rate constant for irreversible mineralization of species i sorbed on the solid, 1/yr. For the local chemical equilibirum case (without mineralization), we set:

$$\vec{k}_i = 0 \qquad (2.1.5)$$

in Eq. (2.1.4). See also Appendix A.

$-D \frac{\partial^2 N_i}{\partial z^2}$ represents the rate of transport by dispersion.

$v \frac{\partial N_i}{\partial z}$ represents the rate of transport by convection

$K_i \frac{\partial N_i}{\partial t}$ represents the accumulation rate.

$\lambda_{i-1} K_{i-1} N_{i-1}$ represents the rate of production of i by decay of its parent, (i-1),

$\eta_i K_i N_i$ represents the decay rate plus the irreversible mineralization rate (if present).

The quantities D, K_i and v are assumed to be constant. When the only source is the dissolution of waste in an array within the repository, we imagine that radionuclides are dissolved into groundwater from an equivalent plane source at the position $z = 0$, and we represent $\phi_i'''(z,t)$ by:

$$\phi_i'''(z,t) = \phi_i''(t)\delta(z) \qquad (2.1.6)$$

where:

$\phi_i''(t)$ = rate of dissolution of nuclide i from a plane source in the water phase, at $z = 0$, atoms/(m^2)(yr)

$\delta(z)$ = Dirac delta function, 1/m

Eq. (2.1.1) must be solved with the following conditions:

Boundary Conditions:

$N_i(z,t)$ and its derivatives tend to zero with a suitable exponential order as z tends to $+\infty$ or $-\infty$ (2.1.7)

Initial Conditions:

$$N_i(z,t = 0) = 0 \text{ for all } z. \qquad (2.1.8)$$

The case without dispersion is obtained by setting $D = 0$ in eq. (2.1.2).

The analytical solution, presented in Appendix, B uses a Laplace Transform for t and a Fourier Transform for z. By integration we have obtained the solution for the following special cases:

(a) Generalized plane source of radionuclides at $z = 0$.

$$\phi_i'''(z,t) = \phi_i''(t)\,\delta(z) \qquad (2.1.9)$$

(b) Band and step release of radionuclides at $z = o$.

The band release is characterized by the following assumptions:

(a) a constant amount of the total waste material dissolves into ground water per unit time,

(b) all of the waste material begins to dissolve at $t = 0$. Dissolution is complete within a leach time T,

(c) all radionuclides contained within the waste material go into solution when the waste matrix dissolves, and

(d) the radionuclides do not migrate inside the waste's matrix.

As shown in Section 3.2, ref. (H1), we obtain:

from assumptions (a) and (b): $\dot{W}_s$, the rate of dissolution of total waste material per unit area of plane source within the water phase, is given by:

$$\dot{W}_s = \frac{W_s^o}{T}\,[h(t) - h(t-T)] \text{ atoms}/(m^2)(yr) \qquad (2.1.10)$$

where

W_s^o = initial density of total waste material in the plane source within the water phase, atoms/m^2.

$h(\xi)$ = Heaviside step function, $h(\xi > o) = 1$, $h(\xi < 0) = 0$.

From assumption (d), the atom fraction $n_i(t)$ of nuclide i in the total waste material is given by:

$$n_i(t) = B_i(t) \qquad (2.1.11)$$

where

$B_i(t)$ is given by the Bateman equation,

$$B_i(t) = \sum_{q=1}^{i} B_{i,q}\, e^{-\lambda_q t} \quad , \qquad (2.1.12)$$

$B_{i,q}$ are the so called "Bateman coefficients," defined by:

$$B_{i,q} = \sum_{m=1}^{q} n_m^o\, X_{i,q}^m \qquad (2.1.13)$$

$$X_{i,q}^m = \begin{cases} 1 & \text{if } m = q = i \\ \frac{1}{\lambda_i}\left(\prod\limits_{r=m}^{i} \lambda_r\right) \prod\limits_{\substack{r=m \\ r\neq q}}^{i} & (\lambda_r - \lambda_q)^{-1} \end{cases} \qquad (2.1.14)$$

n_m^o = atoms of nuclide m per total atoms of waste material at beginning of leaching.

$$\text{When } i = j,\ B_{i,j} = B_{i,i} = n_i^o \qquad (2.1.15)$$

Finally, assumption (c) and the preceding results yield:

$$\phi_i''(t) = n_i(t)\dot{W}_s = \frac{W_s^o}{T}\, B_i(t)[h(t) - h(t-T)] \qquad (2.1.16)$$

$\phi_i''(t)$, as given by (2.1.16), characterizes the band release.

The step release, on the other hand, is described by the following equation:

$$\phi_i''(t) = \frac{W_s^0}{T} B_i(t)\, h(t) \qquad (2.1.17)$$

The step-release solutions resulting from (2.1.17) are relatively simple: they are used in the superposition equation (3.60) in ref. (H1) to construct the more complicated band-release solutions, resulting from (2.1.16). The superposition principle is expressed as (F1,H1):

$$N_i^b(z,t) = N_i^s(z,t;B_{i,j}) - h(t-T)\, N_i^s(z,t-T;B'_{i,j}) \qquad (2.1.18)$$

where

$N_i^b(z,t)$ = band-release solution

$N_i^s(z,t;B_{i,j})$ = step-release solution. The Bateman coefficients $B_{i,j}$, given as an argument, denote the dependence of N_i^s on $B_{i,j}$.

$$B'_{i,j} = B_{i,j} e^{-\lambda_j T} \qquad (2.1.19)$$

2.1.2 General solution

The general solution to Eq. (2.1.1), as derived in Appendix B, is:

$$N_i(z,t) = F_{i,i}^i(z,t) +$$

$$\sum_{j=i}^{i-1} A_i^j \sum_{m=j}^{i} \frac{1}{B_m^{i,j}} \sum_{\substack{r=j \\ r\neq m}}^{i} G_{r,m}^{i,j} F_{r,m}^{i,j}(z,t) \qquad (2.1.20)$$

for: $-\infty<z<\infty, t>0$ and: $v>0$, $v_r \neq v_m$ if $r \neq m$; $\beta_{r,m} \neq \beta_{l,k}$ if $r,m \neq l,k$.

where:

$$v_i = v/K_i \tag{2.1.21}$$

$$A_i^j = \frac{v_i}{\lambda_i} \prod_{l=j}^{i} \frac{\lambda_l}{v_l} \tag{2.1.22}$$

$$B_m^{i,j} = \prod_{\substack{l=j \\ l\neq m}}^{i} \Gamma_{l,m} \tag{2.1.23}$$

$$G_{r,m}^{i,j} \quad \begin{matrix} 1 \ ; \text{ if } j = i-1 \\ \prod_{\substack{l=j \\ l\neq m \\ l\neq r}}^{i} (\beta_{l,m} - \beta_{r,m})^{-1} \ ; \text{ if } j < i-1 \end{matrix} \tag{2.1.24}$$

$$\alpha = D/v \tag{2.1.25}$$

$$\beta_{r,m} = \begin{cases} \lambda_m; \text{ if } r=m \\ \Lambda_{r,m} / \Gamma_{r,m}; \text{ if } r\neq m \end{cases} \tag{2.1.26}$$

$$\gamma_{i,j,k} = 1 + \frac{4\alpha}{v_k} (\eta_k - \beta_{i,j}) \tag{2.1.27}$$

$$\Lambda_{r,m} = (\eta_r \, v_m - \eta_m \, v_r)/(v_r v_m) \tag{2.1.28}$$

$$\Gamma_{r,m} = (v_m - v_r)/(v_r v_m) \tag{2.1.29}$$

The functions $F_{i,i}^{i}(z,t)$ and $F_{r,m}^{ij}(z,t)$ are specified for cases (a1-4) and (b1-4) below:

(a1) General time-dependent source $\phi_i'''(z,t)$ of radionuclide i at position z:

BEST DOCUMENT AVAILABLE

$$F^{i}_{i,i}(z,t) = \frac{1}{2D}\sqrt{\frac{v_i\alpha}{\pi}}\int_{-\infty}^{\infty}\left[\int_0^t \frac{e^{-\eta_i\theta}}{\sqrt{\theta}}\ \cdot\right.$$

$$\left. e^{-(z-\rho-v_i\theta)^2/4\theta v_i\alpha}\ .\phi_i^{'''}(\rho,t-\theta)d\theta\right]d\rho \qquad (2.1.30)$$

$$F^{j}_{r,m}(z,t) = \frac{1}{v}\int_{-\infty}^{\infty}\left[\int_0^t \phi_j^{'''}(\rho,t-\theta)E_{r,m,m}(z-\rho,\theta)d\theta\right]d\rho\ ;\ (r\neq m) \qquad (2.1.31)$$

where

$$E_{i,j,k}(z,t) \equiv e^{-z/2\alpha-\beta_{ij}t}\ .$$

$$\cdot\int_0^{\sqrt{v_k t/4\alpha}} \frac{2}{\sqrt{\pi}}\exp\left[-(\gamma_{ijk}y^2 + \frac{z^2}{16\alpha^2y^2}\right]dy =$$

$$= \frac{e^{z/2\alpha}}{2\sqrt{\gamma_{ijk}}}\cdot e^{-\beta_{ij}t}\ .$$

$$\cdot\left\{e^{-|z|\sqrt{\gamma_{ijk}/2\alpha}}\ \mathrm{erfc}\left[\frac{|z|-v_k t\sqrt{\gamma_{ijk}}}{\sqrt{4\alpha v_k t}}\right] -\right.$$

$$-e^{|z|\sqrt{\gamma_{ijk}/2\alpha}}\ \mathrm{erfc}\left[\frac{|z| + v_k t\sqrt{\gamma_{ijk}}}{\sqrt{4\alpha v_k t}}\right] \text{ for } \gamma_{ijk}>0 \qquad (2.1.32)$$

(a2) General time-dependent plane source $\theta_i^{''}(t)$ of radionuclide i of z=o

$$F^{i}_{i,i}(z,t) = \frac{1}{2D}\left(\frac{v_i\alpha}{\pi}\right)^{1/2}\int_0^t \frac{e^{-\eta_i\theta}}{\sqrt{\theta}}\,e^{-(z-v_i\theta)^2/4\theta v_i\alpha}\ .\ \phi_i^{''}(t-\theta)d\theta \qquad (2.1.33)$$

$$F^{j}_{r,m}(z,t) = \frac{1}{v}\int_0^t \phi_j^{''}(t-\theta)E_{r,m,m}(z,\theta)d\theta \quad (r\neq m) \qquad (2.1.34)$$

(a3) Step release from a plane source at z=o, for a time-dependent plane source given by Eq. (2.1.17). The functions are:

$$F^{i}_{i,i}(z,t) = \frac{W_s^0}{Tv}\sum_{q=1}^{i} B_{i,q}E_{q,q,i}(z,t) \qquad (2.1.35)$$

$$F^j_{r,m}(z,t) = \frac{W^o_s}{Tv} \sum_{q=1}^{j} \frac{B_{j,q}}{(\lambda_q - \beta_{r,m})} \left[E_{r,m,m}(z,t) - E_{q,q,m}(z,t) \right] \quad ,(r \neq m) \qquad (2.1.36)$$

The functions $E_{r,m,m}(z,t)$ and $E_{q,q,m}(z,t)$ are given by (2.1.32).

(a4) Band release from a plane source at z=o:

For a time-dependent plane source extending over time T, as given by Eq. (2.1.16), the functions are the same as in Eqs. (2.1.32), (2.1.35), and (2.1.36). The solution is obtained by using the step-release solution in the superposition equation (2.1.18).

(b1) General time-dependent source at position $z, \theta_i'''(z,t)$:

$$F^i_{i,i}(z,t) = \frac{1}{v}\int_0^{tv_i} e^{-\rho\eta_i/v_i} \, \phi_i'''(z-\rho, t - \frac{\rho}{v_i}) d\rho \qquad (2.1.37)$$

$$F^j_{r,m}(z,t) = \frac{1}{v}\int_0^{\infty} e^{-\rho\eta_m/v_m} \left[\int_0^t \phi_j'''(z-\rho, t-\theta) \right. .$$

$$\left. \exp[-\beta_{r,m}(\theta-\rho/v_m)] \, .h(\theta - \frac{\rho}{v_m}) d\theta \right] d\rho \quad (r \neq m) \qquad (2.1.38)$$

(b2) General time dependent plane source $\phi_i''(t)$ of radionuclide i at z=o:

$$F^i_{i,i}(z,t) = \frac{1}{v} e^{-z\eta_i/v_i} \, \theta_i''(t - z/v_i) h(z) h(t - \frac{z}{v_i}) \qquad (2.1.39)$$

$$F^j_{r,m}(z,t) = \frac{1}{v} e^{-z\eta_m/v_m} \int_0^t \phi_j''(t-\theta) \quad .$$

$$. \, e^{-\beta_{r,m}(\theta - z/v_m)} \, .h(\theta - \frac{z}{v_m}) \, .h(z) d\theta \quad (r \neq m) \qquad (2.1.40)$$

(b3) Step release from a plane source at z=o. For a time-dependent plane source given by Eq. (2.1.17), the functions are:

BEST DOCUMENT AVAILABLE

$$F^{i}_{i,i}(z,t) = \frac{W_s^o}{Tv} e^{-\eta_i z/v_i} \sum_{q=1}^{i} B_{i,q} e^{-\lambda_q (t-z/v_i)} .h(t - \frac{z}{v_i}) .h(z) \qquad (2.1.41)$$

$$F^{j}_{r,m}(z,t) = \frac{W_s^o}{Tv} e^{-\eta_m z/v_m} \sum_{q=1}^{j} B_{j,q} \frac{1}{(\lambda_q - \beta_{r,m})}$$

$$\cdot \left[e^{-\beta_{r,m}(t - z/v_m)} - e^{-\lambda_q (t - z/v_m)} \right] h(t - \frac{z}{v_m})\ h(z) \qquad (2.1.42)$$
$$(r \neq m)$$

(b4) Band release from a plane source at z=o. For time-dependent plane source extending over time T, as given by Eq. (2.1.16), the functions are the same as in Eqs. (2.1.41) and (2.1.42). The solution is obtained by using the step-release solution in the superposition equation (2.1.18).

Summary

Equation (2.1.20) and the associated functions for specific source conditions, are the generalized solutions for one-dimensional transport of a radionuclide in a decay chain of arbitrary length, with local chemical equilibrium between a species in groundwater and that same species sorbed on the adjacent solid.

The application of these solutions is demonstrated in Section (2.2) of this report.

2.2 Effect of Time of Start of Leaching on the Transport of ^{226}Ra and its Precursors

2.2.1 Specification of the problem

One of the most important chains to be considered in the study of the hydrological transport of radionuclides, here given with the half-lives, is:

$$^{242m}\text{Am} \xrightarrow[152y]{} {}^{242}\text{Cm} \xrightarrow[163d]{} {}^{238}\text{Pu} \xrightarrow[86y]{} {}^{234}\text{U} \xrightarrow[2.4\text{x}10^5 y]{} {}^{230}\text{Th} \xrightarrow[7.7\text{x}10^4 y]{} {}^{226}\text{Ra} \xrightarrow[1.6\text{x}10^3 y]{}$$

The most important species is usually ^{226}Ra, due to its relatively high biological hazard and relatively high mobility in geological media.

Here we will be interested in the propagation of radionuclides over time periods of the order of many hundreds of years. Due to the relatively short half-lives of ^{242m}Am, ^{242}Cm and ^{238}Pu, we can assume that these nuclides have already decayed to ^{234}U. The chain to consider then becomes:

$$^{234}U \rightarrow {}^{230}Th \rightarrow {}^{226}Ra$$

Table 2.2.1 shows half lives and assumed sorption retardation coefficients K_i:

Table 2.2.1: Half lives and sorption retardation coefficients

	U-234	Th-230	Ra-226
Half life (yr)	2.4×10^5	7.7×10^4	1.6×10^3
Sorption retardation coefficient	1×10^4	5×10^4	5×10^2

The K_i values are obtained from (B3) and characterize a "western desert soil."

The numerical application to follow deals with the time interval t_s between the burial of the waste and the start of leaching of radionuclides into ground water. t_s characterizes the time interval until water intrudes and until the waste canister is breached by corrosion. Here we assume that there is no leaching of waste radionuclides from burial up to a time t_s, and then the waste matrix and the contained radionuclides begin to dissolve at a rate given by the band release model, with an assumed leach time $T=3\times10^4$ yr. The time t is still measured from the beginning of dissolution of the waste material. We assume no decay daughters of ^{234}U are present at the time of burial (i.e. at $t= -t_s$).

The three nuclides are represented by:

$^{234}U = 1$

$^{230}Th = 2$

$^{226}Ra = 3$

At the start of leaching, the concentration in the matrix is given by the Bateman equation:

$$n_i^o = \sum_{q=1}^{i} B_{i,q}^b e^{-\lambda_q t_s} \qquad (2.2.1)$$

where

$$B_{i,q}^b = \sum_{m=1}^{q} n_m^b X_{i,q}^m \qquad (2.2.2)$$

$X_{i,q}^m$ is given by (2.1.14), and

n_m^b = atoms of nuclide m per total atoms of waste material at burial time.

We assume that:

$n_1^b = 1$

$n_2^b = n_3^b = 0$

We then use n_i^o, given by (2.2.1), as input for the band-release form of (2.1.20), (2.1.41), (2.1.42), and (2.1.18), to calculate the time dependent concentration of Ra-226, N_3 (z,t).

For simplicity, dispersion-free transport is assumed. Our previous report (Hl) Sect. 5.5, shows that neglecting dispersion introduces little error when calculating one-dimensional transport in the chain leading to Ra-226. For no dispersion Eq. (2.1.21) and its auxiliary equations can be expressed in terms of the transit time, τ, for transport of water from the waste to a distance z, i.e.:

$$\tau = z/v, \qquad (2.2.2)$$

The variables z and v no longer appear independently.

For each of the assumed values of t_s and τ, the maximum concentration of Ra-226, $N_3^*(t_s,\tau)$, was calculated by assuming different values of t until a maximum was obtained at $t = t^*$.

2.2.2 Results and discussion

The results are shown in Figs. (2.2.1) - (2.2.8), where the maximum Ra-226 concentration $N_3^*(t_s,\tau)$, normalized to the constant concentration $N_1(0,0)$ of U-234 in groundwater at $t_s = 0$, is plotted against the water-transport time τ, for different values of t_s. On each plot the maximum concentration $N_3^*(t_s,\tau)$ increases with water transport time to a global maximum $N_3^{**}(t_s)$, which occurs at a water-transport time τ^{**}. The values of τ^{**} and the time t^{**} at which the global maximum occurs are indicated on each figure. Increasing t_s causes τ^{**} and t^{**} to decrease, as shown by the results in Table 2.2.2.

Table 2.2.2 Global maximum concentrations of Ra-226 occurring after various dissolution-delay time.

dissolution delay time t_s,yr	global maximum relative concentration of Ra-226, $N_3^{**}/N_1(0,0)$	water-transport time of location global maximum τ^{**},yr	time[a] at which global maximum occurs t^{**}, yr
1	2.03×10^{-2}	8.1	1×10^5
1×10^3	2.03×10^{-2}	8.1	1×10^5
1×10^4	2.07×10^{-2}	6.7	8.6×10^4
3×10^4	2.58×10^{-2}	0.78	3.04×10^4
4×10^4	2.93×10^{-2}	0.606	3.03×10^4
1.7×10^5	4.58×10^{-2}	0.606	3.03×10^4
5×10^5	2.5×10^{-2}	0.606	3.03×10^4

[a] time after beginning of waste dissolution

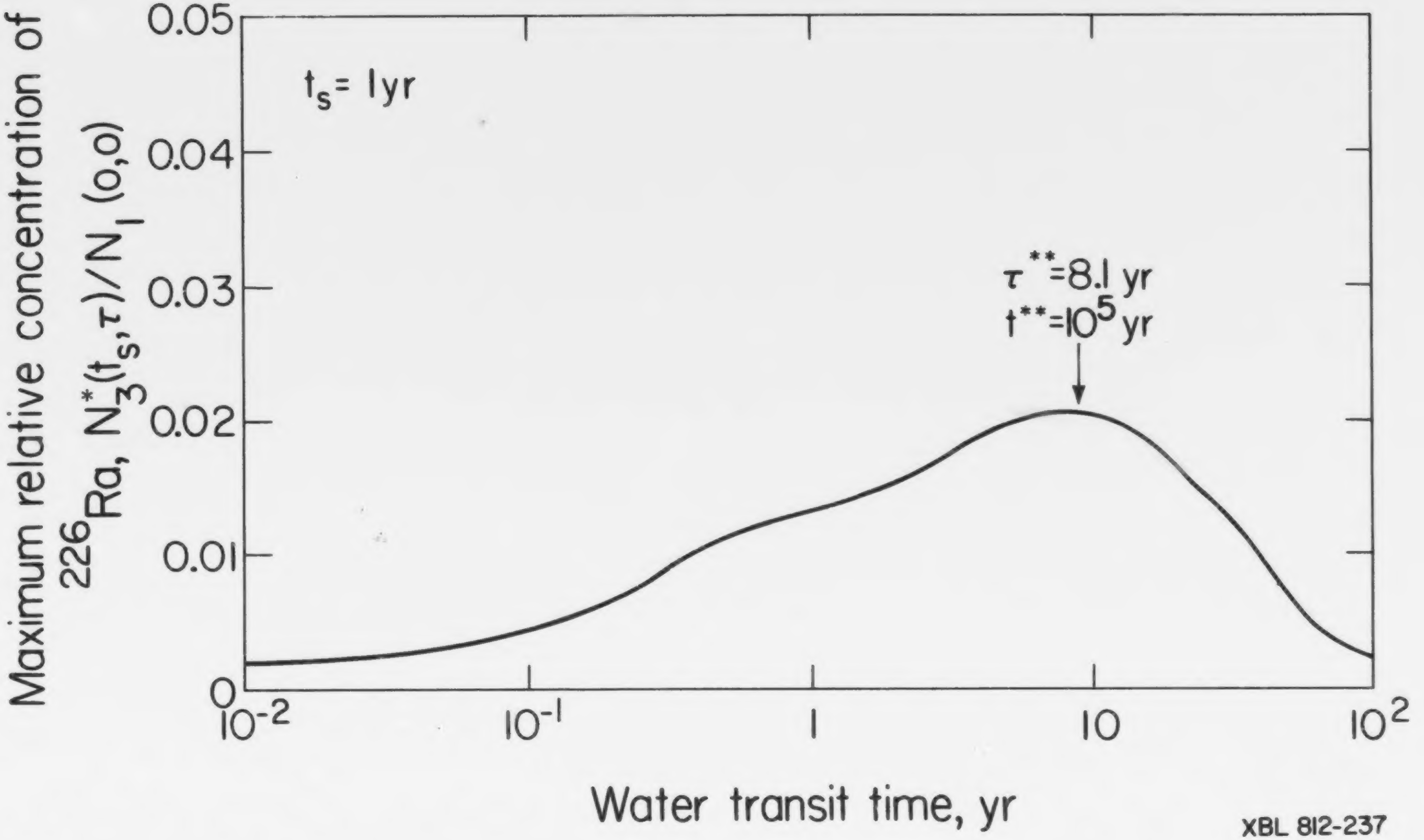

Figure 2.2.1 Profiles of maximum concentration of ^{226}Ra for the $^{234}U \rightarrow {}^{230}Th \rightarrow {}^{226}Ra$ decay chain. $N_3^*(t_s,\tau)$ = atoms/m^3$_{water}$ of ^{226}Ra. $N_1(0,0)$ = atoms/m^3$_{water}$ of ^{234}U at $\tau = 0$, $t = 0$ and $t_s = 0$. t_s = time to start of leaching, yr. τ = water transit time, yr. τ^{**} = water transit time of highest concentration, yr. t^{**} = time of highest concentration, yr. $T = 3 \times 10^4$ yr. $K_U = 10^4$; $K_{Th} = 5 \times 10^5$; $K_{Ra} = 500$. No dispersion. No ^{234}U daughters at burial time.

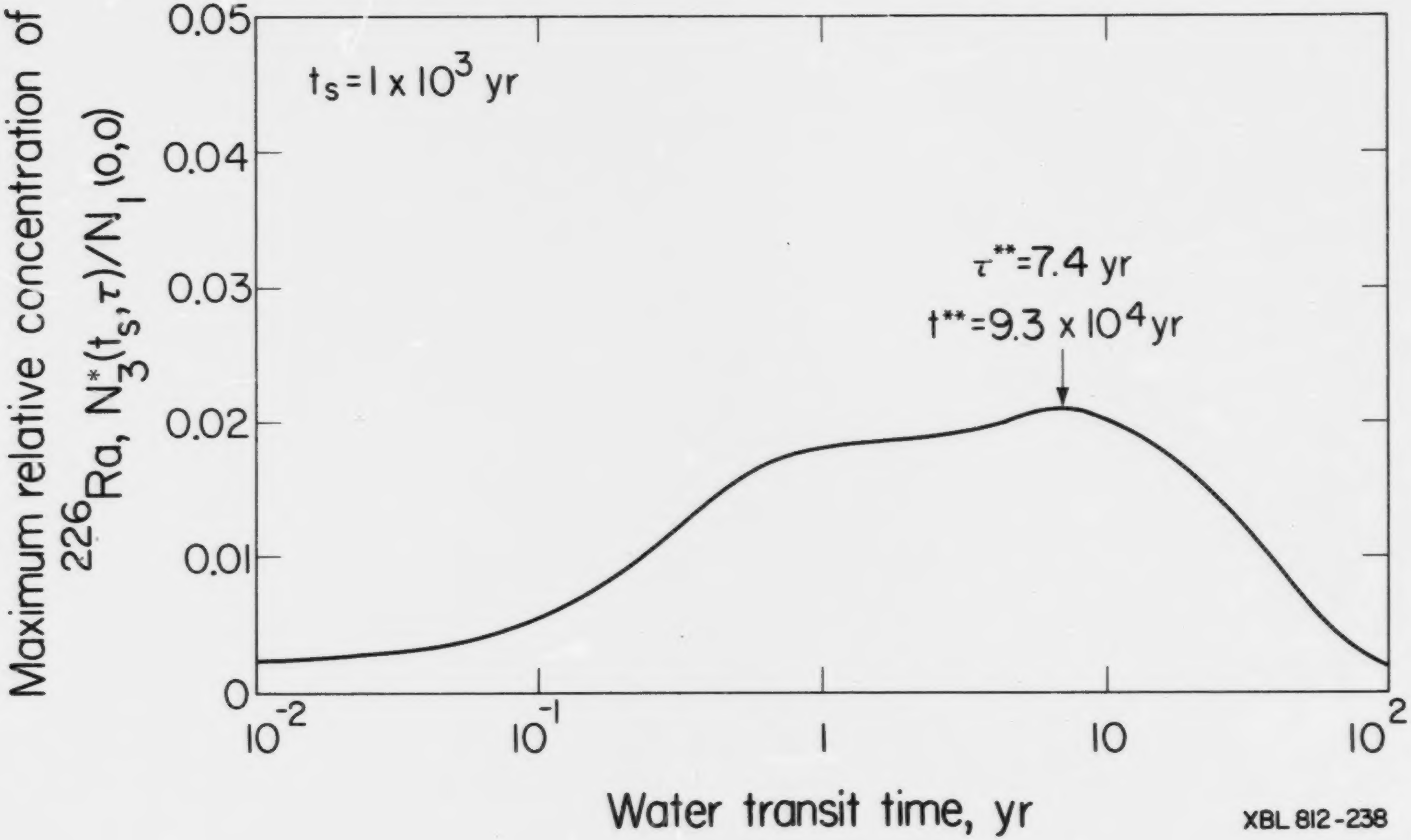

XBL 812-238

Figure 2.2.2 Profiles of maximum concentration of ^{226}Ra for the $^{234}U \rightarrow {}^{230}Th \rightarrow {}^{226}Ra$ decay chain. $N_3^*(t_s,\tau)$ = atoms/m^3_{water} of ^{226}Ra. $N_1(0,0)$ = atoms/m^3_{water} of ^{234}U at $\tau = 0$, $t = 0$ and $t_s = 0$. t_s = time to start of leaching, yr. τ = water transit time, yr. τ^{**} = water transit time of highest concentration, yr. t^{**} = time of highest concentration, yr. $T = 3 \times 10^4$ yr. $K_U = 10^4$; $K_{Th} = 5 \times 10^5$; $K_{Ra} = 500$. No dispersion. No ^{234}U daughters at burial time.

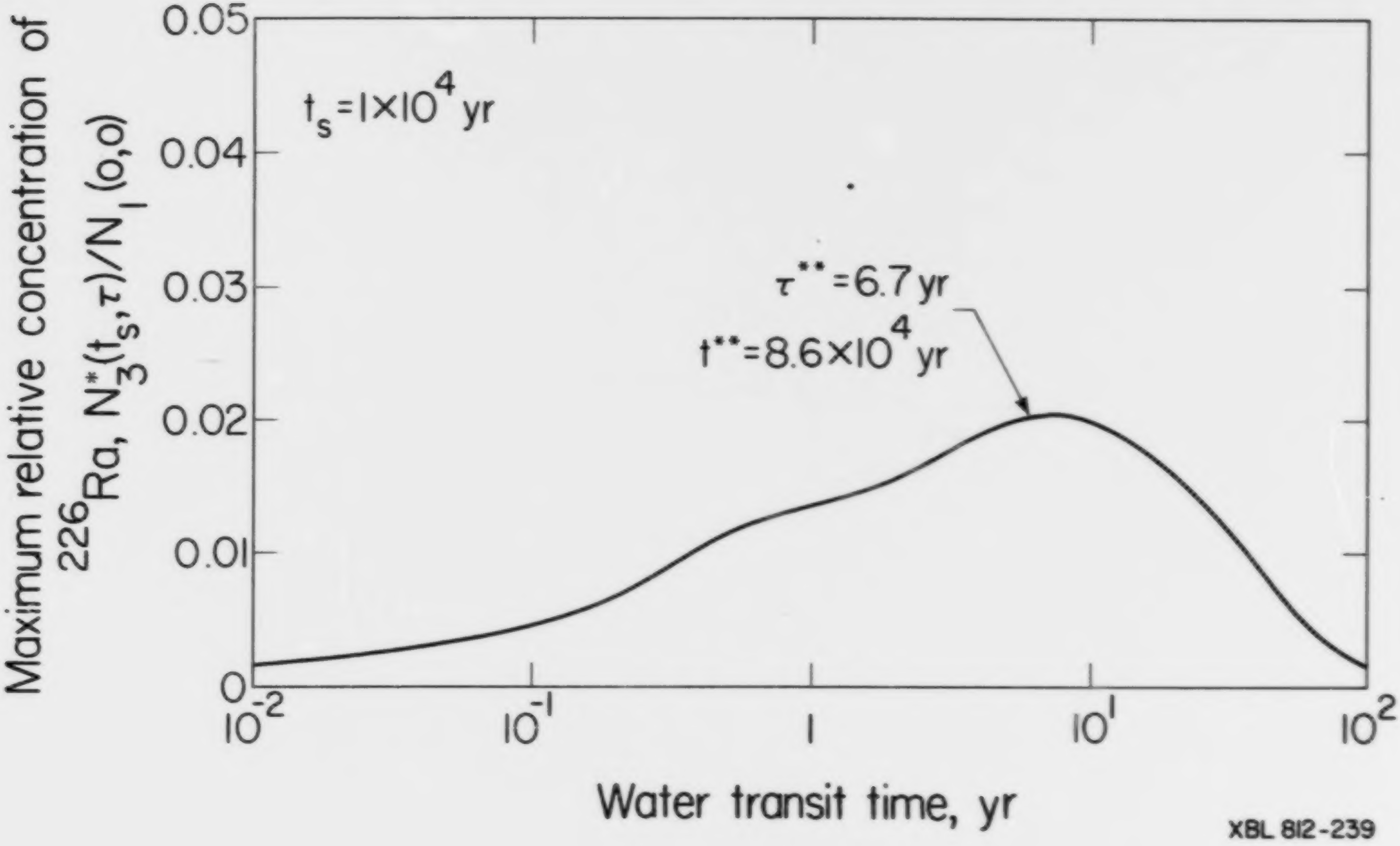

Figure 2.2.3 Profiles of maximum concentration of ^{226}Ra for the $^{234}U \rightarrow {}^{230}Th \rightarrow {}^{226}Ra$ decay chain. $N_3^*(t_s,\tau)$ = atoms/m$^3_{water}$ of ^{226}Ra. $N_1(0,0)$ = atoms/m$^3_{water}$ of ^{234}U at $\tau = 0$, $t = 0$ and $t_s = 0$. t_s = time to start of leaching, yr. τ = water transit time, yr. τ^{**} = water transit time of highest concentration, yr. t^{**} = time of highest concentration, yr. $T = 3 \times 10^4$ yr. $K_U = 10^4$; $K_{Th} = 5 \times 10^5$; $K_{Ra} = 500$. No dispersion. No ^{234}U daughters at burial time.

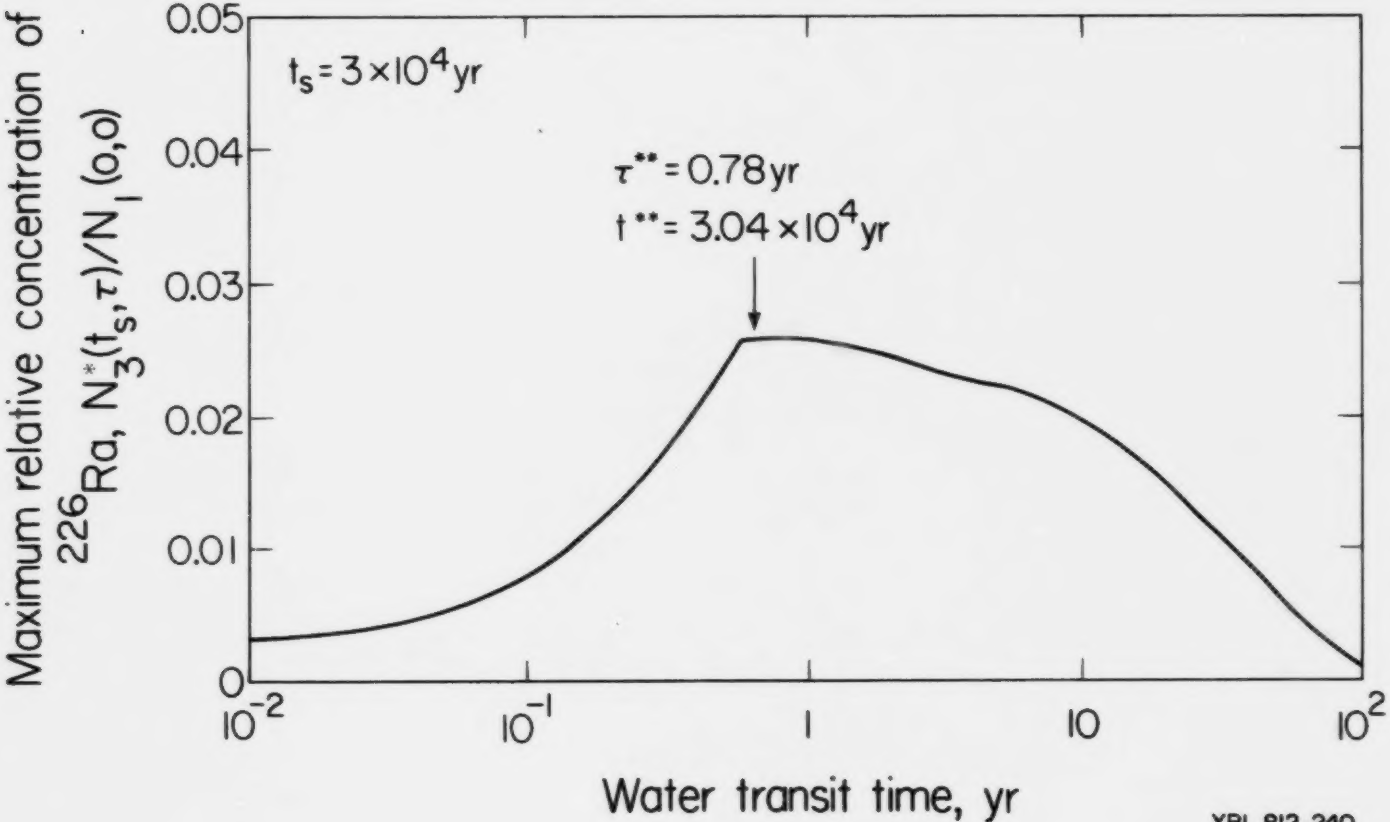

XBL 812-240

Figure 2.2.4 Profiles of maximum concentration of ^{226}Ra for the ^{234}U → ^{230}Th → ^{226}Ra decay chain. $N_3^*(t_s,\tau)$ = atoms/m$^3_{\text{water}}$ of ^{226}Ra. $N_1(0,0)$ = atoms/m$^3_{\text{water}}$ of ^{234}U at $\tau = 0$, $t = 0$ and $t_s = 0$. t_s = time to start of leaching, yr. τ = water transit time, yr. τ^{**} = water transit time of highest concentration, yr. t^{**} = time of highest concentration, yr. $T = 3 \times 10^4$ yr. $K_U = 10^4$; $K_{Th} = 5 \times 10^5$; $K_{Ra} = 500$. No dispersion. No ^{234}U daughters at burial time.

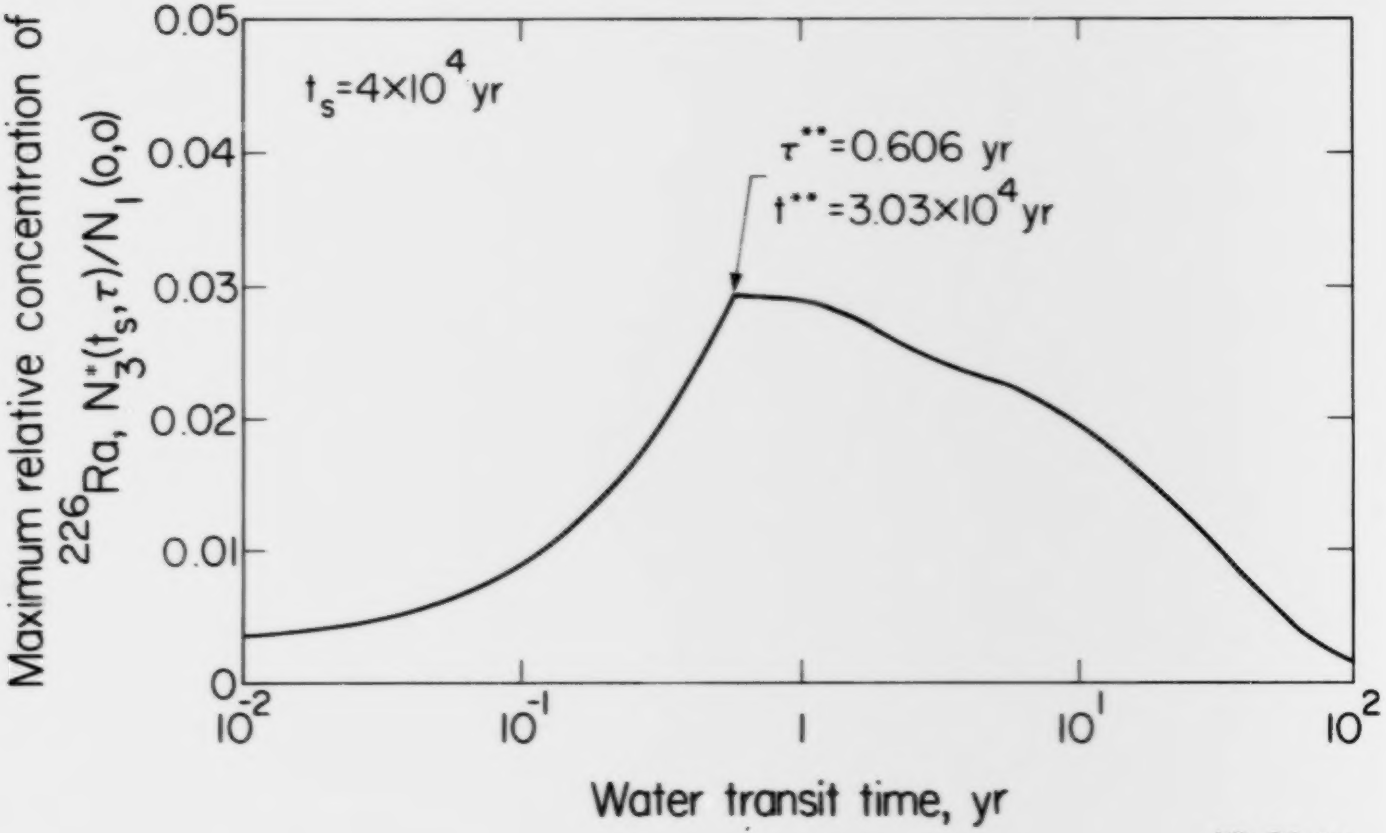

XBL 812-241

Figure 2.2.5 Profiles of maximum concentration of ^{226}Ra for the $^{234}U \rightarrow {}^{230}Th \rightarrow {}^{226}Ra$ decay chain. $N_3^*(t_s,\tau)$ = atoms/m$^3_{water}$ of ^{226}Ra. $N_1(0,0)$ = atoms/m$^3_{water}$ of ^{234}U at $\tau = 0$, $t = 0$ and $t_s = 0$. t_s = time to start of leaching, yr. τ = water transit time, yr. τ^{**} = water transit time of highest concentration, yr. t^{**} = time of highest concentration, yr. $T = 3 \times 10^4$ yr. $K_U = 10^4$; $K_{Th} = 5 \times 10^5$; $K_{Ra} = 500$. No dispersion. No ^{234}U daughters at burial time.

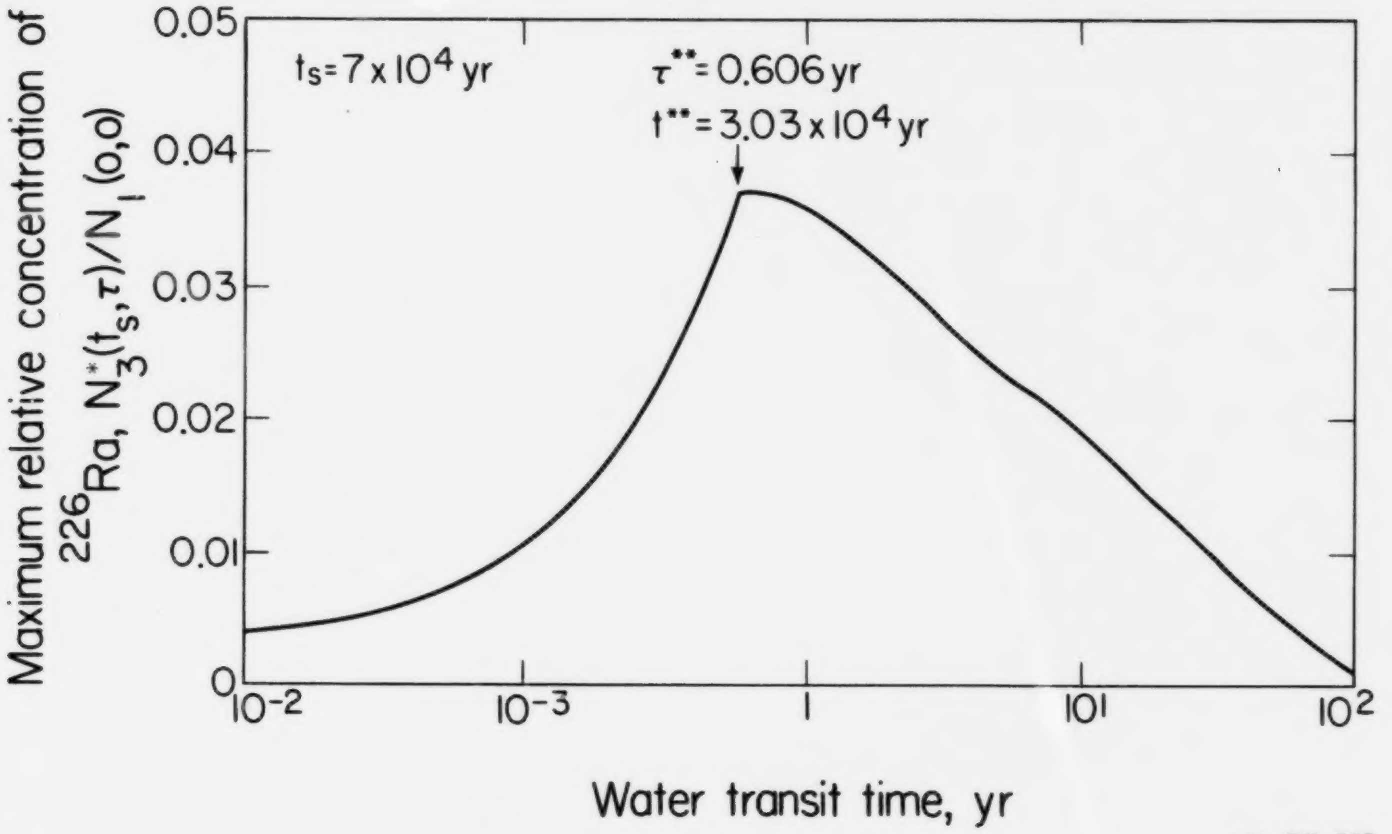

XBL 812-242

Figure 2.2.6 Profiles of maximum concentration of ^{226}Ra for the $^{234}U \rightarrow {}^{230}Th \rightarrow {}^{226}Ra$ decay chain. $N_3^*(t_s,\tau)$ = atoms/m^3_{water} of ^{226}Ra. $N_1(0,0)$ = atoms/m^3_{water} of ^{234}U at $\tau = 0$, $t = 0$ and $t_s = 0$. t_s = time to start of leaching, yr. τ = water transit time, yr. τ^{**} = water transit time of highest concentration, yr. t^{**} = time of highest concentration, yr. $T = 3 \times 10^4$ yr. $K_U = 10^4$; $K_{Th} = 5 \times 10^5$; $K_{Ra} = 500$. No dispersion. No ^{234}U daughters at burial time.

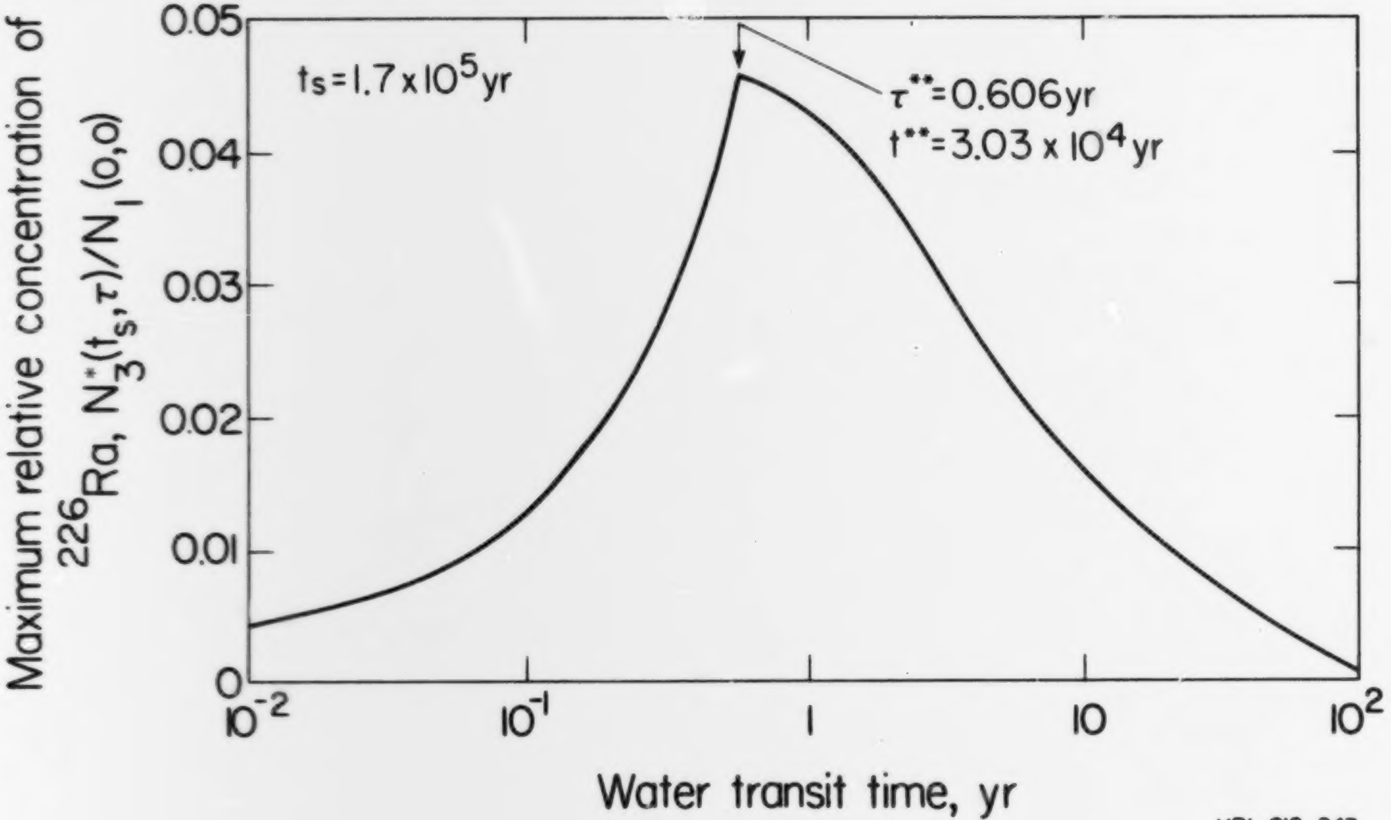

XBL 812-243

Figure 2.2.7 Profiles of maximum concentration of ^{226}Ra for the ^{234}U → ^{230}Th → ^{226}Ra decay chain. $N_3^*(t_s,\tau)$ = atoms/m$^3_{water}$ of ^{226}Ra. $N_1(0,0)$ = atoms/m$^3_{water}$ of ^{234}U at $\tau = 0$, $t = 0$ and $t_s = 0$. t_s = time to start of leaching, yr. τ = water transit time, yr. τ^{**} = water transit time of highest concentration, yr. t^{**} = time of highest concentration, yr. $T = 3 \times 10^4$ yr. $K_U = 10^4$; $K_{Th} = 5 \times 10^5$; $K_{Ra} = 500$. No dispersion. No ^{234}U daughters at burial time.

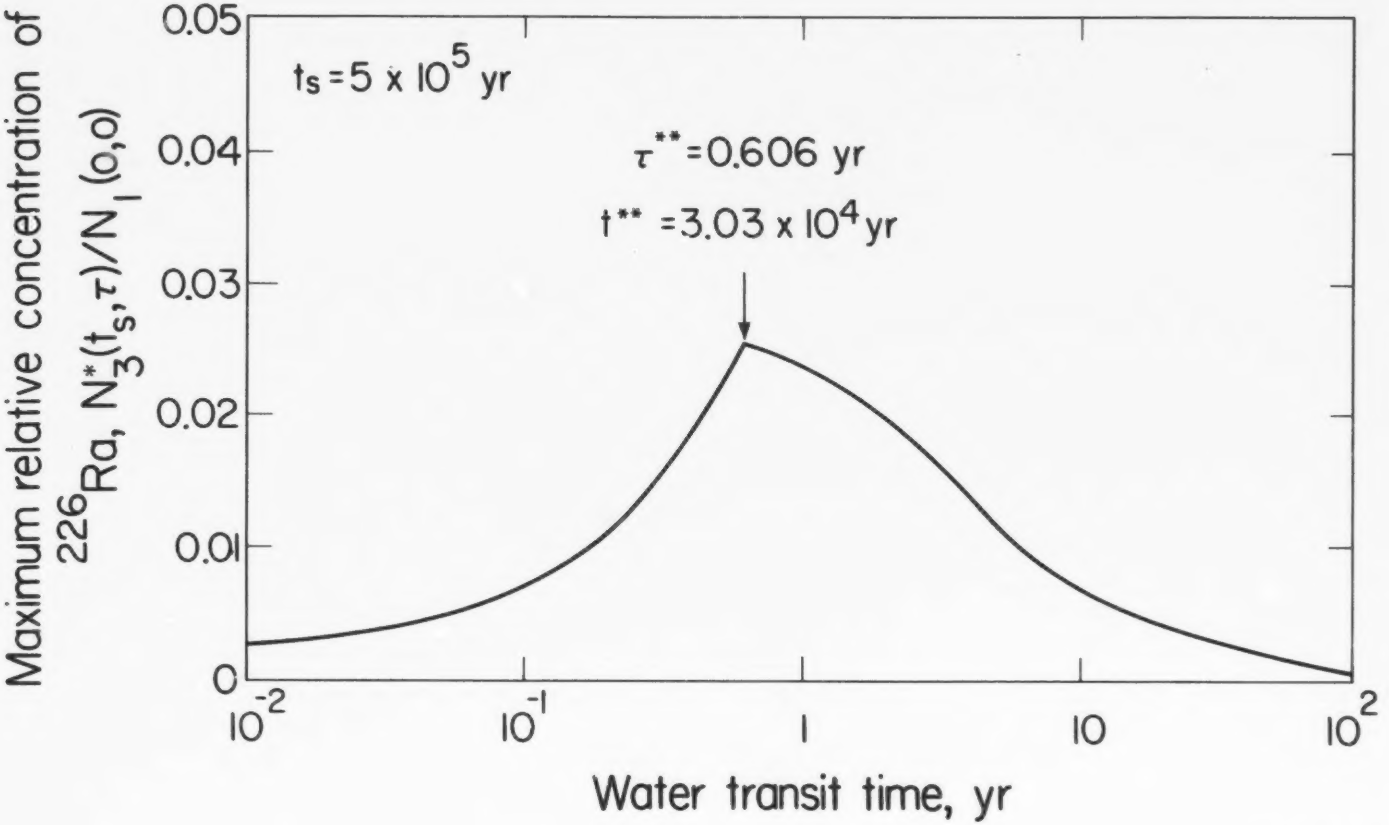

XBL 812-244

Figure 2.2.8 Profiles of maximum concentration of ^{226}Ra for the $^{234}U \rightarrow {}^{230}Th \rightarrow {}^{226}Ra$ decay chain. $N_3^*(t_s,\tau)$ = atoms/m$^3_{water}$ of ^{226}Ra. $N_1(0,0)$ = atoms/m$^3_{water}$ of ^{234}U at $\tau = 0$, $t = 0$ and $t_s = 0$. t_s = time to start of leaching, yr. τ = water transit time, yr. τ^{**} = water transit time of highest concentration, yr. t^{**} = time of highest concentration, yr. $T = 3 \times 10^4$ yr. $K_U = 10^4$; $K_{Th} = 5 \times 10^5$; $K_{Ra} = 500$. No dispersion. No ^{234}U daughters at burial time.

[redacted]

This shows that near-field phenomena involving Ra-226 become more important at long delay times for dissolution, as would be expected.

As shown in Fig. 2.2.9, the largest value of the global maximum Ra-226 concentration $N_3^{**}(t_s)$ occurs at $\tau^{**} = 0.606$ yr and $\tau^{**} = 3.03 \times 10^4$ years, at a delay time of $t_s = 1.7 \times 10^5$ yr. For these parameters the last of the Ra-226 leached from the waste in the repository has just overtaken the first of the Th-230 leached from the waste in the repository. This phenomenon was noted in our previous report ((H1), Section 5.5), and it is theoretically predicted in Section 2.7 of the present report. At greater t_s the global maximum decreases exponentially, with a decay constant equal to the radioactive decay constant of U-234.

As the leaching delay time t_s is increased, increasing amounts of Th-230 and Ra-226 are present in the waste in the repositiory at the beginning of leaching, thereby causing the position of the global maximum Ra-226 concentration to move closer to the repository and the magnitude of this global maximum to increase. For leaching delay times up to about 2,000 years the daughters of U-234 in the waste at the onset of dissolution can be neglected. For delay times greater than a few hundred thousand years it is sufficient to assume that the U-234 decay daughters are in transient equilibrium in the undissolved waste.

As shown in Figure 2.2.10, the maximum Ra-226 concentration $N_3^{*}(t_s,\tau)$ is insensitive to increases in leaching delay time t_s, at constant water-transport time , until the leaching delay time is made as large as about 100,000 yr, of the order of the half life of the controlling precursor ^{234}U.

2.3 Effect of Waste Geometry on Dissolution Rate and Radionuclide Transport

In our previous calculations we have assumed a band release of radionuclides from the waste, which corresponds to a constant rate of dissolution of the total waste matrix and its contained radionuclides. This may be reasonable if the waste geometry is a planar surface, with a constant penetration rate due to corrosion by the surrounding ground water. However, other waste geometries can result in a decreasing dissolution rate as the surface area for dissolution decreases due to corrosion. The calculation of the effect of source geometry upon radionuclide transport is the subject of the present section.

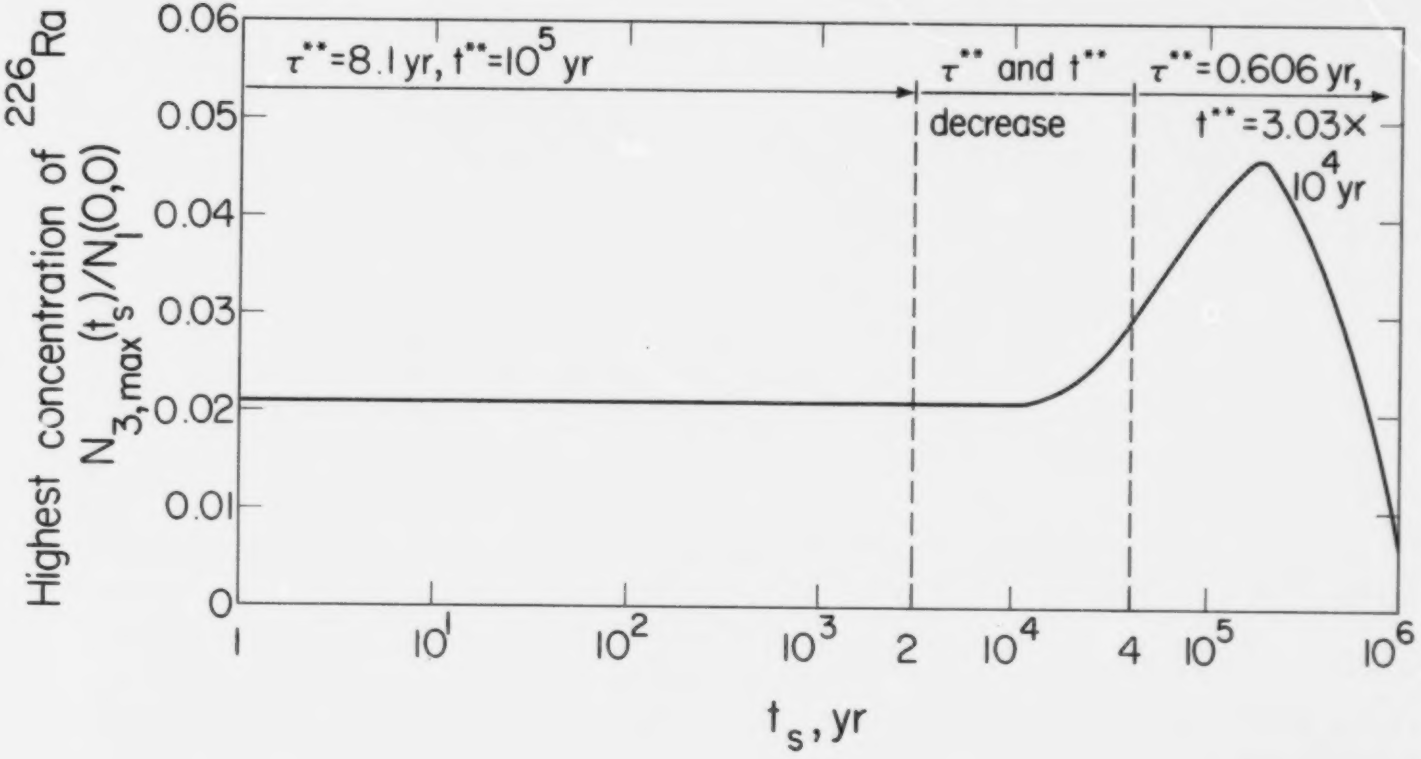

XBL 812-245

Figure 2.2.9 Highest ^{226}Ra concentration for the $^{234}U \rightarrow {}^{230}Th \rightarrow {}^{226}Ra$ decay chain. $N_{3,max}(t_s)$ = atoms/m^3 of ^{226}Ra. $N_1(0,0)$ = atoms/m^3 of ^{234}U at $\tau = 0$, $t = 0$, $t_s = 0$. t_s = time to start of leaching. τ^{**} = water transit time of highest concentration. t^{**} = time of highest concentration. $T = 3 \times 10^4$ yr. $K_U = 1 \times 10^4$, $K_{Th} = 5 \times 10^4$, $K_{Ra} = 5 \times 10^2$. No dispersion. No ^{234}U daughters at burial time.

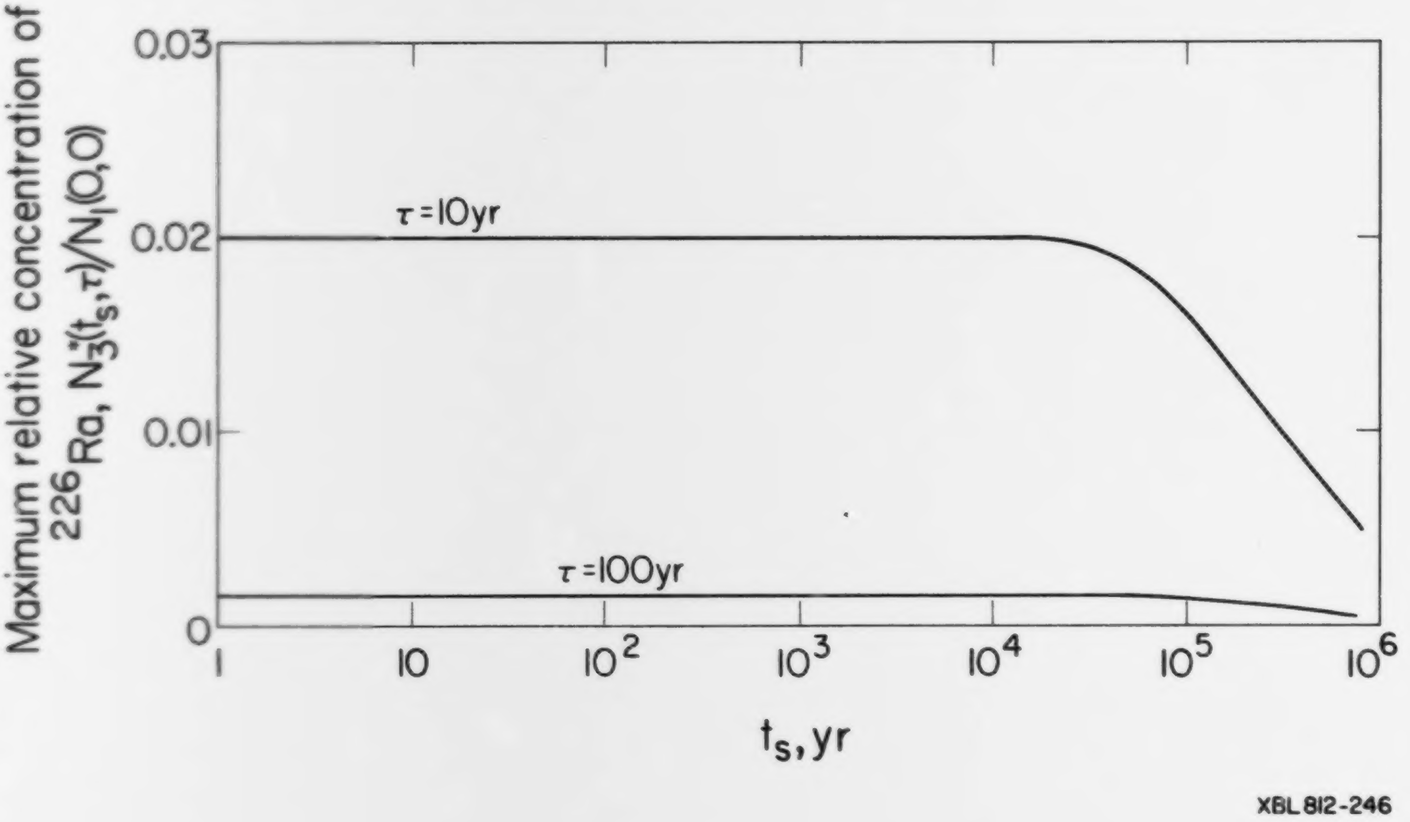

Figure 2.2.10 Maximum ^{226}Ra concentration at fixed τ for the $^{234}U \rightarrow {}^{230}Th \rightarrow {}^{226}Ra$ decay chain. $N_3^*(t_s,\tau)$ = atoms/m^3 of ^{226}Ra. $N_1(0,0)$ = atoms/m^3 of ^{234}U at $\tau = 0$, $t = 0$, $t_s = 0$. t_s = time to start of leaching. τ = water transit time. $K_U = 10^4$, $K_{Th} = 5 \times 10^4$, $K_{Ra} = 500$. T = 3×10^4 hr. No dispersion. No ^{234}U daughters at burial time.

A constant rate of penetration of the waste surface due to corrosion will be assumed for the purpose of this demonstration. Experimental data (B1, H2) indicate that after a short diffusion-controlled corrosion transient, penetration rate appears to be constant for typical waste materials. These experiments are not carried out under repository conditions of groundwater surrounding a waste canister, where a boundary-layer-controlled concentration profile of dissolved waste material in the liquid adjacent to a waste canister can materially alter the dissolution rate. However, in the absence of more relevant experimental data or analysis, a constant penetration rate is assumed for the present calculation.

To use the equations for one-dimensional transport summarized in Sect. 2.1, we must express the source dissolution rate in terms of dissolution rate of an equivalent plane source. As has been discussed previously for the band-release model, we assume that when any portion of the waste matrix dissolves the contained radionuclides also dissolve.

If the waste material is imagined to be in the form of an infinite slab source, of thickness L in the direction of water flow, a constant rate $\dot{R}$ of penetration due to corrosion results in the leach time T given by:

$$T = \frac{L}{2\dot{R}} \tag{2.3.1}$$

The source term for the dissolution rate of radionuclide i from the equivalent plane source is given by adapting Eq. (2.1.16):

$$\phi_i''(t) = 2\,\frac{\rho \dot{R} B_i(t)}{\epsilon}\,[h(t) - h(t-T)] \tag{2.3.2}$$

where ρ is the overall density of the waste material and ϵ is the porosity of the surrounding radionuclides. $B_i(t)$ is given by (2.1.12) - (2.1.14). In writing Eq. (2.3.2) it is assumed that the entire surface of the waste is exposed to water and is being corroded at the uniform penetration rate $\dot{R}$. The dissolved material is channeled into the water pores adjacent to the waste, so the equivalent plane-source dissolution rate per unit cross-sectional area of water flow is the overall plane-source dissolution rate divided by the porosity ϵ of the porous medium adjacent to the waste.

[redacted]

If each waste canister is in the form of a parallelpiped of initial dimensions L_1, L_2, L_3, and if each surface is accessible to corrosion by the surrounding groundwater at a penetration rate R, the leach time becomes:

$$T = \frac{\min(L_1,L_2,L_3)}{2\dot{R}} \qquad (2.3.3)$$

The nuclide source term can be written as:

$$\phi_i''(t) = \frac{\dot{R}\rho}{S\epsilon} \sum_{q=1}^{i} B_{i,q}\, e^{-\lambda_q t} (C_o+C_1t+C_2t^2)\,[h(t)-h(t-T)] \qquad (2.3.4)$$

The coefficients C_o,C_1,C_2 for the parallelpiped are given in Table 2.3.1. S is the surface area of an equivalent plane source in water for each waste canister, determined by the spacing of waste canisters. For canisters spaced in a square array normal to the direction of water flow, with a distance H between the centerline-position of each canister,

$$S = H^2\epsilon$$

Equation (2.3.4) can be used to express the source terms for different waste geometries, using the quantities C_o,C_1,C_2 given in Table 2.3.1. Also listed in Table 2.3.1 are the values of the leach time for each of the waste geometries, calculated on the basis of assumed 0.2 cubic meter of waste material, a distance H between the centerline-position of each canister of 10 m, and an assumed penetration rate $\dot{R}$ of 5 x 10^{-5}m/yr.

For each of the three waste-canister geometries listed in Table 2.3.1, the source terms for the three-member radionuclide chain

$$^{234}U \longrightarrow {}^{230}Th \longrightarrow {}^{226}Ra$$

were calculated from the dispersion-free equations of Sect. 2.1, with the superposition technique presented in Appendix C, using the assumed sorption retardation coefficients given in Table 2.2.1. The resulting space-dependent concentrations at assumed times of 10^3 and 10^4 yr after the beginning of dissolution, normalized to the initial concentration of ^{234}U in the groundwater at the onset of dissolution from the parallelpiped, are shown in

Figures 2.3.1 and 2.3.2. Also shown in Figure 2.3.1 is the concentration profile for a step release, with constant rate of matrix dissolution equal to the initial rate for the cube. The different source geometries affect the shape of the trailing edges of the chromatographic bands, but the leading edge and normalized maximum concentrations are essentially the same for all three geometries.

However, if the waste is subdivided into smaller pieces of greater surface-to-volume ratio, as could occur from fragmentation of the matrix or from dissolution of waste particles previously distributed through a relatively soluble matrix, the leach times can be significantly increased. Although, as shown in (H1), this may not strongly affect the concentration of ^{226}Ra from this chain, the magnitudes of the peak concentrations of other radionuclides can be significantly increased.

Table 2.3.1: Values for C_0, C_1, C_2 and T

	Parallelpiped	Cylinder[a]	Sphere[a]
$C_o(m^2)$	$2(L_1L_2+L_2L_3+L_1L_3)$	$2\pi r_o(L_o+r_o)$	$4\pi\ r_o^{\ 2}$
$C_1(\frac{m^2}{yr})$	$-8\dot{R}(L_1+L_2+L_3)$	$-2\pi\ \dot{R}^2(L_o+4r_o)$	$-8\pi\ r_o\dot{R}$
$C_2(\frac{m^2}{yr^2})$	$24\dot{R}^2$	$6\pi\dot{R}^3$	$4\pi\dot{R}^2$
T(yr)	5850^b	6300^c	7260

[a] r_0 = radius at t=o, m; L_0=cylinder length at t=o,m.
[b] for a cube
[c] for a right circular cylinder

2.4 Nuclide Migration Through a Multi-layer System

Solutions of the problem posed by a multi-layer system have been presented in detail in our previous report ((H1), Chap. 6). For the dispersion-free case, a recursive solution is given by Eq. (6.21) of (H1). A non-recursive solution for a two-medium system, and for a step release from the waste source, is given by Eq. (6.22) of (H1).

BEST DOCUMENT AVAILABLE

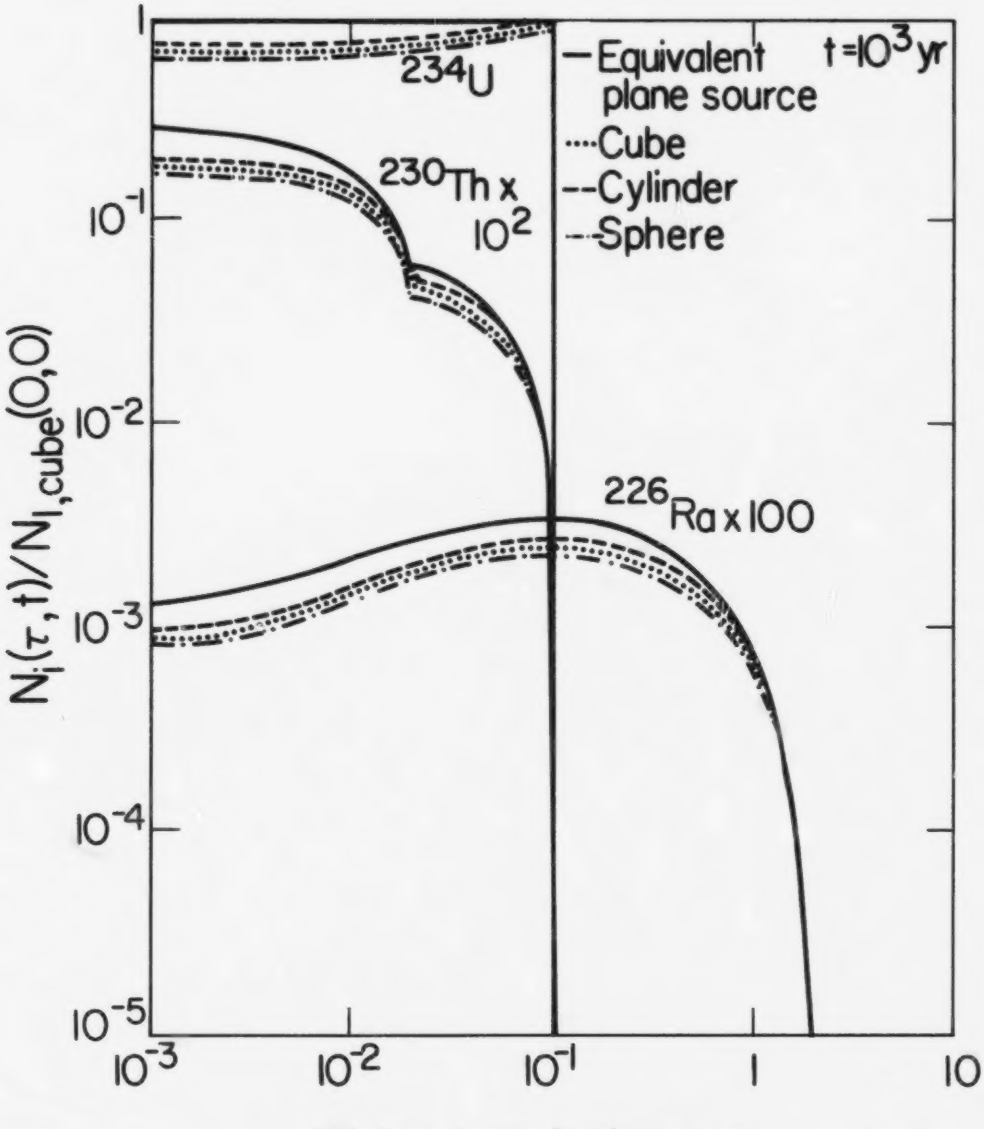

XBL 812-247

Figure 2.3.1 Concentration profiles for the $^{234}U \rightarrow {}^{230}Th \rightarrow {}^{226}Ra$ decay chain. $N_i(\tau,t)$ = atoms/m^3, $N_{1,cube}(0,0)$ = atoms/m^3 of ^{234}U at $\tau = 0$, $t = 0$, for the release from the cube. Penetration rate $R = 5 \times 10^{-5}$ m/yr. 0.2 m^3 of matrix at $t = 0$. τ = water transit time. No dispersion. No ^{234}U daughters.

BEST DOCUMENT AVAILABLE

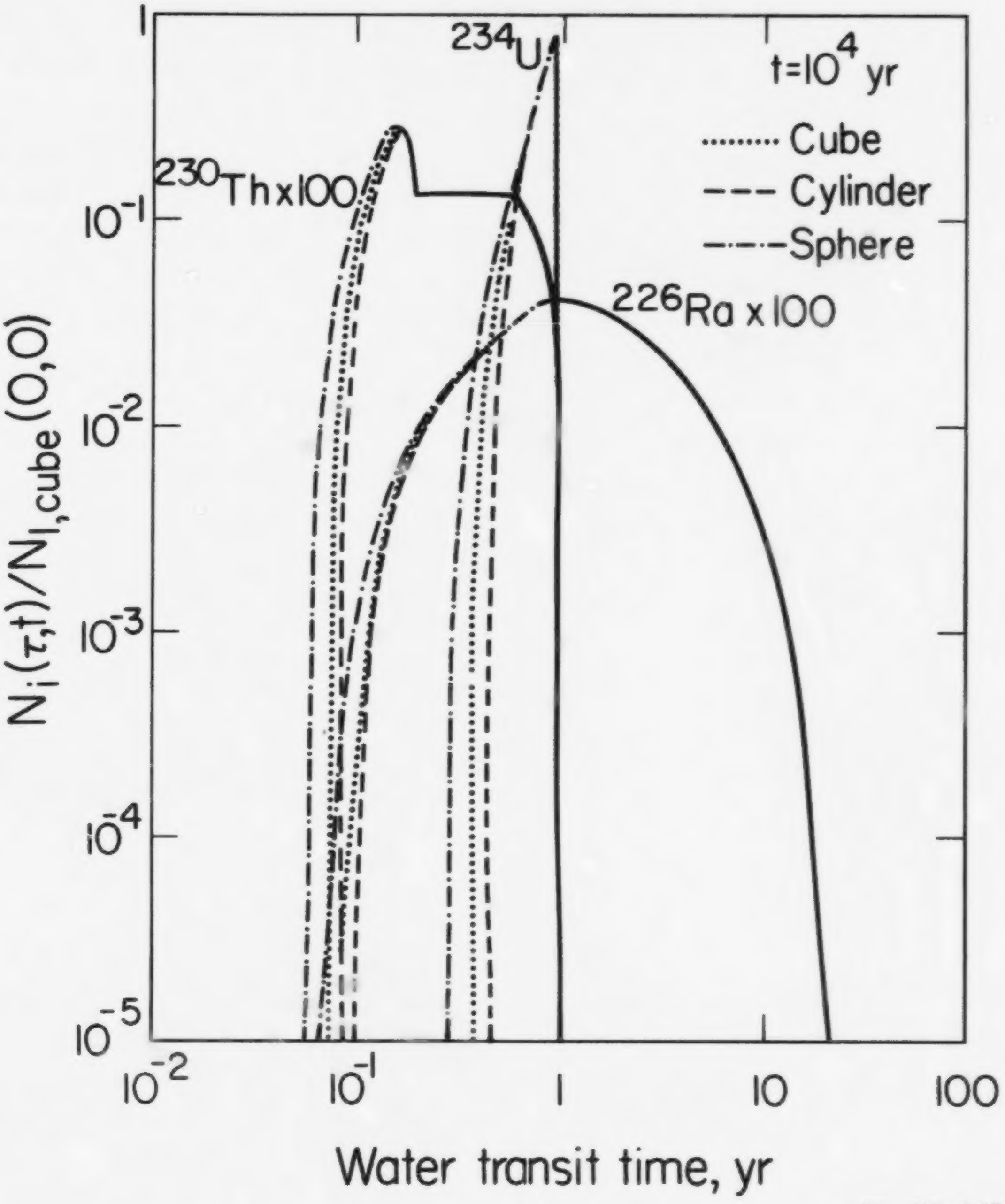

XBL 812-248

Figure 2.3.2 Concentration profiles for the $^{234}U \rightarrow ^{230}Th \rightarrow ^{226}Ra$ decay chain. $N_i(\tau,t)$ = atoms/m^3, $N_{1,cube}(0,0)$ = atoms/m^3 of ^{234}U at $\tau = 0$, $t = 0$, for the release from the cube. Penetration rate $\dot{R} = 5 \times 10^{-5}$ m/yr. 0.2 m^3 of matrix at $t = 0$. τ = water transit time. No dispersion. No ^{234}U daughters.

For finite dispersion, a recursive solution for a two-medium system is presented in Sect. 6.5 of (H1).

We present here applications of the equations derived in (H1). The medium is denoted by a left superscript, e.g.:

${}^2v$ = water velocity in the second medium

$${}^1\eta_i = \lambda_i + \frac{1-{}^1\epsilon}{{}^1\epsilon}\,\frac{{}^1\vec{k}_{D,i}}{{}^1K_i}$$

2.4.1 Near-field transport of a single radionuclide through overpack and rock.

A possible engineered barrier to radionuclide transport involves filling the space between a waste canister and rock with "overpack" material, selected to be nearly impermeable to water or to be specially sorptive for selected radionuclides. The analysis of radionuclide transport through the overpack and rock, assuming one-dimensional transport and an equivalent plane source of dissolving radionuclides, is an application of the multi-layer analysis. The dispersion-free solution for a single radionuclide will be adopted for this purpose.

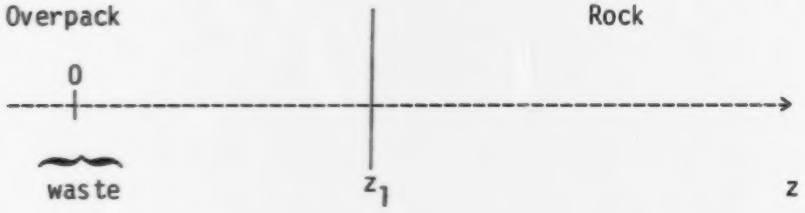

Figure 2.4.1 Overpack surrounding the waste.

The coordinate system is shown in Fig. (2.4.1). The interface between the two media occurs at z_1. The sorption constants in the overpack and rock are ${}^1K$ and ${}^2K$, respectively, and it is assumed that ${}^1K > {}^2K$.

By the superscript "w" we denote the two-medium case with overpack and by the superscript "n" the single-medium case with rock replacing the overpack, e.g.,

t_a^w = arrival time of the radionuclide at position z, when the overpack is present. We denote by ${}^1v$ and ${}^2v$ the water velocity in the overpack and in the rock, respectively. For local chemical equilibrium among all species, with no mineralization ($\vec{k}=o$):

$$ {}^1\eta_1 = {}^2\eta_1 = \lambda_1 $$

Assuming a simple band release of a nuclide with no precursors or decay daughters, the maximum concentration occurs at position z upon the arrival of the convection band at time t_a. When we have an overpack, $t_a = t_a^w$. The step solution without dispersion, eq. (2.1.20), (2.1.41) and (2.1.42), obtained in Section 2.1, by introducing the nuclides release at t=o as a source term in the transport equation, is identical with the solution obtained in our previous report (H1), eq. (4.127).

We then can express the two-medium solution without dispersion, given in Section 6 of (H1), which was obtained using Eq. (4.127), by the notation introduced in Section 2.1 of the present report. In particular, from Eq. (6.22) in (H1), we obtain

$$ t_a^w = \frac{z-z_1}{{}^2v_1} + \frac{z_1}{{}^1v_1} = {}^2\tau^w\,{}^2K_1 + {}^1\tau^w\,{}^1K_1 \text{ , for } z>z_1 \qquad (2.4.1) $$

where ${}^2\tau^w$ is the water transit time from the inner surface of the rock to position z in the rock:

$$ {}^2\tau^w = \frac{z-z_1}{{}^2v} \qquad (2.4.2) $$

and ${}^1\tau^w$ is the water transit time through the overpack:

$$ {}^1\tau^w = \frac{z_1}{{}^1v} \qquad (2.4.3) $$

If there is no overpack, $t_a = t_a^n$, so that:

$$t_a^n = \frac{z}{{}^2v_1} = {}^2K_1 \, {}^2\tau^n \tag{2.4.4}$$

where:

$${}^2\tau^n = \frac{z}{{}^2v} \tag{2.4.5}$$

The maximum concentration of the first nuclide of the decay chain occurs at each position z at time t_a:

$$N_{1,max}(z) = N_1(z,t_a) = \frac{w_s^o}{Tv} B_{1,1} e^{-\lambda_1 t_a} \tag{2.4.6}$$

where:

$$B_{1,1} = n_1^o \quad , \tag{2.4.7}$$

as given by (2.1.13). From (2.4.1) and (2.4.4), we get t_r, the increased transport time, i.e., the "retardation time" caused by replacing rock with overpack:

$$t_r = t_a^w - t_a^n = \frac{z_1}{{}^1v_1} - \frac{z_1}{{}^2v_1} = {}^1\tau^w \left({}^1K_1 - {}^2K_1 \right) \tag{2.4.8}$$

One of the effects of the overpack is then a retardation of the chromatographic band.

Due to radioactive decay, this retardation causes a reduction in the maximum concentration at each position in the rock by a factor f, where:

$$f \equiv \frac{N_1^w(z,t_a^w)}{N_1^n(z,t_a^n)} \quad , \tag{2.4.9}$$

From (2.4.6), (2.4.8), and (2.4.9):

$$f = e^{-\lambda_1 t_r} \tag{2.4.10}$$

or

$$\ln(f) = \lambda_1 \left(\frac{z_1}{{}^2v_1} - \frac{z_1}{{}^1v_1} \right) = \lambda_1 {}^1\tau^W \left({}^2K_1 - {}^1K_1 \right), \text{ for } z > z_1 \tag{2.4.11}$$

Equations (2.4.10) or (2.4.11) allow an analytical study of the relationship between: f, z_1, ${}^1K_1$ and ${}^2K_1$.

If we consider irreversible mineralization, i.e., $\vec{K}_1 > o$, the expression for t_r is left unchanged, but, if we use eq. (2.1.20) and (2.1.41) to express $N_1(z, t_a^{\cdot})$, Eq. (2.4.10) becomes:

$$f = \exp\left[-\lambda_1 t_r + \frac{z_1}{{}^1v_1} (\lambda_1 - {}^1\eta_1) - \frac{z_1}{{}^2v_1} (\lambda_1 - {}^2\eta_1)\right] \tag{2.4.12}$$

2.4.2 Equations for the Concentration of i nuclides in the second medium for a band release and no dispersion:

From the non-recursive solution (eq. (6.22) of (H1)) in the second medium for a step release and the superposition equation (Eq. (3.60) of (H1)), we obtain the following non-recursive formula for the concentrations in the second medium for a band release without dispersion:

$$N_i^b(z,t) = \frac{{}^2\rho}{{}^1\rho} \frac{W_s^o}{Tv} \left[h(\theta_{ii}) - h(\theta_{ii} - T)\right] \cdot \sum_{q=1}^{i} B_{i,q} \exp\left({}_qC_i^i\right) +$$

$$\frac{{}^2\rho}{{}^1\rho} \frac{W_s^o}{Tv} \sum_{j=1}^{i-1} \sum_{m=j}^{i-1} \sum_{r=m+1}^{i} \sum_{q=1}^{j} B_{j,q} \left\{ {}^1A_i^j \, {}^1C_{r,m}^{i,j} \, \frac{1}{{}^1\omega_{r,m}^q} \right. \cdot$$

$$\exp\left(E_i^{r,m}\right) \cdot \left[h(\theta_{mi}) - h(\theta_{ri})\right] - \exp\left(E_i^{r,m} - {}^1\omega_{r,m}^q T\right) \cdot \left[h(\theta_{mi} - T) - h(\theta_{ri} - T)\right] -$$

$$- \exp\left({}_qC_i^m\right) \cdot \left[h(\theta_{mi}) - h(\theta_{mi} - T)\right] + \exp\left({}_qC_i^r\right) \cdot \left[h(\theta_{r,i}) - h(\theta_{r,i} - T)\right] +$$

$${}^2A_i^j\ {}^2C_{r,m}^{i,j}\ \frac{1}{{}^2\omega^q_{r,m}} \cdot \Big[\exp(A^j_{r,m}).[h(\theta_{jm})-h(\theta_{jr})] -$$

$$\exp(A^j_{rm}-{}^2\omega^q_{r,m}T).[h(\theta_{jm}-T) - h(\theta_{jr}-T)] - \exp({}_qC^j_m).[h(\theta_{jm})-h(\theta_{jm}-T)]$$

$$+ \exp({}_qC^j_r)[h(\theta_{jr})-h(\theta_{jr})]\Big] +$$

$$\frac{{}^2\rho}{{}^1\rho}\ \frac{W_s^0}{Tv}\ \sum_{j=1}^{i-1}\ \sum_{m=j}^{i-1}\ \sum_{r=m+1}^{i}\ \sum_{\alpha=1}^{j-1}\ \sum_{\beta=\alpha}^{j-1}\ \sum_{\omega=\beta+1}^{j}\ \sum_{q=1}^{\alpha}\ B_{\alpha,q}\ .$$

$${}^1A_j^\alpha\ {}^1C^{j,\alpha}_{\omega,\beta}\ \frac{1}{{}^1\omega^q_{\omega,\beta}} \cdot {}^2A_i^j\ {}^2C^{i,j}_{r,m}\ \frac{1}{{}^2\omega^q_{r,m}}\ .$$

$$\cdot\Big\{\exp({}_qC^\beta_m) \cdot [h(\theta_{\beta m})-h(\theta_{\beta m}-T)]-\exp({}_qC^\beta_r)[h(\theta_{\beta r}).h(\theta_{\beta r}-T)]$$

$$-\exp({}_qC^\omega_m)[h(\theta_{\omega m})-h(\theta_{\omega m}-T)] +$$

$$+\left(\frac{{}^1B_{\omega,\beta}-\lambda_q}{{}^2B_{m,r}-{}^1B_{\omega,\beta}}\right) \cdot \Big[\exp(A^\beta_{r,m}) \cdot \big[h(\theta_{\beta,m})-h(\theta_{\beta,r})\big] -$$

$$-\exp(A^\beta_{r,m} - {}^2\omega^q_{r,m}T).[h(\theta_{\beta m}-T)-h(\theta_{\beta r}-T)] - \exp(A^\omega_{r,m})[h(\theta_{\omega,m})-h(\theta_{\omega,r})] +$$

$$+\exp(A^\omega_{r,m} - {}^2\omega^q_{r,m}T)[h(\theta_{\omega,m}-T)-h(\theta_{\omega,r}-T)]\Big] +$$

$$+\left(\frac{{}^2B_{r,m}-\lambda_q}{{}^2B_{r,m}-{}^1B_{\omega,\beta}}\right)\Big[\exp(E^{\omega\beta}_m)[h(\theta_{\omega,m})-h(\theta_{\beta m})] -$$

$$-\exp(E^{\omega\beta}_m-{}^1\omega^q_{\omega\beta}T).[h(\theta_{\omega,m}-T)-h(\theta_{\beta,m}-T)] - \exp(E^{\omega,\beta}_r).[h(\theta_{\omega,r})-h(\theta_{\beta,r})] +$$

$$\exp(E^{\omega,\beta}_r-{}^1\omega_{\omega\beta}T).[h(\theta_{\omega,r}-T)-h(\theta_{\beta,r}-T)]\Big]\Big\}\ :\ \text{for } t>0,\ z_1<z<\infty,\ {}^1v>0,\ {}^2v>0 \qquad (2.4.13)$$

where:

$$ {}^{1}v_{i} = {}^{1}v / {}^{1}K_{i} \qquad (2.4.14) $$

$$ A^{\beta}_{r,m} = -\,{}^{2}\beta_{r,m}t + {}^{2}\alpha_{r,m}(z-z_{1}) + \frac{z_{1}}{{}^{1}v_{\beta}}\left({}^{2}\beta_{r,m} - {}^{1}\eta_{\beta}\right) \qquad (2.4.15) $$

$B_{i,q}$ = Bateman coefficient, given by (2.1.12), (2.1.13) and (2.1.14).

${}^{1}\beta^{i,j}_{m}$ is defined by (2.1.23)

$$ {}_{q}C^{\beta}_{m} = -\,\lambda_{q}t + \frac{z-z_{1}}{{}^{2}v_{m}}\left(\lambda_{q} - {}^{2}\eta_{m}\right) + \frac{z_{1}}{{}^{1}v_{\beta}}\left(\lambda_{q} - {}^{1}\eta_{\beta}\right) \qquad (2.4.16) $$

$$ {}^{1}C^{i,j}_{r,m} = {}^{1}G^{i,j}_{r,m} \Big/ {}^{1}B^{i,j}_{m} \qquad (2.4.17) $$

$$ {}^{1}G^{i,j}_{r,m} = \begin{cases} 1 \;;\; \text{if } j = i-1 \\ \displaystyle\prod_{\substack{\alpha=j \\ \alpha\neq m \\ \alpha\neq S}}^{i} \left({}^{1}\beta_{\alpha m} - {}^{1}\beta_{r,m}\right) \;; \quad \text{if } j<i-1 \end{cases} \qquad (2.4.18) $$

$$ E^{\beta\omega}_{m} = -\,{}^{1}\beta_{\omega,\beta}t + \left(\frac{z-z_{1}}{{}^{2}v_{m}}\right)\left({}^{1}\beta_{\omega,\beta} - {}^{2}\eta_{m}\right) + z_{1}\,{}^{1}\alpha_{\omega,\beta} \qquad (2.4.19) $$

$$ {}^{1}\alpha_{r,m} = \left({}^{1}\eta_{r} - {}^{1}\eta_{m}\right) / \left({}^{1}v_{m} - {}^{1}v_{r}\right) \qquad (2.4.20) $$

$$ {}^{1}\beta_{r,m} = \left({}^{1}v_{m}\,{}^{1}\eta_{r} - {}^{1}v_{r}\,{}^{1}\eta_{m}\right) / \left({}^{1}v_{m} - {}^{1}v_{r}\right) \qquad (2.4.21) $$

$$ \theta_{jp} = t - \frac{z-z_{1}}{{}^{2}v_{p}} - \frac{z_{1}}{{}^{1}v_{j}} \qquad (2.4.22) $$

$$ {}^{1}\omega^{q}_{r,m} = \lambda_{q} - {}^{1}\beta_{r,m} \qquad (2.4.23) $$

2.4.3 Effect of an overpack on the transport of ^{237}Np, ^{233}U, ^{229}Th, and ^{225}Ra

Eq. (2.4.10) predicts the effect of an overpack on the first member in a radioactive chain. Here we give a numerical demonstration of the effect of a overpack on the chain:

$$^{241}\text{Pu} \xrightarrow[13y]{} {}^{241}\text{Am} \xrightarrow[458y]{} {}^{237}\text{Np} \xrightarrow[2.14\times10^{6}y]{} {}^{233}\text{Pa} \xrightarrow[7.4\times10^{-2}y]{} {}^{233}\text{U} \xrightarrow[1.62\times10^{5}y]{} {}^{229}\text{Th} \xrightarrow[7.34\times10^{3}y]{} {}^{225}\text{Ra} \xrightarrow[4.1\times10^{-2}y]{}$$

If waste dissolution does not begin until several decades after burial, and since ^{233}Pa and ^{225}Ra will each be in secular equilibrium with its decay parent, the 4n+1 chain reduces to:

$$^{241}\text{Am} \rightarrow {}^{237}\text{Np} \rightarrow {}^{233}\text{U} \rightarrow {}^{229}\text{Th} \rightarrow$$

After calculating the concentration of ^{229}Th, the concentration of ^{225}Ra can be obtained from (Eq. (4.134) of (H1)):

$$N_{Ra} = \frac{\lambda_{Th} K_{Th} N_{Th}}{\lambda_{Ra} K_{Ra}} \qquad (2.4.24)$$

where Th refers to ^{229}Th and Ra to ^{225}Ra.

As input for our calculations we adopt a calculation (B2) of the quantities of actinides in the unreprocessed discharge fuel from a light water nuclear power reactor, resulting from 1 Gw(e)yr of reactor operation, and after all ^{241}Pu has decayed to ^{241}Am:

^{241}Am = 29.0 Kg/Gw(e)yr
^{237}Np = 20.4 Kg/Gw(e)yr

No daughters of ^{237}Np are initially present.

The sorption retardation coefficients are assumed to be those quoted for a western desert soil (B3), as shown in Table 2.4.1.

Table 2.4.1: Half lives and sorption retardation coefficients

	^{241}Am	^{237}Np	^{233}U	^{229}Th
Half life (yr)	458	2.14×10^6	1.62×10^5	7.34x103
Sorption retardation coefficient	1×10^4	1×10^2	1.4×10^4	5×10^4

Assuming no dispersion, we can express the results in terms of the water transport time τ. The water transport time ${}^{1}\tau$ to the interface between the two media at $z=z_1$ is:

$$ {}^{1}\tau = \frac{z_1}{{}^{1}v} \tag{2.4.25} $$

The total water transport time τ to position z is:

$$ \tau = \begin{cases} z/{}^{1}v \ ; \text{ if } z \le z_1 \\ \dfrac{z-z_1}{{}^{2}v} + {}^{1}\tau \ : \text{ if } z > z_1 \end{cases} \tag{2.4.26} $$

where:

${}^{1}v$ = water velocity in the inner (first) medium
${}^{2}v$ = water velocity in the outer (second) medium.

We assume a band-release dissolution of the buried unreprocessed fuel, with a leach time T of 3×10^4 yr. We assume that the sorption-retardation coefficients to be the same in the overpack and surrounding medium for all nuclides except for ^{237}Np, for which we assume:

${}^{1}K_{Np} = 2 \times 10^4$ in the overpack.

Results

Figures 2.4.2, 2.4.3, and 2.4.4 show the space-time-dependent discharge rates of ^{237}Np, ^{233}U, and ^{229}Th/^{225}Ra as a function of the water transport time from the waste source, at a time $t=10^5$ yr after the beginning of waste dissolution. The discharge rate is the rate at which radionuclide activity, expressed in Curies, is transported past the location z by convection. These quantities were calculated by applying Eq. (2.1.20), (2.1.41), and (2.1.42) for the overpack medium (since D=0) and the equations of Sect. 2.4.2 for the surrounding rock. The parameter expressing the thickness of overpack is:

BEST DOCUMENT AVAILABLE

$^1\tau = 0$ no overpack (Figure 2.4.2)

$^1\tau = 5$ yr (Figure 2.4.3)

$^1\tau = 10$ yr (Figure 2.4.4)

Because its half life is only 458 yr, there is negligible ^{241}Am remaining at the time of 10^5 yr adopted for these illustrations. However, the earlier and relatively rapid transport of ^{241}Am does affect the profile of its decay daughter ^{237}Np, as may be seen from Figure 2.4.3. There, for the overpack water-transport time of 5 yr and for the assumed ^1K for neptunium, ^{237}Np leached from the waste can migrate only as far as the overpack-rock interface. The presence of ^{237}Np beyond this interface is due to the earlier migration of ^{241}Am into the surrounding rock.

The effect of the Np-sorbing overpack is to delay the propagation of ^{237}Np and its decay daughters into the surrounding rock. It does significantly increase the local concentrations of ^{233}U and ^{229}Th that appear in the near-field groundwater.

Figures 2.4.5-2.4.8 show the time-dependent discharge rates at a distance from the waste corresponding to a total water transport time of 100 yr. The different figures are for different values of the transport time of water through the overpack, varying from 0 to 100 yr.

The effect of the neptunium-sorbing overpack is to retard but only slightly attenuate the discharge rate of ^{237}Np. However, increasing the residence time of water in the overpack results in an increase in the maximum discharge rate of ^{233}U, ^{229}Th, and ^{225}Ra. When there is no overpack, this maximum discharge rate of ^{233}U occurs when the trailing edge of the band of ^{237}Np reaches the discharge location, and the maximum discharge rates for ^{229}Th and ^{225}Ra occur shortly thereafter. These maxima are followed, at a time about a million years later, by additional peak concentrations of the ^{237}Np daughters, a result of the longer-term transport of the decay daughters which were formed within the waste material. When overpack is added to delay the discharge of ^{237}Np, there is more time for the formation of the decay daughters before the discharge of the parent ^{237}Np, and the peak concentrations and discharge rates of these daughters increase.

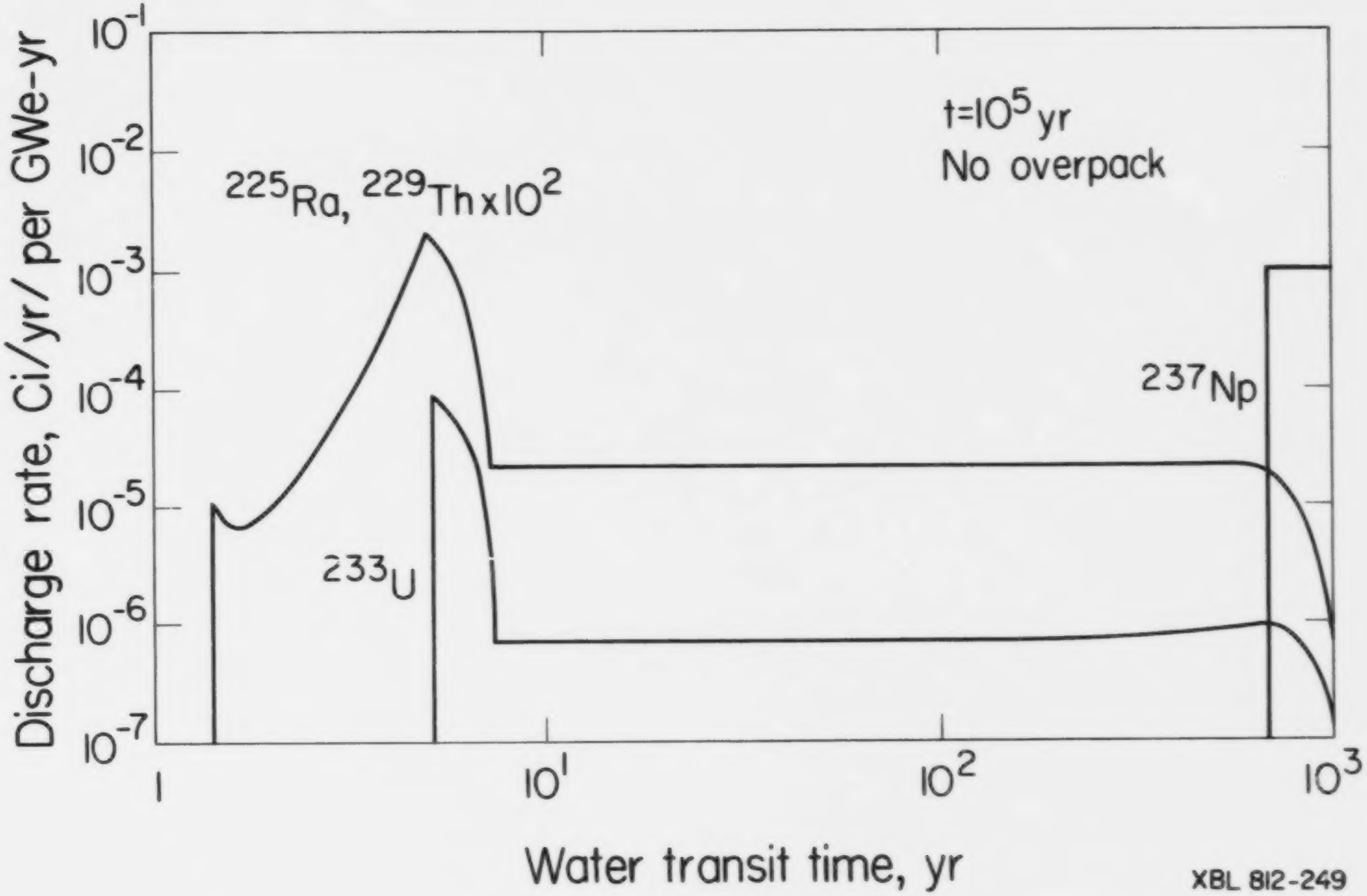

Figure 2.4.2 Discharge rate profiles for the ^{242m}Am → ^{242}Cm → ^{238}Pu → ^{234}U → ^{230}Th → ^{226}Ra decay chain. Unreprocessed discharge fuel. $^{1}\tau$ = water transit time to the interface between the two media, yr. T = 3 x 10^4 yr. No dispersion. K_{Am} = 10^4; K_U = 1.4 x 10^4; K_{Th} = 5 x 10^4, in both media, and K_{Np} = 2 x 10^4 in overpack, K_{Np} = 100 in rock.

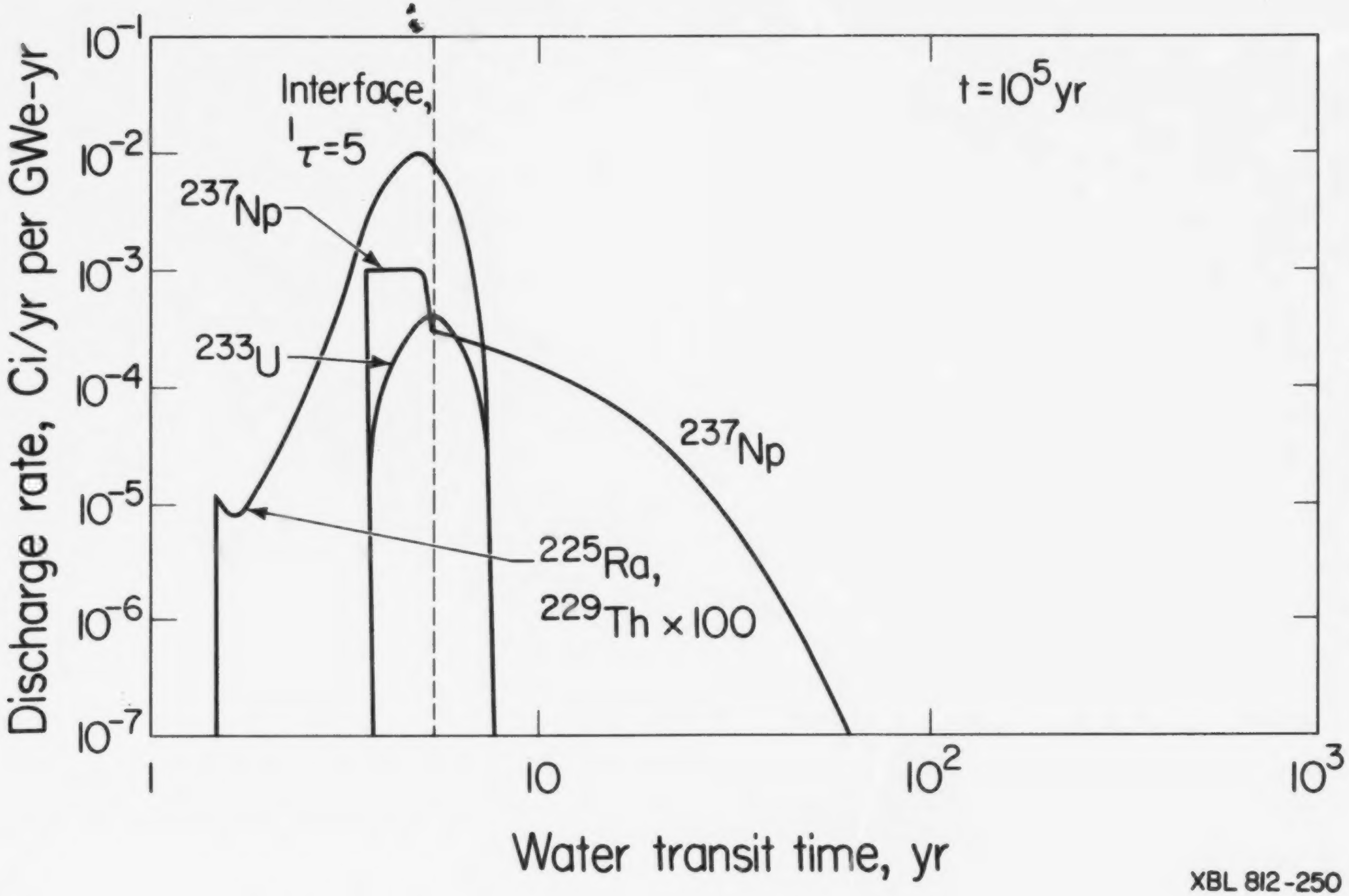

XBL 812-250

Figure 2.4.3 Discharge rate profiles for the $^{242m}\text{Am} \rightarrow {}^{242}\text{Cm} \rightarrow {}^{238}\text{Pu} \rightarrow {}^{234}\text{U} \rightarrow {}^{230}\text{Th} \rightarrow {}^{226}\text{Ra}$ decay chain. Unreprocessed discharge fuel. $^1\tau$ = water transit time to the interface between the two media, yr. $T = 3 \times 10^4$ yr. No dispersion. $K_{Am} = 10^4$; $K_U = 1.4 \times 10^4$; $K_{Th} = 5 \times 10^4$, in both media, and $K_{Np} = 2 \times 10^4$ in overpack, $K_{Np} = 100$ in rock.

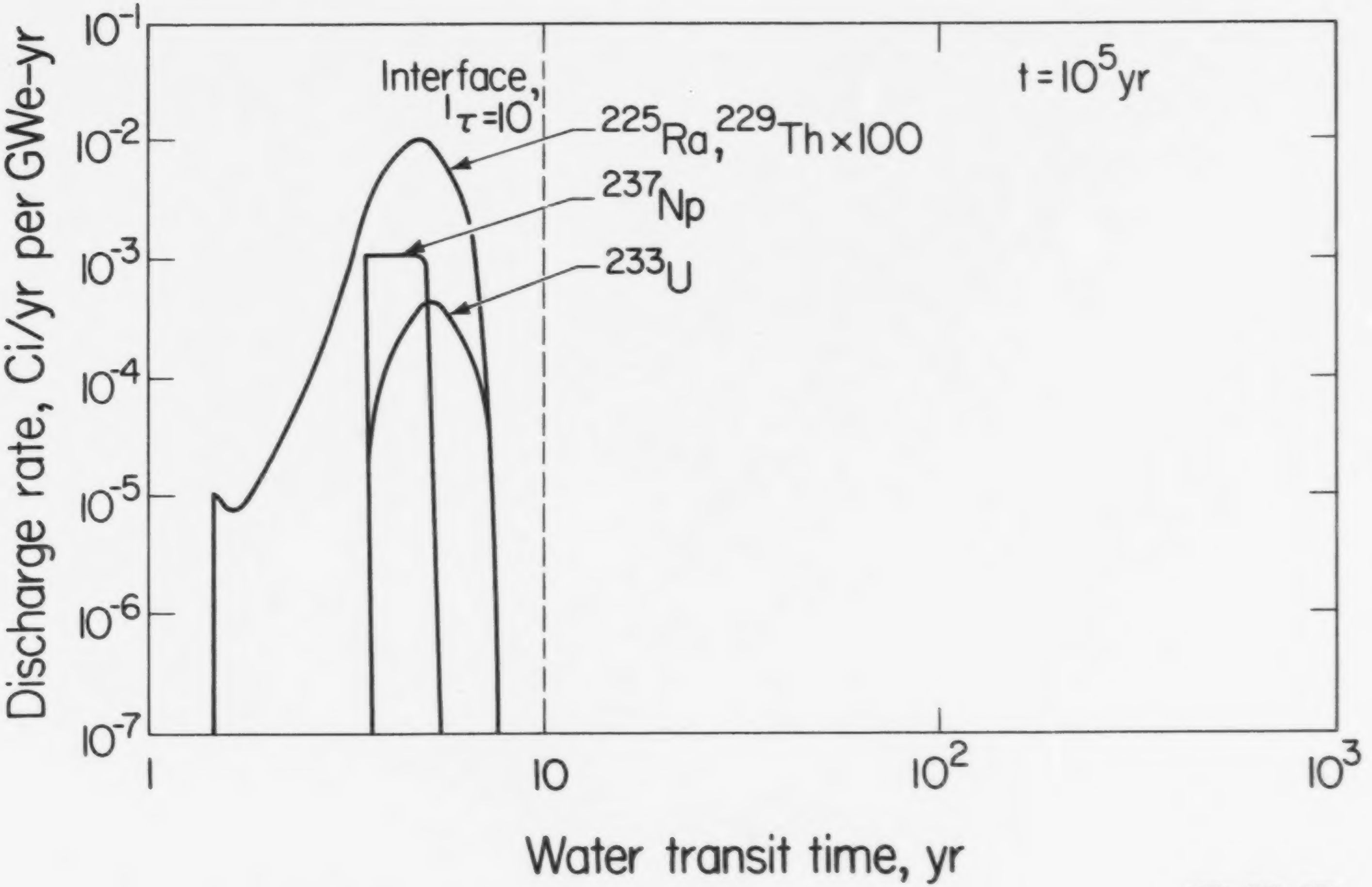

XBL 812-251

Figure 2.4.4 Discharge rate profiles for the ^{242m}Am → ^{242}Cm → ^{238}Pu → ^{234}U → ^{230}Th → ^{226}Ra decay chain. Unreprocessed discharge fuel. $^1\tau$ = water transit time to the interface between the two media, yr. $T = 3 \times 10^4$ yr. No dispersion. $K_{Am} = 10^4$; $K_U = 1.4 \times 10^4$; $K_{Th} = 5 \times 10^4$, in both media, and $K_{Np} = 2 \times 10^4$ in overpack, $K_{Np} = 100$ in rock.

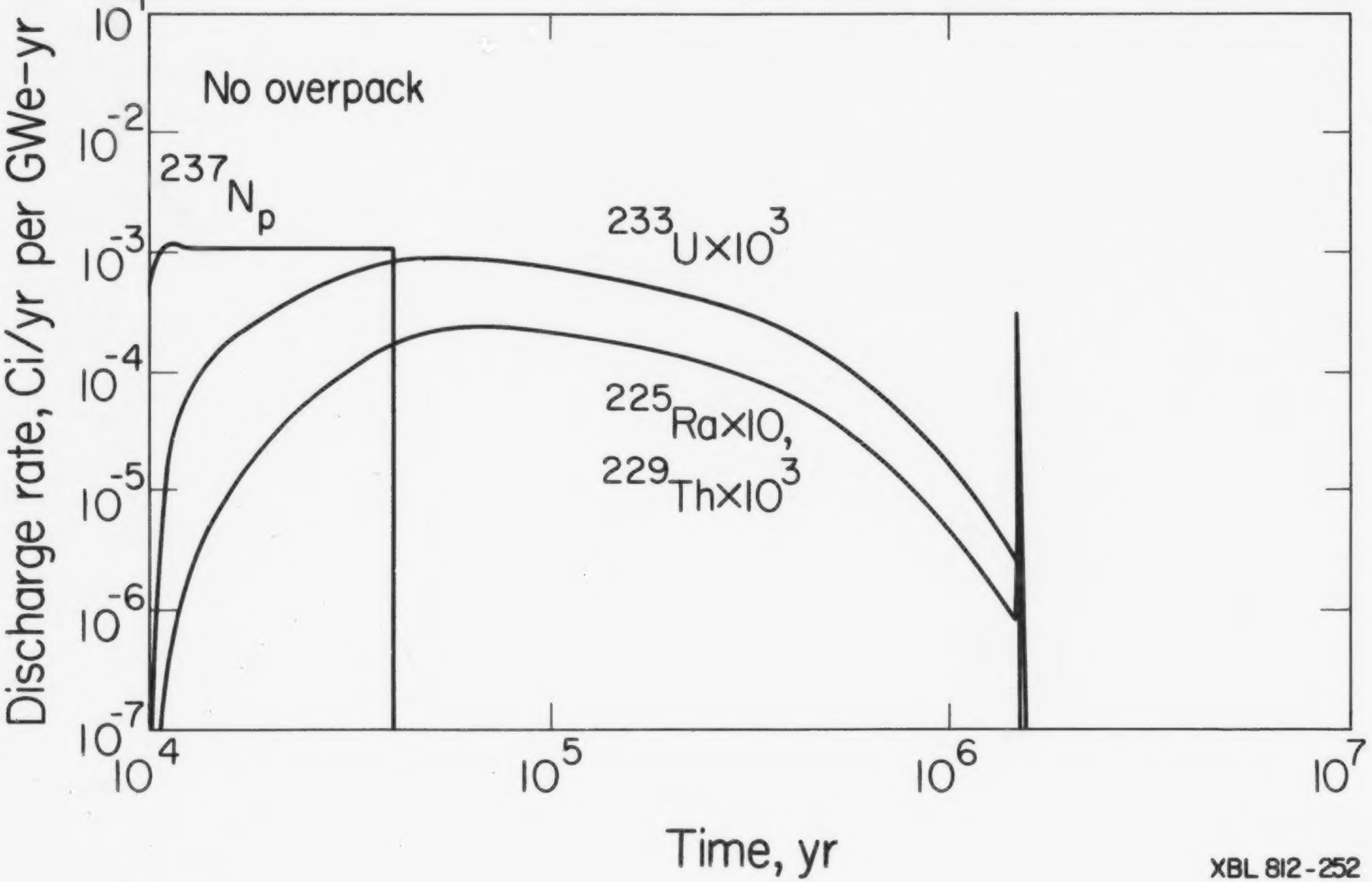

XBL 812-252

Figure 2.4.5 Discharge rate profiles at τ = 100 yr for the $^{242m}Am \rightarrow {}^{242}Cm \rightarrow {}^{238}Pu \rightarrow {}^{234}U \rightarrow {}^{230}Th \rightarrow {}^{226}Ra$ decay chain. Unreprocessed discharge fuel. τ = total water transit time, yr. $^{1}\tau$ = water transit time to the interface between the two media, yr. T = 3 x 10^4 yr. No dispersion. K_{Am} = 10^4; K_U = 1.4 x 10^4; K_{Th} = 5 x 10^4, in both media, and K_{Np} = 2 x 10^4 in overpack, K_{Np} = 100 in rock.

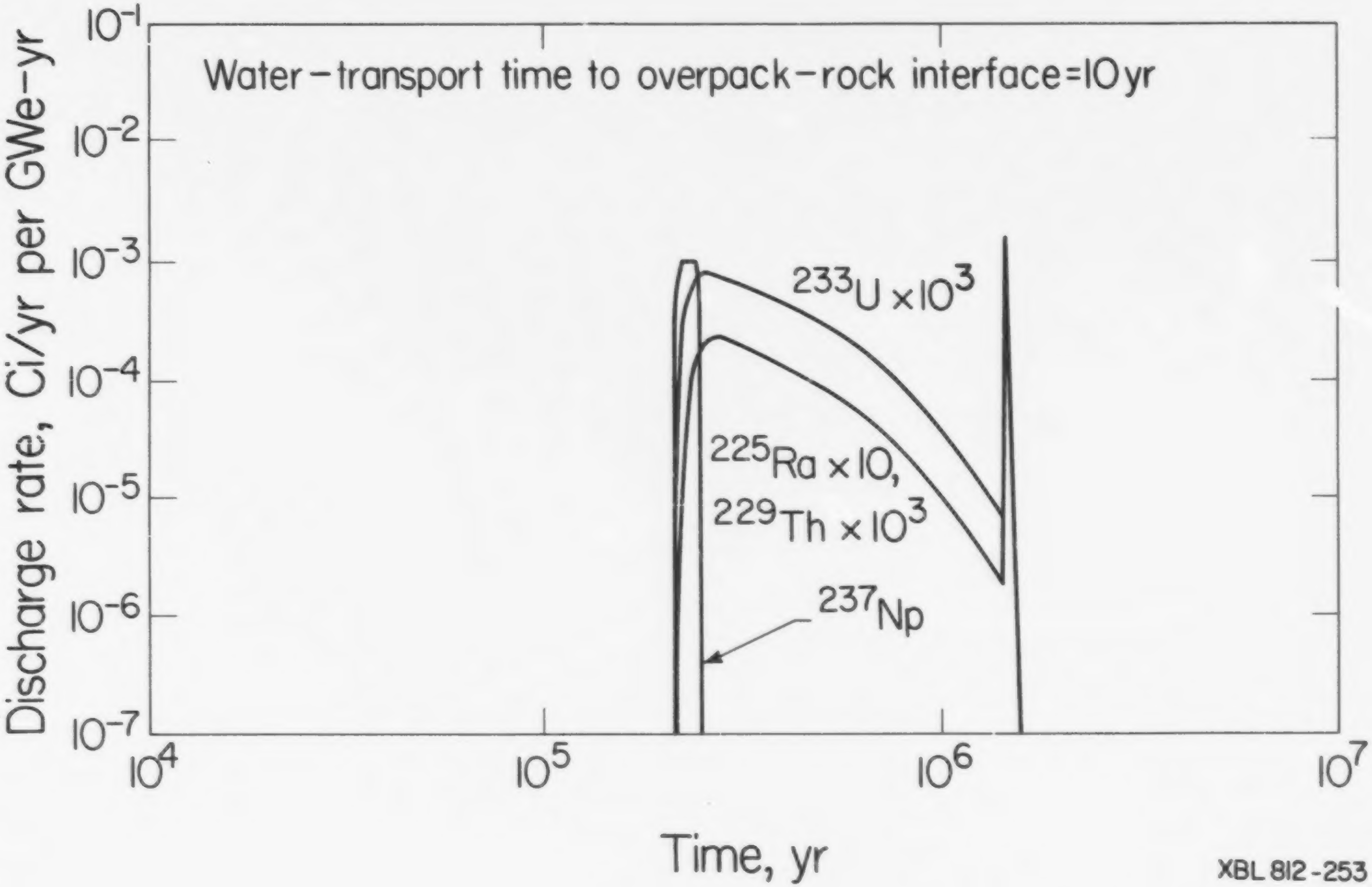

XBL 812-253

Figure 2.4.6 Discharge rate profiles at τ = 100 yr for the ${}^{242m}\mathrm{Am} \rightarrow {}^{242}\mathrm{Cm} \rightarrow {}^{238}\mathrm{Pu} \rightarrow {}^{234}\mathrm{U} \rightarrow {}^{230}\mathrm{Th} \rightarrow {}^{226}\mathrm{Ra}$ decay chain. Unreprocessed discharge fuel. τ = total water transit time, yr. ${}^{1}\tau$ = water transit time to the interface between the two media, yr. T = 3×10^4 yr. No dispersion. $K_{Am} = 10^4$; $K_U = 1.4 \times 10^4$; $K_{Th} = 5 \times 10^4$, in both media, and $K_{Np} = 2 \times 10^4$ in overpack, K_{Np} = 100 in rock.

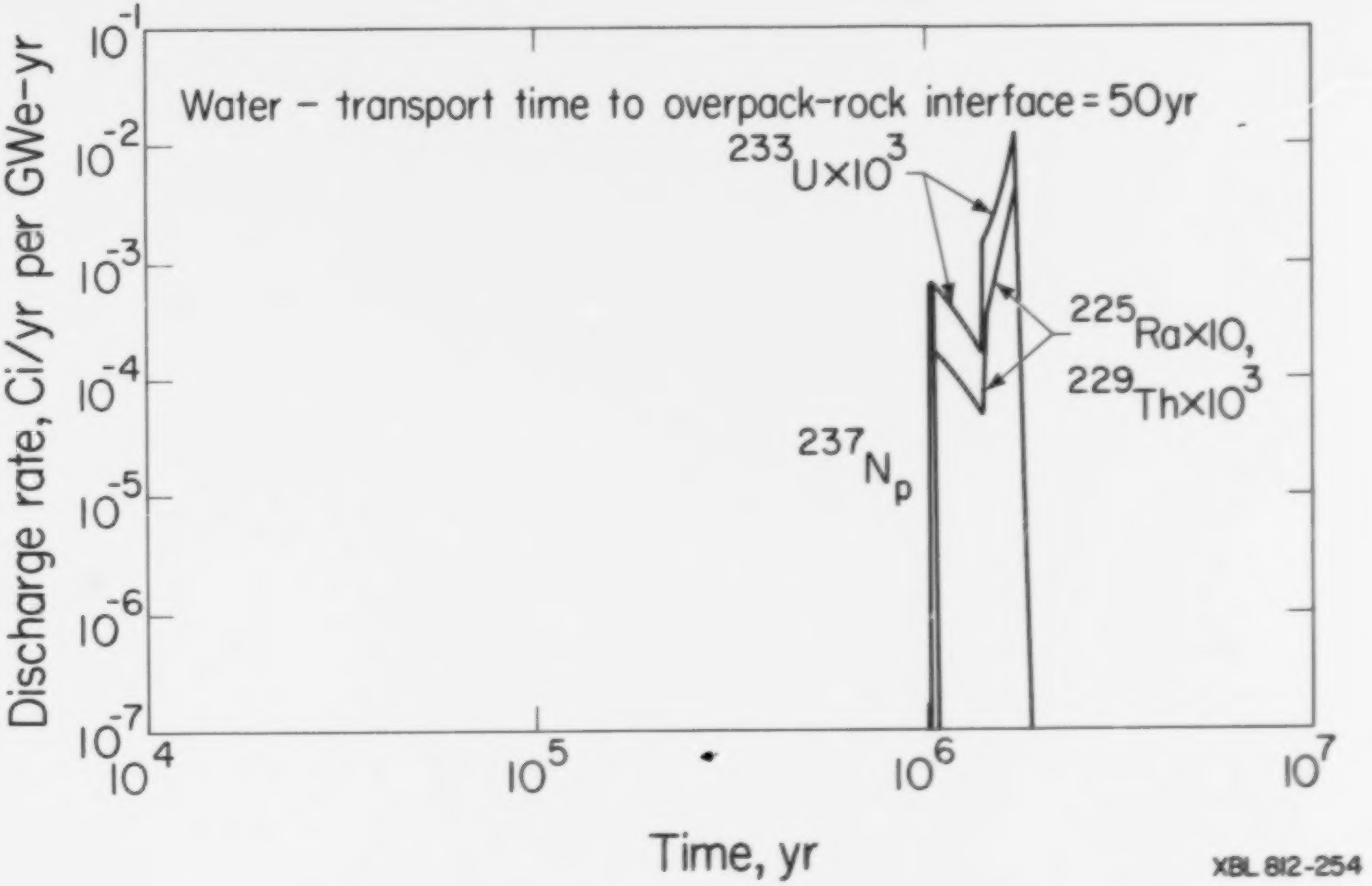

Figure 2.4.7 Discharge rate profiles at τ = 100 yr for the $^{242m}Am \rightarrow {}^{242}Cm \rightarrow {}^{238}Pu \rightarrow {}^{234}U \rightarrow {}^{230}Th \rightarrow {}^{226}Ra$ decay chain. Unreprocessed discharge fuel. τ = total water transit time, yr. $^{1}\tau$ = water transit time to the interface between the two media, yr. $T = 3 \times 10^4$ yr. No dispersion. $K_{Am} = 10^4$; $K_U = 1.4 \times 10^4$; $K_{Th} = 5 \times 10^4$, in both media, and $K_{Np} = 2 \times 10^4$ in overpack, $K_{Np} = 100$ in rock.

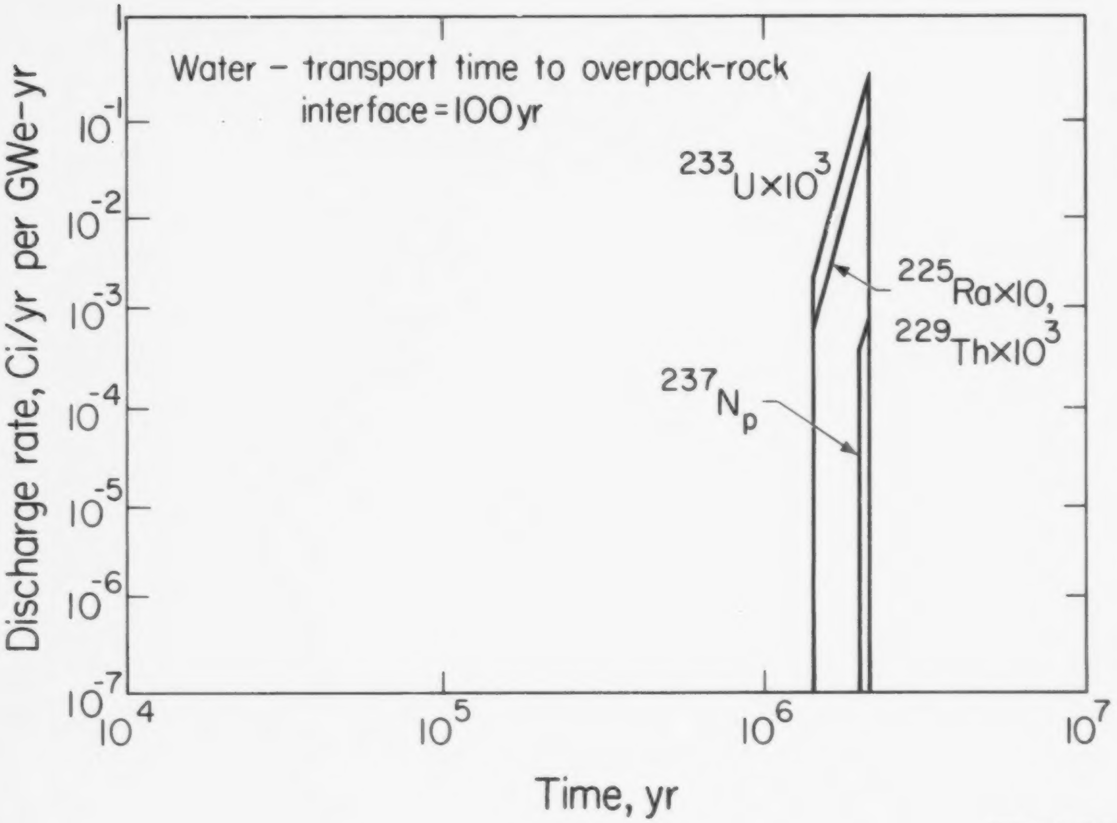

XBL 812-255

Figure 2.4.8 Discharge rate profiles at τ = 100 yr for the $^{242m}Am \rightarrow {}^{242}Cm \rightarrow {}^{238}Pu \rightarrow {}^{234}U \rightarrow {}^{230}Th \rightarrow {}^{226}Ra$ decay chain. Unreprocessed discharge fuel. τ = total water transit time, yr. $^1\tau$ = water transit time to the interface between the two media, yr. $T = 3 \times 10^4$ yr. No dispersion. $K_{Am} = 10^4$; $K_U = 1.4 \times 10^4$; $K_{Th} = 5 \times 10^4$, in both media, and $K_{Np} = 2 \times 10^4$ in overpack, $K_{Np} = 100$ in rock.

[redacted]

Figure 2.4.9 shows the local maximum discharge rates of ^{237}Np and its daughters as a function of the water transport time through the overpack. The times of maximum discharge, at a water-transport time of 100 yr, for various values of the water-transport time in the overpack, are shown in Table 2.4.2.

If we assume that the overpack does not change the water velocity, then the fixed total water transport time of 100 yr corresponds to a fixed position, $z = 100\ v$ meters, where v is the water velocity in m/yr. But if we allow the overpack to change the water velocity, then a fixed total water transport time corresponds to different positions z, for different values of the transport time of water through the overpack.

For example, Figure 2.4.5, for which there is no overpack, presents the discharge rate from rock for which the water-transport time is 100 years. At the other extreme, Figure 2.4.8 is for a water-transport time through the overpack of 100 years, so the discharge here is measured at the outer surface of the overpack.

If the water velocity in the overpack is the same as that in the surrounding rock, then as we proceed from the conditions of Figure 2.4.5 to 2.4.8, overpack replaces the rock initially contained within a fixed distance z from the waste. If, on the other hand, the water velocity in the overpack is much lower than that in the rock, overpack replaces less of the initial rock and the position of discharge moves inward towards the waste as overpack is substituted for rock, holding the total water transport time constant. However, these calculations can be reasonably applied to estimate the discharge ratios at a fixed position z from the source, where z is here assumed to be the thickness of rock that would give a water transport time of 100 yr. Even though insertion of an overpack with lower permeability than the rock would increase the total water-transport time to this fixed position, the effect of an increase in this total transport time of water is small compared to the much larger increase in the transport time of neptunium due to the neptunium-sorbing overpack.

It is apparent that a neptunium-sorbing overpack with the parameters assumed here accomplishes little. For significant benefits to be obtained the overpack must be substantially thicker, have substantially greater sorption retardation of the nuclides in this chain, and/or must have substantially lower water velocity than assumed herein.

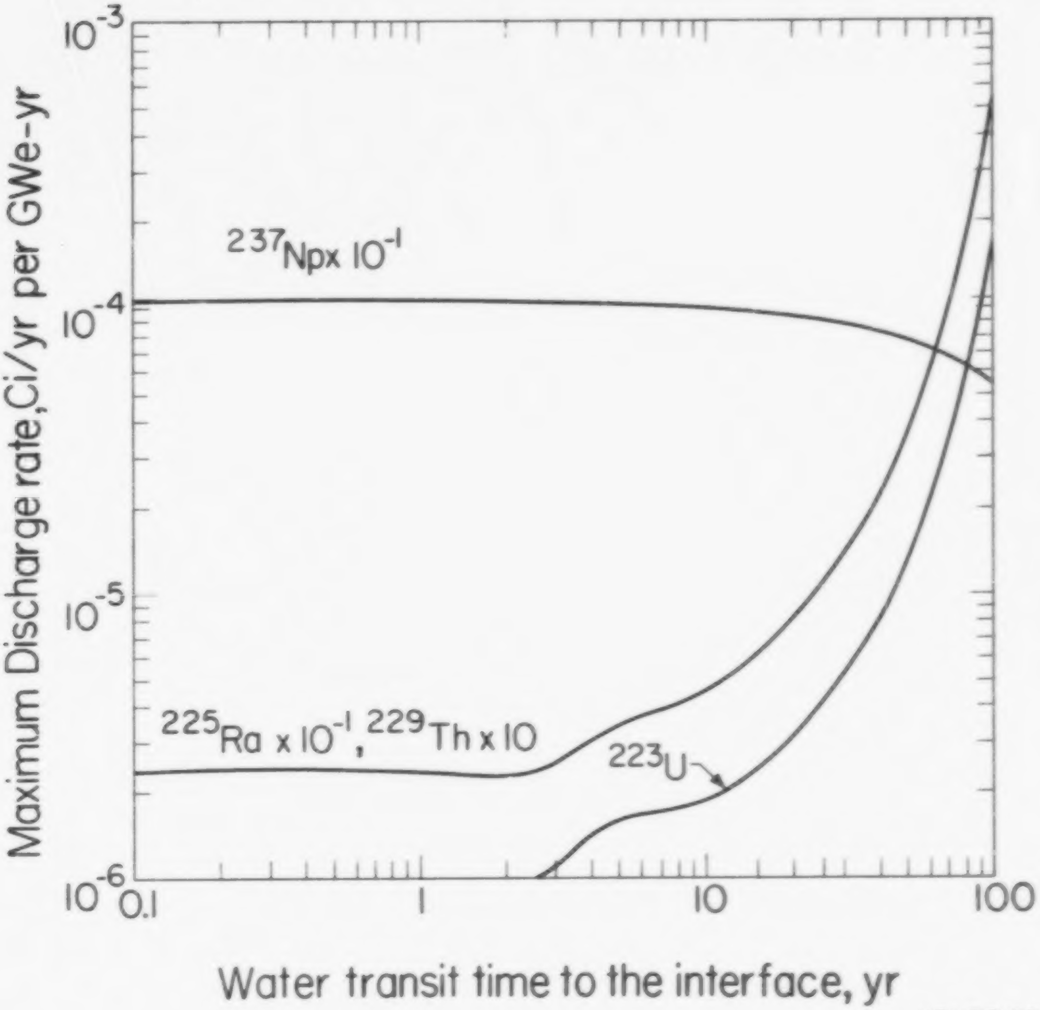

XBL 812-256

Figure 2.4.9 Maximum discharge rate at τ = 100 yr, for the $^{241}\mathrm{Am} \rightarrow {}^{237}\mathrm{Np} \rightarrow {}^{233}\mathrm{U} \rightarrow {}^{229}\mathrm{Th}$ (^{225}Ra) decay chain. Unreprocessed discharge fuel. τ = total water transit time. T = 3×10^4 yr. No dispersion. $K_{Am} = 1 \times 10^4$, $K_U = 1.4 \times 10^4$, $K_{Th} = 5 \times 10^4$ in both media. $K_{Np} = 2 \times 10^4$ in overpack, $K_{Np} = 10^2$ in rock.

Table 2.4.2 Time of maximum discharge rate, for a water-transport time of 100 yr.

Water-Transport Time in in Overpack, yr	Time for Maximum Discharge, yr. ^{237}Np	^{233}U	^{229}Th(^{225}Ra)
0.1	1.6×10^4	4.2×10^4	6.4×10^4
1.0	3.4×10^4	6×10^4	8.2×10^4
10	2.1×10^5	1.4×10^6	1.4×10^6
100	2×10^6	2×10^6	2×10^6

2.4.4 Effect of fuel reprocessing on the transport of ^{237}Np and its daughters

The calculations in Section 2.4.3 assumed that unreprocessed discharge fuel is buried as high-level waste. Instead, if the fuel is reprocessed to recover uranium and plutonium, only about 0.5 percent of the uranium and plutonium in the discharge fuel appears in the high-level reprocessing wastes (B2). If the discharge fuel has been stored for many decades prior to reprocessing, the quantity of ^{237}Np precursors in the high-level reprocessing wastes will be about the same as in the discharge fuel, because most of the ^{241}Pu in the discharge fuel will have decayed to ^{241}Am prior to reprocessing, and all of the americium appears in the high-level reprocessing waste. However, if the discharge fuel is reprocessed within a year or so after discharge, relatively little of the contained ^{241}Pu will have decayed to ^{241}Am. Recovering and recycling this plutonium then results in a two-fold reduction in the total amount of ^{237}Np and its precursors in the high-level waste. This results in about a two-fold reduction in all of the discharge rates presented in Figures 2.4.2-9.

2.4.5. Effect of a 1000-yr delay in waste dissolution

The calculations in Section 2.4.3 were made on the assumption that dissolution is initiated shortly after the Pu in the waste has decayed to ^{241}Am. Actually, because of the short half life and relatively slow transport speed of ^{241}Pu, assuming that waste dissolution begins at the instant of burial would have not perceptible effect on these results.

[redacted]

The calculations for the ^{237}Np chain in unreprocessed discharge fuel were repeated for an assumed delay of one thousand years prior to the initiation of dissolution. This allows time for 78 percent of the ^{241}Am to decay prior to dissolution, resulting in five-fold reduction in the magnitude of the concentration of ^{237}Np in the outer rock region of Figure 2.4.3. This slightly increases the magnitude of the near-field peak discharge rate of ^{237}Np in and near the overpack, but the effect on the discharge rates of ^{237}Np and its daughters in the far-field rock is negligible.

2.5 Solubility-limited dissolution and transport of a radionuclide

2.5.1 Introduction

Analyses which neglect the effect of solubility limits of dissolving radioelements can overestimate the concentrations of low-solubility radionuclides in groundwater. When the radioactive wastes begin to dissolve in groundwater, some radioelements may appear in chemical forms of very low solubility, and they may not go into solution when the surrounding waste matrix dissolves. Radioelements which exhibit solubility-limited transport, depending upon the waste composition, dissolution rate, water flow rate, and the groundwater conditions, are technetium, zirconium, thorium, uranium, neptunium, and plutonium.

Here we present an analysis of the space-time-dependent concentration of a radionuclide which is limited in concentration by solubility in the groundwater. We will adopt the one-dimensional transport analyses presented in our previous report (H1) and in the present report, which assume that the waste is represented by an infinite plane source normal to the direction of water flow. Radioelements dissolved from the waste are assumed to be instantly well mixed in the water at the waste location. Radioelements which may be released from the waste by dissolution of the waste matrix are not necessarily all dissolved, depending upon the elemental solubility limit. Undissolved radionuclides are assumed to exist as a precipitate at the dissolution location.

As has been pointed out in Section 2.3, the full effects of a solubility limit cannot be taken into account by a one-dimensional model. Groundwater flowing slowly across a waste surface will develop a near-stagnant boundary layer adjacent to the surface, and there will exist boundary-layer-controlled concentration profiles of dissolved radioelements in the liquid adjacent to the waste canister. The higher concentration near the surface is likely to affect the dissolution rate of that radioelement. Likewise, the dissolving radioelement will approach its solubility limit far sooner in the boundary layer than in the bulk of the groundwater at the waste location. Therefore, solubility-limited transport will occur well before the average concentration of the dissolving radioelement in the groundwater adjacent to the waste reaches the solubility limit. These important boundary-layer effects will be the subject of a later report, but they are neglected in the present analysis.

The analyses presented here are limited to a radionuclide which has no decay parents. It is assumed that local chemical equilibrium exists with respect to sorption and with respect to formation or dissolution of the immobile precipitate. Dispersion-free transport is assumed, and the solutions are expressed for step release, band release, and exponential release (H1).

2.5.2 Analysis

We assume first that the radionuclide of interest is the only isotopic form of that element present in the waste, so that a concentration solubility limit N* for that element becomes a concentration limit for that radionuclide. The governing transport equation for the radionuclide with no precursors, ignoring axial dispersion, is:

$$K \frac{\partial N}{\partial t} + v \frac{\partial N}{\partial z} + \lambda K\ N = 0 \qquad (2.5.1)$$

where N = concentration of nuclide in water phase

K = overall sorption retardation coefficient

v = velocity of groundwater

λ = decay constant of nuclide

From Eq. (2.5.1)

$$\frac{\partial N}{\partial t} + v_1 \frac{\partial N}{\partial z} + \lambda N = 0 \qquad (2.5.2)$$

where $v_1 = v/K_1$ is the effective migration velocity of the nuclide.

If some of the radionuclide contained in the dissolved waste does not go into solution, it will exist as a precipitate at the dissolution location. The material balance for the precipitate is:

$$\frac{dP(t)}{dt} = \phi''(t) - N_1^*v - \lambda P(t) \qquad (2.5.3)$$

$$\phi''(t) = n^O\dot{W}_S\, e^{-\lambda t} \qquad (2.5.4)$$

where $P(t)$ = amount of precipitate per unit surface of plane source in the water phase.

$\phi''(t)$ = rate of release of nuclide from the source, per unit area of source in the water phase.

n^O = atom fraction of the radionuclide in the waste at t=o.

N^* = solubility-limited concentration in water phase

$\dot{W}_S$ = dissolution rate of the total waste material per unit area of the plane source in the water phase.

In the case of a step release, we assume a constant dissolution rate $\dot{W}_S$. From Eqs. (2.5.3) and (2.5.4):

$$\frac{dP(t)}{dt} = n^O\dot{W}_S e^{-\lambda t} - N^*v - \lambda P(t) \qquad (2.5.5)$$

The initial condition is $P(0) = 0$. Solving the differential equation (2.5.5), we obtain:

$$P(t) = n^O\dot{W}_S t - \lambda t - \frac{N^*v}{\lambda}(1-e^{-\lambda t}) \qquad (2.5.6)$$

For a band release, we assume a constant dissolution rate $\dot{W}_S$, given by

$\frac{W_S^O}{T}$ (see Eq. (2.1.10)), where T is the leach time. Eq. (2.5.3) becomes:

$$\frac{dP(t)}{dt} = \frac{n^O W_S^O}{T} e^{-\lambda t}\,[1-h(t-T)] - N^*v - \lambda P(t) \qquad (2.5.7)$$

Solving the Eq. (2.5.7) with the initial condition; $P(0) = 0$:

$$P(t) = n^O \frac{W_S^O}{T} e^{-\lambda t}\,[t-(t-T)h(t-T)] - \frac{N^*v}{\lambda}(1-e^{-\lambda t}) \qquad (2.5.8)$$

In the case of an exponential release mode, the nuclide is leached at a fractional rate k from the source. The amount $W_{S,1}(t)$ of the nuclide within the source at time t, per unit area is:

$$W_{S,1}(t) = n^o W_S^o e^{(-\lambda+k)t} \qquad (2.5.9)$$

So the release rate is:

$$\phi''(t) = kW_{S,1}(t) = kn^o W_S^o \, e^{-(\lambda+k)t} \qquad (2.5.10)$$

In this case, Eq. (2.5.3) becomes:

$$\frac{dP(t)}{dt} = kn^o W_S^o \, e^{-(\lambda+k)t} - N^* v - \lambda P(t) \qquad (2.5.11)$$

We can now use Eq. (2.5.8) to find the time t* at which all of the precipitate has dissolved, i.e., P(t*) = 0.

The initial condition is P, as in P(0) = 0. Solving Eq. (2.5.10), we obtain:

$$P(t) = \left(\frac{N^* v}{\lambda} + W_S^o n^o\right) e^{-\lambda t} - W_S^o n^o \, e^{-(\lambda + k)t} - \frac{N^* v}{\lambda} \qquad (2.5.12)$$

The transport equation (2.5.2) is solved separately for the two time domains corresponding to (1) P > 0, and (2) P = 0. The precipitate begins to form at t=0, and finite precipitate exists until t=t*. The solubility-limited conditions are:

(1) $P(t) > 0$, $N(0,t) = N^*$ at $t^* > t > 0$.

Initial condition: $N_1(z,0) = 0$ (2.5.13)

Boundary condition: $N_1(0,t) = N^*$ (2.5.14)

The solution for a step release is:

$$N_1(z,t) = N^* e^{-\frac{\lambda}{v_1} z} \, h(t - z/v_1) \qquad (2.5.15)$$

(2) $P(t) = 0$, $N\,(0,t) \leq N^*$, at $t > t^*$.

Here one of two conditions can occur: (a) $T > t^*$, or (b) $T < t^*$. Each has different solutions, as shown below.

(2.1) When $T > t^*$

Let $t = t' + t^*$, $z = v_1 z'$ (2.5.16)

Eq. (2.5.1) becomes:

$$\frac{\partial N_1}{\partial t'} + \frac{\partial N_1}{\partial z'} + \lambda N = 0 \tag{2.5.17}$$

Initial condition:

$$N(z',t'=0) = N(z',t=t^*) = N^* e^{-\lambda z'} \, h(t^*-z'), \; z'>0 \tag{2.5.18}$$

Boundary condition

$$N(z'=0,t') = N^0 e^{-\lambda(t'+t^*)} \, [1-h(t'-(T-t^*))], \; t'>0 \tag{2.5.19}$$

where $N^0 = n^0 W_s^0 / vT$

Due to the linear nature of the initial and the boundary conditions Eq. (2.5.17) can be solved by separating the side conditions (2.5.18) and (2.5.19) into two sets of side conditions as follows:

$$\text{Let } N = N_a + N_b \tag{2.5.20}$$

$$\frac{\partial N_a}{\partial t'} + \frac{\partial N_a}{\partial z'} + \lambda \, N_a = 0 \tag{2.5.21}$$

Solving Eq. (2.5.21) with the initial and boundary conditions shown below:

$$\begin{aligned} N_a(z',t'=0) &= N^* e^{-\lambda z'} \, h(t^*-z') \, , \; z'>0 \\ N_a(z'=0,t') &= 0 \quad , \quad t' > 0 \end{aligned} \tag{2.5.22}$$

We obtain

$$N_a(z,t) = N^* e^{-\lambda z/v_1}[h(t-z/v_1) - h(t-t^*-z/v_1)] \tag{2.5.23}$$

$N_b(z,t)$ is also obtained in a similar way:

$$\frac{\partial N_b}{\partial t'} + \frac{\partial N_b}{\partial z'} + \lambda N_b = 0 \tag{2.5.24}$$

with the initial and the boundary conditions:

$$\begin{aligned} &N_b(z',t'=0) = 0 &&, z' > 0 \\ &N_b(z'=0,t') = N^0 e^{-\lambda(t'+t^*)}[1-h(t'-(T-t^*))] &&, t' > 0 \end{aligned} \tag{2.5.25}$$

We obtain:

$$N_b(z,t) = N^0 e^{-\lambda t} [h(t-t^*-z/v_1) - h(t-T-z/v_1)] \tag{2.5.26}$$

(2.2) When $T < t^*$

We will solve Eq. (2.5.2) with the initial and the boundary conditions shown below:

$$\begin{aligned} &N(z,t'=0) = N^* e^{-\lambda z/v_1} h(t^*-z/v_1) &&, z' > 0 \\ &N(z=0,t') = 0, \text{ since } t^* > T &&, t' > 0 \end{aligned} \tag{2.5.27}$$

We obtain

$$N(z,t) = N^* e^{-\lambda z/v_1} [h(t-z/v_1) - h(t-t^*-z/v_1)] \tag{2.5.28}$$

So the complete solutions for the entire time domain for the band release are:

(2.1) $T > t^*$, from Eq. (2.5.15), 2.5.23) and (2.5.26):

$$N(z,t) = N^* e^{-\lambda z/v_1} [h(t-z/v_1)-h(t-t^*-z/v_1)] + \frac{n^0 W_S^0}{vT} e^{-\lambda t} [h(t-t^*-z/v_1)-h(t-T-z/v_1)] \tag{2.5.29}$$

(2.2) $T < t^*$, from Eq. (2.5.15) and (2.5.28):

$$N(z,t) = N^* e^{-\lambda z/v_1} [h(t-z/v_1)-h(t-t^*-z/v_1)] \qquad (2.5.30)$$

Furthermore, solutions to the transport equation for the step release and for the exponential release are derived in a similar way:

For the step release, with $\dot{W}_S = W_S^o/T$:

$$N(z,t) = N^* e^{-\lambda z/v_1} [h(t-z/v_1)-h(t-t^*-z/v_1)] + \frac{n^o W_S^o}{vT} e^{-\lambda t} h(t-t^*-z/v_1) \qquad (2.5.31)$$

For the exponential release:

$$N(z,t) = N^* e^{-\lambda z/v_1} [h(t-z/v_1- h(t-t^*-z/v)] + \frac{kn^o W_S^o}{v} e^{-(\lambda+k)t} h(t-t^*-z/v_1) \qquad (2.5.32)$$

Figure 2.5.1 shows the space-time-dependent concentration of a radionuclide with a solubility limited concentration, for no precursors, no axial dispersion, and for a band release. Here it is assumed that the precipitate dissolves before the waste is completely leached, i.e., $t^* < T$. Time-dependent concentrations in the water adjacent to the source are shown by the solid line on the N-t plane. There, when $0 \leq t \leq t^*$, the concentration is at a constant value equal to the solubility limit N^*. At $t > t^*$ the concentration adjacent to the source coincides with the broken line which shows the concentration with no solubility limit.

At $t > t^*$ there are two characteristic regions in the space-dependent concentration profile at a given time. The region from $v_1(t-t^*)$ to $v_1 t$ is the profile decaying exponentially with distance, which was established when saturation ($N=N^*$) occurred adjacent to the source. The region from $v_1(t-T)$ to $v_1(t-t^*)$ is typical of the concentration profile with a source decaying exponentially with time and with no solubility limit. The discontinuity in N at $z = v_1(t-t^*)$, with $t > t^*$, occurs because at the time t^*, when all

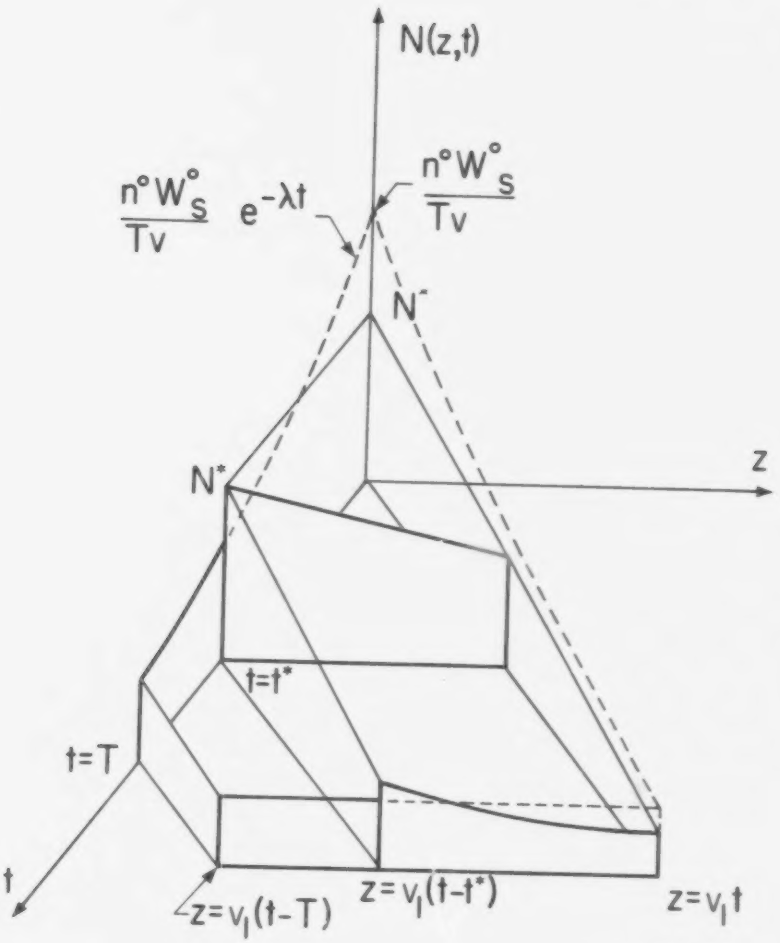
N(z,t)
$\frac{n^\circ W_s^\circ}{Tv}$
$e^{-\lambda t}$
$\frac{n^\circ W_s^\circ}{Tv}$
N'
z
N*
t=t*
t=T
t
$z=v_l(t-T)$
$z=v_l(t-t^*)$
$z=v_l t$

XBL 812-257

Figure 2.5.1 Space-time-dependent concentration of a radionuclide with a limited solubility. The waste remains after the precipitate dissolves ($T > t^*$).

[redacted]

precipitate has dissolved, the rate of release from the dissolving waste is too small to establish a concentration as high as the solubility limit. The broken line in the cross-hatched region is the concentration profile that would result if there were no solubility limit throughout.

Figure 2.5.2 shows similar space-time-dependent concentrations, with the assumption that precipitate remains after all the waste has been dissolved, i.e., $t^* > T$. Broken lines show concentration profiles in the absence of any solubility limit. Here, the leach time T does not affect the concentration profile. The concentration adjacent to the waste is at the solubility limit until all precipitate disappears. Consequently, the concentration in the chromotographic band decreases exponentially with distance at a given time. The final width of the band is given by the product $v_1 t^*$, where t^* is the time for all precipitate to dissolve.

In either case, the maximum concentration of the radionuclide experienced at position z is:

$$N(z)_{\max} = N^* e^{\frac{-\lambda z K}{v}} \qquad (2.5.33)$$

In Section 2.5.3 these equations will be used to estimate the solubility limited concentration profiles resulting from the assumed dissolution of discrete waste canisters. Applying these equations derived for an infinite plane source to the dissolution in the neighborhood of a waste canister will considerably overestimate the far-field concentrations, because of transverse dispersion due to discrete sources (see Sects. 5.1.3). However, the ratio of the far-field concentration for one-dimensional transport in the absence of solubility limits to the far-field concentration for a similar one-dimensional transport with a solubility limit is a meaningful estimate of the correction that would be expected when transverse dispersion is taken into account. The actual concentration ratio for dissolution and three-dimensional transport from a discrete waste source would likely be greater than that estimated here because of the boundary-layer effects near the dissolving waste, as discussed in Section 2.5.

From the equation for one-dimensional transport of a radionuclide without dispersion (Sect. 2.1 or (H1)) and from Eq. (2.5.33), we find the ratio of maximum concentrations experienced at any position z to be:

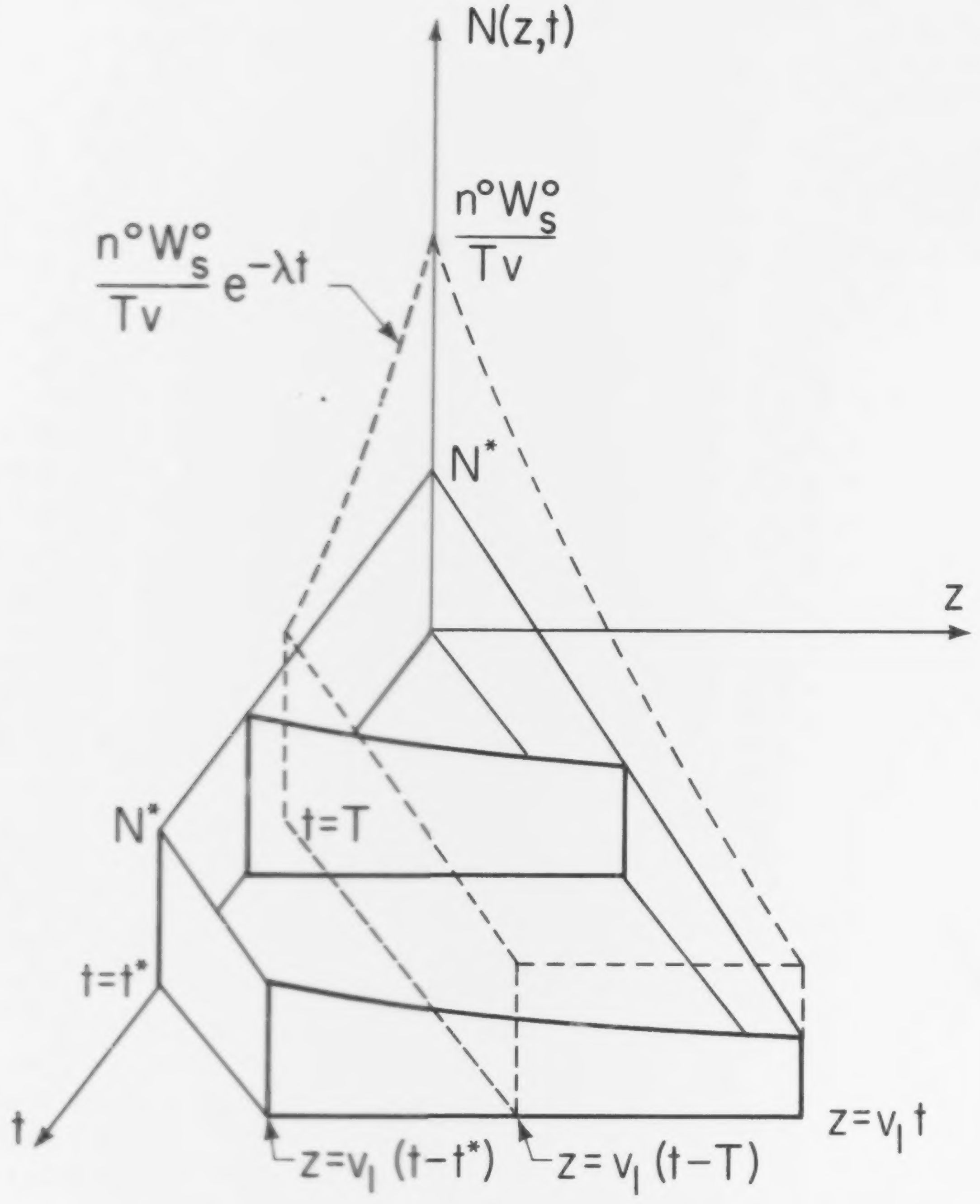
N(z,t)
$\frac{n^\circ W_s^\circ}{Tv}$
$\frac{n^\circ W_s^\circ}{Tv} e^{-\lambda t}$
N*
z
N*
t=T
t=t*
t
z=v$_l$ t
z=v$_l$ (t−t*)
z= v$_l$ (t−T)

XBL 812-258

Figure 2.5.2 Space-time-dependent concentration of a radionuclide with a limited solubility. Precipitate remains after the waste dissolves ($t^* > T$).

$$\frac{N_{s,max}(z)}{N_{l,max}(z)} = \frac{W_S^o n^o}{TvN^*} \tag{2.5.34}$$

where $N_{s,max}$ is the maximum concentration for no solubility limit, $N_{l,max}$ is the maximum concentration with a solubility limit, and W_S^o is the total amount of dissolving waste per unit area of equivalent plane source in the water phase.

2.5.3 Solubility-limited transport of ^{239}Pu

The band-release equations (2.4.24) and 2.4.25) are applied here to estimate the effect of solubility limits on the transport of ^{239}Pu. It is expected that dissolved plutonium will be in the Pu(IV) oxidation state. In the absence of complexing agents Pu(IV) in water solution tends to form $Pu(OH)_4$ or a hydrated polymer (B2). The solubilities of these species in water are given by the data of Rai and Serne (R1). As shown by Benedict, et al (B2), these data lead to a solubility of Pu(IV) in a neutral aqueous solution at room temperature of approximately:

$$N^* = 2.39 \times 10^{-5} \text{ kg Pu/m}^3$$

(a) ^{239}Pu in unreprocessed spent fuel

The waste is assumed to be unreprocessed fuel discharged from a pressurized water reactor. Each fuel assembly is packaged separately in a cylindrical canister. Assuming an irradiation exposure of 33,000 MW-day per metric ton of uranium in the initial fuel, and an initial fuel enrichment of 3.3 isotopic percent ^{235}U, the amount of ^{239}Pu per canister is estimated to be 2.9 kg. The plutonium in the discharge fuel is only 58 percent ^{239}Pu (P1), and the presence of other plutonium isotopes will be neglected. Likewise, we neglect the fact that the amount of ^{239}Pu increases with time, for a period of about 20,000 years after the waste is buried, due to the decay of the precursors ^{243}Am and ^{243}Cm (P1).

The waste canister is assumed to be a cylinder of the following dimensions (S1):

height = 4.6 m

diameter = 0.30 m

The cylinder is assumed to be oriented with its axis normal to the direction of water flow, with a cross-sectional area normal to water flow of 1.4 m^2. Assuming a water pore velocity of 10 m/yr and a porosity of 1 percent for the surrounding rock, the volumetric flow rate of water associated with the projected cross-sectional area of this canister is 0.14 m^3/yr. For the purpose of the present estimate, it will be assumed that this is the flow rate of water into which radionuclides from the dissolving fuel element are released. As has been explained in the Introduction (Sect. 2.5.1), this assumption of a water flow rate for dissolution and the assumption that the dissolved radionuclides are well mixed in this water at the position of dissolution are the major and most uncertain assumptions of the entire calculation.

Assuming a band-release dissolution time T of 3×10^4 yr, we then have the effective plane-source release rate of ^{239}Pu from the waste, in mass per unit time per unit cross-sectional area of water flow:

$$\phi''(t) = 6.9 \times 10^{-3}\, e^{-\lambda t}\ \text{kg/m}^2\ \text{yr}$$

where $\lambda = 2.84 \times 10^{-5}$/yr

At the beginning of dissolution (t=0), the concentration $N_s(0,0)$ in the water adjacent to the waste, in the absence of a solubility limit, would be $N_s(0,0) = 6.0 \times 10^{-4}$ kg/m^3. Since this is a hundred-fold greater than the solubility limit N^*, a plutonium precipitate will form. From Eq. (2.5.8), the plutonium precipitate is expected to exist for $t^* = 1.13 \times 10^5$ yr.

We now wish to calculate the concentration $N_1(z,t)$ of ^{239}Pu at position z and time t. From (B3), we assume a sorption retardation coefficient for plutonium of $K=10^4$. The results are shown in Figure 2.5.3, where the distance from the source is expressed in terms of the water-transport time $=z/v$. On the basis of these estimates for unreprocessed spent fuel, neglecting the solubility limit of plutonium may overestimate the far-field concentration of plutonium in groundwater by a factor of about 30. A larger correction could occur if the analysis were to include the boundary-layer effects discussed in Section 2.4.1.

BEST DOCUMENT AVAILABLE

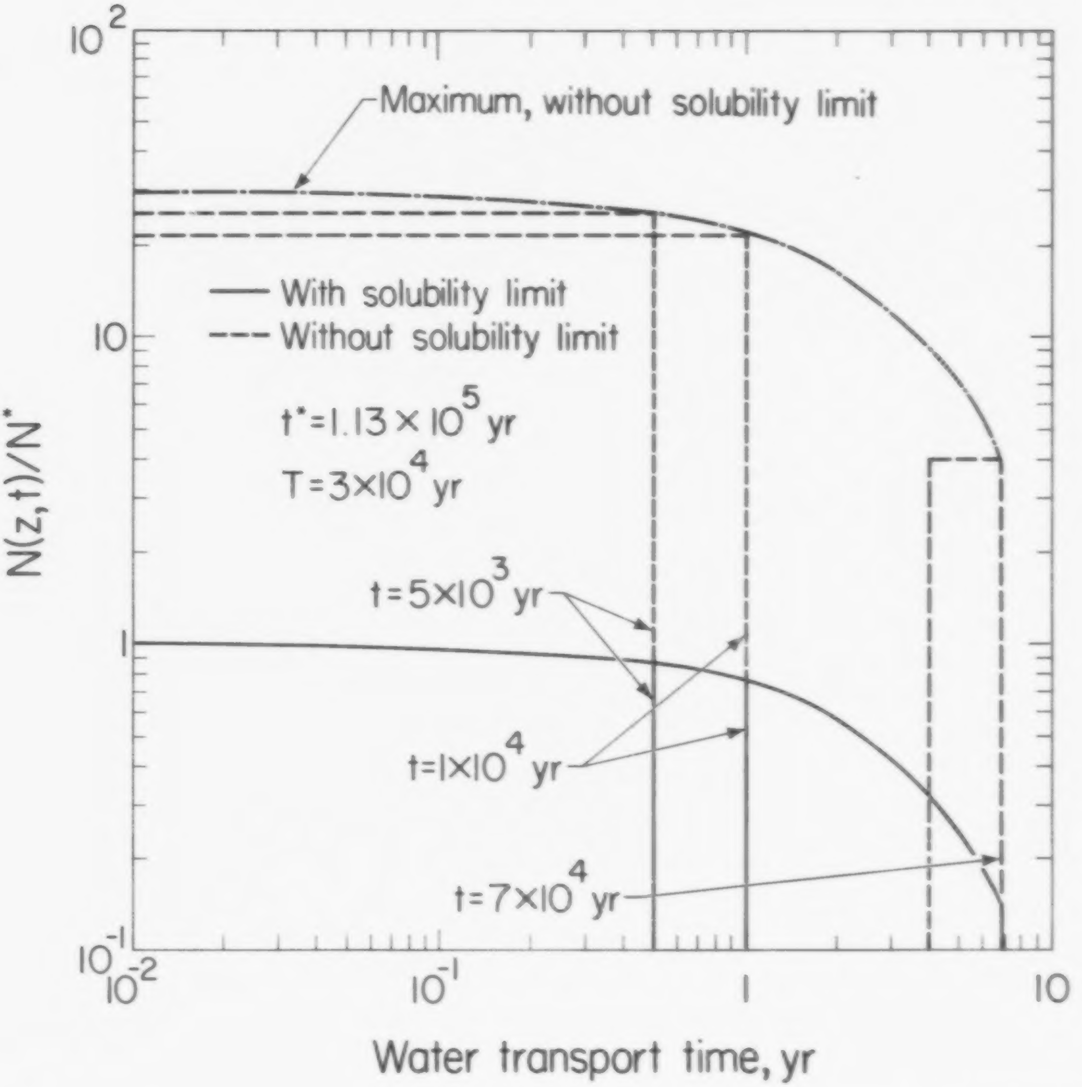

XBL 812-259

Figure 2.5.3 Concentration profiles of ^{239}Pu nuclide with and without a solubility limit, for unreprocessed spent fuel. (Water velocity = 10 m/yr; porosity = 0.1, leach time = 3 x 10^4 yr, ^{239}Pu solubility = 2.39 x 10^{-5} kg/m^3, K_{Pu} = 1 x 10^4.)

A similar calculation is now made for the release of plutonium by dissolution of the glass matrix of reprocessed high-level waste. The waste canister is assumed to be a cylinder of the following dimensions:

height = 3.0 m
diameter = 0.30 m

The matrix of borosilicate glass is assumed to contain 25 weight percent of calcined fission products and actinides, with an inventory of 0.084 kg of ^{239}Pu. A leach time of 3 x 10^4 yr is assumed, the same as in the case of unreprocessed spent fuel. Even though there is a lower inventory of plutonium in the reprocessed waste, the assumed dissolution rate of the waste matrix is such that the plutonium will reach its solubility limit in the adjacent groundwater.

From Eq. (2.5.8), with $P(t^*) = 0$, it is estimated that a plutonium precipitate will exist for 1.55 x 10^4 yr. Since this is less than the assumed leach time, the concentration profiles of plutonium in the surrounding medium will be similar to the profiles in Figure 2.5.1. The calculated concentration profiles of plutonium, are plotted in Figure 2.5.4 versus the water transport time at various assumed times after the beginning of dissolution. Here the solubility limited transport of plutonium results in peak concentrations at any distance which are a factor of 1.3 below the local maximum concentration that would be predicted without consideration of a solubility limit.

As has been pointed out earlier, a larger correction occurs if the analysis were to include the boundary-layer effects discussed in Section 2.4.1.

2.6 Transport of radionuclides with equilibrium between different chemical species in the liquid

2.6.1 Introduction

Many of the radioactive fission products and actinides, when dissolved in groundwater, can exist in different chemical forms which have different sorption equilibrium constants. For example, depending upon the acidity and oxidation potential of the groundwater, different oxidation states of neptunium may exist. These would result in different ionic species, such as Np^{4+} for Np(IV) and NpO_2^+ for the more common Np(V). These two species would be expected to have quite different sorption equilibrium constants (B2). There

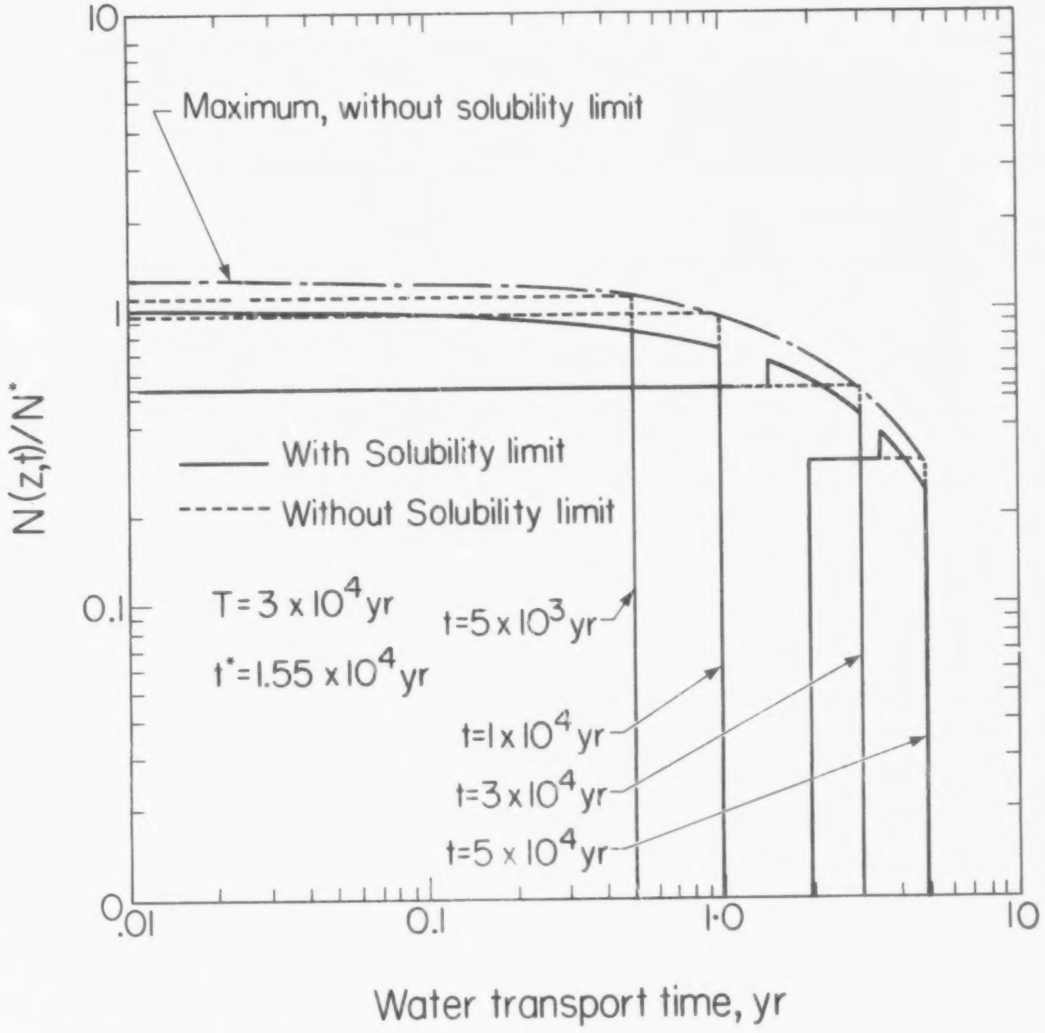

XBL 812-260

Figure 2.5.4 Concentration profiles of ^{239}Pu nuclide with and without solubility limit for HLN. (Water velocity = 10 m/yr, porosity = 0.01, leach time = 3 x 10^4 yr, ^{239}Pu solubility = 2.39 x 10^{-5} kg/m^3 of H_2O, K_{Pu} = 1 x 10^4.)

can also exist different actinide carbonate complexes in water at intermediate pH, such as $Pu(CO_3)_n^{4-2n}$, and the carbonate complexing can be expected to affect the sorption equilibrium. Therefore, for a given dissolved radionuclide, we must consider the possibility of the coexistence of chemical states of quite different characteristic migration velocities, and we must consider the effect of a continuous equilibrium between these different chemical states.

The effect of assumed noninteraction between species of different sorption coefficients on the transport of ^{237}Np has been demonstrated by Hill (H5). In the absence of a continuous equilibrium between these species, preferential sorption can perform a chromatographic separation of the different chemical states. However, the net transport of the radioelement will be quite different if there is a continued re-equilibrium between strongly sorptive and weakly sorptive species, as is considered herein.

The analysis of transport with continuous equilibrium of a radioelement between different chemical states in a given phase is the subject of the present chapter. Here we show that equations for the transport of a nuclide $\underline{i}$ in a radioactive decay chain, with the radionuclide continuously equilibrated between $\underline{n}$ chemical states, each state with a different sorption retardation coefficient, can be transformed into the transport equations for an equivalent single chemical species. Thus, our existing analysis for the transport of a nuclide in any –member decay chain, each nuclide existing in a single chemical species in the aqueous phase, can now be applied to the solution of this multi-species problem.

2.6.2. Formulation

Consider the one-dimensional transport of a radioelement through a porous sorbing medium. There can exist $\underline{n}$ different chemical states of that element in the liquid phase, and there are $\underline{n}$ corresponding states sorbed on the solid. Here we will assume that there is only one isotope of the chemical element being considered, so that we can speak meaningfully of an equilibrium between the $\underline{n}$ chemical states of the radionuclide. Let c_i^m and s_i^m be the concentrations of the m^th^ chemical species of the i^th^ nuclide in the water and in the solid, respectively. The equation for the one-dimensional transport of species $\underline{m}$ of the $\underline{i}$ nuclide is:

$$\frac{\partial}{\partial t}(\epsilon c_i^m) + v\frac{\partial}{\partial z}(\epsilon c_i^m) - D\frac{\partial^2}{\partial z^2}(\epsilon c_i^m) - \dot{\Delta}_c(\epsilon c_i^m) - \dot{\Delta}_n(\epsilon c_i^m) + j_i^m = \epsilon\phi_i^m \qquad (2.6.1)$$

$$\frac{\partial}{\partial t}[(1-\epsilon)s_i^m] - \dot{\Delta}_c[(1-\epsilon)s_i^m] - \dot{\Delta}_n[(1-\epsilon)s_i^m] - j_i^m = 0 \qquad (2.6.2)$$

$$i = 1.2,\ldots., \qquad m = 1,2,\ldots \quad n$$

where v is the velocity of water, D is the dispersion coefficient, ϵ is the porosity of the sorbing medium, z is the distance from the waste source, and t is the time measured from initial leach time. The terms $\dot{\Delta}_c(\epsilon c_i^m)$ and $\dot{\Delta}_c[(1-\epsilon)s_i^m]$ denote the volumetric rate of production of chemical species m by chemical reaction, $\dot{\Delta}_n(\epsilon c_i)$ and $\dot{\Delta}_n[(1-\epsilon)s_i^m]$ denote the volumetric rate of generation of the same species by radioactive decay in water and in solid phases, respectively. j_i^m denotes the rate of sorption this chemical species from the water to the solid phases. ϕ_i^m is the source term of mth chemical species of nuclide i.

Consider the following system of chemical reactions:

$$c_1^1 \underset{k_{fi}^{21}}{\overset{k_{fi}^{12}}{\rightleftharpoons}} c_i^2 \; . \; . \; . \; c_i^m \underset{k_{fi}^{m+1,m}}{\overset{k_{fi}^{m,m+1}}{\rightleftharpoons}} c_1^{m+1} \; . \; . \; . \; c_i^n \qquad (2.6.3)$$

$$s_i^1 \underset{k_{si}^{21}}{\overset{k_{si}^{12}}{\rightleftharpoons}} s_i^2 \; . \; . \; . \; s_i^m \underset{k_{si}^{m+1,m}}{\overset{k_{si}^{m,m+1}}{\rightleftharpoons}} s_i^{m+1} \; . \; . \; . \; s_i^n \qquad (2.6.4)$$

Eqautions (2.6.3) and (2.6.4) assume that in a given phase, liquid or solid, there is the same number of atoms of i per molecule in each chemical species containing nuclide i. The net rate of production of chemical species m by chemical reaction can then be expressed as:

$$\dot{\Delta}_c(c_i^m) = -k_{fi}^{m,m-1}\,c_i^m - k_{fi}^{m,m+1}\,c_i^m + k_{fi}^{m-1,m}\,c_i^{m-1} + k_{fi}^{m+1,m}\,c_i^{m+1} \qquad (2.6.5)$$

$$\dot{\Delta}_c(s_i^m) = -k_{si}^{m,m-1}\, s_i^m - k_{si}^{m,m+1} s_i^m + k_{si}^{m-1,m}\, s_i^{m-1} + k_{si}^{m+1,m}\, s_i^{m+1} \qquad (2.6.6)$$

where $k_{fi}^{m,m+1}$ and $k_{si}^{m,m+1}$ are the first-order rate constants of chemical reaction of m^{th} chemical species to the $(m+1)^{th}$ species in water and solid phases.

The rate of transport of chemical species m from water to solid phases can be written as

$$j_i^m = k_i^m\, a\, (c_i^m - \frac{1}{K_{Di}^m}\, s_i^m) \qquad (2.6.7)$$

where k_i^m is the mass-transfer coefficient at the interface between water and solid phases, a is the interfacial area per unit volume of the geologic medium, and K_{Di}^m is the sorption distribution coefficient of the m^{th} chemical species.

When the physiochemical equilibrium is locally established in the entire system, the expressions for the chemical reaction and sorption processes can be simplified as:

$$\frac{c_i^{m+1}}{c_i^m} = K_{ei}^m \text{ , } i = 1,2, \ldots , m = 1,2, \ldots n \qquad (2.6.8)$$

$$\frac{s_i^m}{c_i^m} = K_{Di}^m \text{ , } i = 1,2, \ldots , m = 1,2, \ldots n \qquad (2.6.9)$$

where K_{ei}^m is the equilibrium constant for the chemical reaction between the m^{th} and $(m+1)^{th}$ chemical species. Then, we find that the rate terms for chemical reaction and interfacial transport in Eqs. (2.6.1) and and (2.6.2) cancel in favor of the equilibrium conditions.

The concentration of any m^{th} chemical species can be expressed by the concentration of a given reference chemical species with the aid of the equilibrium relation given by Eq. (2.6.8). If we arbitrarily select the first species for the reference species, the concentration c_i^m can be expressed in terms of c_i^1 as

$$c_i^m = \prod_{j=1}^{m-1} (K_{ei}^j)\, c_i^1 \tag{2.6.10}$$

With the assumptions that any chemical species consists of only one nuclide, we can replace the concentrations c_i^m and s_i^m by the concentrations N_i^m and M_i^m of nuclide i in the m^{th} chemical state. The chemical and nuclear reactions occur independently from each other. A chemical reaction within aqueous phase acts on each element only to change the chemical form but does not change the total amount of contained nuclide. Suppose that the l^{th} chemical state of nuclide i-1 decays to the m^{th} chemical state of nuclide i. Then the nuclear reaction terms can be expressed simply as:

$$\dot{\Delta}_n(c_i^m) = \dot{\Delta}_n(N_i^m) = -\lambda_i N_i^m + \lambda_{i-1} N_{i-1}^l \tag{2.6.11}$$

$$\dot{\Delta}_n(s_i^m) = \dot{\Delta}_n(M_i^m) = \lambda_i \, M_i^m + \lambda_{i-1} M_{i-1}^l \tag{2.6.12}$$

Substituting Eqs. (2.6.11) and (2.6.12) into Eqs. (2.6.1) and (2.6.2) and replacing c_i^m and s_i^m by N_i^m and M_i^m, we have

$$\frac{\partial}{\partial t}(\epsilon N_i^m) + v \frac{\partial}{\partial z}(\epsilon N_i^m) - D \frac{\partial^2}{\partial z^2}(\epsilon N_i^m) + \epsilon \lambda_i N_i^m = \epsilon \lambda_{i-1} N_{i-1}^l + \epsilon \phi_i^m \tag{2.6.13}$$

$$\frac{\partial}{\partial t}[(1-\epsilon) M_i^m] + (1-\epsilon)\lambda_i M_i^m = (1-\epsilon)\lambda_{i-1} M_{i-1}^l \tag{2.6.14}$$

Summing up Eqs. (2.6.13) and (2.6.14) and eliminating M_i^m with the aid of Eq. (2.6.9), we have the transport equation which governs the aqueous concentration of the m^{th} chemical species of nuclide i:

$$\frac{\partial}{\partial t}(K_i^m N_i^m) + v \frac{\partial N_i^m}{\partial z} - D \frac{\partial^2 N_i^m}{\partial z^2} + \lambda_i K_i^m N_i^m = \lambda_{i-1} K_{i-1}^l N_{i-1}^l + \phi_i^m \tag{2.6.15}$$

where K_i^m is the sorption retardation coefficient of the m^{th} chemical species of the i^{th} nuclide

$$K_i^m = 1 + \frac{(1-\epsilon)K_{Di}^m}{\epsilon} \tag{2.6.16}$$

Substituting Eq. (2.6.10) into Eq. (2.6.15) and summing up the resultant equations with respect to each of n species, we have the single transport equation

$$K_i \frac{\partial N_i^1}{\partial t} + v \frac{\partial N_i^1}{\partial z} - D\frac{\partial^2 N_i^1}{\partial z^2} + \lambda_i K_i N_i^1 = \frac{K_{e,i-1}^{E,1}}{K_{e,i}^{E,1}} \lambda_{i-1} K_{i-1} N_{i-1}^1 + \frac{\phi_i'''}{K_{e,i}^{E,1}} \tag{2.6.17}$$

where K_i is the effective retardation coefficient of nuclide i, defined by:

$$K_i = \frac{K_i^{E,1}}{K_{e,i}^{E,1}} \tag{2.6.18}$$

with

$$K_i^{E,1} = K_i^1 + \sum_{m=2}^{n} K_i^m \prod_{j=1}^{m-1} (K_{e,i}^j) \tag{2.6.19}$$

$$K_{e,i}^{E,1} = 1 + \sum_{m=2}^{n} \prod_{j=1}^{m-1} K_{e,i}^j \tag{2.6.20}$$

The ϕ_i''' is the volumetric source term for the total amount of the i^{th} nuclide:

$$\phi_i''' = \sum_{m=1}^{n} \phi_i^m \tag{2.6.21}$$

When the source term is given by a step release from an infinite plane source at z=0, the ϕ_i is given by Eq. (2.1.9), namely:

$$\phi_i(z,t) = \frac{M_T^0}{T} B_i(t)\ \delta(z)\ h(t) \tag{2.6.22}$$

where M_T^0 is the initial amount of total waste within the water phase, T is the leach time, and $B_i(t)$ is the Bateman equation given by Eq. (2.1.12).

The initial and infinite-medium boundary conditions are

$$N_i^m(z,0) = 0 \tag{2.6.23}$$

$$N_i^m(\pm\infty,t) = 0 \tag{2.6.24}$$

$i = 1,2, \dots \quad , \quad m = 1,2, \dots m$

2.6.3 Application of the general solution

The basic transport equation has the same form as that given earlier by Eq. (2.1.1) which governs the aqueous concentration of an arbitrary nuclide chain of single chemical species, with the exception of the difference of the constant factors in decay and source terms. Therefore, we can apply the solution given in Section 2.1 of this report.

The solution for a release can be written as:

$$N_i^{m,s}(z,t) = f_i^m F_{ii}^i(z,t) + f_i^m \sum_{j=1}^{i-1} A_i^j \sum_{m=j}^{i} \frac{1}{B_m^{ij}} \sum_{\substack{r=j \\ r\neq m}}^{i} G_{rm}^{ij} F_{rm}^{j}(z,t) \tag{2.6.25}$$

where

$$f_i^m = \begin{cases} 1/K_{ei}^{Ei} & \text{if } m=1 \\ \prod_{j=1}^{m-1} (K_{ei}^j \,/\, K_{ei}^{E1}) & \text{if } m\neq j \end{cases} \tag{2.6.26}$$

The constants A_i^j, $B_m^{i,j}$, and $G_{rm}^{i,j}$ and functions F_{ii}^i and F_{rm}^j are given by Eqs. (2.1.22), (2.1.23), (2.1.24), (2.1.35), and (2.1.36).

For a band release, the solution can be obtained by the superposition theorem given by Eq. (2.1.18).

$$N_i^{m,b}(z,t) = N_i^{m,s}(z,t,B_{ij}) - h(t-T)\, N_i^{m,s}(z,t-T,B_{ij}') \tag{2.6.27}$$

B_{ij}' is given by Eq. (2.1.19).

2.6.4 Effects of two chemical species of neptunium on the migration of $^{237}Np \rightarrow {}^{233}U \rightarrow {}^{229}Th \rightarrow {}^{225}Ra$

To illustrate the solutions, let us suppose the following nuclide chain,

m	i=1	2	3	4
1	$^{237}NpO_2^+$	^{233}U	^{229}Th	^{225}Ra
2	$^{237}Np^{4+}$			

in which the mother nuclide ^{237}Np forms two chemical species in the aqueous phase, Np^{4+} and NpO_2^+. For the purpose of this illustration, assumed values for the retardation coefficients are:

$K_1^1 = 100$ $K_2^1 = 14{,}000$ $K_3^1 = 50{,}000$ $(K_4^1 = 500)$

$K_1^2 = 10{,}000$

Given the Eh and pH values of the ground water, and assuming an ideal solution, we can evaluate the concentration ratio N_1^2/N_1^1 of the two chemical species of neptunium at equilibrium from the Nernst equation. The standard half-cell potential E^0 for the oxidation of Np^{4+} to NpO_2^+ is 0.739 volts (B2). To illustrate, we assume Eh=0.2 volts and pH=2.41. The calculated equilibrium ratio for neptunium in the aqueous phase is:

$K_{el}^1=[Np^{4+}]/[NpO_2^+]/=N_1^2\ N_1^1=0.3$, for Eh=2, pH=2.41, and $K_{el}^1=0.7$ for Eh=2, pH=2.32.

In Fig. 2.6.1, the concentration profiles of $^{237}Np \rightarrow {}^{233}U \rightarrow {}^{229}Th \rightarrow {}^{225}Ra$ in the aqueous phase for species equilibrium of Np, with $K_{el}^1=0.3$ and those for neptunium existing only as NpO_2^+ $(K_{el}^1=0)$ are shown. The concentration profile of ^{225}Ra was calculated on the basis of local secular equilibrium with ^{229}Th (see Sec. 4.5 of the previous report (H1)). Although the shape of concentration band of ^{237}Np is not changed by the existence of the second equilibrium species Np^{4+}, the leading edge of the equilibrium neptunium band occurs at much a smaller distance from the waste than the band for the single species of neptunium, NpO_2^+. Although the concentration profiles of ^{233}U and ^{225}Ra near the waste are not greatly changed, the plateaus in their concentrations are shrunk and the concentrations in these plateaus are decreased.

BEST DOCUMENT AVAILABLE

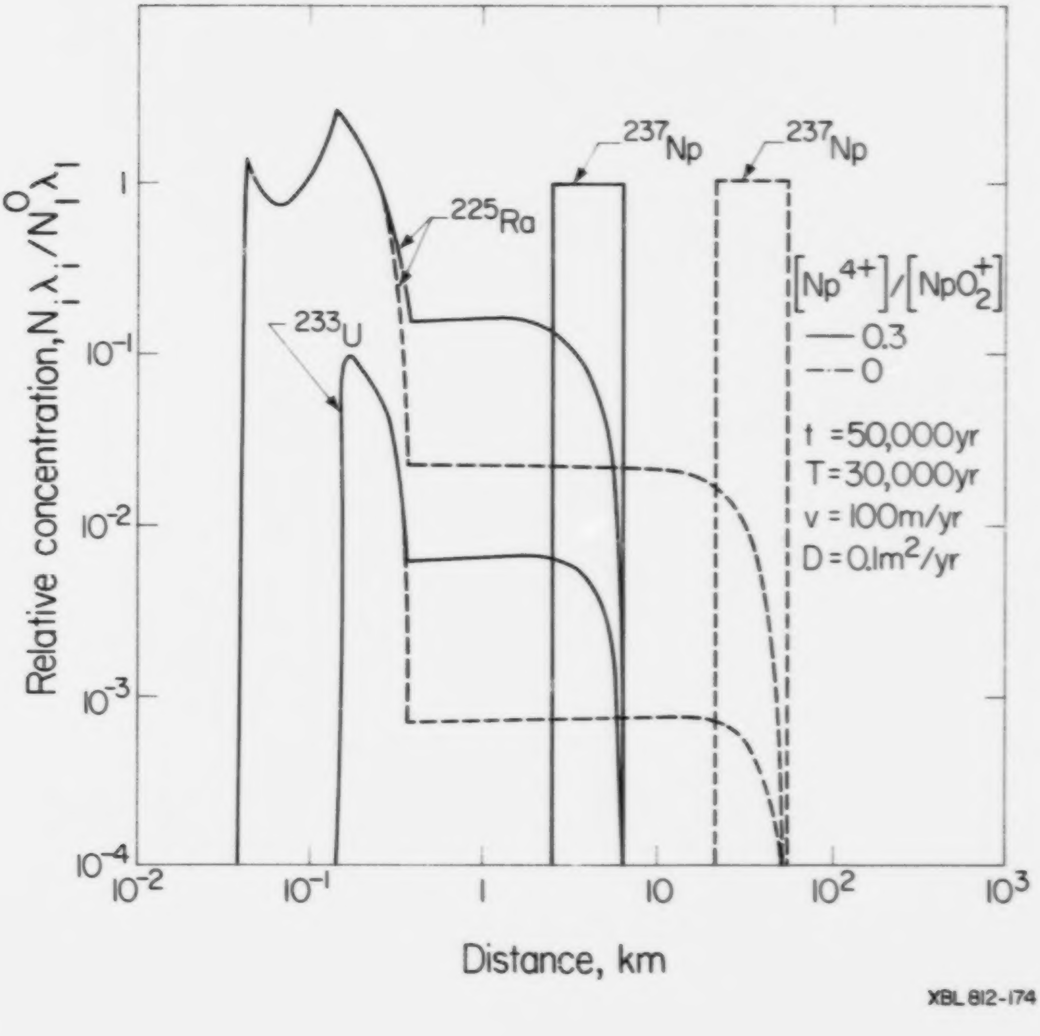

Figure 2.6.1 Effects of two chemical compounds of mother nuclide on aqueous concentrations of three members nuclide chain; concentration profiles of $^{237}Np \rightarrow {}^{233}U \rightarrow {}^{229}Th({}^{225}Ra)$ at t = 50,000 yr. (T = 30,000 yr, v = 100 m/yr, D = 0.1 m^2/yr, $K_{NpO_2^+} = 100$, $K_{Np^{4+}} = 10,000$, $K_U = 14,000$, $K_{Th} = 50,000$, $K_{Ra} = 500$, $K_{el}^1 = 0.3$).

Figure 2.6.2 shows a similar comparison of the concentration profiles of the ^{237}Np chain but for the cases of $K_{el}^{1}=0.7$ and $K_{el}^{1}=0$. As the equilibrium concentration of the less mobile species N_p^{4+} is increased by increasing K_{el}^{1}, the migration distance of the equilibrium neptunium becomes much smaller. The effect of increasing the species equilibrium of Np^{4+} is to cause the neptunium band to move with the speed of the more sorptive less mobile species.

The concentration profiles of the daughters, ^{233}U and ^{225}Ra, are appreciably changed by the higher retardation coefficient of the mother nuclide. The broad plateaus in their concentration profiles, which appear when neptunium exists as a single relatively mobile species, are not present when equilibrium with the less mobile Np^{4+} occurs. The greater peak concentrations of ^{233}U and ^{225}Ra with less mobile neptunium have been observed in our previous report (H1).

The importance of the effects of coexistence of chemical species in various valence states on the migration behaviour has been studied by Hill (H5). She assumed that the fraction of the initial inventory of ^{237}Np in each valence state remains constant in transport through the geologic medium, i.e., no interaction between the species. The total concentration of neptunium was calculated as the sum of the concentration of each separately migrating chemical species. Species equilibrium was not considered in Hill's calculations. Figure 2.6.3 shows a comparison between the concentration profiles of ^{237}Np (50% strongly sorbed Np^{4+} and 50% weakly sorbed NpO_2^+) $\rightarrow {}^{233}U \rightarrow {}^{229}Th$ ($\rightarrow {}^{225}Ra$) calculated from the equilibrium model and those calculated from the noninteraction model of Hill. The figure shows that these two different models give concentration curves quite different from each other. The non-equilibrium model shows two chromatographic bands for neptunium, whereas the more appropriate equilibrium model shows a single band. The plateaus in concentrations of ^{233}U and ^{225}Ra which are predicted from the noninteraction model are not present in the concentration profiles predicted from the equilibrium model, developed in the present study. Although the hydrolytic oxidation

$$Np^{4+} + 2H_2O \rightleftarrows NpO_2^+ + 4H^+ + e^-$$

is not rapid in the time scale of laboratory experiments (B2), equilibrium would be expected in the near stagnant conditions of slow flow of groundwater.

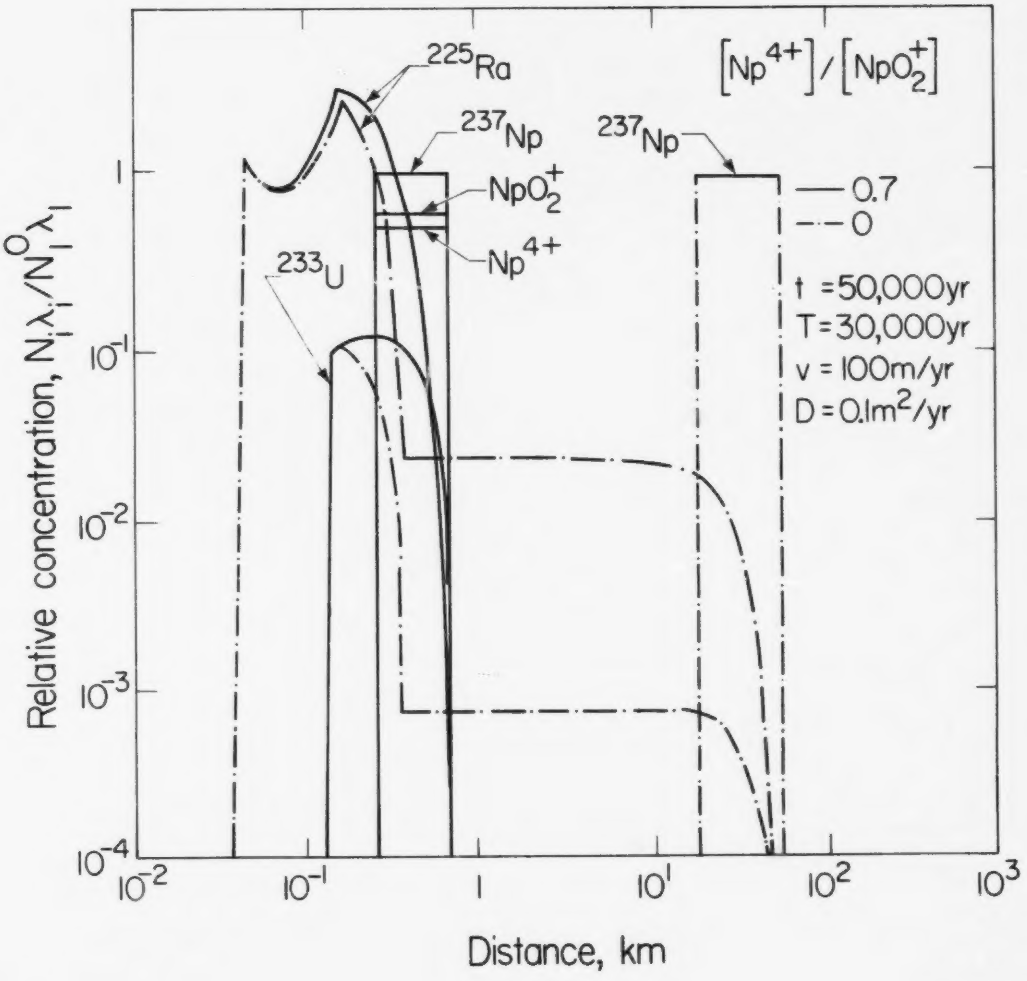

XBL 812-175Y

Figure 2.6.2 Effects of two chemical compounds of mother nuclide on aqueous concentrations of three members nuclide chain; concentration profiles of $^{237}Np \rightarrow {}^{233}U \rightarrow {}^{229}Th({}^{225}Ra)$ at $t = 50{,}000$ yr. ($T = 30{,}000$ yr, $v = 100$ m/yr, $D = 0.1$ m^2/yr, $K_{NpO_2^+} = 100$, $K_{Np^{4+}} = 10{,}000$, $K_U = 14{,}000$, $K_{Th} = 50{,}000$, $K_{Ra} = 500$, $K_{el}^1 = 0.7$).

BEST DOCUMENT AVAILABLE

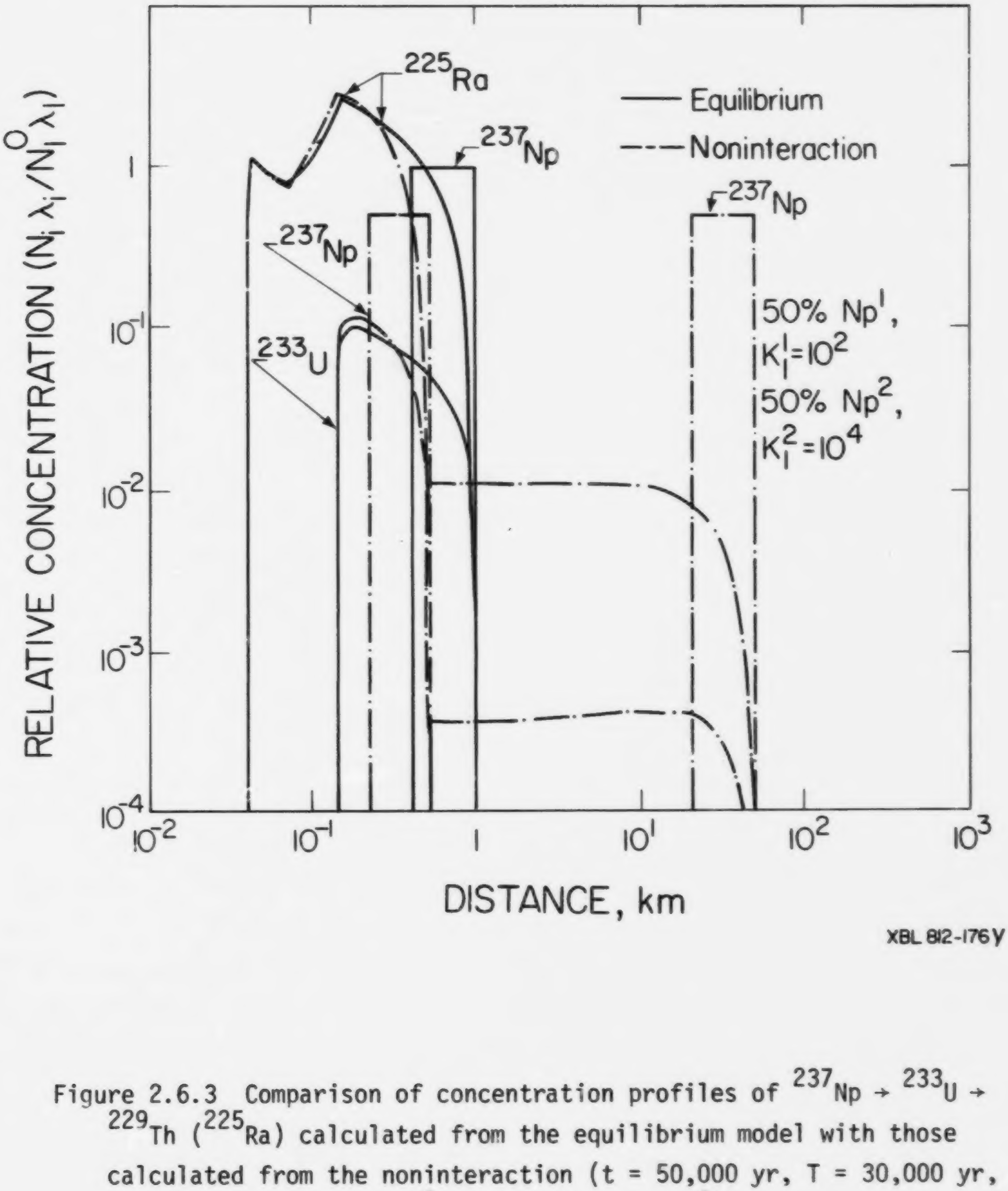

Figure 2.6.3 Comparison of concentration profiles of $^{237}Np \rightarrow ^{233}U \rightarrow ^{229}Th$ (^{225}Ra) calculated from the equilibrium model with those calculated from the noninteraction (t = 50,000 yr, T = 30,000 yr, v = 100 m/yr, D = 0.1 m^2/yr, $K_{NpO_2^+} = 100$, $K_{Np}^{4+} = 10,000$, $K_U = 14,000$, $K_{Th} = 50,000$, $K_{Ra} = 500$, $K_{el}^1 = 0.5$).

2.7 Maxima of Release Bands

2.7.1 Introduction

This research is concerned with the determination of the maxima values of nuclide concentrations which occur during the migration of nuclide chains in geologic media. One is interested in the determination of the position of the maximum concentration of a given nuclide at a fixed time as well as the time at which the maximum is observed at a fixed position in the field. The analysis should be applicable to actinide chains present in high level reprocessed waste and in unreprocessed spent fuel.

Normally, the most direct method for the determination of the maxima concentrations would be to solve the appropriate system of transport equations and then to search for the extrema of the solutions. Instead of doing this we present an approximation method which allows us to determine the extrema in concentrations without having to calculate the entire concentration history. The method concentrates entirely on the determination of the extrema: their positions in space at a fixed time and their occurrence at a fixed position.

In this study we are neglecting dispersion effects. The results obtained by using this assumption are more conservative than those which take dispersion into account. We are assuming one dimensional water transport and sorption equilibrium for the nuclides in the soil and in the water. The soil and water properties as well as the water velocity are considered constant.

The basic idea in the approximation method is that when the leach time is small compared with a radionuclide half-live, the exact solutions to a band release boundary condition can be approximated by solutions which have forms similar to those when a impulse release boundary condition is used. The extrema are then easily and directly determined from these approximate solutions and the results have a simple and compact form. The approximation method has been extensively tested for all nuclides which are present in high level unreprocessed and reprocessed wastes by comparing it with available results obtained from the exact solution. The range of values for the leach time for which the approximation is accurate has been determined.

Use of this method avoids time consuming evaluation of the complicated exact solution formulas and it provides a quick insight into the effects of the physical parameters on the extremum. As an additional result, the time interval during which a given position is contaminated (contamination time) and the spatial region that is contaminated at a given time (extend of the contaminated region) can be also readily obtained. The method will evaluate with good accuracy the extremum of the exact solutions to a decaying band release (without dispersion) and it is shown to work provided the leach time is smaller than the half-lives of the nuclides involved. Most of the waste forms considered have predicted lifetimes which satisfy such a condition.

The effects on the maxima concentrations (expressed in terms of peak water dilution rates) due to the variation of a number of parameter values were studied. The parameters were: the water travel time, the leach time, the time for begining of leaching and the sorption coefficients. Results are presented in tables and graphs.

Finally, to obtain a qualitative comparison of the potential harm to the biosphere caused by the groundwater leaching of the solid waste we evaluated water dilution rates of the leaching of an equivalent amount of natural uranium ore mill tailings generated in producing the fuel needed to generate 1 Gw(e) yr of electricity in a PWR which produced such a solid waste.

2.7.2 The governing equations and initial conditions

The system considered is a one-dimensional single region where the flowing water velocity and the soil and water properties are constant. The sorption-desorption process is in equilibrium and dispersion is negligible.

The governing equation for the concentration $N_i(z,t)$ of the i^{th} member of a radioactive chain is written as (H1, Eq. (4.102)):

$$\frac{\partial N_i}{\partial t} + v_i \frac{\partial N_i}{\partial z} + \lambda_i N_i = \frac{K_{i-1}}{K_i} \lambda_{i-1} N_{i-1} \qquad i = 1,2,3 \qquad \lambda_0 = 0, \; v_i = \frac{v}{K_i} \tag{2.7.1}$$

The initial conditions are expressed as (H1, Eq. (4.103b)):

$$N_i(z,0) = 0, \text{ for all } z>0 \quad . \tag{2.7.2}$$

2.7.3 The boundary conditions

When a decaying band release occurs at the repository, the boundary condition can be expressed by the following (H1, Eq. (3.8)):

$$N_i(0,t) = N_i^0 \, \phi_i(t) \, [h(t) - h(t-T)] \qquad (2.7.3)$$

where $\phi_i(t)$ is a prescribed positive function of the time t (generally, it is a Bateman's function (H1, Eq. (3.11)), h(t) is the step function and T is the leach time and N_i^0 the initial concentration of the i^{th} nuclide present at the beginning of leaching.

2.7.4 The general solution to a decaying band release

The general solution to the governing equation Eq. (2.7.1) subject to the initial condition Eq. (2.7.2) and the boundary condition Eq. (2.7.3) was developed in the previous report (H1, Eq. (4.127)). It is here rewritten:

$$N_i(z,t) = N_i^0 \, e^{-(\lambda_i z/v_i)} \phi\left(t - \frac{z}{v_i}\right) \left[h\left(t - \frac{z}{v_i}\right) - h\left(t - \frac{z}{v_i} - T\right)\right] + \qquad (2.7.4)$$

$$\sum_{j=1}^{i-1} A_i^{(j)} N_j^0 \sum_{m=j}^{i} \frac{e^{-(\lambda_m z/v_m)}}{B_m^{(j)}} \sum_{\substack{r=j \\ r\neq m}}^{i} D_{rm}^{(j)} [g_{rm}(t) * \phi_i(t)(h(t)-h(t-T))]$$

where

$$A_i^{(j)} = \prod_{r=j}^{i-1} \frac{\lambda_r}{v_r} \qquad (2.7.5)$$

$$B_m^{(j)} = \prod_{\substack{r=j \\ r\neq m}}^{i} \frac{v_m - v_r}{v_m v_r} \qquad (2.7.6)$$

$$D_{rm}^{(j)} = \prod_{\substack{q=j \\ q\neq m\neq r}}^{i} \left[(\Delta_{qm} - \Delta_{rm})\right]^{-1} \qquad (2.7.7)$$

$$\Delta_{qm} = \frac{\lambda_q v_m - \lambda_m v_q}{v_m - v_q} = \Delta_{mq} \qquad (2.7.8)$$

$$\Delta_{rm} = \frac{\lambda_r v_m - \lambda_m v_r}{v_m - v_r} = \Delta_{mr} \tag{2.7.8}$$

$$g_{rm}(t) = e^{-\Delta_{rm}(t-z/v_m)} h(t - \frac{z}{v_m}) \tag{2.7.9}$$

The symbol $*$ represents the convolution integral of the functions in the bracketed term, i.e.:

$$g_{rm}(t) \; * \; \phi_j(t)[h(t)-h(t-T)] = \int_0^t g_{rm}(\tau) \, \phi_j(t-\tau)[h(t-\tau-T)]d\tau \tag{2.7.9a}$$

The task of finding the extremum of the general solution Eq. (2.7.4) for an arbitrary i^{th} member is too complex to be performed analytically. This is caused by the presence of step functions which can result in a discontinuous first order derivative inside the domain where the concentration is non trivial.

The maximum could eventually be located at that point where the discontinuity occurs and the methods provided by calculus would fail detect them.

Such a situation is depicted in the following sketch:

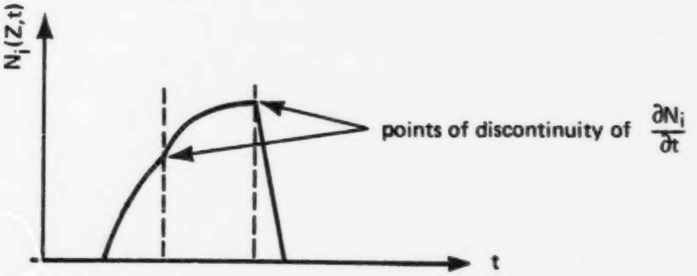
$N_i(Z,t)$
points of discontinuity of $\frac{\partial N_i}{\partial t}$
t

The general solution Eq. (2.7.4) can be seen to be a function of the leach time T as well as z and t, i.e.: $N_i(z,t,T)$.

Furthermore, one can notice that the solution Eq. (2.7.4) can be rewritten in the following form:

$$N_i(z,t,T) - N_i^0 \, e^{\frac{-\lambda_i}{v_i} z} \, \phi_i(t-\frac{z}{v_i})[h(t-\frac{z}{v_i})-h(t-\frac{z}{v_i}-T)] = G_i(z,t,T)$$

where $G_i(z,t,T)$ is readily identified from Eq. (2.7.4).

Since most difficulties in evaluating analytically the extremum resulted from the terms represented by $G_i(z,t,T)$, we will approximate these functions by simpler forms in order to enable us to obtain the solution extremum in compact and closed form.

2.7.5 Approximate solution to a decaying band release

Let us rewrite the function $G_i(z,t,T)$:

$$G_i(z,t,T) = \sum_{j=1}^{i-1} A_i^{(j)} N_j^o \sum_{m=j}^{i} \frac{e^{-(\lambda_m/v_m)z}}{B_m^{(j)}} \sum_{\substack{r=j \\ r\neq m}}^{i} D_{rm}^{(j)} \left[g_{rm}^{(t)} * \phi_j(t)(h(t)-h(t-T))\right] \tag{2.7.10}$$

For small values of the leach time T, $T \ll 1/\lambda_j$, $j = 1,2\ldots i$, an approximation to the function $G_i(z,t,T)$ is obtained by using a modified form of the law of the mean for continuous functions:

$$G_i(z,t,T) \cong G_i(z,t,T=0) + T \frac{\partial}{\partial T}[G_i(z,t,T=0)] \tag{2.7.11}$$

By setting T=0 in Eq. (2.7.10) one can readily see that $G_i(z,t,T=0)=0$ and Eq. (2.7.11) is rewritten as

$$G_i(z,t,T) \cong T \left[\frac{\partial}{\partial T} G_i(z,t,T=0)\right] \tag{2.7.12}$$

Eq. (2.7.12) is next used to simplify Eq. (2.7.10). First note that:

$$\left[\frac{\partial}{\partial T}[h(t-T)]\right]_{T=o} = -\delta(t) \tag{2.7.13}$$

where $\delta(t)$ is the Dirac's delta function.

By using Eq. (2.7.12) in Eq. (2.7.10) one has:

$$G_i(z,t,T) \cong \sum_{j=1}^{i-1} A_i^{(j)} N_j^o \sum_{m=j}^{i} \frac{e^{-(\lambda_m/v_m)z}}{B_m^{(j)}} T \sum_{\substack{r=j \\ r\neq m}}^{i} D_{rm}^{(j)}$$

$$\times \left\{\frac{\partial}{\partial T}\left[g_{rm}(t) * \phi_j(t)(h(t)-h(t-T))\right]\right\}_{T=0} \tag{2.7.14}$$

The bracketed term is expanded below:

$$\frac{\partial}{\partial T}\left[\int_0^t g_{rm}(\tau)\,\phi_j(t-\tau)[h(t-\tau)-h(t-T-\tau)]d\tau \qquad (2.7.15)$$

by using Eq. (2.7.13) there results:

$$= \int_0^t g_{rm}(\tau)\phi_j(t-\tau)\delta(t-\tau)d\tau =$$

by using the integration property of the delta function, it yields:

$$= g_{rm}(t)\phi_j(0) = g_{rm}(t)\ , \text{ since } \phi_j(0) = 1 \qquad (2.7.16)$$

with the help of Eq. (2.7.16) one can rewrite Eq. (2.7.14)

$$G_i(z,t,T) \cong \sum_{j=i}^{i-1} A_i^{(j)}\ N_j^0 \sum_{m=j}^{i} \frac{e^{-(\lambda_m/v_m)z}}{B_m^{(j)}} \sum_{\substack{r=j\\ r\neq m}}^{i} D_{rm}^{(j)}\ Tg_{rm}(t) \qquad (2.7.17)$$

The above expression for the function $G_i(z,t,T)$ has the same form as if we had solved Eq. (2.7.1) using the impulse release boundary condition instead of a decaying band release boundary condition.

The solution to Eq. (2.7.1), Eq. (2.7.2) and an impulse release boundary condition which can be mathematically represented by $\phi_i(t)=T\delta(t)$ has been obtained in the previous report H1, Eq. (5.10), (5.20), (5.21), (5.22), where they are explicitly written for i=1,2,3. Those equations can be used here to explicitly express the approximate form of the function $G_i(z,t,T)$ for i=1,2,3.

Therefore, the concentration of a ith member nuclide, Eq. (2.7.4) can be rewritten in its approximate form with the help of Eq. (2.7.17) as:

$$N_i(z,t,T) = N_i^0\, e^{\frac{-\lambda_i z}{v_i}}\ \phi_i(t - \frac{z}{v_i})\ [h(t - \frac{z}{v_i}) - h(t - \frac{z}{v_i} - T)] +$$

$$\sum_{j=i}^{i-i} A_i^{(j)}\ N_j^0 \sum_{m=j}^{i} \frac{e^{(-\lambda_m/v_m)z}}{B_m^{(j)}} \sum_{\substack{r=j\\ r\neq m}}^{i} D_{rm}^{(j)} Tg_{rm}(t) \qquad (2.7.18)$$

The above general approximate solution for the concentration of an i^{th} member is specifically rewritten for the first three members of a radionuclide chain.

With the help of Eq. (5.20) from reference H1 the solution for the 1^{st} member is:

$$N_1(z,t) = N_1^0 \exp(-\lambda_1 t)\ s[v_1 t;\ v_1(t-T)] \qquad (2.7.19)$$

by using Eq. (5.21) from reference H1, the concentration of the 2^{nd} member is:

$$N_2(z,t) \cong N_2^0 \exp(-\frac{\lambda_2}{v_2} z)\ S[v_2 t, v_2\ (t-T)]\ \phi_2(t) +$$

$$(N_1^0 T)\ B_{12} \exp(-\Delta_{21} t - \alpha_{21} z)\ S(v_1 t; v_2 t) \qquad (2.7.20)$$

Finally, with the help of Eq. (5.22) from reference H1, one writes the solution for the 3^{rd} member:

$$N_3(z,t) \cong N_3^0 \phi_3(t) \exp(-\frac{\lambda_3}{v_3} z) S[v_3 t; v_3(t-T)] +$$

$$(N_2^0 T)\ B_{23} \exp(-\Delta_{23} t - \alpha_{23} z)\ S(v_2 t; v_3 t) +$$

$$(N_1^0 T)\ A \Big\{ \exp(-\Delta_{31} t - \alpha_{31} z)\ S(v_1 t; v_3 t) + \exp\ (-\Delta_{32} t - \alpha_{32} z) S(v_3 t : v_2 t) +$$

$$+ \exp\ (-\Delta_{21} t - \alpha_{21} z)\ S(v_2 t; v_1 t) \Big\} \qquad (2.7.21)$$

The constants in above equations are defined below:

$$B_{ij} = \frac{\lambda_i v_j}{v_i v_j} \qquad (2.7.22)$$

$$\Delta_{ij} = \Delta_{ji} = \frac{\frac{\lambda_i}{v_i} - \frac{\lambda_j}{v_j}}{\frac{1}{v_i} - \frac{1}{v_j}} = \frac{\lambda_i v_j - \lambda_j v_i}{v_j - v_i} \text{ (repeated from Eq. (2.7.8))} \qquad (2.7.23)$$

$$\alpha_{ij} = \alpha_{ji} = \frac{\lambda_i - \lambda_j}{v_i - v_j} \qquad (2.7.24)$$

$$A = \lambda_1\lambda_2 v_3/[v_1(\lambda_2-\lambda_3)+ v_2(\lambda_3-\lambda_1) + v_3(\lambda_1-\lambda_2)] \qquad (2.7.25)$$

The function $S[a(t); b(t)]$ which is actually a short hand notation for a difference of step functions is defined as follows:

$$S[a(t): b(t)] = h[a(t) - z] - h[b(t)-z] \qquad (2.7.26)$$

We have therefore obtained an approximate solution which represents the decaying band release problem for a small leach time but which has a simpler form. In the next sections analytical formulas for the extremum of this solution are derived.

We have therefore obtained an approximate solution which represents the decaying band release problem for a small leach time but which has a simpler form. In the next sections analytical formulas for the extremum of this solution are derived.

2.7.6 Extremum of the solution for the 1st member:

Let us denote the time of the maximum concentration of a given i^{th} member at a fixed position z by t_i^* and the corresponding concentration by $N_i^*(z,t_i^*)$.

Conversely, the position of maximum concentration at a given fixed time t will be denoted by z_i^*. The corresponding concentration will be $N_i^*(z_i^*,t)$.

The solution for the 1st member is the simplest and reads:

$$N_1(z,t) = N_1^0 \exp(-\lambda_1 t)\ S[v_1 t;v_1(t-T)] \qquad (2.7.27)$$

One should note that for the 1st member, the approximate solution is equal to the exact solution. The problem can be divided into two parts:

2.7.6.A Determination of the time of the maximum concentration at a given fixed position

At a fixed position, the solution Eq. (2.7.19) can be visualized by the following sketch:

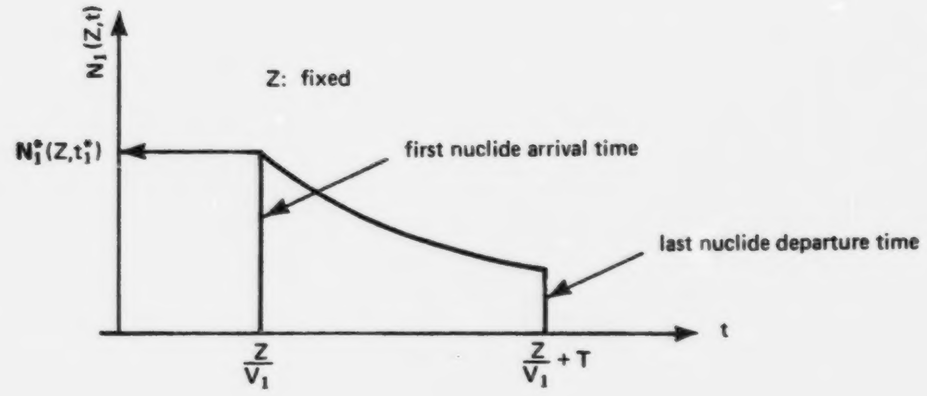

It is apparent that the maximum at a fixed position z occurs at the first nuclide arrival time:

$$t_1^* = \frac{z}{v_1} \tag{2.7.28}$$

and the corresponding concentration is:

$$N_1^*(z,t_1^*) = N_1^0 \exp(-\frac{\lambda_1}{v_1} z) \tag{2.7.29}$$

2.7.6.B Determination of the position of the maximum concentration at a given fixed time

At a fixed time the concentration is constant with respect to position and the position of maximum could be any value of z between v_1t and $v_1(t-T)$. The following sketch illustrates this case:

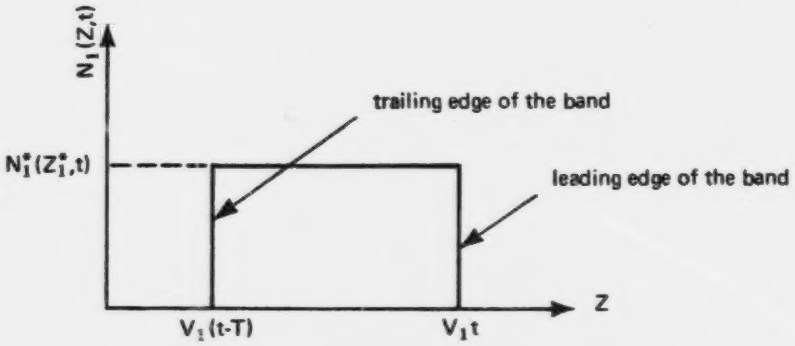

The maximum concentration is:

$$N_1^*(z_1^*,t) = N_1^0 \exp(-\lambda_1 t) \tag{2.7.30}$$

but the position of the extremum is not singular:

$$v_1(t-T) \leq z_1^* \leq v_1 t \tag{2.7.31}$$

2.7.7 Extremum of the solution for the 2^{nd} member (1^{st} daughter)

The determination of t_2^* and z_2^* can be divided into two stages:

1) The 2^{nd} member (1^{st} daughter) is not present at the repository initially ($N_2^o = 0$, $N_1^o \neq 0$)

2) The initial amount of 1^{st} daughter is significant ($N_2^o \neq 0$, $N_1^o \neq 0$)

2.7.7.A 1st daughter is not present initially at repository:

By setting $N_2^o = 0$ in Eq. (2.7.20) one has:

$$N_2(z,t) = \left[N_1^o T \frac{\lambda_1 v_2}{v_1 - v_2} S(v_1 t; v_2 t) \right] \exp\left(-\Delta_{21} t - \alpha_{21} z\right) \tag{2.7.32}$$

Note that the coefficient of the exponential term is always positive. This is because when

$$\begin{aligned} &v_1 > v_2;\ S(v_1;v_2) = h(v_1 t - z) - h(v_2 t - z) = 1 \\ &v_1 > v_2;\ S(v_1;v_2) = h(v_1 t - z) - h(v_2 t - z) = -1 \end{aligned} \tag{2.7.32a}$$

The exponential term is a monotonically decreasing or increasing function of either z or t, depending on the sign of either α_{12} or Δ_{12}, respectively.

a) Determination of the time t_2^* of the maximum concentration at a given fixed position z. ($N_2^o = 0$).

At a fixed position z, the concentration of the 1^{st} daughter is an exponential function of time. It will be a monotonically increasing or decreasing function of time depending if Δ_{12} is negative or positive, respectively.

When Δ_{12} is positive the concentration $N_2(z,t)$ will decrease monotonically as t increases. Therefore, the maximum will always occur on the "first nuclide arrival time" at a fixed position z. When $v_1 < v_2$ the first nuclide arrives at z in a time $t_2^* = \frac{z}{v_2}$ and when $v_1 > v_2$ the first nuclide arrives at $t_2^* = \frac{z}{v_1}$. Figures (2.7.1a) and (2.7.1b) represent schematically such situations.

Conversely, when Δ_{12} is negative the concentration $N_2(z,t)$ will increase monotonically as t increases. Therefore, the maximum in this case will occur on the "last nuclide departure time" from that position z. When $v_1 > v_2$ the last nuclide departs from z at a gime $t_2^* = \frac{z}{v_2}$ and when $v_1 < v_2$ the last nuclide departs at a time $t_2^* = \frac{z}{v_1}$.

Figures (2.7.1c) and (2.7.1d) represent schematically these cases. Above four possibilities are summarized in Table 2.7.1. In this case the maximum at a fixed position z occurs always at a time determined by the velocity of the nuclide which has the smaller product $\lambda_i K_i$ according to Table 2.7.1. One

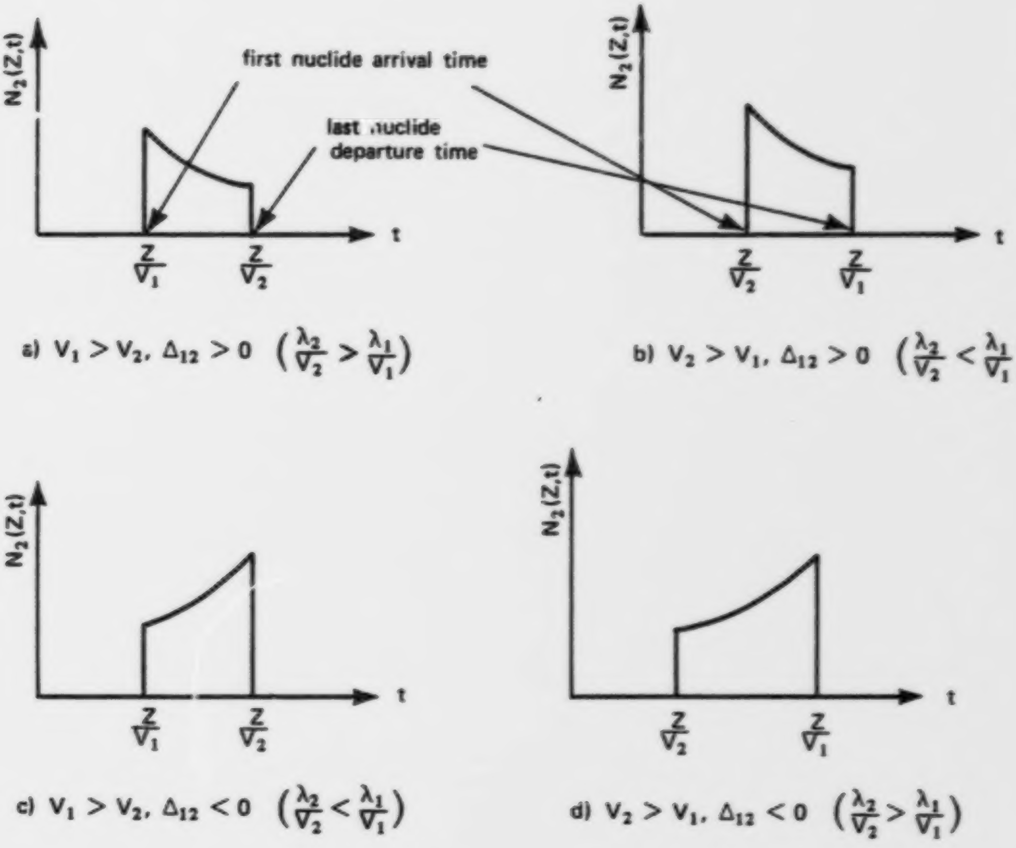

a) $V_1 > V_2$, $\Delta_{12} > 0$ $\left(\frac{\lambda_2}{V_2} > \frac{\lambda_1}{V_1}\right)$

b) $V_2 > V_1$, $\Delta_{12} > 0$ $\left(\frac{\lambda_2}{V_2} < \frac{\lambda_1}{V_1}\right)$

c) $V_1 > V_2$, $\Delta_{12} < 0$ $\left(\frac{\lambda_2}{V_2} < \frac{\lambda_1}{V_1}\right)$

d) $V_2 > V_1$, $\Delta_{12} < 0$ $\left(\frac{\lambda_2}{V_2} > \frac{\lambda_1}{V_1}\right)$

Figure 2.7.1 Different possibilities for the maximum of a 2nd member at a fixed position when $N_2^0 = 0$.

can therefore reduce Table 2.7.1 into the following more compact form (Table 2.7.2): The corresponding concentrations can be obtained from Eq. (2.7.32):

Case:	$\Delta_{12} = \frac{\lambda_1 K_1 - \lambda_2 K_2}{K_1 - K_2} > 0$	$\Delta_{12} = \frac{\lambda_1 K_1 - \lambda_2 K_2}{K_1 - K_2} < 0$
$K_2 > K_1$	$t_2^* = \frac{z}{v_1}$ $(\lambda_2 K_2 > \lambda_1 K_1)$	$t_2^* = \frac{z}{v_2}$ $(\lambda_1 K_1 > \lambda_2 K_2)$
$K_2 < K_1$	$t_2^* = \frac{z}{v_2}$ $(\lambda_1 K_1 > \lambda_2 K_2)$	$t_2^* = \frac{z}{v_1}$ $(\lambda_2 K_2 > \lambda_1 K_1)$

Table 2.7.1 Different possibilities of the maxima concentrations for 2nd members ($N_2^o = o$).

$\lambda_1 K_1 > \lambda_2 K_2$	$\lambda_1 K_1 < \lambda_2 K_2$
$t_2^* = \frac{z}{v} K_2$	$t_2^* = \frac{z}{v} K_1$

Table 2.7.2: Time of maximum concentration for the 2nd member ($N_2^o = o$).

$$N_2^*(z, t_2^*) = (N_1^o T)\ B_{12}\ \exp(-\lambda_m K_m \frac{z}{v}) \qquad (2.7.33)$$

where

$$\lambda_m K_m = \min[\lambda_1 K_1, \lambda_2 K_2]$$

b) Determination of the position of the maximum concentration at a given fixed time:

One sees from Eq. (2.7.32) with a fixed time t, that when α_{12} is positive the concentration $N_2(z,t)$ will decrease monotonically as z increases. Therefore, the maximum will always occur at the "trailing edge" of the band. When $v_1 > v_2$, the "trailing edge" is given by $z_2^* = v_2 t$ and when $v_2 > v_1$, $z_2^* = v_1 t$. These situations are represented schematically by Figures (2.7.2a) and (2.7.2b).

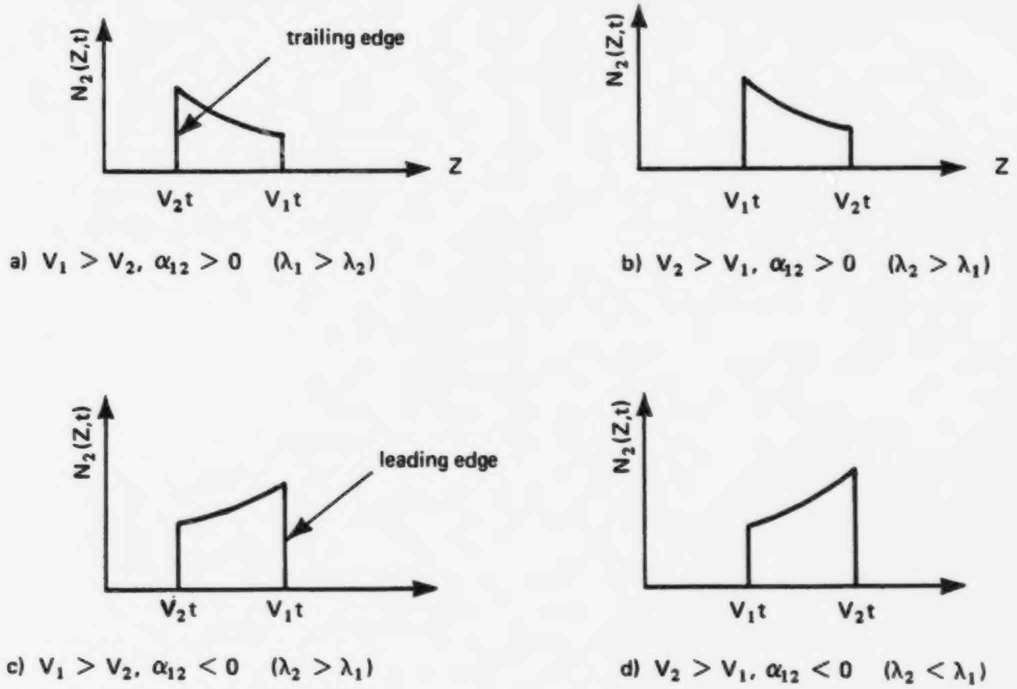

a) $V_1 > V_2$, $\alpha_{12} > 0$ $(\lambda_1 > \lambda_2)$

b) $V_2 > V_1$, $\alpha_{12} > 0$ $(\lambda_2 > \lambda_1)$

c) $V_1 > V_2$, $\alpha_{12} < 0$ $(\lambda_2 > \lambda_1)$

d) $V_2 > V_1$, $\alpha_{12} < 0$ $(\lambda_2 < \lambda_1)$

Figure 2.7.2 Different possibilities for the maximum of a 2nd member at a fixed time when $N_2^0 = 0$.

Conversely, when α_{12} is negative the concentration $N_2(z,t)$ will increase monotically as z increases. Thus, the maximum will always occur on the leading edge of the band. In this case, when $v_1 > v_2$ the leading edge is $z_2^\star = v_1 t$ and when $v_1 < v_2$, it is $z_2^\star = v_2 t$. Thus, the maximum will always occur on the leading edge of the band. Figures (2.7.2c) and (2.7.2d) represent schematically these cases.

The four possibilities for the location of the maxima at a fixed time t are summarized in Table (2.7.3) below:

	$\alpha_{12} = \frac{\lambda_1 - \lambda_2}{v_1 - v_2} > 0$	$\alpha_{12} = \frac{\lambda_1 - \lambda_2}{v_1 - v_2} < 0$
$v_1 > v_2$	$z_2^\star = v_2 t \ (\lambda_1 > \lambda_2)$	$z_2^\star = v_1 t \ (\lambda_2 > \lambda_1)$
$v_1 < v_2$	$z_2^\star = v_1 t (\lambda_2 > \lambda_1)$	$z_2^\star = v_2 t \ (\lambda_1 > \lambda_2)$

Table (2.7.3): The different possibilities of extremum at a fixed time $(N_2^0=0)$

In this case one notices that the maxima always occurs at the location determined by the velocity of the nuclide with the smaller decay constant. Regardless of which nuclide travels faster.

Therefore, one can conclude that at a fixed time, the position of the maximum is determined by the decay constant of the nuclides. Therefore, one can further simplify Table (2.7.3) into the following table:

$\lambda_2 > \lambda_1$	$\lambda_2 < \lambda_1$
$z_2^\star = v_1 t$	$z_2^\star = v_2 t$

(2.7.34)

Table (2.7.4); The position of maximum for the 2nd member at a fixed time ($N_2^0 = 0$)

And the corresponding concentration can be obtained from Eq. (2.7.31)

$$N_2^\star(z_2^\star, t) = B_{12} \exp(-\lambda_m t) \qquad (2.7.35)$$

where $\lambda_m = \min[\lambda_1, \lambda_2]$

Consider for instance the chain:

$$^{246}\mathrm{Cm} \xrightarrow[4.76 \times 10^3 \mathrm{yr}]{\alpha} {}^{242}\mathrm{Pu} \xrightarrow[287 \times 10^5 \mathrm{yr}]{\alpha}$$

For the purpose of illustration let us assume the following values (H5):

$$\lambda_1 = 1.46 \times 10^{-4} \mathrm{yr}^{-1}, \; K_1 = 3000 \; : \lambda_1 K_1 = 4.38 \times 10^{-1}$$

$$\lambda_2 = 1.79 \times 10^{-6} \mathrm{yr}^{-1}, \; K_2 = 10^4 \; : \lambda_2 K_2 = 1.79 \times 10^{-2}$$

The time of maximum concentration at a fixed z can be readily read from Table (2.7.2) by using the condition $\lambda_1 K_1 > \lambda_2 K_2$, and it is:

$$t_2^\star = \frac{z}{v_2}$$

and the corresponding maximum concentration is

$$N_2^\star(z,t_2^\star) = (N_1^0 T)\,\frac{\lambda_1\,v_2}{v_1-v_2}\,\exp(-\lambda_2 K_2\,\frac{z}{v})$$

Similarly, the position of maximum concentration at a fixed t can be obtained from Table (2.7.4) by using the condition $\lambda_1 > \lambda_2$ and it is:

$$z_2^\star = v_2 t$$

Hence, the maximum concentration at a fixed time t is:

$$N_2^\star(Z_2^\star,t) = (N_1^0 T)\,\frac{\lambda_1\,v_2}{v_1-v_2}\,\exp(-\lambda_2 t)$$

To illustrate this example numerically consider:

$z = 10^3$m, $t = 10^3$ years, $v = 10$ m/yr and $T = 10^4$ years.

Then, at the position $z = 10^3$ meters the maximum concentration occurs at a time

$$t_2^\star = \frac{10^3}{10^{-3}} = 10^6 \text{ years}$$

and it has a magnitude of:

$$\frac{N_2^\star(z,t_2^\star)}{N_1^0} = 0.104$$

Conversely, after $t = 10^3$ years the maximum concentration occurs at a position

$$z_2^\star = \frac{10 \times 10^3}{10^4} = 1\text{m}$$

with a concentration:

$$\frac{N_2^*(z_2^*,t)}{N_1^0} = 0.625$$

Besides the determination of the extremum of the solution, another features of the solution can be deduced, namely: the contamination region at a fixed time and the contamination time at a given fixed position.

Let us denote by R_i the region which is contaminated by the i-th nuclide at a given time. For the 1st daughter, from Eq. (2.7.32) one notices that the solution is non trivial in the region defined by:

$$R_2 = v_f t - v_s t \qquad (2.7.36)$$

where $v_f t$ is the front edge of the band and v_f is the fastest nuclide velocity, $v_s t$ is the trailing edge of the band and v_s is the slowest nuclide velocity.

Similarly, we denote by θ_i the contamination time which is the time interval in which there are i-th nuclides present at a given position z. For the 1st daughter from Eq. (2.7.31) one concludes that:

$$\theta_2 = \frac{z}{v_s} - \frac{z}{v_f} \qquad (2.7.37)$$

where $\frac{z}{v_f}$ is the first nuclide arrival time at a given position z and $\frac{z}{v_s}$ is the last nuclide departure time.

The effect of a large value of $|v_1 - v_2|$ is a large contamination time and contaminated region (see Eq. (2.7.36) and Eq. (2.7.37)), but the corresponding maxima concentrations are reduced by an increase in $|v_1 - v_2|$, according to Eq. (2.7.32).

Consider again the example previously used $({}^{246}\mathrm{Cm} \rightarrow {}^{242}\mathrm{Pu})$, the contaminated region at a given time t would be:

$$R_2 = \left(\frac{1}{K_1} - \frac{1}{K_2}\right) vt = 2.33 \times 10^{-4}\ vt$$

while the contamination time at a given position z would be:

$$\theta_2 = (K_2 - K_1)\frac{z}{v} = 7 \times 10^3 \frac{z}{v}$$

As a numerical example, suppose we are interested again in $t = 10^3$ yrs, $z = 1000$ m, and $v = 10$m/yr, then:

$$\theta_2 = 7 \times 10^5 \text{ years and } R_2 = 2.33 \text{ meters}$$

Therefore, at a position 10^3m away from the repository, ^{242}Pu will be present during 7.0×10^5 years and after 10^3 years of the beginning of leaching the ^{242}Pu band has spread to a extension of 2.33 meters.

The next case considers a non zero initial concentration of the daughter, $(N_2^0 \neq 0)$.

2.7.7.B First daughter has non zero initial concentration at the repository $(N_2^0 \neq 0)$:

In this case Eq. (2.7.20) keeps both terms:

$$N_2(z,t) = N_2^0 \exp\left(-\frac{\lambda_2 z}{v_2}\right) S[v_2 t; v_2(t-T)]\, \phi_2(t) +$$

$$N_1^0 \frac{T\lambda_1 v_2}{v_1 - v_2} \exp(-\Delta_{21} t - \alpha_{21} z)\; S(v_1 t, v_2 t) \qquad (2.7.38)$$

The added term represents those 2^{nd} member nuclides initially emitted at the repository and it has the same form as the first member solution Eq. (2.7.19). The second term represents the decay of the 1^{st} member nuclides which were emitted at the repository generating daughter nuclides. Evaluation of the extremum of each of these individual term was done in past sections.

Eq. (2.7.38) can be seen as a superposition of two functions represented by each one of the terms described above. Let us consider a fixed position z, the first term is non trivial in the time interval $\frac{z}{v_2}, \frac{z}{v_2} + T$ and $\phi_2(t)$ is an exponential function of λ_2, λ_1. But since we have assumed $T \ll \frac{1}{\lambda_j}$, $j=1,2$, the exponential decay during this time interval T is negligible and we can assume this term as being a band of constant magnitude. Hence, one can set $\phi_2(t) \cong 1$ in Eq. (2.7.38).

The different configurations that Eq. (2.7.38) can take depending on the relative magnitude of the nuclide velocities are illustrated in Figure (2.7.3).

The dotted lines in Figure (2.7.3) represent the case where the 1^{st} term contribution is smaller than the second term contribution.

In cases (a) and (d), one must evaluate $N_2(z,t = \frac{z}{v_1})$ and $N_2(z,t = \frac{z}{v_2})$ using Eq. (2.7.38) to decide whether the extremum occurs at $\frac{z}{v_1}$ or $\frac{z}{v_2}$. At $t = \frac{z}{v_2}$, by using Eq. (2.7.38): $N_2(z,t = \frac{z}{v_2}) = [N_2^0 + (N_1^0 T)\ B_{12}\ ]\exp(- \frac{\lambda_2 z}{v_2})$

At $t = \frac{z}{v_1}$, by using (2.7.38): $N_2(z,t = \frac{z}{v_1}) = (N_1^0 T)\ B_{12}\ \exp(- \frac{\lambda_1}{v_1} z)$.

Taking the ratio of the two concentrations and denoting it by R:

$$R = \frac{N_2(z,t = \frac{z}{v_2})}{N_2(z,t = \frac{z}{v_1})} = \frac{N_2^0 + (N_1^0 T)\ |B_{12}|}{(N_1^0 T)\ |B_{12}|} \exp\left[\left(\frac{\lambda_1}{v_1} - \frac{\lambda_1}{v_2} z\right)\right] \qquad (2.7.41)$$

$$\text{when } R \geq 1;\ t_2^* = \frac{z}{v_2} \text{ and when } R < 1,\ t_2^* = \frac{z}{v_1} \qquad (2.7.41a)$$

The inequalities in Eq. (2.7.41a) are solved for z resulting:

$$z \geq W = \frac{\ln\left[\frac{N_2^0 + (N_1^0 T)|B_{12}|}{(N_1^0 T)|B_{12}|}\right]}{\left(\frac{\lambda_1}{v_1} - \frac{\lambda_2}{v_2}\right)} \text{ yields: } t_2^* = \frac{z}{v_1} \qquad (2.7.42)$$

$$Z \leq W = \frac{\ln\left[\frac{N_2^0 + (N_1^0 T)\ |B_{12}|}{(N_{10}^0 T)\ |B_{12}|}\right]}{\left(\frac{\lambda_1}{v_1} - \frac{\lambda_2}{v_2}\right)} \text{ yields: } t_2^* = \frac{z}{v_2} \qquad (2.7.43)$$

The following table summarizes the time for the maximum concentration of the 1^{st} daughter at a fixed position when its initial concentration is non zero.

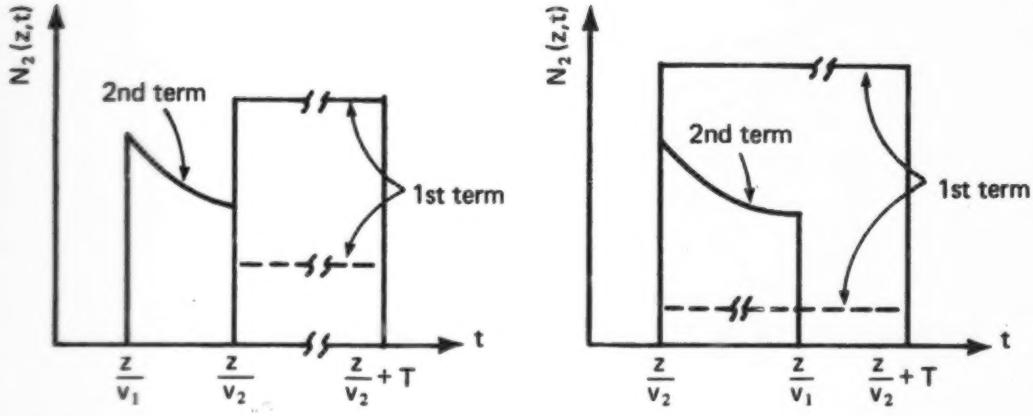
N₂(z,t)
2nd term
1st term
t
z/v₁
z/v₂
z/v₂ + T
N₂(z,t)
2nd term
1st term
t
z/v₂
z/v₁
z/v₂ + T

a) $v_1 > v_2$, $\lambda_2 k_2 > \lambda_1 k_1$, z fixed

b) $v_2 > v_1$, $\lambda_2 k_2 < \lambda_1 k_1$, z fixed

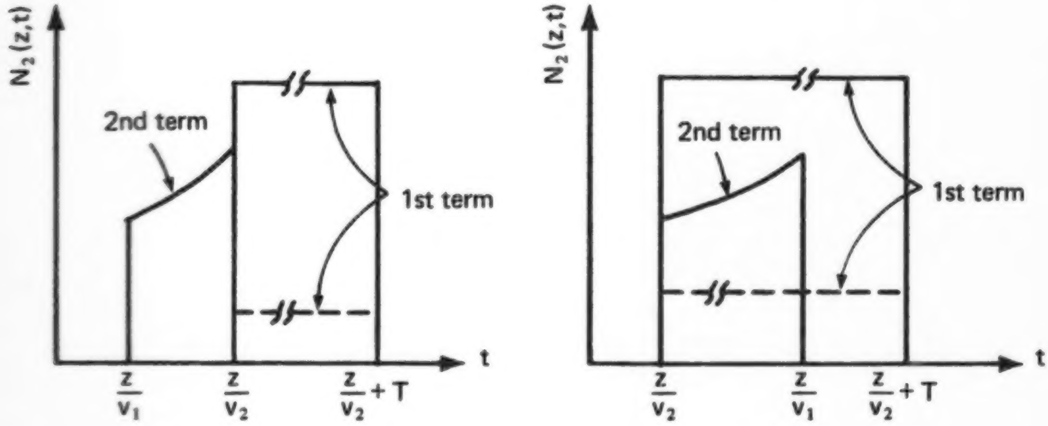
N₂(z,t)
2nd term
1st term
t
z/v₁
z/v₂
z/v₂ + T
N₂(z,t)
2nd term
1st term
t
z/v₂
z/v₁
z/v₂ + T

c) $v_1 > v_2$, $\lambda_2 k_2 < \lambda_1 k_1$, z fixed

d) $v_2 > v_1$, $\lambda_2 k_2 > \lambda_1 k_1$, z fixed

Figure 2.7.3 Possible configurations for the concentration $N_2(z,t)$ at a fixed position z ($N_2^0 \neq 0$).

	$z < W$	$z > W$
$\lambda_1 K_1 > \lambda_2 K_2$	$t_2^* = \frac{z}{v_2}$	$t_2^* = \frac{z}{v_2}$
$\lambda_1 K_1 < \lambda_2 K_2$	$t_2^* = \frac{z}{v_2}$	$t_2^* = \frac{z}{v_1}$

Table 2.7.5: The time for maxima for the 2nd member at a fixed position ($N_2^0 \neq 0$)

By an analogous development, the position of extremum z_2^* at a fixed time can be determined. They are summarized below:

	$t < W'$	$t > W'$
$\lambda_1 > \lambda_2$	$z_2^* = v_2 t$	$z_2^* = v_2 t$
$\lambda_1 < \lambda_2$	$z_2^* = v_2 t$	$t_2^* = v_1 t$

where

$$W' = \frac{\ln \left[\frac{N_2^0 + (N_1^0 T) |B_{12}|}{(N_1^0 T) |B_{12}|} \right]}{\lambda_1 - \lambda_2}$$

Table 2.7.6: The position for maxima for the 2nd member at a fixed time ($N_2^0 \neq 0$)

When the 1st daughter is initially present at the repository the contamination time and the contaminated region can be determined according to Eq. (2.7.38). They are summarized below:

Cases	Contamination time	Contaminated region
$v_1 > v_2$	$\theta_2 = \left(\frac{z}{v_2} - \frac{z}{v_1}\right) + T$	$R_2 = v_1 t - v_2 (t-T)$
$v_1 < v_2$	$\theta_2 = \frac{z}{v_1} - \frac{z}{v_2}$ if $\frac{z}{v_1} - \frac{z}{v_2} > T$	$R_2 = (v_2-v_1)t$ if $(v_2-v_1)t > v_2T$
	$\theta_2 = T$ if $\frac{z}{v_1} - \frac{z}{v_2} < T$	$R_2 = v_2T$ if $(v_2-v_1)t < v_2T$

Table 2.7.7: Contamination time and contamination region for the 2nd member when $N_2^0 \neq 0$.

One should notice that when $N_2^0 = 0$, Tables (2.7.5) and (2.7.6) reduce to Tables (2.7.2) and (2.7.4), respectively.

2.7.8 Extremum of the solution for the 3rd member (2nd daughter).

This problem is again subdivided into two stages:

1) The initial amount of the 3rd member present at the repository is zero ($N_3^0 = 0$, $N_2^0 \neq 0$, $N_1^0 \neq 0$).

2) The initial amount of the 3rd member is significant at the repository ($N_3^0 \neq 0$, $N_1^0 \neq 0$, $N_1^0 \neq 0$).

2.7.8.A The initial amount of the 3rd member at the repository is zero:

By setting $N_3^0 = 0$ in Eq. (2.7.21) the solution reads:

$$N_3(z,t) = T(B_{23}N_2^0 - AN_1^0) \exp(-\Delta_{23}t - \alpha_{23}z)\, S(v_2t;\, v_3t) +$$

$$N_1^0 TA \exp(-\Delta_{13}t - \alpha_{13}z)\, S(v_1t; v_3t)$$

$$- TAN_1^0 \exp(-\Delta_{12}t - \alpha_{12}z)\, S(v_1t;\, v_2t) \qquad (2.7.21)$$

Depending on the relative magnitudes of the nuclide velocities, the functions $S(v_i t, v_j t)$ can assume the values of -1, 0 or 1. Therefore, for each one of the six possible different combinations of the three nuclide velocities, different terms in Eq. (2.7.21) will arise.

The task of determining the extremum of the Eq. (2.7.21) is indeed expanded to the task of determining the extremum of six different functions, depending on the relative magnitude of the nuclide velocities.

In order to determine the time of the maximum concentration at a fixed position, the following procedure is adopted:

For a particular set of nuclide velocities, say for generality (v_s, v_m, v_f, where subscript s stands for slowest, m for medium and f for fastest) the solution can be sketched as follows:

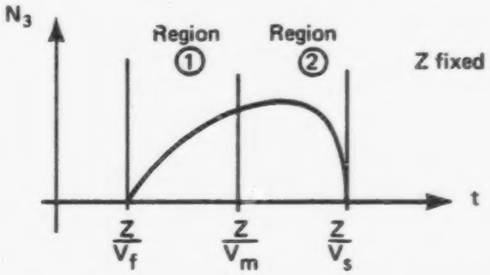

There are two distinct regions. The solution (2.7.21) takes different form in each of this region, because the functions $S(v_i t; v_j t)$ assumes different values in each region for the same set of nuclide velocities.

Let us summarize in Table 2.7.8 the values of the functions $S(v_i; v_j t)$ in each region and for the six possible combinations of the nuclide velocities: (see Eq. (2.7.26))

The procedure adopted to evaluate the time of maximum for each of the six cases will be to evaluate the individual maximum of the concentration for each region and then to compare them in order to decide which one is actually the true extremum of the solution in both regions.

We will next evaluate the maximum for the first of the six cases listed in Table (2.7.8). For the case (1) where $v_1 > v_2 > v_3$ each region is studied individually. In Region (1), from Eq. (2.7.21) and Table (2.7.8) the concentration distribution in this region is given by:

$$\frac{N_3}{N_1^0}(z,t) = TA\exp(-\Delta_{13}t - \alpha_{13}z) - TA\exp(-\Delta_{12}t - \alpha_{12}z) \qquad (2.7.44)$$

and it is nontrivial for a given $z>0$ in the interval:

		Region 1			Region 2		
Case	$v_f>v_m>v_s$	$S(v_2t;v_3t)$	$S(v_1t;v_3t)$	$S(v_1t;v_2t)$	$S(v_2t;v_3t)$	$S(v_1t;v_3t)$	$S(v_1t,v_2t)$
1	$v_3>v_2>v_1$	0	1	1	1	1	0
2	$v_3>v_2>v_1$	-1	-1	0	0	-1	-1
3	$v_1>v_3>v_2$	0	1	1	-1	0	1
4	$v_2>v_3>v_1$	1	0	-1	0	-1	-1
5	$v_3>v_1>v_2$	-1	-1	0	-1	0	1
6	$v_2>v_1>v_3$	1	0	-1	1	1	0

Table 2.7.8: Values for the functions $S(v_it;v_jt)$

$\frac{z}{v_1} \leq t \leq \frac{z}{v_2}$ which is the domain of definition of (2.7.44)

The partial derivative with respect to time of Eq. (2.7.44) is:

$$\frac{1}{TN_1^0}\frac{\partial N_3}{\partial t}(z,t) = A\Delta_{12}\exp(-\Delta_{13}t - \alpha_{13}z) - A\Delta_{13}\exp(-\Delta_{12}t-\alpha_{12}z) \tag{2.7.45}$$

The function described by Eq. (2.7.44) can have, if any, only one extremum in its domain of definition because Eq. (2.7.45) can have only one zero, if any, in its domain of definition (region 1). The zero of Eq. (2.7.45) (if any) occurs at:

$$t_3^* = \frac{1}{\Delta_{21}-\Delta_{31}}\left[\ln \frac{\Delta_{21}}{\Delta_{31}} - (\alpha_{21}-\alpha_{31})z\right] \tag{2.7.46}$$

By evaluating Eq. (2.7.45) at the beginning of its domain of definition $t = \frac{z}{v_1}$ one has:

$$\frac{1}{N_1^0}\ \frac{\partial N_3}{\partial t}\ (z,t = \frac{z}{v_1}) = AT\ (\Delta_{21}-\Delta_{31})\ \exp(- \frac{\lambda_1}{v_1} z) \tag{2.7.47}$$

Furthermore, one can show that

$$A(\Delta_{21}-\Delta_{31}) = \frac{v_1 v_3 \lambda_2 \lambda_1 (N_1^0 T)}{v_1-v_3} > 0 \tag{2.7.48}$$

hence $\frac{\partial N_3}{\partial t}\ (z,t = \frac{z}{v_1}) > 0$ for any $z > 0$.

Therefore, Eq. (2.7.44) is initially increasing and if the zero of Eq. (2.7.45) lies inside the domain of definition the extremum will be a maximum, i.e., if

$$\frac{z}{v_1} < \ t_3^*\ (\text{Eq. } (2.7.46) < \frac{z}{v_2} \tag{2.7.49}$$

t_3^* will be a point of maximum.

On the other hand, if t_3^* given by Eq. (2.7.46) does not exist or it is outside the domain of definition, the function Eq. (2.7.44) is monotonically increasing in its domain of definition and the maximum will occur at the end of region 1, i.e.:

$$t_3^* = \frac{z}{v_2} \tag{2.7.50}$$

The inequality Eq. (2.7.49) can be rewritten by using Eq. (2.7.46) to express this condition in terms of the position z:

$$\frac{z}{v_1} < \frac{1}{\Delta_{21}-\Delta_{31}} \left[\ln \frac{\Delta_{12}}{\Delta_{13}} - (\alpha_{21}-\alpha_{31})z \right] \leq \frac{z}{v_2} \tag{2.7.51}$$

In Region 2, from Eq. (2.7.21) and using Table (2.7.8) the concentration distribution in this region is given by:

$$\frac{N_3}{N_1^0}(z,t) = T(\frac{N_2^0 B_{23}}{N_1^0} - A) \exp(-\Delta_{23}t-\alpha_{23}z) + TA \exp(-\Delta_{13}t-\alpha_{13}z) \tag{2.7.52}$$

and it is non trivial for a given $z>o$ in the interval $\frac{z}{v_2} \leq t \leq \frac{z}{v_3}$ which is the domain of definition of Eq. (2.7.52).

The partial derivative with respect to time of Eq. (2.7.52) is:

$$\frac{1}{N_1^0} \frac{\partial N_3}{\partial t}(z,t) = \left(T\ A - \frac{B_{23}N_2^0}{N_1^0}\right) \Delta_{23} \exp(-\Delta_{23}t-\alpha_{23}z) -$$

$$TA\Delta_{13} \exp(-\Delta_{13}t-\alpha_{13}z) \tag{2.7.53}$$

Again, the function described by Eq. (2.7.52) can have, if any, only one extremum in its domain of definition.

This is because Eq. (2.7.53) can have, if any, only one zero in its domain of definition. The zero of Eq. (2.7.53) (if any) occurs at:

$$t_3^* = \frac{1}{\Delta_{32}-\Delta_{31}} \left[\ln \left(\frac{A - B_{23}N_2^0/N_1^0}{A} \frac{\Delta_{32}}{\Delta_{13}} \right) - (\alpha_{23}-\alpha_{13})z \right] \tag{2.7.54}$$

Let us evaluate Eq. (2.7.53) at the end of the domain,

$t = \frac{z}{v_3}$:

$$\frac{1}{N_1^0}\frac{\partial N_3}{\partial t}\left(z, t = \frac{z}{v_3}\right) = T\left[A(\Delta_{23}-\Delta_{13}) - \frac{N_2^0 B_{23}\Delta_{23}}{N_1^0}\right] \exp\left(-\frac{\lambda_3}{v_3} z\right) \qquad (2.7.55)$$

Two possibilities results from Eq. (2.7.55):

$$\frac{N_2^0}{N_1^0}\frac{B_{23}\Delta_{23}}{A\ (\Delta_{23}-\Delta_{31})} \geq 1 \text{ yields } \frac{\partial N_3}{\partial t}\left(z, t = \frac{z}{v_3}\right) \geq 0 \qquad (2.7.56)$$

$$\frac{N_2^0}{N_1^0}\frac{B_{23}\Delta_{23}}{A\ (\Delta_{23}-\Delta_{31}} < 1 \text{ yields } \frac{\partial N_3}{\partial t}\left(z, t = \frac{z}{v_3}\right) < 0 \qquad (2.7.57)$$

Suppose t_3^* given by Eq. (2.7.54) exists and it is interior, i.e.:

$$\frac{z}{v_2} \leq t_3^* \text{ (Eq. (2.7.54))} \leq \frac{z}{v_3} \qquad (2.7.58)$$

Then, when Eq. (2.7.56) is true:

$\frac{\partial N_3}{\partial t}(z, t = \frac{z}{v_3}) \geq 0$, t_3^* is necessarily a point of minimum, while if the inverse occurs, $\frac{\partial N_3}{\partial t}(z, t = \frac{z}{v_3}) < 0$, then t_3^* given by Eq. (2.7.54) is a point of maximum.

On the other hand, if t_3^* give by Eq. (2.7.54) does not exist or it is outside of its domain of definition, the function Eq. (2.7.52) is monotonically increasing if $\frac{\partial N_3}{\partial t}(z, t = \frac{z}{v_3}) \geq 0$ and the extremum occurs at $t_3^* = \frac{z}{v_3}$. Conversely, $N_3(z,t)$ is monotonically decreasing if $\frac{\partial N_3}{\partial t}(z, t = \frac{z}{v_3}) < 0$ and there results $t_3^* = \frac{z}{v_2}$.

The inequality Eq. (2.7.58) can be rewritten by using Eq. (2.7.54) to express this condition in terms of the position z:

$$\frac{z}{v_2} \leq \frac{1}{\Delta_{32}-\Delta_{31}} \left[\ln \left(1 - \frac{N_2^0 B_{23}}{N_1^0 A}\right) \frac{\Delta_{32}}{\Delta_{13}} - (\alpha_{32}-\alpha_{32})z \right] \leq \frac{z}{v_3} \qquad (2.7.59)$$

After having determined the time of the maximum in each region, one substitutes these values of time back into the corresponding Eq. (2.7.44) and Eq. (2.7.53) to evaluate the maxima concentrations in each region. By comparing these concentrations one can finally decide about the actual maximum for both regions.

This procedure is repeated for the other five cases listed in Table 2.7.8 and the following general form of the extremum can be obtained and it is summarized in Table (2.7.9). As before, a given case is denoted by: $v_f > v_m > v_s$ where the subscripts indicate:

f = fastest nuclide velocity, f = 1,2,3
m = intermediate nuclide velocity, m = 1,2,3
s = slowest nuclide velocity, s = 1,2,3

(For example, the case 1 in Table 2.7.8 would be f = 1, m = 2, s = 3).

2.7.8.B Extremum of the solution for the 3rd member when its initial amount at the repository is non zero ($N_3^0 \neq 0$, $N_2^0 \neq 0$, $N_1^0 \neq 0$).

In this case the complete solution Eq. (2.7.21) is required:

$$\begin{aligned} N_3(z,t) = {} & N_3^0 \exp\left(-\frac{\lambda_3 z}{v_3}\right) S[v_2 t; v_3(t-T)]\, \phi_3(t) + \\ & \Big\{ (N_2^0 T B_{23} - N_1^0 T A) \exp(-\Delta_{23} t - \alpha_{23} z)\, S(v_2 t; v_3 t) + \\ & N_1^0 T A \exp(-\Delta_{31} t - \alpha_{31} z)\, S(v_1 t; v_3 t) + N_1^0 T A \exp(-\Delta_{21} t - \alpha_{21} z)\, S(v_2 t, v_1 t) \Big\} \end{aligned} \qquad (2.7.60)$$

Region 1		Region 2	
Condition: $\frac{z}{v_f} \leq \frac{\ln(\frac{M\Delta_{mf}}{\Delta_{fs}}) - (\alpha_{mf}-\alpha_{fs})z}{\Delta_{mf}-\Delta_{fs}} \leq \frac{z}{v_m}$		Condition: $\frac{z}{v_m} \leq \frac{\ln(\frac{M\Delta_{ms}}{\Delta_{fs}}) - (\alpha_{ms}-\alpha_{fs})z}{\Delta_{ms}-\Delta_{fs}} \leq \frac{z}{v_s}$	
Satisfied	Not Satisfied	Satisfied	Not Satisfied
$t_3^* = \frac{\ln(\frac{M\Delta_{mf}}{\Delta_{fs}}) - (\alpha_{mf}-\alpha_{fs})z}{\Delta_{mf}-\Delta_{fs}}$	Cases 1,3: $t_3^* = \frac{z}{v_m}$	$t_3^* = \frac{\ln \frac{M\Delta_{ms}}{\Delta_{fs}} - (\alpha_{ms}-\alpha_{fs})z}{\Delta_{ms} - \Delta_{fs}}$	Cases 2,4: $t_3^* = \frac{z}{v_m}$
Note: Cases 1, 3: M = 1 Cases 2,4: $M = 1 - \frac{N_2^0 B_{23}}{N_1^0 A}$ Cases 5, 6: $M = 1 - \frac{N_1^0 A}{N_2^0 B_{23}}$ $W_1 = \frac{B_{23}\Delta_{23}}{A(\Delta_{mf}-\Delta_{fs})} \ (\frac{N_2^0}{N_1^0})$	Cases 2,4: if: $W_1 \geq 1: t_3^* = \frac{z}{v_f}$ $W_1 < 1: t_3^* = \frac{z}{v_m}$ Cases 5, 6; if: $W_1 \leq 1: t_3^* = \frac{z}{v_f}$ $W_1 > -1 : t_3^* = \frac{z}{v_m}$	Note: Cases 2, 4: M = 1 Cases 1, 3: $M = 1 - \frac{N_2^0 B_{23}}{N_1^0 A}$ Cases 5, 6: $M = 1 - \frac{N_1^0 A}{N_2^0 B_{23}}$ $W_2 = \frac{B_{23}\Delta_{23}}{A(\Delta_{ms}-\Delta_{fs})} \ (\frac{N_2^0}{N_1^0})$	Cases 1,3: if $W_2 \geq 1: t_3 = \overset{*}{v_s} \ \underline{z}$ $W_2 < 1: t_3^* = \frac{z}{v_m}$ Cases 5, 6; if: $W_2 \leq 1: t_3^* = \frac{z}{v_s}$ $W_2 > -1 : t_3^* = \frac{z}{v_m}$

Table 2.7.9 Summary of the determination of the extremum for the 3rd member ($N_3^0 = 0$)

The second term which is inside the bracklet was analyzed in the previous section and its extremum can be determined by using Table (2.7.9). When $N_3^0 \neq 0$, a new term (1^{st} term on the right hand side) is superimposed.

Recalling the assumption of small leach time, i.e., $T \ll \frac{1}{\lambda}$, j=1,2,3, and by realizing that this added term is non trivial in the interval $(z/v_3, z/v_3 + T)$ of duration T, one can neglect changes in the Bateman's function $\phi_3(t)$, and consider $\phi_3^0(t)=1$. Therefore, the first term can be seen as a band of duration T and constant magnitude $N_3^0 \exp(\lambda_3 z/v_3)$.

Depending on the relative magnitude of the nuclide velocities, different configurations result from the superimposition of the two terms. (Consider for example Figure 2.7.4.)

In case (a) of Figure (2.7.4) the two terms are non trivial in independent time domains and one can evaluate the extremum of the 2^{nd} term (use Table (2.7.9)) and the extremum of the first term (use Eq. (2.7.28)) separately. The largest concentration will define the true maximum for both terms.

In case (b) of Figure (2.7.4) we have two possibilities: when the extremum of the 2^{nd} term occurs in region (1) and when it occurs in region (2) (dotted line). In either case, one can decide about the true maximum by evaluating the concentration Eq. (2.7.60) at $t = z/v_3$ which is the point of extrema for the first term and comparing to the concentration (Eq. 2.7.21)) at the point of extrema for the 2^{nd} term alone obtained by using Table (2.7.9) and taking $N_3^0 = 0$ in Eq. (2.7.60).

Again, the larger of them will define the true maximum. In case (c) of Figure (2.7.4) the extremum occurs clearly at the point of extremum of the 2^{nd} term but the magnitude is larger by the addition of $N_3^0 \exp(-\lambda_3 z/v_3)$ to the 2^{nd} term.

Above examples does not exhaust all possibilities, since we might have a sufficiently large z so that $z/v_3 + T$ lies inside the time domain of the 2^{nd} term.

But in any case, it can be shown that the following steps will yield the time of maxima t_3^* at a fixed position z:

1) Evaluate $N_3(z,t=z/v_3)$ using Eq. (2.7.60) with both terms.
2) Use Table (2.7.9) to obtain t_3^* for the 2^{nd} term alone.
3) Evaluate $N_3(z,t_3^*)$ with t_3^* obtained in above step (2) but using Eq. (2.7.60) with both terms.
4) Compare $N_3(z,t=z/V_3)$ from step (1) and $N_3(z,t_3^*)$ from step (3).

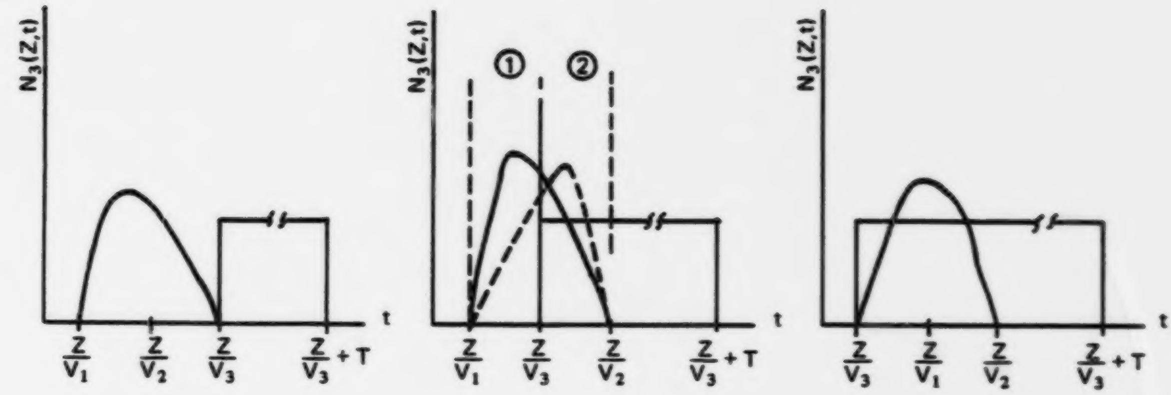

Figure 2.7.4 Possible configurations of the solution for the 3rd member when $N_3^0 \neq 0$.

if $\quad N_3(z, t = \frac{z}{v_3}) > N_3(z, t_3^*); \quad t_3^* = \frac{z}{v_3}$

if $\quad N_3(z, t = \frac{z}{v_3}) < N_3(z, t_3^*); \quad t_3^*$ = from step (2).

2.7.8.C Contamination time and contaminated region for the 3rd member (2nd daughter)

We distinguish two cases:

a) When 2nd daughter is not present at the repository initially ($N_3^0=0$) the contamination time θ_3 as well as the contaminated region R_3 can be readily obtained from Eq. (2.7.21) and Table (2.7.8). They can be expressed by

$$\theta_3 = \left(\frac{1}{v_s} - \frac{1}{v_f}\right) z \qquad (2.7.61)$$

$$R_3 = (v_f - v_s)\, t$$

b) When the 2nd daughter has non zero initial concentration at the repository, ($N_3^0 \neq 0$) using Eq. (2.7.60) and Table (2.7.8) one can construct the following table:

	Θ_3		R_3	
Case:	$\frac{z}{v_3} + T > \frac{z}{v_s}$	$\frac{z}{v_3} + T < \frac{z}{v_s}$	$v_3(t-T > v_sT$	$v_3(t-T < v_sT$
$v_3 < v_2 < v_1$ $v_3 < v_1 < v_2$	$\left(\frac{z}{v_3} - \frac{z}{v_f}\right) + T$	$\left(\frac{z}{v_3} - \frac{z}{v_f}\right) + T$	$v_ft - v_3(t-T)$	$v_ft - v_3(t-T)$
$v_2 < v_3 < v_1$ $v_1 < v_3 < v_2$	$\left(\frac{z}{v_3} - \frac{z}{v_f}\right) + T$	$\left(\frac{z}{v_3} - \frac{z}{v_f}\right) + T$	$(v_f-v_s)t$	$v_ft-v_3(t-T)$
$v_3 > v_2 > v_1$ $v_3 > v_1 > v_2$	T	$\left(\frac{z}{v_s} - \frac{z}{v_3}\right)$	$(v_3 - v_s)t$	v_3T

Table 2.7.10: Contamination time and contaminated region for the 3rd member ($N_3^0 \neq 0$).

2.7.9 Example of the utilization of the method and comparison with the exact solution results

To verify the validy of the approximation and to determine the range in leaching time for which this approximate solution is accurate in representing the exact solution to a decaying band release we compared the results of the approximate solution with those of the exact solutions. These comparisons are done for different leach times.

Comparisons for the first member solutions are not necessary since the exact and approximate solutions have the same form. We studied the ^{234}U and ^{237}Np chains. First, we considered the following chain:

$^{234}U \rightarrow {}^{230}Th \rightarrow {}^{226}Ra$ with the set of parameters given below obtained from reference (H1):

^{234}U: $\lambda_1 = 2.8 \times 10^{-6}\ yr^{-1}$, $K_1 = 1.4 \times 10^4$, $v_1 = 7.8 \times 10^{-3}$ m/yr.

^{230}Th: $\lambda_2 = 9.0 \times 10^{-6}\ yr^{-1}$, $K_2 = 5.0 \times 10^4$, $v_2 = 2.2 \times 10^{-3}$ m/yr.

^{226}Ra: $\lambda_3 = 4.3 \times 10^{-4}\ yr^{-1}$, $K_3 = 5.0 \times 10^2$, $v_3 = 2.2 \times 10^{-1}$ m/yr.

Thus, in this case $v_3 > v_1 > v_2$ and $v = 110$ m/yr.

The case of no initial daughter at the repository is considered initially ($N_2^o = 0$; $N_3^o = 0$).

The extremum for the 2nd member (^{230}Th) can be readily obtained from Table (2.7.2) with the condition below:

$\lambda_2 K_2 = 0.45\ (yr^{-1})$; $\lambda_1 K_1 = 0.039\ (yr^{-1})$, thus $\lambda_2 K_2 > \lambda_1 K_1$

Therefore, the time when the maximum occurs at a fixed position can be obtained from Table (2.7.2) and it is:

$$t_2^* = \frac{z}{v_1}$$

and the corresponding maximum concentration will be:

$$N_2^*(z,t_2^*) = \frac{N_1^o T \lambda_1 v_2}{v_1 - v_2}\, e^{-\frac{\lambda_1}{v_1} z} \tag{2.7.62}$$

consequently the contamination time is:

$$\theta_2 = \left(\frac{1}{v_2} - \frac{1}{v_1}\right) z \tag{2.7.63}$$

The time of maxima for the 3rd member at a fixed position can be obtained from Table (2.7.9). In this present case $v_3 > v_1 > v_2$ ($f = 3$, $m = 1$ and $s = 2$). Therefore, according to Table (2.7.8) we are in case (5).

The coefficients Δ_{ij} and α_{if} are first evaluated:

$$\Delta_{32} = 4.75 \times 10^{-6} (yr^{-1}); \ \Delta_{13} = -1.29 \times 10^{-5} (yr^{-1}); \ \Delta_{12} = 1.14 \times 10^{-5} (yr^{-1})$$

$$\alpha_{32} = 1.92 \times 10^{-3} (m^{-1}); \ \alpha_{13} = 2.01 \times 10^{-3} (m^{-1}); \ \alpha_{12} = -1.11 \times 10^{-3} (m^{-1})$$

Let us assume that $N_2^o = N_3^o = 0$. In the column titled region (1) in Table (2.7.9) we first check the condition for the existence of interior maximum.

Since $N_2^o = 0$ and $B_{23} = 0$; hence: $M = 1$ and $W_1 = 0$.

$$\ln \frac{M\Delta_{mf}}{\Delta_{fs}} = \ln \frac{\Delta_{31}}{\Delta_{32}} \text{ ; but since } \frac{\Delta_{31}}{\Delta_{32}} < 0 \text{ the condition for interior maximum}$$

cannot be satisfied.

From the column, "not satisfied," under case (5) and with $W_1 = 0$, the time of maximum is read: $t_3^* = \frac{z}{v} = \frac{z}{v}$.

Similary, the condition for existence of interior maximum is region 2 is first checked.

$$\ln M \frac{\Delta_{ms}}{\Delta_{fs}} = \ln \frac{\Delta_{21}}{\Delta_{32}} = \ln 2.40 = 0.875$$

Again the condition is not satisfied. And for case (5) with $W_2 = 0$ the time of maximum is

$$t_3^* = \frac{z}{v_m} = \frac{z}{v_1}$$

One can conclude that the time of maxima will be always on:

$t_3^* = \frac{z}{v_1}$ in either region (1) or region (2) and the corresponding maximum maximum concentration is:

$$\frac{N_3^*}{N_1^0}(z,t_3^*) = TA\left[\exp\left(-\frac{\Delta_{32}}{v_1} - \alpha_{32}\right) z - \exp\left(-\frac{\lambda_1}{v_1} z\right)\right] \qquad (2.7.64)$$

and the contaminated time will be given by:

$$\theta_3 = \left(\frac{1}{v_2} - \frac{1}{v_3}\right) z \qquad (2.7.65)$$

The above results agrees well with the exact solution presented by Higashi (H6) for leach times values up to about 3 x 10^4 years. (See Figures 2.7.5a and 2.7.5b).

A more detailed study is presently being conducted to determine upper bounds for the error as one increases the leach time for larger values.

In Fig. (2.7.5a) the maximum concentration of ^{226}Ra ($N_3^*(z,t_3^*)/N_1^0$) is plotted for each fixed position z. The initial concentrations of the daughters were zero and the leach time was 3500 yrs. For this value of leach time the agreement was complete.

Figure (2.7.5b) is a similar plot but for a leach time value of 35000 yrs. Although this value of leach time is larger than the ^{226}Ra half life, thus violating Eq. (2.7.10), the approximate solution deviation from the exact solution is smaller than 10 percent. This is because the ^{226}Ra concentration is controlled by the decay of ^{234}U whose half life is much larger than the leach time used.

In Fig. (2.7.6a) the calculation was the same as in Fig. (2.7.5a) but this time the daughters were initially in transient equilibrium. For this leach time the agreement was complete.

In Fig. (2.7.6b) a leach time of 3.5 x 10^4yrs was used which is about an order of magnitude larger than the half life of ^{226}Ra. Although this fact

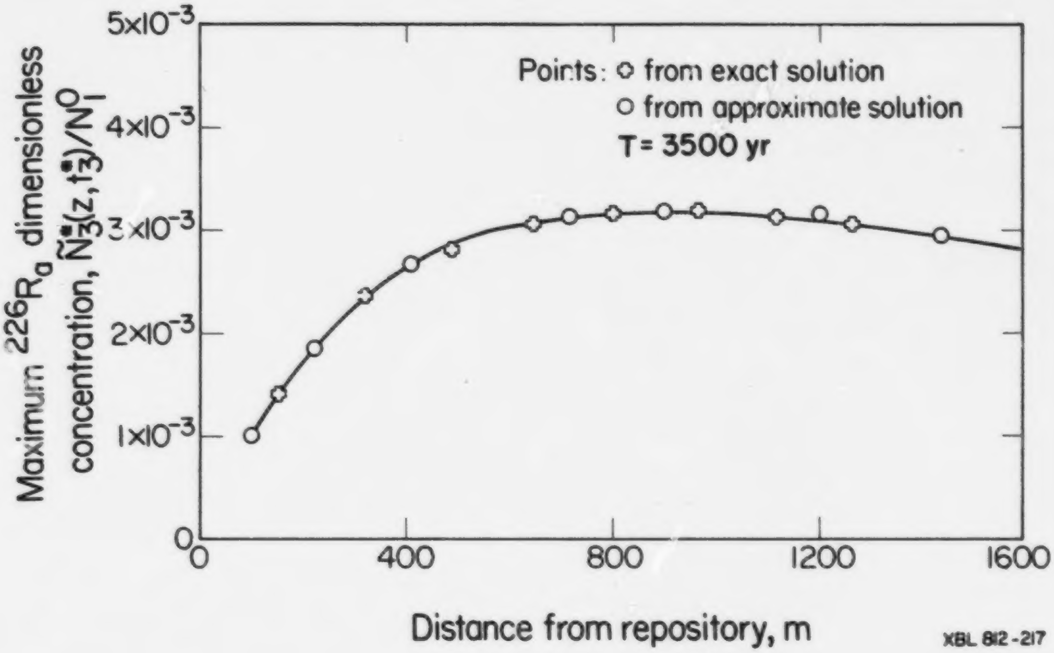

XBL 812-217

Figure 2.7.5a Maxima concentrations of ^{226}Ra at different fixed positions. No initial daughters ($N_2^0 = N_3^0 = 0$). No dispersion. T = 3500 years.

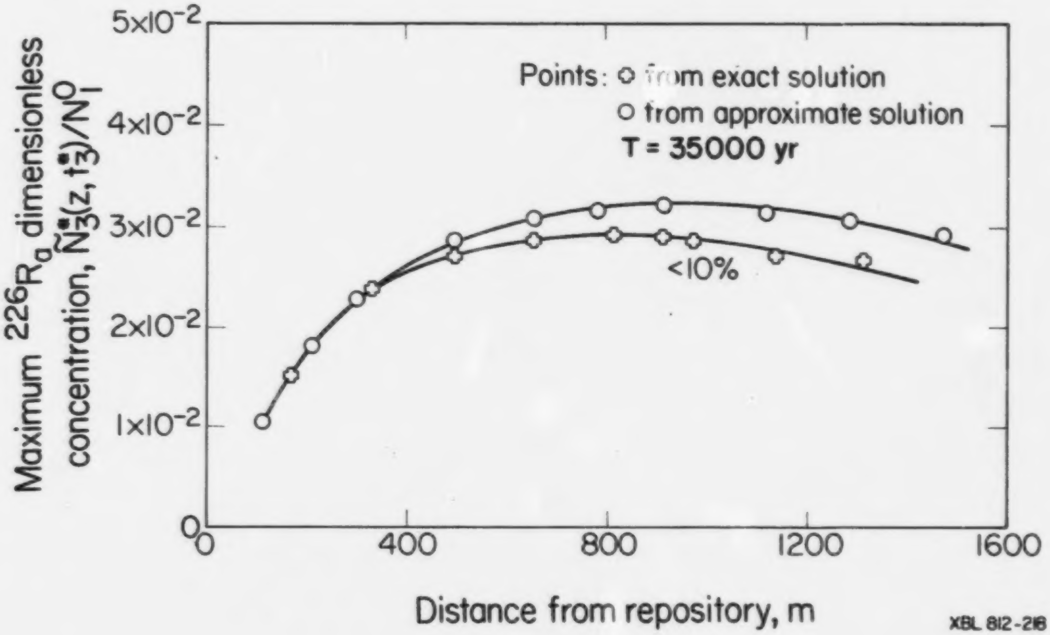

XBL 812-218

Figure 2.7.5b Maxima concentrations of ^{226}Ra at different fixed positions. No initial daughters ($N_2^0 = N_3^0 = 0$). No dispersion. T = 35000 years.

BEST DOCUMENT AVAILABLE

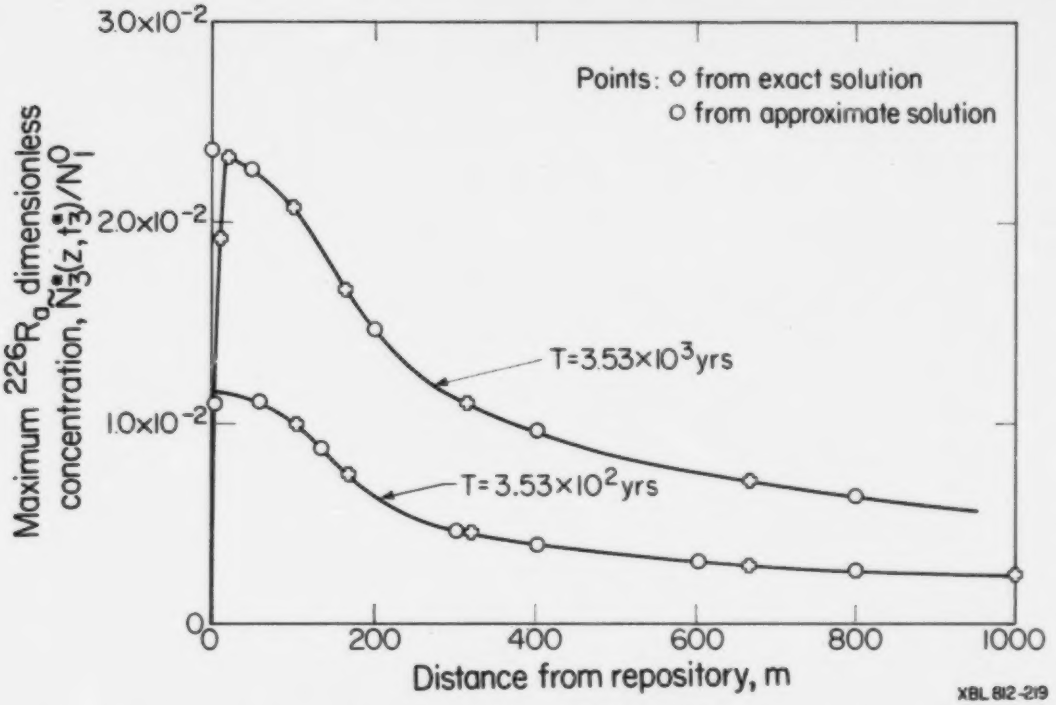

Figure 2.7.6a Maxima concentrations of ^{226}Ra at different fixed positions. Initial transient equilibrium. No dispersion. T = 3500 years.

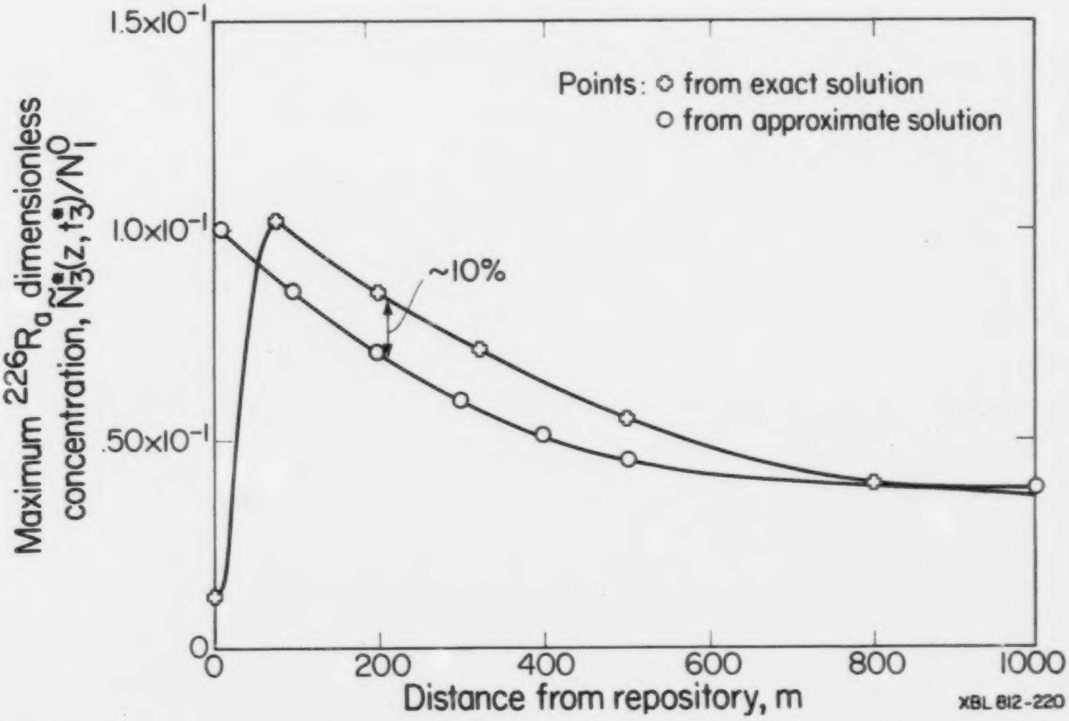

Figure 2.7.6b Maxima concentrations of ^{226}Ra at different fixed positions. Initial transient equilibrium. No dispersion. T = 35000 years.

violates the basic assumption Eq. (2.7.10a) the comparison with the exact solution (Fig. 2.7.6b) shows that the error is larger only for distances $z < 10m$ where the decay of the initial ^{226}Ra nuclides is important. For $z > 10m$ where the concentration of ^{226}Ra is controlled by the decay of ^{234}U the error is smaller than 10 percent.

A second three member chain which is also important starts with ^{237}Np:

$$^{237}Np(^{233}Pa, 27d) \xrightarrow[2.14 \times 10^{6} yr]{\alpha} {}^{233}U \xrightarrow[1.58 \times 10^{5} yr]{\alpha} {}^{229}Th \xrightarrow[7340\ yr]{\alpha}$$

The same calculations done for the ^{234}U chain are repeated here. For the purpose of illustration, the following equilibrium constants were assumed arbitrarily: $K_1 = 10^4$, $K_2 = 1.4 \times 10^4$, $K_3 = 5 \times 10^4$.

Let us first determine the extremum of the solution for the 2nd member. From Table (2.7.2) and with the condition below:

$$\lambda_2 K_2 = 6.14 \times 10^{-2} (yr^{-1}); \ \lambda_1 K_2 = 3.24 \times 10^{-3} (yr^{-1}) \text{ thus } \lambda_2 K_2 > \lambda_1 K_1$$

therefore $t_2^* = \frac{z}{v_1}$, and the corresponding maximum concentration will be:

$$N_2^* (z, t_2^*) = \frac{(N_1^0 T) \lambda_1 v_2}{v_1 - v_2} e^{-\left(\frac{\lambda_1}{v_1} z\right)} \tag{2.7.66}$$

The time of maximum for the 3rd member at a fixed position can be obtained from Table (2.7.9) this is a case (5).

The coefficients Δ_{ij} and α_{ij} are first evaluated:

$$\Delta_{32} = -4.56 \times 10^{-5} (yr^{-1}); \ \Delta_{31} = -9.38 \times 10^{-5} (yr^{-1}); \ \Delta_{12} = 1.45 \times 10^{-5} (yr^{-1})$$

$$\alpha_{32} = 6.37 \times 10^{-3} (m^{-1}); \ \alpha_{31} = 8.55 \times 10^{-3} (m^{-1}); \ \alpha_{12} = -1.20 \times 10^{-3} (m^{-1})$$

Consider the case of no initial daughters, (i.e., $N_2^0 = N_3^0 = 0$).

Under the column titled Region (1) in Table (2.7.9) the condition for the existence of interior maxima is first checked:

Since $N_2^0 = 0$ and $B_{23} = 0$ hence $M = 1$ and $W_1 = 0$, thus;

$$\ln\left(M\frac{\Delta_{mf}}{\Delta_{fs}}\right) = \ln\frac{\Delta_{13}}{\Delta_{32}} = \ln\left(\frac{9.38}{4.56}\right) = 0.721$$

and

$$z\left(1 - \frac{v_f}{v_m}\right)(\alpha_{mf} - \alpha_{fs}) = z\left(1 - \frac{v_3}{v_1}\right)(\alpha_{13} - \alpha_{32}) = (-2.18 \times 10^{-3})\ z$$

Therefore, the condition for interior maxima cannot be satisifed for $z > 0$. Under the column titled "not satisfied," for cases (5).

$$t_3^* = \frac{z}{v_m} = \frac{z}{v_1}$$

Similarly, for Region (2):

$$\ln M\frac{\Delta_{ms}}{\Delta_{fs}} = \ln\frac{\Delta_{21}}{\Delta_{32}} = \ln\left(-\frac{1.45}{4.56}\right) \text{ which is not defined.}$$

Therefore, the condition for interior maxima is again not satisfied. From the column "not satisfied" in Region (2) in Table (2.7.9) and case (5) one reads:

$$t_3^* = \frac{z}{v_m} = \frac{z}{v_1} \quad .$$

Since the maximum concentration in either region occurs at the common boundary $t_3^* = \frac{z}{v_1}$, the maximum concentration for both regions is the same and can be expressed by:

$$\frac{N_3^*(z,t_3^*)}{N_1^0} = TA\left[\exp\left(-\frac{\Delta_{23}}{v_1}z - \alpha_{23}z\right) - \exp\left(-\frac{\lambda_1}{v_1}z\right)\right] \qquad (2.6.67)$$

Figure (2.7.7a) and 2.7.7b) show the case of zero initial daughters concentration for leach times of 3500 yrs and 35000 yrs, respectively. Also for this chain, the agreement between the exact and approximate solutions is quite good for leach times smaller than 35,000 yrs.

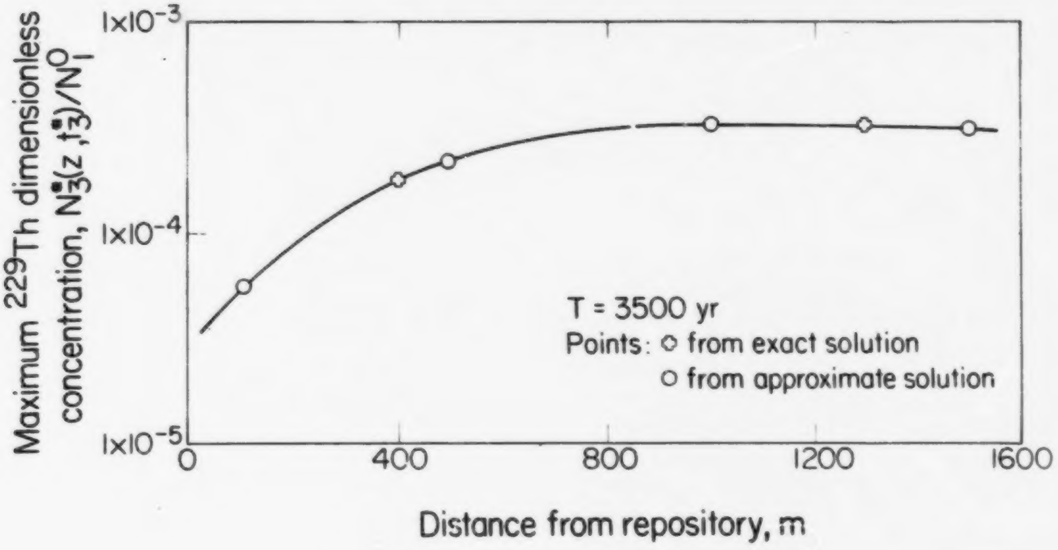

XBL 812-221

Figure 2.7.7a Maxima concentrations of ^{229}Th at different fixed positions. No initial daughters ($N_2^0 = N_3^0 = 0$). No dispersion. T = 3500 years.

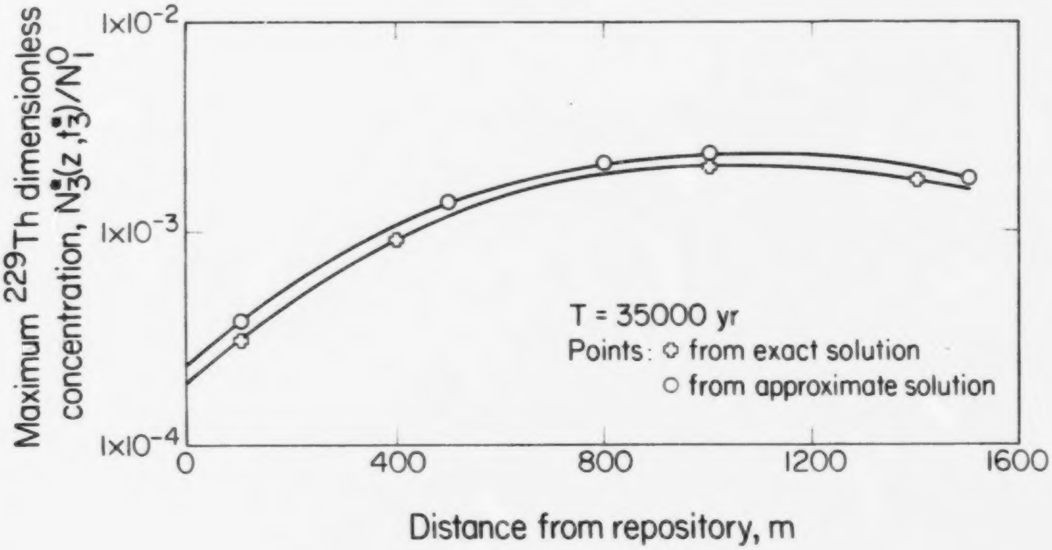

XBL 812-222

Figure 2.7.7b Maxima concentrations of ^{229}Th at different fixed positions. No initial daughters ($N_2^0 = N_3^0 = 0$). No dispersion. T = 35000 years.

Finally, in Figures (2.7.8a) and (2.7.8b) the comparison is made for the case when the initial daughter concentrations are in transient equilibrium. The curves for the case of a leach time of 3500 yr still show good agreements but the curves for the case of a leach time of 35000 yr show a small deviation.

The comparisons between maxima concentrations obtained by evaluating the exact solutions formulas (reference H1, Eq. (4.1.27)) and by using the approximate method developed in this report are summarized below.

Deviations of the values obtained by the approximate method from those of the exact solution are expressed in terms of percent error which is defined as:

$$e = \frac{\text{exact value - approximate value}}{\text{exact value}} \times 100 \quad (\%) \qquad (2.7.67a)$$

Here, the two chains analysed previously in this section are studied again but using instead the initial concentrations and sorption coefficients listed in Table (2.7.14a).

Tables 2.7.10a through 2.7.10d show the percent error in the maxima concentrations calculation of ^{226}Ra, ^{229}Th, ^{230}Th and ^{233}U, respectively, at different values of the ratio path length/groundwater velocity (z/v) and at different leach times.

All four tables show that for leach times smaller than 10^3 years where the condition $T < 1/\lambda_j$ $(j = 1,2,3)$ (Eq. 2.7.10a) is satisfied, the error is negligible for all values of z/v.

For leach times between 10^3 - 10^4 years the error is greater than 10 percent only for path length/groundwater velocity ratios smaller than 1 year.

Since groundwater velocities are expected to be smaller than 10 m/yr, for this leach time the approximate method is applicable for path lengths $z > 10$ meters.

Finally, for leach times of the order of 10^5 years or larger, the error becomes unacceptable for any value of the ratio path length/groundwater velocity.

In view of the above results, the condition $T < 1/\lambda_j$ $(j = 1,2,3)$ can be relaxed and the validity of the method for the adopted set of sorption constant can be extended to leach times of the order of 10^4 years provided that $z/v < 1$ yr.

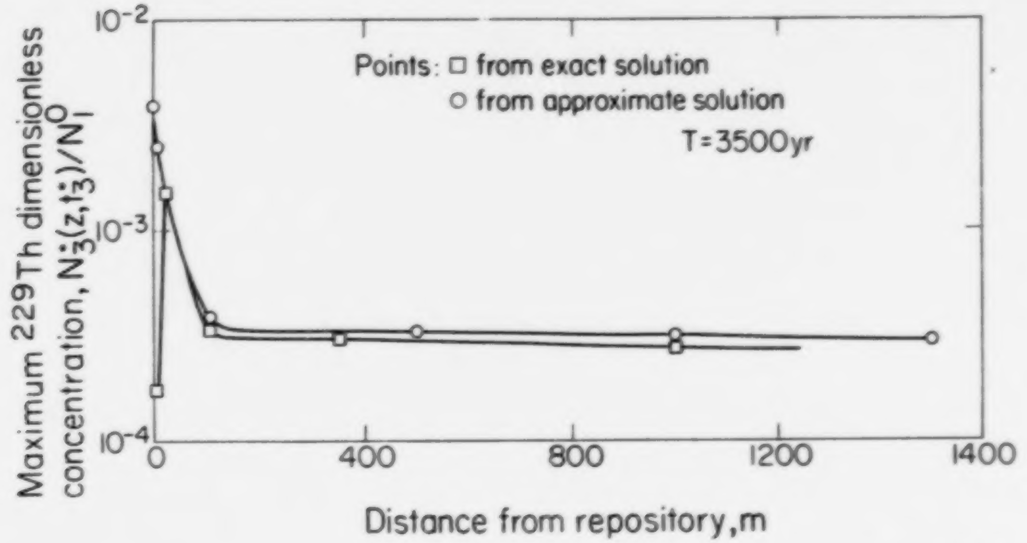

Figure 2.7.8a Maxima concentrations of ^{229}Th at different fixed positions. Initial transient equilibrium. No dispersion. T = 3500 years.

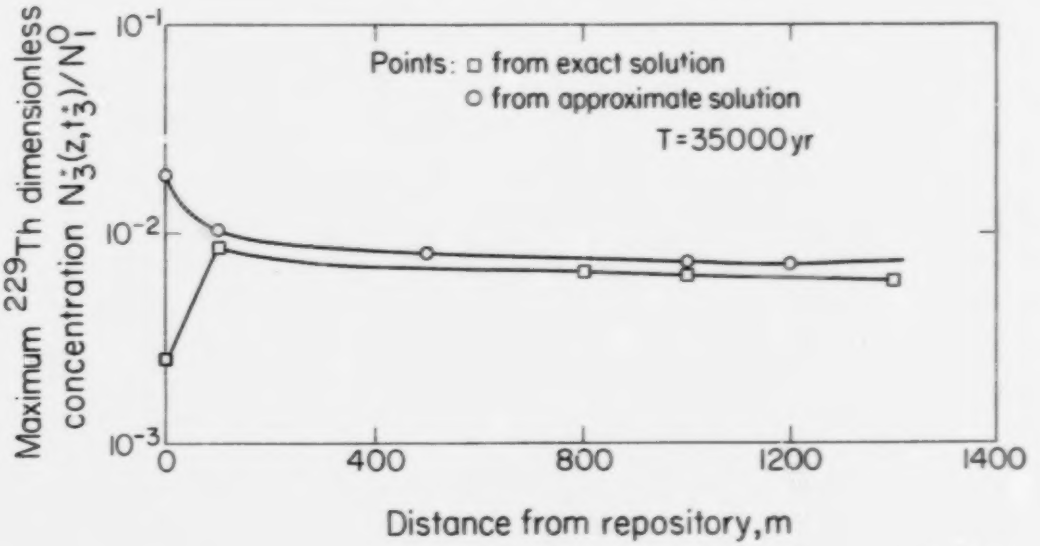

Figure 2.7.8b Maxima concentrations of ^{229}Th at different fixed positions. Initial transient equilibrium. No dispersion. T = 35000 years.

z/v(yr)	T(yr): 10	10^2	10^3	10^4	10^5
10^{-2}	0	8.0	10.0	49.0	24.0
10^{-1}	0	1.0	3.0	38.0	98.0
10^{0}	0	0	0.2	11.0	42.0
10^{1}	0	0	0	3.0	39.0
10^{2}	0	0	0	3.0	43.0
10^{3}	0	0	0	3.0	40.0
10^{4}	-	-	-	-	50.0

Table 2.7.10a: Percent error of the approximate method in the evaluation of the maxima concentrations of ^{226}Ra

z/v(yr)	T(yr): 10	10^2	10^3	10^4	10^5
10^{-2}	0	7.0	55.0	85.0	95.0
10^{-1}	0	7.0	42.0	75.0	93.0
10^{0}	0	5.0	18.0	50.0	82.0
10^{1}	0	4.0	9.0	19.0	82.0
10^{2}	0	0	0	1.0	14.0
10^{3}	0	0	0	1.0	10.0
10^{4}	0	-	0	1.0	10.0

Table 2.7.10b: Percent error of the approximate method in the evaluation of the maxima concentrations of ^{229}Th

z/v(yr)	T(yr) 10	10^2	10^3	10^4	10^5
10^{-2}	0	7.0	19.0	52.0	33.0
10^{-1}	0	5.0	9.0	41.0	30.0
10^{0}	0	0	5.2	22.0	2.0
10^{1}	0	0	1.0	8.0	94.0
10^{2}	0	0	1.0	6.0	96.0
10^{3}	0	0	1.0	6.0	124.0
10^{4}	-	-	-	-	-

Table 2.7.10c: Percent error of the approximate method in the evaluation of the maxima concentrations of ^{230}Th

z/v(yr)	T(yr) 10	10^2	10^3	10^4	10^5
10^{-2}	0	7.0	30.0	81.0	99.0
10^{-1}	0	6.0	22.0	72.0	99.0
10^{0}	0	0	9.0	55.0	99.0
10^{1}	0	0	5.0	23.0	98.0
10^{2}	0	0	1.0	2.0	27.0
10^{3}	0	0	1.0	2.0	33.0
10^{4}	0	-	1.0	2.0	23.0

Table 2.7.10d: Percent error of the approximate method in the evaluation of the maxima concentrations of ^{233}U

2.7.10 Analysis of the effects of variation in parameters values on the maxima concentrations

In this section we apply the method developed in previous sections to analyse the effects on the maximum concentration caused by variations in the values of the parameters.

The main advantage of this present method is that it avoids the need of detailed evaluation of the complete solution and the subsequent search for the extremum. One can use this method to analytically evaluate directly the extremum, saving therefore considerably computing time.

Although this can be done with the help of a pocket calculator, when a large number of cases is to be evaluated as in the case of a parametric analysis, it is very useful to program this method into the computer so that one can evaluate the extremum of any number of nuclides and for any number of sets of parameters all at once.

A computer program called MAX1 (see Appendix D) was developed which uses this method in evaluating the potential hazard at the biosphere resultant from the release of radionuclides present in the high level waste canisters.

According to the assumptions made in the development of the method, MAX1 will be restricted to the following:

a. One dimensional systems
b. Constant water velocity, soil and water properties
c. Negligible dispersion effects
d. Leach times smaller than the half-lives of nuclides envolved.
e. Maximum chain size is three members.

MAX1 will evaluate the following for an i^{th} nuclide:

i) Time of maxima at a fixed given position (t_i^*)

ii) The maximum dimensionless concentration: $N_i^* \frac{z_i, t_i^*}{N_1^o}$

iii) The correspondent maximum water dilution rate (see Section 2.7.10.B).

iv) The contamination time for that position: (θ_i)

In order to apply this method for any nuclide, it is necessary first to reduce the long actinide chains into 3 members or less chains by suitable simplifications.

2.7.10.A Reduction of the actinides chains

The actinides chains present in high level wastes have more than three members and cannot be treated by the method above. But because some elements have very short half lives while some others have very long half-lives, these chains can be broken into shorter chains.

There are four distinct complete actinide chains present in high level wastes. They are shown in Table (2.7.11) below.

In order to reduce these chains into smaller chains, the following factors must be taken into account:

i) Whether the waste is unreprocessed or reprocessed; which type of reactor has generated it; when the leaching starts after the burial. These factors determine basically the initial amount of a given nuclide.

ii) The relative magnitudes of sorption equilibrium coefficients and half-lives of a precursor and its daughters. (See discussion about secular equilibrium for migrating chains in H1, Section 4.5.)

For this present case we will consider the initial amount of actinides in the waste as being that of the reprocessed HLW from spent fuels of a PWR and the range of time for beginning of leaching is below 10^5 yrs.

With these assumptions we have defined the nuclides activities that are initially present in the repository.

In addition, we assume that the sorption equilibrium constants of the actinides do not differ more than four orders of magnitude from each other.

With above assumptions the following simplifications can be made:

A very short-lived nuclide can be considered as being in secular equilibrium with its long-lived precursor, i.e., $\lambda_{i-1}K_{i-1}N_{i-1} = \lambda_i K_i N_i$. According to reference (H1) section 4.5 the necessary conditon to have secular equilibrium is that $\lambda_i K_i >> \lambda_{i-1}K_{i-1}$. Since we have assumed that the equilibrium constants do not differ more than four orders of Table 2.7.11 magnitude from each other, the half-life of the daughter must be four or more orders of magnitude smaller.

Table 2.7.11: Actinides Chains Present in PWR Spent Fuel and Reprocessed Waste.

I) The 4n+3 chain:

$$ {}^{251}\mathrm{Cf}_{98} \xrightarrow[900\ \mathrm{yr}]{\alpha} {}^{247}\mathrm{Cm}_{96} \xrightarrow[1.54\times10^{7}\ \mathrm{yr}]{\alpha} {}^{243}\mathrm{Pu}_{94} \xrightarrow[4.96\ \mathrm{hr}]{\beta^-} {}^{243}\mathrm{Am}_{95} \xrightarrow[7370\ \mathrm{hr}]{\alpha} {}^{239}\mathrm{Np}_{93} \rightarrow $$

$$\begin{tikzcd}
\rightarrow {}^{239}\mathrm{Np}_{93} \arrow[r, "\beta^-", "2350\ \mathrm{d}"'] & {}^{239}\mathrm{Pu}_{94} \arrow[r, "\alpha", "2.44\times10^{4}\ \mathrm{yr}"'] & {}^{235}\mathrm{U}_{92} \arrow[r, "\alpha", "7.0\times10^{8}\ \mathrm{yr}"'] & {}^{231}\mathrm{Th}_{90} \arrow[r, "\beta^-", "25.52\ \mathrm{hr}"'] & {}^{231}\mathrm{Pa}_{91} \rightarrow \\
{}^{243}\mathrm{Cm}_{96} \arrow[ur, "\alpha", "28\ \mathrm{yr}"'] & & & &
\end{tikzcd}$$

$$ \rightarrow {}^{231}\mathrm{Pa}_{91} \xrightarrow[3.25\times10^{4}\ \mathrm{yr}]{\alpha} {}^{227}\mathrm{Ac}_{89} \xrightarrow[21.8\ \mathrm{yr}]{\beta^-} {}^{227}\mathrm{Th}_{90} \xrightarrow[18.27\ \mathrm{d}]{\alpha} {}^{223}\mathrm{Ra}_{88} \xrightarrow[11.43\ \mathrm{d}]{\alpha} {}^{219}\mathrm{Ru}_{86} \rightarrow $$

$$ \rightarrow {}^{219}\mathrm{Ru}_{86} \xrightarrow[3.96\ \mathrm{s}]{\alpha} {}^{215}\mathrm{Po}_{84} \xrightarrow[1.78\ \mathrm{ms}]{\alpha} {}^{211}\mathrm{Pb}_{82} \xrightarrow[36.1\ \mathrm{m}]{\beta^-} {}^{211}\mathrm{Bi}_{83} \xrightarrow[2.14\ \mathrm{m}]{\alpha} {}^{207}\mathrm{Ti}_{81} \rightarrow $$

$$ \rightarrow {}^{207}\mathrm{Ti}_{81} \xrightarrow[4.77\ \mathrm{m}]{\beta^-} {}^{207}\mathrm{Pb}_{82} $$

III) The 4n+1 chain:

$${}^{245}\mathrm{Cm}_{96} \xrightarrow[8.5\times10^{3}\,\mathrm{yr}]{\alpha} {}^{241}\mathrm{Pu}_{94} \xrightarrow[15\ \mathrm{yr}]{\beta^-} {}^{241}\mathrm{Am}_{95} \xrightarrow[433\ \mathrm{yr}]{\alpha} {}^{237}\mathrm{Np}_{93} \xrightarrow[2.14\times10^{6}\,\mathrm{yr}]{\alpha} {}^{233}\mathrm{Pa}_{91} \rightarrow$$

$$\rightarrow {}^{233}\mathrm{Pa}_{91} \xrightarrow[27\ \mathrm{d}]{\beta^-} {}^{233}\mathrm{U}_{92} \xrightarrow[1.58\times10^{5}\,\mathrm{yr}]{\alpha} {}^{229}\mathrm{Th}_{90} \xrightarrow[7340\ \mathrm{yr}]{\alpha} {}^{225}\mathrm{Ra}_{88} \xrightarrow[14.8\,\mathrm{d}]{\beta^-} {}^{225}\mathrm{Ac}_{89} \rightarrow$$

$$\rightarrow {}^{225}\mathrm{Ac}_{89} \xrightarrow[10\ \mathrm{d}]{\alpha} {}^{221}\mathrm{Fr}_{87} \xrightarrow[4.8\ \mathrm{m.}]{\alpha} {}^{217}\mathrm{At}_{85} \xrightarrow[32\ \mathrm{ms}]{\alpha} {}^{213}\mathrm{Bi}_{83} \xrightarrow[46\ \mathrm{m}]{\beta^-} {}^{213}\mathrm{Po}_{84} \rightarrow$$

$$\rightarrow {}^{213}\mathrm{Po}_{84} \xrightarrow[4\ \mu\mathrm{s}]{\alpha} {}^{209}\mathrm{Pb}_{82} \xrightarrow[3.3\ \mathrm{hr}]{\beta^-} {}^{209}\mathrm{Bi}_{83}$$

IV) The 4n chain:

$${}^{244}\mathrm{Cm}_{96} \xrightarrow[17.9\ \mathrm{yr}]{\alpha} {}^{240}\mathrm{Pu}_{94} \xrightarrow[6540\,\mathrm{yr}]{\alpha} {}^{236}\mathrm{U}_{92} \xrightarrow[2.3\times10^{7}\,\mathrm{yr}]{\alpha} {}^{232}\mathrm{Th}_{90} \xrightarrow[1.4\times10^{10}\,\mathrm{yr}]{\alpha} {}^{228}\mathrm{Ra}_{88} \rightarrow$$

$$\begin{tikzcd}
\rightarrow {}^{228}\mathrm{Ra}_{88} \arrow[r, "\beta^-", "5.75\,\mathrm{yr}"'] & {}^{228}\mathrm{Ac}_{89} \arrow[r, "\beta^-", "6.13\,\mathrm{hr}"'] & {}^{228}\mathrm{Th}_{90} \arrow[r, "\alpha", "1.91\,\mathrm{yr}"'] & {}^{224}\mathrm{Ra}_{88} \arrow[r, "\alpha", "3.64\,\mathrm{d}"'] & {}^{220}\mathrm{Ru}_{86} \rightarrow \\
& {}^{232}\mathrm{U}_{92} \arrow[ur, "\alpha", "72\mathrm{yr}"'] & & &
\end{tikzcd}$$

$$\rightarrow {}^{220}\mathrm{Ru}_{86} \xrightarrow[55.6\ \mathrm{s}]{\alpha} {}^{216}\mathrm{Po}_{84} \xrightarrow[0.15\ \mathrm{s}]{\alpha} {}^{212}\mathrm{Pb}_{82} \xrightarrow[10.64\ \mathrm{hr}]{\beta^-} {}^{212}\mathrm{Bi}_{83} \xrightarrow[60\ \mathrm{m}]{\beta^-} {}^{212}\mathrm{Po}_{84} \rightarrow$$

$$\rightarrow {}^{212}\mathrm{Po}_{84} \xrightarrow[45\ \mathrm{s}]{\alpha} {}^{208}\mathrm{Pb}_{82}$$

II) The 4n+2 chain:

$$^{246}Cm_{96} \xrightarrow[4.76\times10^{3}\,yr]{\alpha} {}^{242}Pu_{94} \xrightarrow[3.87\times10^{5}\,yr]{\alpha} {}^{238}U_{92} \xrightarrow[4.47\times10^{9}\,yr]{\alpha} {}^{234}Th_{90} \xrightarrow[24.1\,d]{\beta^-} {}^{234}Pa_{91} \rightarrow$$

$$\rightarrow {}^{234}Pa_{91} \xrightarrow[6.67\,hr]{\beta^-} {}^{234}U_{92} \xrightarrow[2.44\times10^{5}\,yr]{\alpha} {}^{230}Th_{90} \xrightarrow[7.7\times10^{4}\,yr]{\alpha} {}^{226}Ra_{88} \xrightarrow[1600\,yr]{\alpha} {}^{222}Rn_{86} \rightarrow$$

from IIa

$$\rightarrow {}^{222}Rn_{86} \xrightarrow[3.8\,d]{\alpha} {}^{218}Po_{84} \xrightarrow[3.05\,m]{\alpha} {}^{214}Pb_{82} \xrightarrow[26.8\,m]{\beta^-} {}^{214}Bi_{83} \xrightarrow[19.8\,m]{\beta^-} {}^{214}Po_{84} \rightarrow$$

$$\rightarrow {}^{214}Po_{84} \xrightarrow[163.7\,\mu s]{\alpha} {}^{210}Pb_{82} \xrightarrow[22.3\,yr]{\beta^-} {}^{210}Bi_{83} \xrightarrow[5.01\,d]{\beta^-} {}^{210}Po_{84} \xrightarrow[138.4\,d]{\alpha} {}^{206}Pb_{82}$$

IIa): Branch of 4n+2 chain

$$^{242m}Am_{95} \xrightarrow[152\,yr]{I.C.} {}^{242}Am_{95} \xrightarrow[16\,hr]{\beta^-} {}^{242}Cm_{96} \xrightarrow[163\,d]{\alpha} {}^{238}Pu_{94} \xrightarrow[84.8\,yr]{\alpha} {}^{234}U_{92} \rightarrow$$

On the other hand, if a nuclide has a much longer half-life than its precursors one can assume that every short lived precursor initially present in the waste has decayed by the time that waste dissolution begins. The initial concentration of this long-lived nuclide should include those of the precursors which have already decayed.

With these two assumptions, each one of the four chains can be broken into the following smaller chains: (The nuclides in parentheses are in secular equilibrium with its precursor).

The first chain I, (4n+3 chain) can be subdivided into the following chains:

I-1) $^{251}Cf_{98} \xrightarrow[900\ yr]{\alpha}$

I-2) $^{247}Cm_{96}\ (^{243}Pu_{94}) \xrightarrow[1.57x10^{7} yr]{\alpha} {}^{243}Am_{95}(^{230}Np) \xrightarrow[7370\ yr]{\alpha} {}^{239}Pu_{94} \xrightarrow[2.44x10^{4} yr]{\alpha}$

(assume that all $^{243}Cm_{96}$ has decayed to $^{239}Pu_{94}$)

I-3) $^{235}U_{92}(^{231}Th_{90}) \xrightarrow[7.0x10^{8} yr]{\alpha} {}^{231}Pa_{91}(^{227}Ac_{89}) \xrightarrow[3.25x10^{4} yr]{\alpha}$

Subsequent elements are in secular equilibrium with $^{231}Pu_{91}$. The next Chain II (4n+2 chain) can be subdivided into the following chains:

II-1) $^{246}Cm_{96} \xrightarrow[4.76x10^{3} yr]{\alpha} {}^{242}Pu_{94} \xrightarrow[3.87x10^{5} yr]{\alpha}$

If the times of interest are of the order of the $^{234}U_{92}$ half-life or longer one should consider the following chain:

II-2a) $^{238}U_{92}(^{234}U_{92}, {}^{234}Th_{90}, {}^{234}Pa_{91}) \xrightarrow[4.5x10^{9} yr]{\alpha} {}^{230}Th_{90} \xrightarrow[7.7x10^{4} yr]{\alpha} {}^{226}Ra_{88} \xrightarrow[1600\ yr]{\alpha}$

This is because $^{234}U_{92}$ has decayed significantly and the contribution to the concentrations of the daughters $^{230}Th_{90}$ and $^{226}Ra_{88}$ comes from $^{238}U_{92}$ decay.

On the other hand, if the time scale is smaller than $^{234}U_{92}$ half-life the following chains should be considered instead of (II-2a):

II-2b) $^{238}U_{92}(^{234}Th_{90}, ^{234}Pa_{91}) \xrightarrow[4.47\times10^{9}\,yr]{\alpha}$

II-3) $^{234}U_{92} \xrightarrow[2.44\times10^{5}\,yr]{\alpha} {}^{230}Th_{90} \xrightarrow[7.7\times10^{4}\,yr]{\alpha} {}^{226}Ra_{88} \xrightarrow[1600\ yr]{\alpha}$

In this later case, if the dissolution begins after hundreds of years or more one can assume that every nuclide in the branch IIa of the chain 4n+3 has decayed to form $^{234}U_{92}$ nuclides. But sometimes we are interested in the effects of fuel dissolution beginning at the time the waste is emplaced, and at other times we are interested in what happens if dissolution does not begin for hundreds of years or more. The decay of the initial $^{238}Pu_{94}$, $^{242m}Am_{95}$ and $^{242}Cm_{96}$ in the waste to form $^{234}U_{92}$ is important. In waste from fuel reprocessed a few months after discharge, $^{242}Cm_{96}$ is the most important source of $^{234}U_{92}$(B2). This and the less important sources $^{238}Pu_{94}$ and $^{242m}Am_{95}$ would have to be considered as members of the chain if the dissolution were assumed to occur immediately and if we were interested in the contamination of groundwater quite near the repository.

In any of the above cases, all remaining nuclides are in secular equilibrium with $^{226}Ra_{88}$.

In chain III, (the 4n+1 chain) one can neglect the first element $^{245}Cm_{96}$ because of the low quantities present initially in the reprocessed waste.

On the other hand, there is a large amount of $^{241}Pu_{94}$. For practical purposes, the chain beginning with the decay of $^{241}Pu_{94}$, to form $^{241}Am_{95}$ and $^{237}Np_{93}$, is quite important. If waste dissolution were to begin at the time waste is put into a repository, the existing inventory of $^{241}Pu_{94}$ in unreprocessed spent fuel is important, even after a delay time of 10 years from reactor discharge to emplacement in a repository.

If waste dissolution were not to begin for a hundred years or so, from a practical point of view $^{241}Am_{95}$ becomes the first member, i.e., the half-life for the effective decay of the parent of $^{241}Am_{95}$ is only 13 yr instead of 8500 yr.

If waste dissolution begins hundreds of years or more after emplacement the chain III (4n+1 chain) can be reduced to the following chain:

$$^{237}Np_{93}(^{233}Pa_{91}) \xrightarrow[2.14\times10^{6}\text{yrs}]{\alpha} {}^{233}U_{92} \xrightarrow[1.58\times10^{5}\text{yr}]{\alpha} {}^{229}Th_{90} \xrightarrow[7340\text{ yr}]{\alpha}$$

Where the initial amount of $^{237}Np_{93}$ should include the decay of $^{241}Pu_{94}$, $^{241}Am_{95}$.

All other subsequent nuclides are in secular equilibrium with $^{229}Th_{90}$.

Finally, chain IV (4n chain) can be reduced to the following chain:

$$^{240}Pu_{94} \xrightarrow[6540\text{ yr}]{\alpha} {}^{236}U_{92} \xrightarrow[2.3\times10^{7}\text{yr}]{\alpha} {}^{232}Th_{90} \xrightarrow[1.4\times10^{10}\text{yr}]{\alpha}$$

$^{232}U_{92}$ can be neglected, and all other subsequent nuclides are in secular equilibrium with $^{232}Th_{90}$.

2.7.10.B Evaluation of peak water dilution rate

To estimate the potential hazard to the biosphere we use the Maximum Permissible Concentration (MPC) according to 10 CFR Part 20, Appendix B. These are the nuclide concentrations in water which will result in the maximum allowable dose for an average individual who has all his water intake from such a source. The water dilution rate is the volumetric flow rate of aquifer or surface water into which the migrating radionuclides discharge such that the concentration of any nuclide will not be above the MPC concentration.

Therefore, the peak water dilution rate is calculated as follows:

$$I_i = Q\lambda_i N_i^*(z,t_i^*)/(MPC) \qquad (2.7.68)$$

where Q is the volumetric groundwater flow rate (M^3/yr) and $(MPC)_i$ has units of (Curie/m^3). They are listed in Table (2.7.14a).

2.7.10.C The reference case and the range of variation of the parameters

The reference case is defined by the following set of parameters:

i) The time lapsed between the emplacement and the beginning of the waste dissolution is denoted by t_s and is taken to be 1000 yrs. This parameter represents the expected lifetime of the protective canisters and barriers. t_s does not show up directly in the solutions but its variation leads to changes in the initial inventory of each nuclide present in the waste when the leaching starts.

The nuclide inventories present in the waste at $t_s = 10^3$yr are listed in Table (2.7.14a) and they were obtained from reference (B2). These inventories are from the reprocessed waste of spent fuels of a PWR after generating 1GW(e) yr of electricity with a load factor of 80 percent, a thermal efficiency of 34 percent and a burnup of 30.4 MWD/kg.

These spent fuels are reprocessed after 150 days cooling period and 0.5 percent of the Pu and U are lost to the waste. The time elapsed between discharge and emplacement in the repository is assumed to be negligible.

ii) The duration of the release (leach time) is denoted by T and is taken to be 10^4 yrs. This number represents the expected lifetime of a proposed waste form. It is assumed that the waste matrix dissolves at a constant rate over time T and all contained radionuclides dissolve when the matrix dissolves.

iii) The position downstream where the contaminated water streamline meets the aquifer is called the path length. It is denoted by z and for the reference case it will be 1000m.

iv) The reference velocity of the water flowing past the repository will be v=10 m/yr. The reference water travel time will be therefore $z/v = 10^2$ yr.

v) The sorption retardation constant is denoted by K_i. The reference set of values is given in Table (2.7.14a), obtained from reference B2.

The procedure adopted here to analyze the effects of the variation of the parameters values on the maximum water dilution rate is to keep all parameters fixed at the reference values with the exception of one of them which is varied. This is done in turn for each one of the relevant parameters.

Each parameter is varied in the range given by Table (2.7.12) below:

		Minimum	Maximum
Time of beginning of leaching	t_s	1 yr	10^5 yr
Leach time	T	10 yr	50,000 yr
Water travel time	z/v	10^{-3} yr	10^8 yr
Equilibrium constant	K_i	10^2	10^4

Table 2.7.12: Range of variation of the parameters

The analysis of the variation of the sorption equilibrium constant for nuclides which are 1st members of a chain can be studied by the results of the variation in water velocity. This is because they are both related to the same parameter $v_i = v/K_i$. For three-member chains the following cases were calculated:

	Cases:	K_1	K_2	K_3
1	$K_3 > K_2 > K_1$	10^2	Varied	10^4
2	$K_1 > K_2 > K_3$	10^4	Varied	10^2
3	$K_2 > K_3 > K_1$	10^2	10^4	Varied
4	$K_1 > K_3 > K_2$	10^4	10_2	Varied
5	$K_2 > K_1 > K_3$	Varied	10^4	10^2
6	$K_3 > K_1 > K_2$	Varied	10^2	10^4

Table 2.7.13: Variation of equilibrium constants values for three-member chain analysis.

In each one of the six cases described in Table 2.7.13 one of the equilibrium constants is kept fixed at the lower limit (10^2), the other at the upper limit (10^4), while the third is varied inside the range (10^2-10^4). The calculations are done for every one of the six possible combinations described in Table 2.7.13.

With these six cases we cover the possible different combinations of equilibrium constants for three member chains. Consider for instance case 1. When K_2 approaches $K_1 = 10^2$, case 1 tends to case 6 and if K_2 approaches $K_3 = 10^4$, case 1 in this case tends to case 3.

By analyzing these 6 cases one can predict qualitatively the behavior of the solution for a 3 member chain for any different combination of sorption coefficients.

2.7.10.D Results of the calculations

i) The reference case:

Table 2.7.14a and Table 2.7.14b show the results of the calculations for the reference case. In Table 2.7.14a the nuclide parameters are listed. The column titled "Member" indicates whether the element is considered a first, second or third member in a chain. A number 4 indicates that the nuclide is in secular equilibrium with the nearest long lived precursor.

The last column which is titled "Attenuation factor" is the product $\lambda_i K_i$ (1/yr).

Table 2.7.14b actually shows the results of the calculation. The number under the column "1st" is the identification number of the 1st precursor of that nuclide (if any) and the number under the column "2nd" is the identification number of the 2nd precursor (if any).

Let us identify the results in each column with the nomenclature used in past sections:

"TIME OF PEAK (yr)" = t_i^*
"MAXIMUM N/NO" = $N_i^*(z,t_i^*)/N_i^o$
"WATDIL (m^3/yr.Gw(e)yr)" = I_i
"CONTAM. TIME (yr)" = θ_i

For the reference case, the largest peak water dilution rate is that of ^{129}I which is a volatile fission product. Although it has been recovered

Table 2.7.14a: Sample Output - Nuclide Parameters for the Reference Case. (The Nuclide Parameters are Listed Below) Time for Beginning of Leaching is 1.00E+03(YR)

NUMBER	NUCLIDE	MEMBER	HALF-LIFE (YR)	SORPTION CONST.	MPC (CI/M**3)	INITIAL ACTIVITY(CI)	ATTENUATION FACTOR (1/YR)
1	H-3	1	1.20E+01	1.00E+00	3.00E-03	1.58E-21	5.78E-02
2	C-14	1	5.60E+03	1.00E+01	8.00E-04	1.15E+01	1.24E-03
3	SE-79	1	6.50E+04	1.00E+02	3.00E-04	1.09E+01	1.07E-03
4	SR-90	1	2.80E+01	1.00E+02	3.00E-07	3.74E-05	2.48E+00
5	ZR-93	1	9.50E+05	1.00E+04	8.00E-04	5.20E+01	7.29E-03
6	NB-93M	1	1.40E+01	1.00E+04	4.00E-04	1.59E-21	4.95E+02
7	TC-99	1	2.10E+05	1.00E+00	2.00E-04	3.89E+02	3.30E-06
8	RU-106	1	1.00E+00	1.00E+01	1.00E-05	1.00-200	6.93E+00
9	CO-113	1	1.40E+01	1.00E+04	3.00E-05	4.13E-19	4.95E+02
10	SM-126	1	1.00E+05	1.00E+03	2.00E-05	1.49E+01	6.93E-03
11	SB-125	1	2.70E+00	1.00E+02	1.00E-04	7.13-107	2.57E+01
12	I-129	1	1.70E+07	1.00E+00	6.00E-08	1.00E+00	4.08E-08
13	CS-134	1	2.00E+00	1.00E+03	2.00E-05	1.91-144	3.47E+02
14	CS-135	1	3.00E+06	1.00E+03	1.00E-04	7.80E+00	2.31E-04
15	CS-137	1	3.00E+01	1.00E+03	2.00E-05	2.69E-04	2.31E+01
16	CE-144	1	7.80E-01	2.20E+03	1.00E-05	1.00-200	1.95E+03
17	PM-147	1	4.40E+00	2.50E+03	2.00E-04	1.07E-62	3.94E+02
18	SM-151	1	8.70E+01	2.50E+03	4.00E-04	1.18E+01	1.99E+01
19	EU-152	1	1.30E+01	2.50E+03	6.00E-05	2.33E-21	1.33E+02
20	EU-154	1	1.60E+01	2.50E+03	2.00E-05	2.94E-14	1.08E+02
21	EU-155	1	1.80E+00	2.50E+03	2.00E-04	1.06-162	9.62E+02
22	RA-225	4	4.10E-02	5.00E+02	5.00E-07	2.86E-03	8.45E+03
23	RA-226	3	1.60E+03	5.00E+02	3.00E-08	3.25E-03	2.17E-01
24	TH-228	4	1.90E+00	5.00E+04	7.00E-06	2.45E-02	1.82E+04
25	TH-229	3	7.30E+03	5.00E+04	5.00E-07	2.86E-03	4.75E+00
26	TH-230	2	8.00E+04	5.00E+04	2.00E-06	1.72E-02	4.33E-01
27	U-233	2	1.60E+05	1.40E+04	3.00E-05	6.22E-02	6.06E-02
28	U-234	1	2.50E+05	1.40E+04	3.00E-05	1.99E+00	3.88E-02
29	U-235	1	7.10E+08	1.40E+04	3.00E-05	7.60E-03	1.37E-05
30	U-238	1	4.50E+09	1.40E+04	4.00E-05	4.50E-02	2.16E-06
31	NP-237	1	2.10E+06	1.00E+02	3.00E-06	1.44E+01	3.30E-05
32	PU-238	2	8.60E+01	1.00E+04	5.00E-06	2.84E+00	8.06E+01
33	PU-239	2	2.40E+04	1.00E+04	5.00E-06	5.58E+01	2.89E-01

Table 2.7.14a (Continued)

NUMBER	NUCLIDE	MEMBER	HALF-LIFE (YR)	SORPTION CONST.	MPC (CI/M**3)	INITIAL ACTIVITY(CI)	ATTENUATION FACTOR (1/YR)
34	PU-240	2	6.60E+03	1.00E+04	5.00E-06	2.45E+02	1.05E+00
35	PU-241	4	10.3E+01	1.00E+04	2.00E-04	9.10E+00	5.33E+02
36	PU-242	2	3.80E+05	1.00E+04	5.00E-06	1.93E-01	1.82E-02
37	AM-241	2	4.60E+02	1.10E+04	4.00E-06	1.91E+04	1.66E+01
38	AM-42M	1	1.50E+02	1.10E+04	4.00E-06	1.18E+00	5.08E+01
39	AM-243	1	7.90E+03	1.10E+04	4.00E-06	4.40E+02	9.65E-01
40	CM-242	4	4.50E-01	3.00E+03	2.00E-05	1.18E+00	4.62E+03
41	CM-243	1	3.20E+01	3.00E+03	5.00E-06	3.54E-08	6.50E+01
42	CM-244	1	1.80E+01	3.00E+03	7.00E-06	1.41E-12	1.16E+02
43	CM-245	1	9.30E+03	3.00E+03	4.00E-06	9.10E+00	2.24E-01
44	CM-246	1	5.50E+03	3.00E+03	4.00E-06	1.68E+00	3.78E-01

a) 1,2,3 indicate first, second or third member of a chain respectively; 4 indicates secular equilibrium with the nearest long lived precursor

b) Sorption constants are the overall equilibrium constant, i.e., the ratio of the amount in water and solid to the amount in water (see B3)

c) MPC are the maximum permissible concentrations in water (see B2)

d) Nuclide activities in waste, 10^3 yrs after emplacement. High level reprocessing waste from 7Gwe produced in a LWR (see B2)

e) Attenuation factors are the products of decay constants and sorption constants.

LEACH TIME (YR)	PATH LENGTH(M)	WATER VELOCITY (M/YR)
1.0000E+04	1.0000E+02	1.0000E+00

No.	NUCLIDE	MEMBER	1ST	2ND	TIME OF PEAK (YR)	MAXIMUM N/NO	WAT. DIL. (M**3/ GW*YR**2)	CONTAM. TIME (YR)	PERCENTAGE
1	H-3	1	0	0	1.00E+02	3.10E-03	1.63E-25	1.00E+04	.000
2	C-14	1	0	0	1.00E+03	8.84E-01	1.27E+00	1.00E+04	.047
3	SE-79	1	0	0	1.00E+04	8.99E-01	3.26E+00	1.00E+04	.121
4	RB-90	1	0	0	1.00E+04	3.25-108	4.06-110	1.00E+04	.000
5	ZR-93	1	0	0	1.00E+06	4.82E-01	3.13E+00	1.00E+04	.116
6	NB-93M	1	0	0	1.00E+06	0.	0.	1.00E+04	0.
7	TC-99	1	0	0	1.00E+02	1.00E+00	1.94E+02	1.00E+04	7.195
8	RU-106	1	0	0	1.00E+03	0.	0.	1.00E+04	0.
9	CD-113	1	0	0	1.00E+06	0.	0.	1.00E+04	0.
10	SM-126	1	0	0	1.00E+05	5.00E-01	3.72E+01	1.00E+04	1.379
11	SB-125	1	0	0	1.00E+04	0.	0.	1.00E+04	0.
12	I-129	1	0	0	1.00E+02	1.00E+00	1.67E+03	1.00E+04	61.715
13	CS-134	1	0	0	1.00E+05	0.	0.	1.00E+04	0.
14	CS-135	1	0	0	1.00E+05	9.77E-01	7.62E+00	1.00E+04	.282
15	CS-137	1	0	0	1.00E+05	0.	0.	1.00E+04	0.
16	CF-144	1	0	0	2.20E+05	0.	0.	1.00E+04	0.
17	PM-147	1	0	0	2.50E+05	0.	0.	1.00E+04	0.
18	SM-151	1	0	0	2.50E+05	0.	0.	1.00E+04	0.
19	EU-152	1	0	0	2.50E+05	0.	0.	1.00E+04	0.
20	EU-154	1	0	0	2.50E+05	0.	0.	1.00E+04	0.
21	EU-155	1	0	0	2.50E+05	0.	0.	1.00E+04	0.
22	RA-225	4	25	0	4.40E+04	3.77E-01	2.16E+01	4.99E+06	.008
23	RA-226	3	26	28	1.40E+06	2.96E-04	3.07E+02	4.95E+06	11.381
24	TH-228	4	34	0	1.00E+06	2.51E-467	8.78E-43	1.00E+06	.000
25	TH-229	3	27	31	4.40E+04	2.61E-07	2.16E-01	4.99E+06	.008
26	TH-230	2	28	0	1.40E+06	2.22E-04	6.93E-02	5.00E+06	.003
27	U-233	2	31	0	1.00E+04	2.44E-05	1.54E-02	1.40E+06	.001
28	U-234	1	0	0	1.40E+06	2.06E-02	1.37E-01	1.00E+04	.005
29	U-235	1	0	0	1.40E+06	9.99E-01	2.53E-02	1.00E+04	.001
30	U-238	1	0	0	1.40E+06	1.00E+00	1.12E-01	1.00E+04	.004
31	NP-237	1	0	0	1.00E+04	9.97E-01	4.78E+02	1.00E+04	17.710

LEACH TIME (YR)	PATH LENGTH(M)	WATER VELOCITY (M/YR)
1.0000E+04	1.0000E+02	1.0000E+00

No.	NUCLIDE	MEMBER	1ST	2ND	TIME OF PEAK (YR)	MAXIMUM N/NO	WAT. DIL. (M**3/ GW*YR**2)	CONTAM. TIME (YR)	PERCENTAGE
32	PU-238	2	38	0	1.10E+06	0.	0.	1.00E+06	0.
33	PU-239	2	39	0	1.00E+06	2.89E-12	8.37E-09	1.00E+06	.000
34	PU-240	2	42	0	1.00E+06	1.60E-29	1.23E-42	1.00E+06	.000
35	PU-241	4	43	0	3.00E+05	1.96E-10	8.90E-10	1.00E+04	.000
36	PU-242	2	44	0	1.00E+06	1.37E+00	6.65E-01	1.00E+06	.025
37	AM-241	2	43	0	3.00E+05	5.47E-11	2.51E-07	1.10E+06	.000
38	AM-42M	1	0	0	1.10E+06	0.	0.	1.00E+04	0.
39	AM-243	1	0	0	1.10E+06	1.24E-42	1.36E-38	1.00E+04	.000
40	CM-242	4	38	0	1.10E+06	0.	0.	1.00E+04	0.
41	CM-243	1	0	0	3.00E+05	0.	0.	1.00E+04	0.
42	CM-244	1	0	0	3.00E+05	0.	0.	1.00E+04	0.
43	CM-245	1	0	0	3.00E+05	1.96E-10	4.45E-08	1.00E+04	.000
44	CM-246	1	0	0	3.00E+05	3.83E-17	1.16E-15	1.00E+04	.000

---

a) Identification number (first column) of the first precursor;

b) Identification number of the 2nd precursor

c) Time of maximum concentration at the given path length

d) Maximum dimensionless concentration:; $N_i(z,t_i)/N_i$

e) Correspondent maximum water dilution rate (see Eq. (2.7.68))

f) Time interval that this nuclide is present at the given path length

g) Percentage of the sum of all peak water dilution rates (in Column 8) for all nuclides.

separately it is assumed to be also present in the dissolving waste material. In addition, it is also assumed that ^{129}I has a dissolution leach time equal to that of the reprocessing high-level waste. (Similar assumptions are made about ^{3}H and ^{14}C.)

Because of its low sorption constant (K=1), ^{129}I peak is the first to arrive at the reference water travel time.

Following ^{129}I, the next important contributor is the actinide ^{237}Np which has high initial activity and toxicity.

^{226}Ra produced by the decay of the ^{234}U originally present at the repository presents also significant peak water dilution rate at this reference water travel time because of its low MPC value. ^{226}Ra has the smallest MPC value followed by ^{129}I.

In addition to ^{129}I, the fission products ^{99}Tc, ^{126}Sm, ^{135}Cs, ^{79}Se and ^{93}Zr also present significant peak water dilution rates.

ii) Variation of parameters results

The variation of peak water dilution rate I_i with water travel time is shown in Figure 2.7.9.

For water travel times smaller than 10 yr ^{241}Am, and ^{239}Pu produce the largest peak water dilution rates. Their peaks die out quickly for larger water travel times.

^{226}Ra water dilution rate builds up from the decay of ^{234}U and reaches the largest value at a water travel time of about 10^{2}yr. Between 10 yr and 10^{3} yr, ^{226}Ra is the largest contributor.

For water travel times larger than 10^{3} years only those nuclide with small attentuation factor will be present.

This is the case of ^{129}I which has the smallest attenuation factor of them all being the last to die out at about 10^{8} years. Allied to its high toxicity, ^{129}I is one of the most important nuclides to be contained.

Besides ^{129}I, at large water travel times, ^{237}Np and ^{99}Tc also present significant water dilution rates. They roll off at about 10^{5} years.

With the exception of ^{129}I, ^{237}Np, and ^{99}Tc all other significant radionuclide have peak water dilution rate curves which roll-off quickly before water travel time of 10^{3} years.

The variation of the time for peak t_i^* with water travel time is shown in Figure 2.7.10. The linear variation is expected for the 1st and 2nd members of chains according to the results of the method developed in preceding sections.

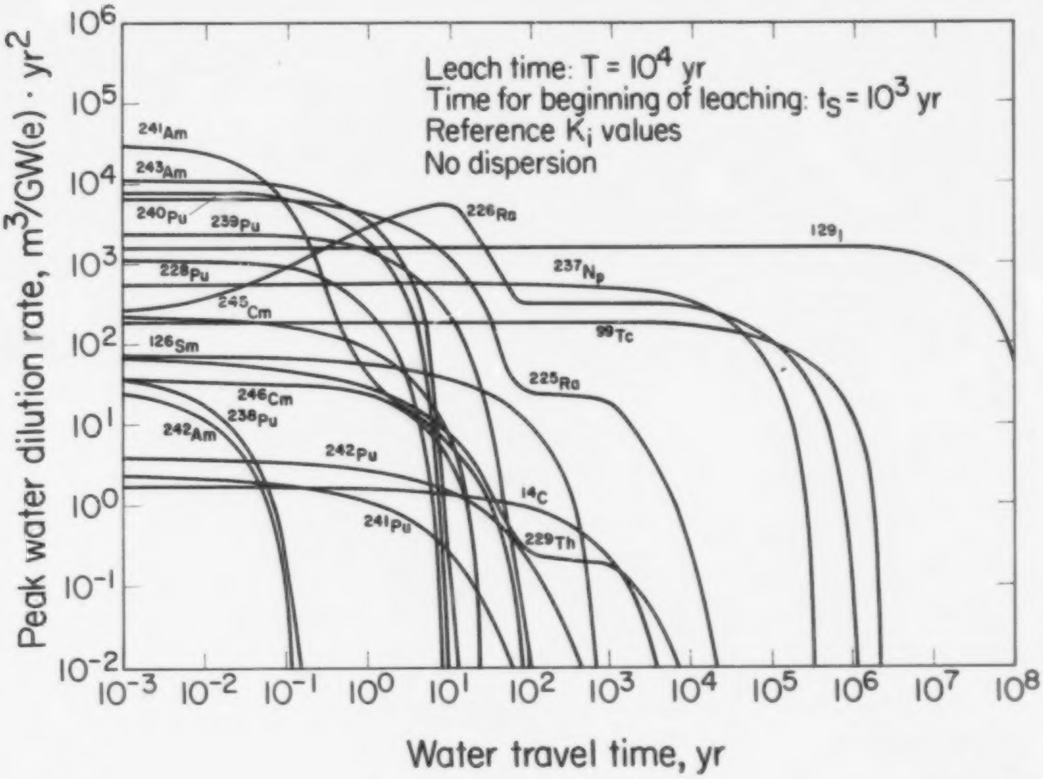

XBL 812-225

Figure 2.7.9 Variation of peak water dilution rate with water travel time for reprocessed PWR high level waste.

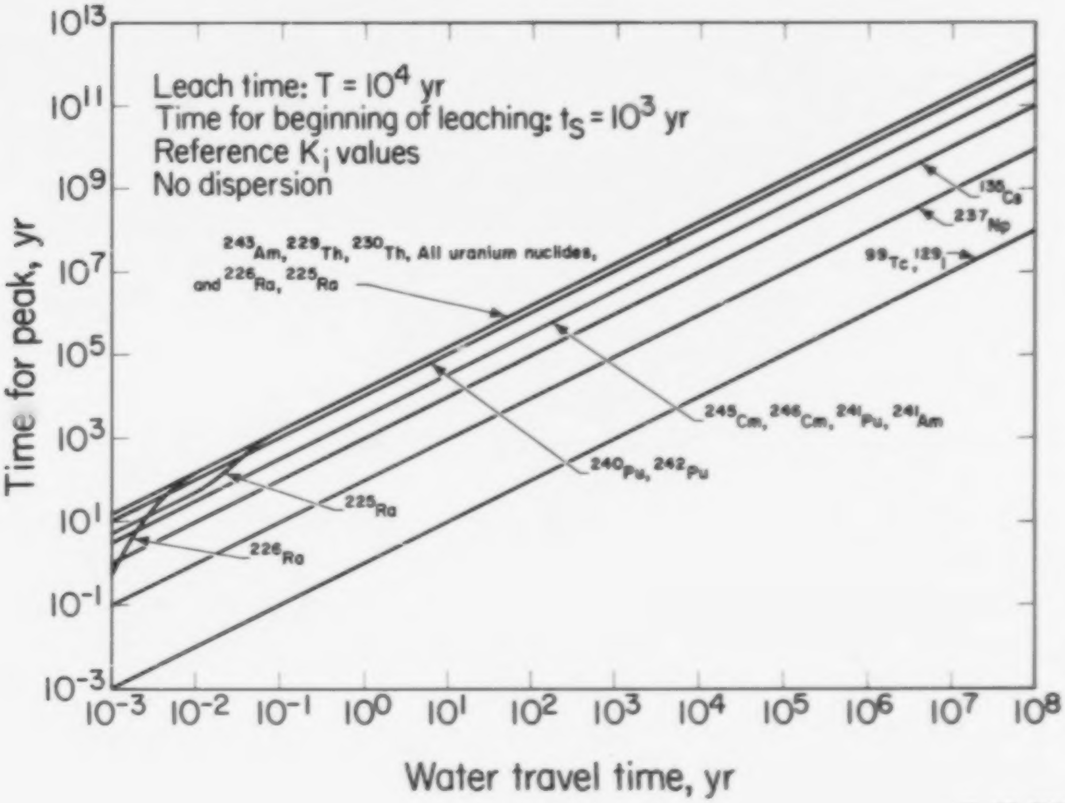

XBL 82-226

Figure 2.7.10 Variation of time for peak with water travel time for reprocessed PWR high level waste.

For the 3rd member nuclides ^{226}Ra and ^{225}Ra we see that their times for peak are interior to the time domain only for very short water travel times ($<10^{-1}$yr).

For larger times their peaks travel on the ^{234}U and ^{233}U characteristics, respectively.

At a given water travel time the first peaks to arrive are those of ^{129}I and ^{99}Tc which travel with the water front velocity because of their assumed equilibrium constant of unity.

One hundred years later the ^{237}Np peak reaches that position followed by the ^{135}Cs peak 10 years later.

Only after about 10^4 years later all other nuclides peaks start to arrive. The nuclides ^{226}Ra , ^{240}Pu, ^{239}Pu, ^{241}Am, and ^{243}Am take a much longer time (10^4 yrs) to reach a given position than ^{129}I and ^{99}Tc.

If these nuclides (^{129}I, ^{99}Tc, ^{226}Ra (thus ^{238}U) and ^{237}Np) could be contained, the range of water travel time of concern would be reduced to 10^3 years, because all other nuclides with significant peak water dilution rates have already decayed to negligible values for water dilution rates before water travel times of 10^3 yrs.

Figure 2.7.11 shows the variation of peak water dilution rate with leach time T for a fixed water travel time.

For all 1st member nuclides for each order of magnitude increase in leach time we have a order of magnitude decrease in its peak water dilution rate.

However, for the 3rd members ^{229}Th(^{225}Ra) and ^{226}Ra changes in leach time have no effect on their peak water dilution rates. Therefore, changes in waste forms will not affect the magnitude of the peak water dilution rates of ^{226}Ra and ^{225}Ra.

Another important result which is not shown graphically but it is implicit in the method is that the time for peak of any nuclide is independent of the leach time.

The effect of variation of the time for beginning of leaching on the peak water dilution rate is minimal as one can see in Figure 2.7.12.

A delay in starting the dissolution can eliminate the shorter lived fission product like ^{3}H, ^{14}C, ^{90}Sr and ^{137}Cs. When leaching begins as early as I year after emplacement the actinides ^{241}Pu, ^{238}Pu and ^{242}Cm have not decayed to their long lived daughters yet and they will be present in the groundwater. But at the assumed reference water travel time of Figure 2.7.12, they have already decayed before they can migrate such a distance.

All other important nuclides have half-lives larger than 10^5 yrs. The initial inventory will not be changed significantly by the presence of engineered barriers. Although these barriers will not affect the magnitude of the peak water dilution rates they will delay the time when these peaks occurs.

The variation of peak water dilution rate of the third members ^{225}Ra and ^{226}Ra with the value of the equilibrium constant are shown in Figures 2.7.13 through 2.7.18.

Each figure shows each of the six cases described in Table 2.7.13. The two chains analyzed are:

1) $$^{234}\text{U} \xrightarrow[2.5.10^5\text{yrs}]{} {}^{230}\text{Th} \xrightarrow[7.7\text{x}10^4\text{yr}]{} {}^{226}\text{Ra} \xrightarrow[1600\text{ yr}]{}$$

2) $$^{237}\text{Np} \xrightarrow[2.14\text{x}10^6\text{yr}]{} {}^{233}\text{U} \xrightarrow[1.6\text{x}10^5\text{yr}]{} {}^{229}\text{Th}({}^{225}\text{Ra}) \xrightarrow[7340\text{ yr}]{}$$

The half lives of the radionuclides in the first chain are ordered in the same way as the half lives of the nuclides in the second chain are ordered. When the equilibrium constant of correspondent nuclides in each chain are equal, the behavior of the solutions is expected to be also the same. In the figures for each one of the six cases, the above mentioned fact is confirmed. The variation of the peak water dilution rates with water travel time for each case shows its own characteristic behavior differing from case to case in each of the six cases.

Figure 2.7.13 shows the case 1 where $K_3>K_2>K_1$. The curves for ^{226}Ra show same behavior as the curves for ^{229}Th differing only in the magnitude of the peak water dilution rate due to different initial activities. In case 1 the value of K_3 and K_1 were fixed at 10^4 and 10^2, respectively and K_2 was varied between those extremes. For all values of K_2 taken the peak water dilution rate is approximately constant for water travel times of up to 10^2 and decaying monotonically thereafter.

When the K_2 value tends to 10^2, case 1 is approaching case 6. This fact can be confirmed by looking at the curves representing the case 6 (Fig. 2.7.18) where $K_3>K_1>K_2$ and comparing to the curves in case 1 when K_2 is smallest.

BEST DOCUMENT AVAILABLE

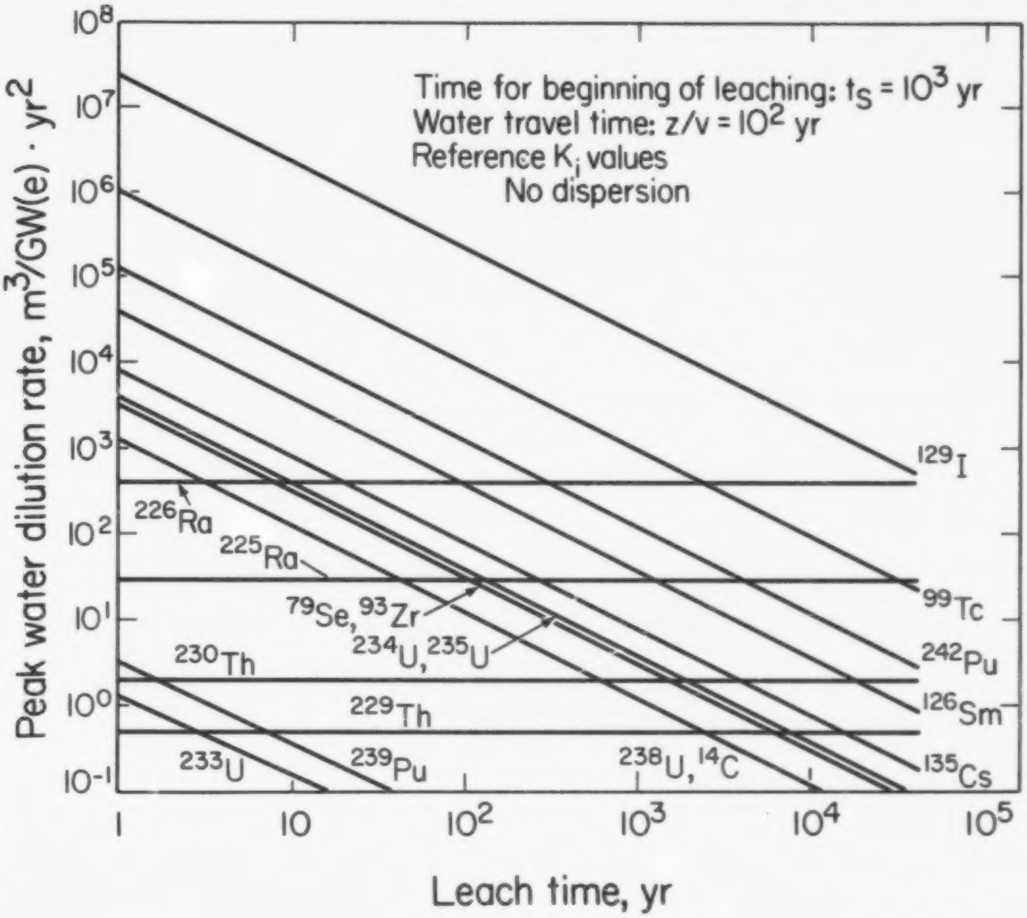

Figure 2.7.11 Variation of peak water dilution rate with leach time for reprocessed PWR high level waste.

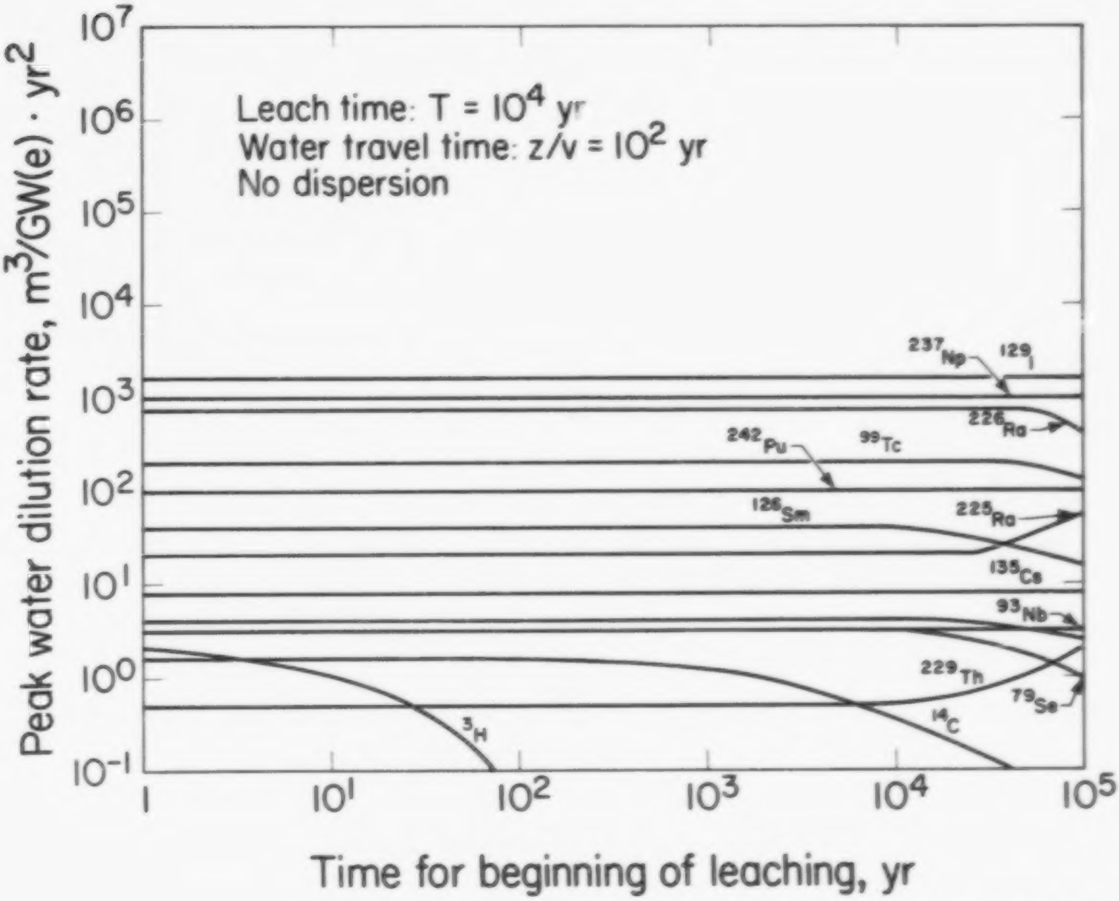

XBL 812-228

Figure 2.7.12 Variation of peak water dilution rate with the time for beginning of leaching for reprocessed PWR high level waste.

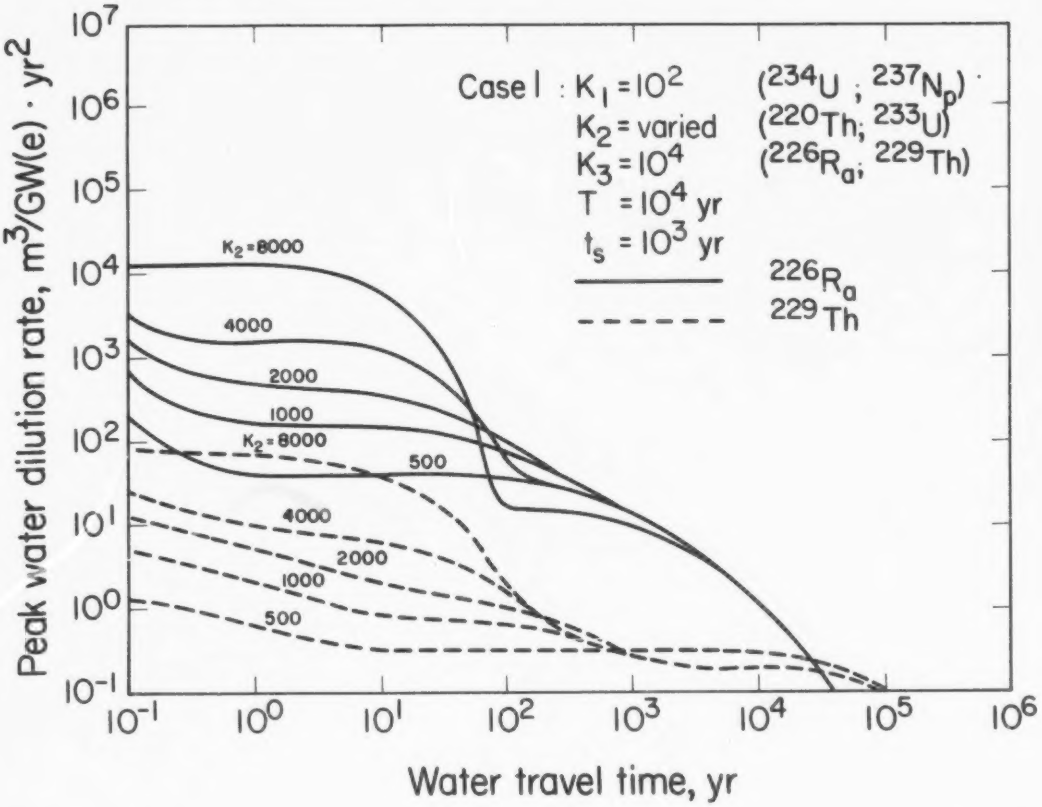

XBL 812-229

Figure 2.7.13 Variation of peak water dilution rate of third members ^{229}Th, ^{226}Ra with the sorption coefficient and with water travel time for reprocessed PWR high level waste.

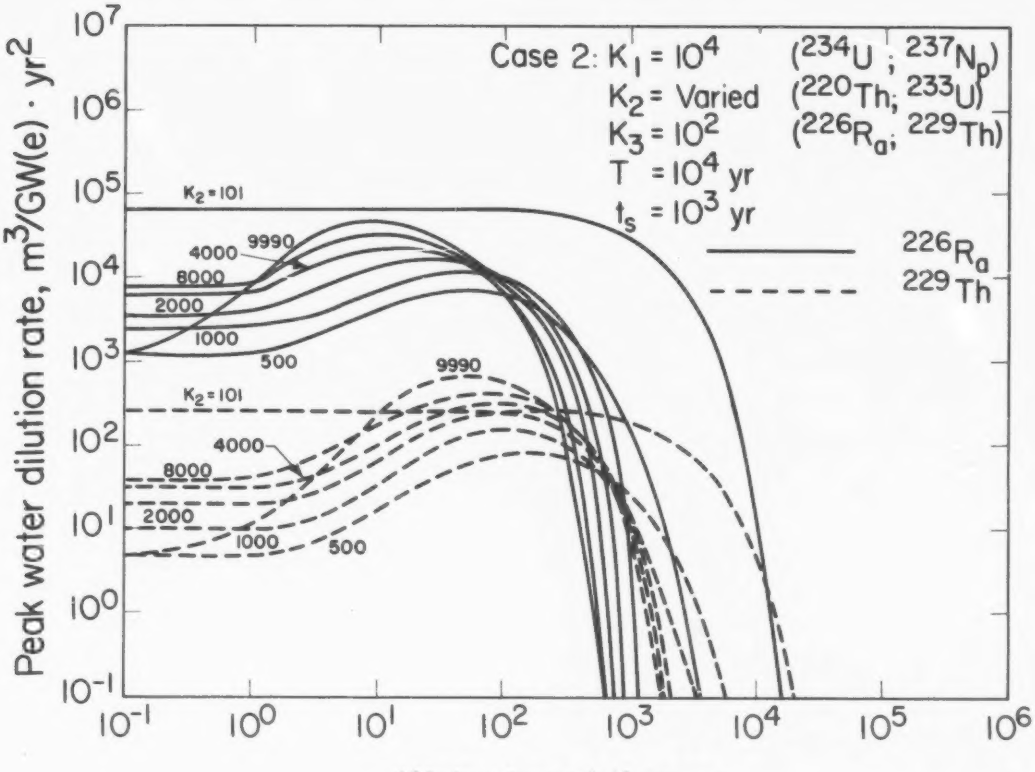

XBL 812-230

Figure 2.7.14 Variation of peak water dilution rate of third members ^{229}Th, ^{226}Ra with the sorption coefficient and with water travel time for reprocessed PWR high level waste.

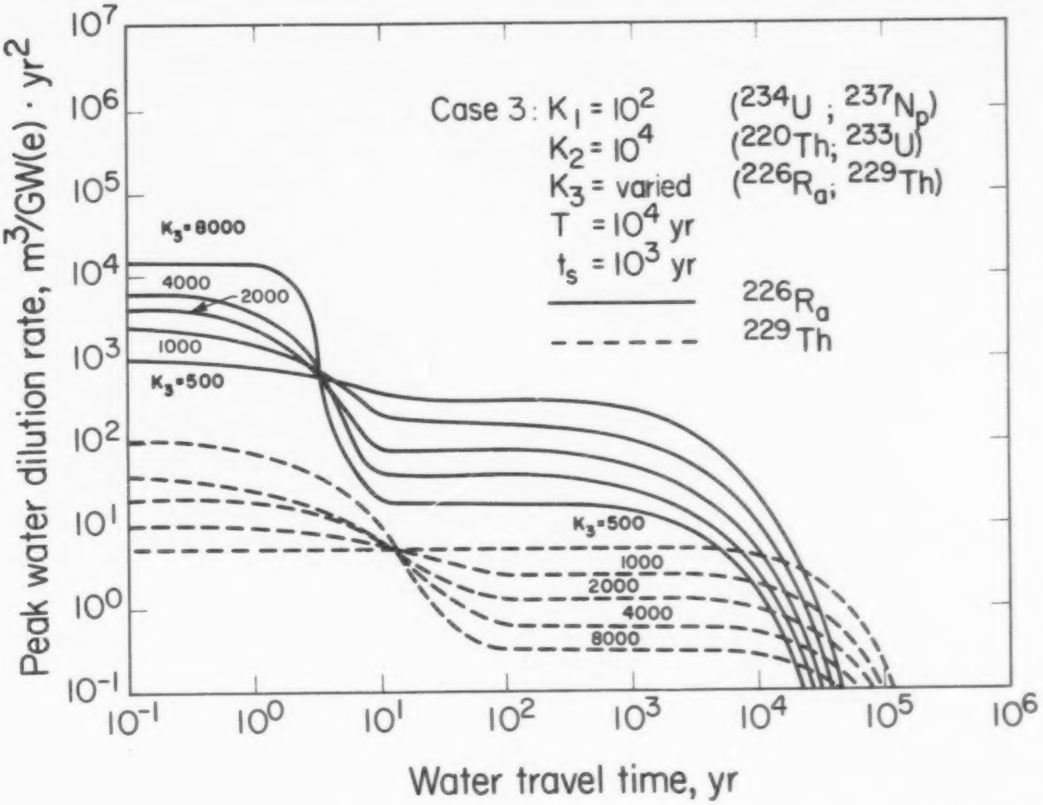

XBL 812-231

Figure 2.7.15 Variation of peak water dilution rate of third members ^{229}Th, ^{226}Ra with the sorption coefficient and with water travel time for reprocessed PWR high level waste.

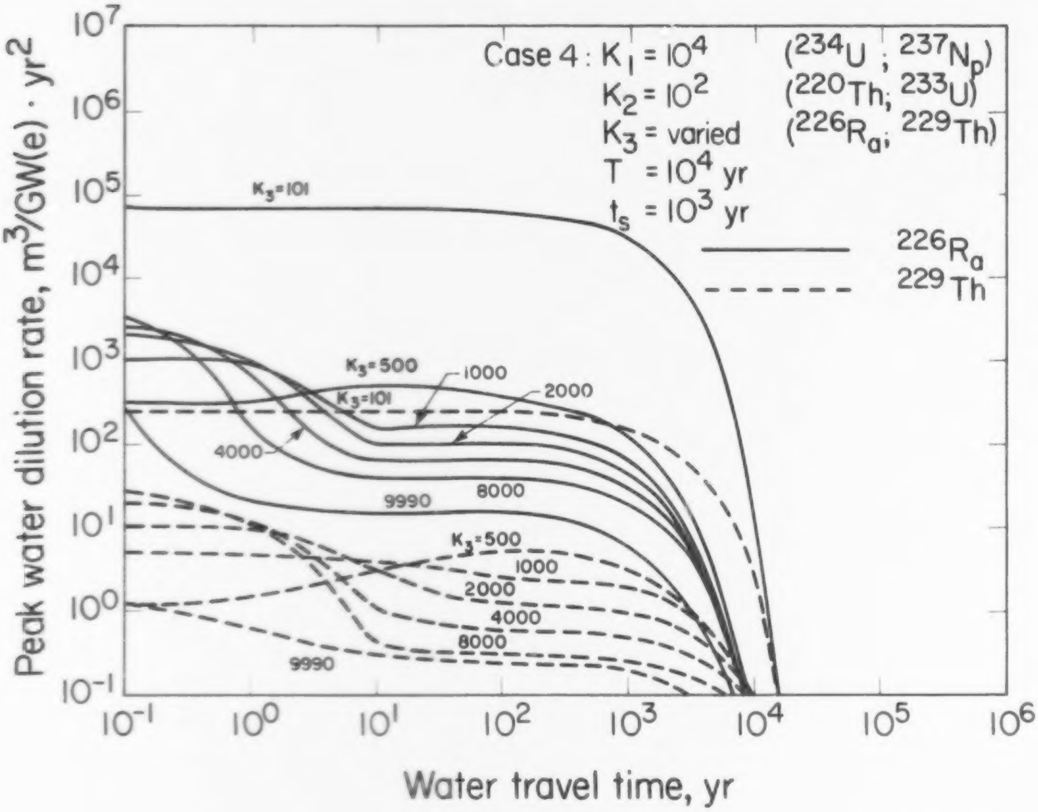

XBL 812-232

Figure 2.7.16 Variation of peak water dilution rate of third members ^{229}Th, ^{226}Ra with the sorption coefficient and with water travel time for reprocessed PWR high level waste.

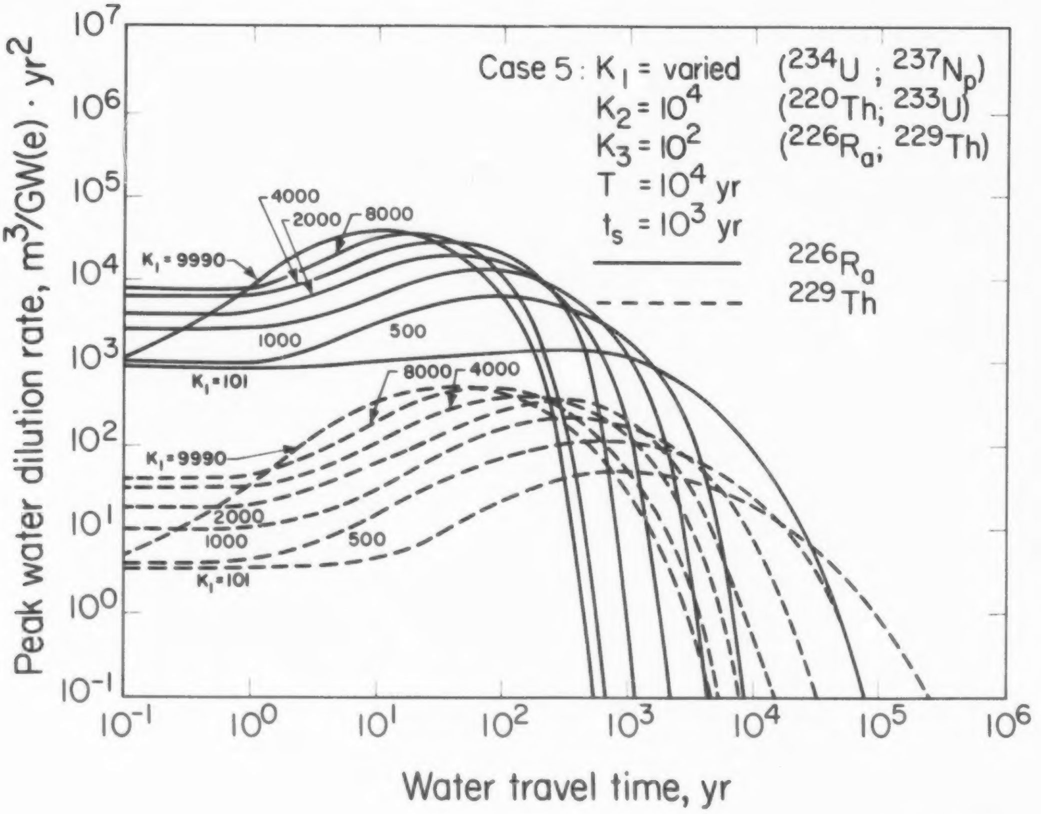

XBL 812-233

Figure 2.7.17 Variation of peak water dilution rate of third members ^{229}Th, ^{226}Ra with the sorption coefficient and with water travel time for reprocessed PWR high level waste.

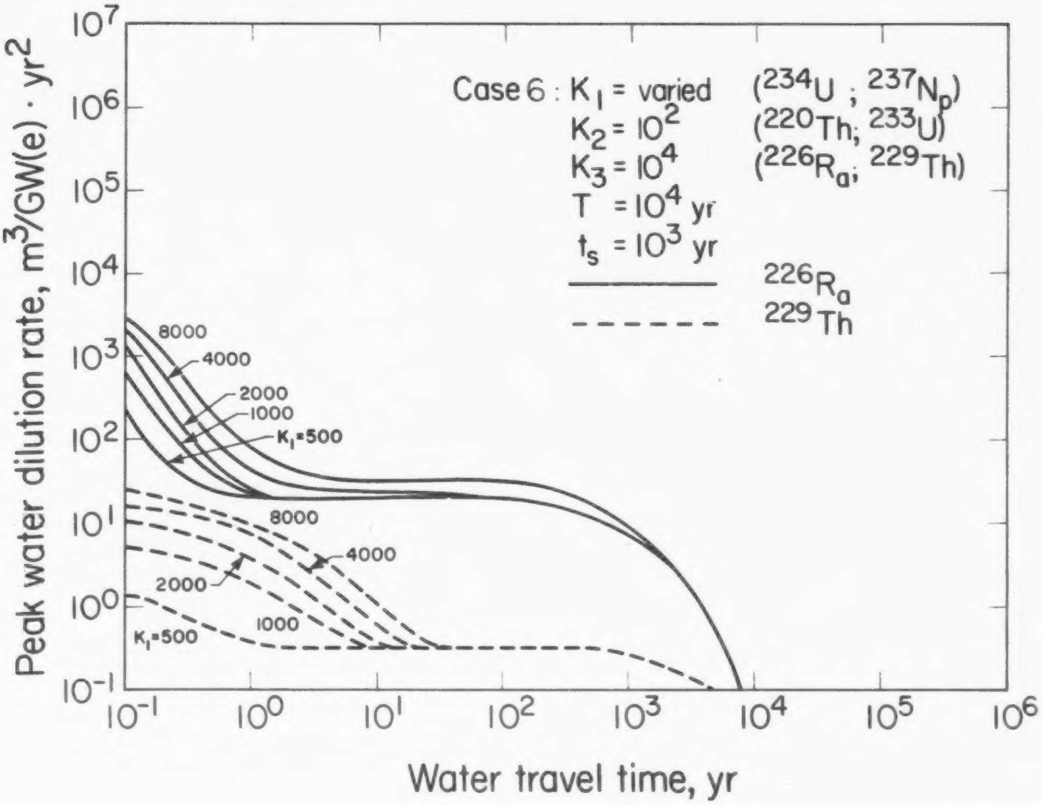

XBL 812-234

Figure 2.7.18 Variation of peak water dilution rate of third members ^{229}Th, ^{226}Ra with the sorption coefficient and with water travel time for reprocessed PWR high level waste.

In case 1 as well as in case 6, no increase in peak water dilution rate with increased water travel time is observed.

Figure 2.7.14 shows case 2 where $K_1 > K_2 > K_3$. In this case, an increase in peak water dilution rate with water travel time is observed. AS K_2 is reduced to values close to 10^2 we are departing from case 2 and entering the case 4 where no increase is observed for any value of K_3 which is being varied. On the other hand, when K_2 approaches 10^4, case 2 tends to case 5 whose curves also show an increase in peak water dilution rate with time. Case 2 and case 5 are the only cases where these build up and subsequent roll off in peak water dilution rate occur. These two cases have the common fact that K_3 has a smaller value than K_1 and K_2.

In all other cases, the peak water dilution rate decreases monotonically with water travel time.

2.7.10.E Leaching of natural uranium ore mill tailings

The nuclide inventories of the reprocessed high level waste used in the reference case is the result of the generation of 1 GW(e) year of electricity by a PWR. They operate at 33 percent thermal efficiency, 80 percent load factor, and with a burnup of 30,500 MwD/Mg.

Such an electric generation requires the total amount of 30.3 Mg of UO_2 fuel enriched to 3.3 percent ^{235}U.

To evaluate the amount of natural uranium ore required to produce this amount of fuel let us consider a gaseous diffusion enrichment plant with a depleted uranium stream with 0.0036 atom fraction of ^{235}U.

By a simple mass balance in both the total number of atoms and in ^{235}U atoms, one concludes that it is required 250 Mg of natural uranium ore. The eventual losses during fabrication are 1 percent, in conversion to hexafluoride is 0.5 percent and in milling and concentration is 5 percent (B2).

The total activity of the uranium present in such ore will be:

^{238}U: 82 Ci
^{235}U: 1.7 Ci

When the uranium ore is processed, it is milled and purified to remove the non-uranium rock. The non-uranium radioactive decay daughters, e.g., ^{230}Th, ^{226}Ra are also separated and are left with the piles of mill tailings.

Suppose these piles of mill tailings are buried in such a way that a equivalent initiating event which started the leaching of the high level reprocessed waste canisters also happens for the piles of mill tailings. One can assume that the leach rate of the mill tailings is the same as the reference value adopted for HLW, i.e., 10^{-4} yrs^{-1}.

Since the ore body is expected to be where it has been for periods longer than 10^5 years, the initial activities of all daughters are in transient equilibrium with ^{238}U.

Also, for the purpose of this illustration, one can assume that ^{238}U and ^{234}U are in the solution with the same chemical form (thus, with the same equilibrium constant) which allows us to consider the following reduced chain:

$$^{238}U(^{234}U) \dashrightarrow {}^{230}Th \dashrightarrow {}^{226}Ra$$

where ^{234}U is in secular equilibrium with ^{238}U because the intermediates ^{234}Th and ^{234}Pa have very short-lives.

The peak water dilution rates resulting from the leaching of such piles of mill tailings are calculated and shown in Fig. (2.7.19) and for the uranium ore in Fig. (2.7.20).

The peak water dilution rate for ^{226}Ra from the mill tailings as well as the envelope of the peak water dilution rates of all nuclides present in a reprocessed HLW are plotted against water travel time.

^{226}Ra peak water dilution rate due to the dissolution of mill tailings is larger than the envelope of the HLW peaks for water travel times up to 10^6 years and it decays rapidly thereafter.

BEST DOCUMENT AVAILABLE

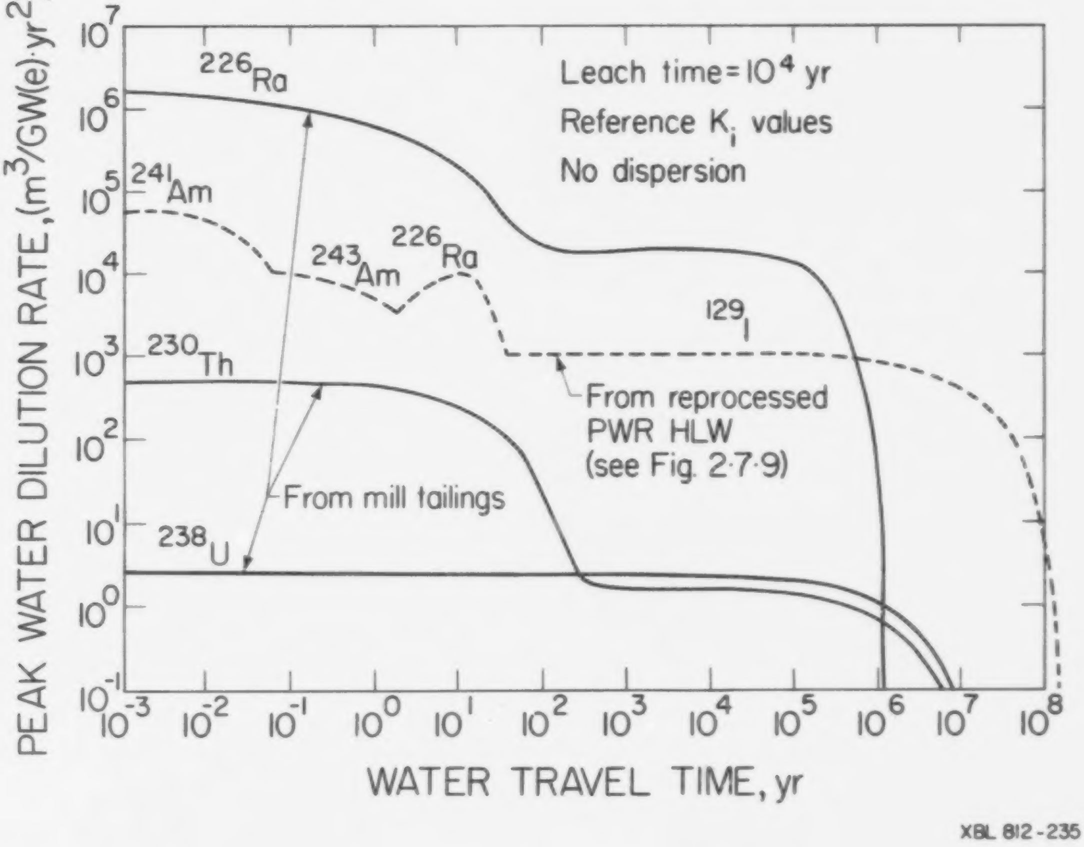

Figure 2.7.19 Variation of peak water dilution rate from natural uranium ore mill tailings with water travel time.

BEST DOCUMENT AVAILABLE

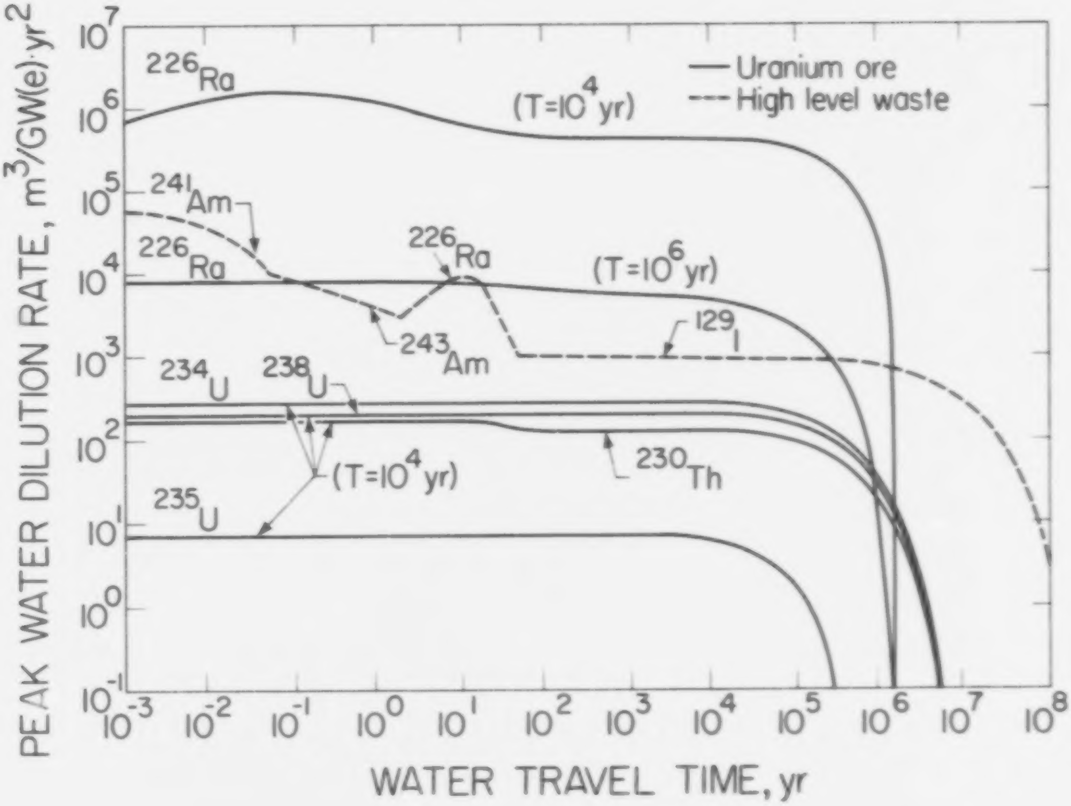

XBL 812-236

Figure 2.7.20 Variation of peak water dilution rate with water travel time from leaching of natural uranium ore.

2.8 Nomenclature

A_i^j : Defined by Eq. (2.1.22)

$A_{s,m}^B$: Defined by Eq. (2.4.15)

$B_i(t)$: Bateman equation, Eq. (2.1.12)

$B_{i,q}$: Bateman coefficient defined by Eq. (2.1.13)

$B_{i,q}^b$: defined by Eq. (2.2.2)

$B_{i,q}'$: $B_{i,q}e^{-\lambda_q T}$

$X_{B_{i,q}}$: Constant defined in Appendix C

$X_{B_{i,q}}^1$: Constant defined in Appendix C

$B_m^{i,j}$: Constant defined by Eq. (2.1.23)

c_0, c_1, c_2 : Coefficients introduced in Section 2.3

$c_i^m(z,t)$: Concentration in water of the m^th^ chemical compounds of the i^th^ nuclide

${}_qC_m^B$: Defined by Eq. (2.4.16)

$C_{r,m}^{i,j}$: Defined by Eq. (2.4.17)

C_m^-, C_m^+ : Constants introduced in Appendix B

D : Axial dispersion coefficient, m^2/yr

$E_{ijk}(z,t)$: Defined by Eq. (2.1.32)

$E_m^{B,\omega}$: Defined by Eq. (2.4.19)

f : Reducing factor defined by Eq. (2.4.9)

f_i^m : Fraction defined by Eq. (2.6.26)

$F_i(s,p)$: Defined in Appendix B

$F_{i,i}^i(z,t), F_{r,m}^j(z,t)$: given in section 2.1.2

F : Fourier transform

g_i : Defined in Appendix B

$G_{r,m}^{i,j}$: Defined by Eq. (2.1.24)

$h(t)$: Heaviside step function

H : Centerline distance between waste canisters, m

$k_{fi}^{m,m+1}$: Rate constant for chemical reaction in the water phase, 1/yr

$k_{si}^{m,m+1}$: Rate constant for chemical reaction in the solid phase, 1/yr

$\vec{k}_i$: First order reaction rate for irreversible minieralization, 1/yr

$K_{D,i}$: Distribution coefficient, $(\text{atoms}/m^3 s)/(\text{atoms}/m^3 f)$

$K_{D,i}^m$: Distribution coefficient for the m^{th} compound of the i^{th} nuclide

$K_{e,i}^m$: Equilibrium constant for chemical reaction between the m^{th} and $(m+1)^{th}$ compounds

$K_{e,i}^{E,m}$: Constant defined by Eq. (2.6.20)

K_i : Sorption retardation coefficient or effective retardation coefficient defined by Eq. (2.6.18)

K_i^m : Sorption retardation coefficient of the m^{th} compound of the i^{th} nuclide defined by Eq. (2.6.16)

$K_i^{E,m}$: Constant defined by Eq. (2.6.19)

$L_j(t)$ $j=1,2,3$: Dimensions of parallelepiped at $t=0$, m

L_0 : Length of cylinder at $t = 0$, m

$\hat{L}_i$: Defined by Eq. (2.1.2)

α : Laplace transform

$m_i(z,t)$: Concentration of mineralized atoms in solid, atoms/m^3

$M_i(z,t)$: Concentration in solid of atoms in equilibrium with liquid, atoms/m^3

$M_i^m(z,t)$: Concentration in the solid of nuclide i which forms the m^{th} chemical compounds.

M_T^0 : Initial amount of total waste

$n_i(t)$: Atom fraction of nuclide i in the total waste material

n_i^0 : Atom fraction of nuclide i in the total waste material at t=0

n_i^b : Atom fraction of nuclide i in the total waste material at burial time

${}^{x}n_i^{s}(z,t), {}^{x}n_i^{b}(z,t)$, $x=0,1,2$: defined in Appendix C

$N_i(z,t)$: Concentration in water of the i^{th} nuclide

$N_i^m(z,t)$: Concentration in water of the m^{th} chemical compounds of the i^{th} nuclide

N_i^s, N_i^b : Concentration resulting from a step, or a band
release

$N_i(z,p)$: Laplace transforms of $N_i(z,t)$

$N_i^*(t_s, \tau)$: Maximum concentration of nuclide i

$N_i^{**}(t_s)$: Highest concentration of nuclide i over all   and all t

p : Laplace transform variable for t

$r(t)$: Radius of cylinder or sphere, m

r_i : Sorption rate of nuclide i, atoms/yr m^3

R : Penetration rate, m/yr

R_i : Chemical reaction rate, atoms/yr m^3

s : Fourier transform variable for t or

S : Interfacial area per unit volume of sorbing medium

$s_i^m(z,t)$: Concentration of the m^{th} chemical compounds of the i^{th} nuclide in the solid phase

$\mathcal{S}$: Surface area of equivalent plane source, m^3

t : Time, yr

t_s : Time to start of leaching, yr

t^{**} : Time of global maximum ^{226}Ra concentration

t_r : Retardation time, yr

t_a : Arrival time, yr

T : Leach time, yr

v : Water velocity, m/yr

v_i : v/K_i, m/yr

$\dot{w}_s$: Rate of dissolution of total waste material, atoms/m^2 yr

w_s^o : Initial density of total waste material in the plane source in the water phase, atoms/m^2

$\tilde{y}_i$: Defined in Appendix B

$\hat{y}_i$: Defined in Appendix B

z : Distance from repository

α : Longitudinal dispersivity factor D/v

$\ell_{\alpha_{s,m}}$: Defined by Eq. (2.4.20)

$\tilde{\beta}_{s,m}$: Defined by Eq. (2.1.26)

β_i : Defined in Appendix B

$\gamma_{i,j,k}$: Defined by Eq. (2.1.27)

γ_i : Defined in Appendix B

$\Gamma_{r,m}$: Defined by Eq. (2.1.29)

$\delta(z)$: Dirac delta function, 1/m

$\delta(t)$: Dirac delta function, 1/yr

ε : Porosity of sorbing medium

θ_{jp} : Defined by Eq. (2.4.22)

η_i : Defined by Eq. (2.1.4)

λ_i : Decay constant, 1/yr

$\Lambda_{r,m}$: Defined by Eq. (2.1.28)

ρ : Overall density of waste material, atoms/m^3

${}^{l}\rho$: Density of water in l^{th} medium, kg/m^3

τ : Water transit time, yr

τ^{**} : Water transit time value at global maximum ^{226}Ra concentration

1_{τ} : Water transit time to the interface between two media, yr

$\chi^{m}_{i,q}$: Defined by Eq. (2.1.14)

$\phi_i'''(z,t)$: General source term in water phase, atoms/m^3 yr

$\phi_i''(t)$: Plane source term in water phase, atoms/m^3 yr

$\phi_i^m(z,t)$: Plane source term in water phase, of mth chemical compound of ith nuclide

$\phi_i'''(z,p)$: Defined in Appendix B

Subcripts

f : Fluid

s : Solid

Superscripts

b : Band release

s : Step release

n : No overpack

w : With overpack

3.1. Non Equilibrium Sorption in Chromatographic Columns: Impulse Release

3.1.1. Introduction

In the analysis of migration of radionuclide through geologic media, related to high level waste disposal it is commonly assumed that the sorption reactions between radionuclides in the solid phase with those in the liquid phase are pointwise in equilibrium.

In this present report, a non-equilibrium model described by different authors (L1,H2) is used to assess the effects of the departure from equilibrium sorption models.

A one dimensional chromatographic column with constant solution velocity is considered. Effects associated with hydrodynamic dispersion and diffusion are neglected and soil properties are constant.

The main objective of this study is to recognize the physical processes involved in a non-equilibrium sorption. For this purpose it is necessary to obtain a simple analytical solution whose terms can be easily identified with the different processes occurring. With this in mind, the simplest of all boundary conditions was choosen, namely a impulse release boundary condition at the origin of the column.

In order to obtain estimates of numerical values for the mass transfer rate coefficient, the solution is applied to interpret stationary (batch) as well as flowing sorption experiments done at ANL (S1).

Comparison of the analytical solutions against experimental data (S1) shows agreement for the case of groundwater solutions containing Pu^{4+} and Am^{3+} flowing in limestone.

3.1.2. The Governing Equations

By considering the volume averaged (H1) mass balances in the liquid phase and in the solid phase one writes the following governing equations for a first member of a chain:

$$\frac{\partial}{\partial t}(\varepsilon N) + \vec{\nabla}\cdot(\vec{v}N\varepsilon) = \vec{\nabla}\cdot\vec{D}\cdot\vec{\nabla}(N\varepsilon) - R - \lambda N\varepsilon \tag{3.1.1}$$

$$\frac{\partial}{\partial t}[(1-\varepsilon)M] = \vec{\nabla}\cdot\vec{D}\cdot\vec{\nabla}[(1-\varepsilon)M] - \lambda M(1-\varepsilon) + R \tag{3.1.2}$$

Here (see nomenclature in Section 2.8) the mass transfer rate R is defined to be positive when the nuclides are going from the liquid phase to the solid phase.

Assuming that the system considered is one dimensional where the solution velocity is constant and where the dispersion coefficient is negligible, the Eqs. (3.1.1) and (3.1.2) are reduced to:

$$\varepsilon \frac{\partial N}{\partial t} + \varepsilon v \frac{\partial N}{\partial z} = -R - \lambda N \varepsilon \qquad (3.1.3)$$

$$(1 - \varepsilon) \frac{\partial M}{\partial t} = R - \lambda M(1 - \varepsilon) \qquad (3.1.4)$$

(For a stationary system one sets $v = 0$ in Eq. (3.1.3)

3.1.2.2 Initial and Boundary Conditions

The initial conditions can be expressed as:

$$N(z,0) = M(z,0) = 0 \quad ; \quad t = 0 \quad , \quad z > 0 \qquad (3.1.7)$$

The boundary condition can be obtained as follows: Suppose we have a waste canister which leaches in such a way that produces a concentration boundary condition represented generically by:

$$N(0,t) = \phi(t) \, [h(t) - h(t - T)] \qquad (3.1.8)$$

where $\phi(t)$ is a arbitrary positive function of time, $h(t)$ is a step function, and T is the duration of the release. One can define a equivalent constant band release boundary condition by the following:

$$N(0,t) = N_0[h(t) - h(t - T)] = \frac{1}{T} \int_0^T \phi(t)[h(t) - h(t - T)] \, dt \qquad (3.1.9)$$

Finally, the impulse release boundary condition can be obtained by taking the limit when the leach time T tends to zero, i.e.:

$$N(0,t) = \lim_{T \to 0} N(0,t) = \lim_{T \to 0} N_0[h(t) - h(t - T)] \qquad (3.1.10)$$

which yields the impulse release boundary condition: $N(0,t) = N_0 T \delta(t)$; $z = 0$, $t > 0$, where $\delta(t)$ is the Dirac's delta function

B. Model for the Sorption Reactions

The mechanisms of sorption in a geologic media are expected to be very complex. They will depend on a large range of parameters and physical processes.

A most general relation for the mass-transfer rate would be a function of the concentrations in each phase:

$$R = f(N,M) \qquad (3.1.11)$$

Consider a stationary system consisting of a solid phase immersed in a solution. Assume that the concentration M in the solid phase is uniform

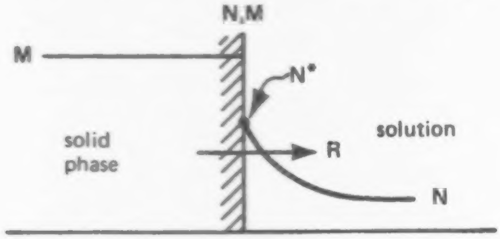

N is the concentration at the bulk of the solution and N* is the atom concentration in the liquid at the interface. The flux of radionuclide from (or to) the solid phase can be expressed through a empirical "mass transfer coefficient K_m" defined by the following relationship

$$R = sK_m(N - N^*) \quad \text{(atoms/yr m}^3\text{ of bed)} \qquad (3.1.12)$$

where s is the specific interface area (m^2 of interface/m^3 of bed) and k_m should include effects of geometry, temperature, acidity of solution, etc. and it has units of [m^3 of solution/m^2 of interface x year].

The basic assumption made is that although the bulk concentration N has not reached equilibrium yet the concentration at the interface (N*) has already reached and it can be related to the concentration in the solid phase by:

$$\gamma N^* = M \qquad (3.1.13)$$

and

$$\gamma = K_D \rho_s \qquad (3.1.13a)$$

where:

K_D = equilibrium distribution coefficient, $\frac{\text{atoms/g of solid}}{\text{atoms/cm}^3 \text{ of solution}}$

ρ_s = solid phase density, [g of solid/cm^3 of solid]

substituting for N* from Eq. (3.1.13) into Eq. (3.1.12) one has:

$$R = \frac{sk_m}{\gamma}(\gamma N - M) \tag{3.1.14}$$

Let us define:

$$\beta = \frac{k_m}{\gamma} \quad [\text{m}^3 \text{ of solid/m}^2 \text{interface x year] hence:} \tag{3.1.15}$$

$$R = s\beta(\gamma N - M) \tag{3.1.16}$$

Above relation can then be substituted into Eq. (3.1.3) and Eq. (3.1.4). In the next section we non-dimensionalize Eq. (3.1.3) and Eq. (3.1.4) after having substituted Eq. (3.1.16) and they are solved for a impulse release boundary condition Eq. (3.1.10).

The mass transfer rate expressed by Eq. (3.1.16) is similar to the relationship used by Lapidus and Amundson (L1).

3.1.3. Analytical Solutions

3.1.3.1. Solution to the Flowing System

Let us consider the following dimensionless variables:

Dimensionless concentrations:

$$n = \frac{N}{N_0} \quad , \quad m = \frac{M}{\gamma N_0} \tag{3.1.16a}$$

Dimensionless time:

$$\tau = \frac{(t - z/v)}{\left(\frac{s\beta}{\varepsilon}\right)^{-1} \frac{(1 - \varepsilon)}{\varepsilon}} \tag{3.1.17}$$

where $t_0 = \left(\frac{s\beta}{\epsilon}\right)^{-1}$ is a characteristic reaction time. Dimensionless distance:

$$\xi = z\gamma/vt_0 \tag{3.1.18}$$

Dimensionless mass-transfer rate:

$$r = \frac{R}{N_0 s\beta\gamma} = n - m \tag{3.1.18a}$$

substituting these dimensionless groups into Eqs. (3.1.3), (3.1.4), (3.1.7) and (3.1.10) and using Eq. (3.1.16) results:

$$\frac{\partial n}{\partial \xi} + (1 + \lambda t_0)\, n - m = 0 \tag{3.1.19}$$

$$\frac{\partial m}{\partial \tau} - n + (1 + \lambda t_0)\, m = 0 \tag{3.1.20}$$

In general, $\lambda t_0 << 1$ so that it can be neglected. The boundary and initial conditions can be written as:

$$m(\xi,0) = 0 \quad , \quad \tau \leq 0 \quad , \quad \text{all } \xi \tag{3.1.21}$$

$$n(0,\tau) = \delta(\tau) \quad , \quad \xi = 0 \quad , \quad \tau \geq 0 \tag{3.1.22}$$

Defining the following Laplace's transformation with respect to time:

$$\bar{n}(\xi,p) = \int_0^\infty e^{-p\tau} n(\xi,\tau)\, d\tau \tag{3.1.23}$$

$$\bar{m}(\xi,p) = \int_0^\infty e^{-p\tau} m(\xi,\tau)\, d\tau$$

and applying above relations to Eq. (3.1.19) and Eq. (3.1.23) results:

$$\frac{d\bar{n}}{d\xi} + \bar{n} - \bar{m} = 0 \tag{3.1.24}$$

from Eq. (3.1.20), Eq. (3.1.23) and using Eq. (3.1.21) one obtains:

$$\bar{m} = \frac{\bar{n}}{1 + p} \qquad (3.1.25)$$

substituting Eq. (3.1.25) back into Eq. (3.1.24) yields:

$$\frac{d\bar{n}}{d\xi} = \frac{\bar{n}}{1 + p} - \bar{n} \qquad (3.1.26)$$

the integration of Eq. (3.1.26) results:

$$\bar{n}(\xi,p) = c \exp\left(- \frac{p}{1 + p}\xi\right) \qquad (3.1.27)$$

The Laplace transform of the boundary condition Eq. (3.1.22) is:

$$\bar{n}(0,p) = 1 \qquad (3.1.29)$$

by using Eq. (3.1.29), Eq. (3.1.27) reduces to:

$$\bar{n}(\xi,p) = \exp\left(- \frac{p}{1 + p}\xi\right) \qquad (3.1.30)$$

To invert above expression back to the variable τ one considers the rule:

$$\mathcal{L}^{-1}\{pf(p)\} = \frac{dF}{d\tau} + F(0)\cdot\delta(\tau) \qquad (3.1.31)$$

where

$$\mathcal{L}^{-1}\{f(p)\} = F(\tau)$$

taking $f(p) = e^{\xi/P}/P$ results:

$$\mathcal{L}^{-1}\left\{\frac{e^{\xi/p}}{p}\right\} = I_0(\sqrt{4\xi\tau})$$

since $I_0(0) = 1$ and

BEST DOCUMENT AVAILABLE

$$\frac{dI_0}{d\tau} = 2\xi \, \frac{I_1(\sqrt{4\xi\tau})}{\sqrt{4\xi\tau}}$$

from Eq. (3.1.31) one has:

$$\mathcal{L}^{-1}\left\{e^{\xi/p}\right\} = 2\xi \, \frac{I_1(\sqrt{4\xi\tau})}{\sqrt{4\xi\tau}} + \delta(\tau)$$

thus:

$$\mathcal{L}^{-1}\left\{e^{\xi/p+1}\right\} = 2\xi e^{-\tau} \frac{I_1(\sqrt{4\xi\tau})}{\sqrt{4\xi\tau}} + \delta(\tau)\, e^{-\tau}$$

hence:

$$\mathcal{L}^{-1}\left\{e^{-\xi} e^{\xi/p+1}\right\} = 2\xi e^{-(\tau+\xi)} \, \frac{I_1(\sqrt{4\xi\tau})}{\sqrt{4\xi\tau}} + \delta(\tau)\, e^{-(\tau+\xi)}$$

Hence the solution for the radionuclide concentration in the liquid phase will be:

$$n(\xi,\tau) = \left[2\xi e^{-(\tau+\xi)} \, \frac{I_1(\sqrt{4\xi\tau})}{\sqrt{4\xi\tau}} + \delta(\tau)\, e^{-(\tau+\xi)}\right] h(\tau) \qquad (3.1.32)$$

In order to obtain the solution for the concentration in the solid phase, one substitutes Eq. (3.1.30) into Eq. (3.1.25) yielding:

$$\bar{m}(\xi,p) = \frac{1}{1+p} \exp\left(-\frac{p}{1+p}\,\xi\right) \qquad (3.1.33)$$

the inversion of above Laplace's transform is immediate and there results the concentration in the solid phase:

$$m(\xi,\tau) = e^{-(\tau+\xi)}\, I_0(\sqrt{4\xi\tau})\, h(\tau) \qquad (3.1.34)$$

3.1.3.2. Solution to the Stationary System

Consider the following system:

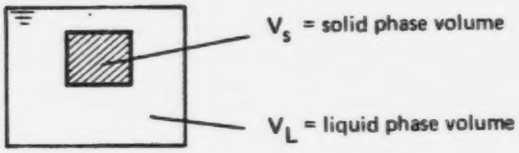

Considering a nuclides balance in the solid phase one has:

$$\frac{dM}{dt} = (V_S + V_L)\, R$$

where $R = s\beta(\gamma N - M)$. A similar nuclides balance in the liquid phase yields:

$$\frac{dN}{dt} = -(V_S + V_L)\, R$$

Again, we have neglected radioactive decay. By denoting $\alpha = (V_S + V_L)s$ (total interface area)

$$\frac{dM}{dt} = \alpha\beta(\gamma N - M) \qquad (3.1.37)$$

$$\frac{dN}{dt} = -\alpha\beta(\gamma N - M) \qquad (3.1.38)$$

An overall atoms balance in both phases will yield:

$$V_S M + V_L N = \text{constant} = V_S M(0) + V_L N(0) \qquad (3.1.39)$$

where M(0), N(0) are the initial concentrations in the solid phase and liquid phase, respectively. Two practical cases are considered:

$$\begin{aligned} &\text{i)} \quad N(0) = 0 \;, \quad M(0) \neq 0 \\ &\text{ii)} \quad N(0) \neq 0 \;, \quad M(0) = 0 \end{aligned} \tag{3.1.40}$$

The solutions for each case are easily obtained and are:

Case i:

$$N(t) = \frac{\frac{V_s}{V_L} M(0)}{K} [1 - \exp(-\alpha\beta K t)] \tag{3.1.41}$$

$$M(t) = \gamma \frac{V_s}{V_L} \frac{M(0)}{K} [1 - \exp(-\alpha\beta K t)] + M(0) \exp(-\alpha\beta K t) \tag{3.1.42}$$

where

$$K = 1 + \gamma \frac{V_s}{V_L} = 1 + K_D \rho_s \frac{(1 - \epsilon)}{\epsilon} \tag{3.1.43}$$

Case ii:

$$N(t) = \frac{\gamma N(0)}{K} [1 - \exp(-\alpha\beta K t)] + N(0) \exp(-\alpha\beta K t) \tag{3.1.44}$$

$$M(t) = \frac{N(0)}{K} [1 - \exp(-\alpha\beta K t)] \tag{3.1.45}$$

One should note that when β tends to infinity the terms $\exp(-\alpha\beta K t)$ tend to zero. A very large value for β represents a very fast mass transfer rate leading to an almost instantaneous equilibrium condition. This fact can be seen from the ratio of either Eq. (3.3.41) and Eq. (3.3.42) or Eq. (3.3.45) and Eq. (3.3.44) when $\beta \rightarrow \infty$ which yields

$$\gamma = \frac{M(t)}{N(t)}$$

resulting in $R = 0$, which is the definition of equilibrium.

3.1.4. Discussion about the Characteristics of the Analytical Solution for the Flowing System

We rewrite the solution for the concentration in the liquid phase Eq. (3.1.32):

$$n(\xi,\tau) = \left[e^{-(\tau+\xi)}\delta(\tau) + 2\xi\, e^{-(\tau+\xi)}\, \frac{I_1(\sqrt{4\xi\tau})}{\sqrt{4\xi\tau}}\right] h(\tau) \qquad (3.1.32)$$

Each term on the right of Eq. (3.1.32) has its particular meaning.

3.1.4.1. The individual pulses

The first term represents the original impulse released at the origin at $\tau = \xi = 0$ and which travels along the characteristic $\tau = 0$. In other words, this pulse moves with the groundwater velocity and has the shape of a delta function.

To obtain a better physical interpretation of this pulse one can integrate this term with respect to time and denote it by $n_1(\xi,\tau = 0)$ as follows:

$$n_1(\xi,\tau = 0) = \int_{\tau-\varepsilon}^{\tau+\varepsilon} \delta(\tau)\, e^{-(\tau+\xi)}\, d\tau$$

where ε is any positive number and by using the integration property of the delta function one has:

$$n_1(\xi,\ \tau = 0) = e^{-\xi} \quad \text{when} \quad \tau = 0 \qquad (3.1.46)$$

This pulse will be called the seed pulse, because it will be the first contaminated groundwater to reach a given position ξ leaving at that position a certain amount of nuclides in the solid phase. The seed pulse concentration "decays" exponentially with ξ.

The second term in the solution will be called "the secondary pulse" and it is generated by those nuclides left behind by the seed pulse. Let us denote it by $n_2(\xi,\tau)$:

$$n_2(\xi,\tau) = 2\xi e^{-(\tau+\xi)}\, \frac{I_1(\sqrt{4\xi\tau})}{\sqrt{4\xi\tau}}\, h(\tau) \qquad (3.1.47)$$

this pulse has zero concentration along the characteristic $\tau = 0$ and for a given ξ reaches its maximum value along the "equilibrium characteristic" $\tau = \xi$, decreasing thereafter. This equilibrium characteristic would be the characteristic along which the equivalent solution to the equilibrium sorption problem would travel.

The behavior of these pulses can be seen in Fig. 3.1.1 which is a conceptual view of the analytical solution Eq. (3.1.32).

One should note that the seed pulse is represented by a straight vertical line of magnitude $e^{-\xi}$ and it exists at only a particular (z,t), while the secondary pulse is actually a continuous surface.

At any given position ξ, the first contaminated water to arrive is the seed pulse at the time $\tau = 0$, and it has a concentration $n_1(\xi, \tau = 0) = e^{-\xi}$. At this time $\tau = 0$ the mass transfer rate is given by $r(\tau = 0) = n_1 - m$. Due to the characteristic of the function n_1, Eq. (3.1.32), the mass transfer rate along the ground-water characteristics yields a concentration in the solid phase given by:

$$m(\xi, \tau = 0) = e^{-\xi} \tag{3.1.48}$$

The mass transfer rate due to the seed pulse is always positive. This is physically equivalent to say that the seed pulse always gives nuclides to the solid phase.

At this same position, for a time $\tau > 0$ the secondary pulse follows.

Due to the imposition of a impulse release boundary condition, only the seed pulse is initially contaminated at the origin $\tau = \xi = 0$. The subsequent flow of groundwater past the origin is not contaminated. This later ground water as it flows away from the origin is contaminated by the nuclides in the solid phase which were left by the seed pulse. For times $\tau > 0$ the mass transfer rate is given by:

$$r(\tau > 0) = n_2 - m \tag{3.1.49}$$

where n_2 is given by Eq. (3.1.47) and m is given by Eq. (3.1.34). The above mass transfer rate can be either positive or negative corresponding to the cases where the flux of nuclides is from the secondary pulse to the solid phase or vice-versa respectively.

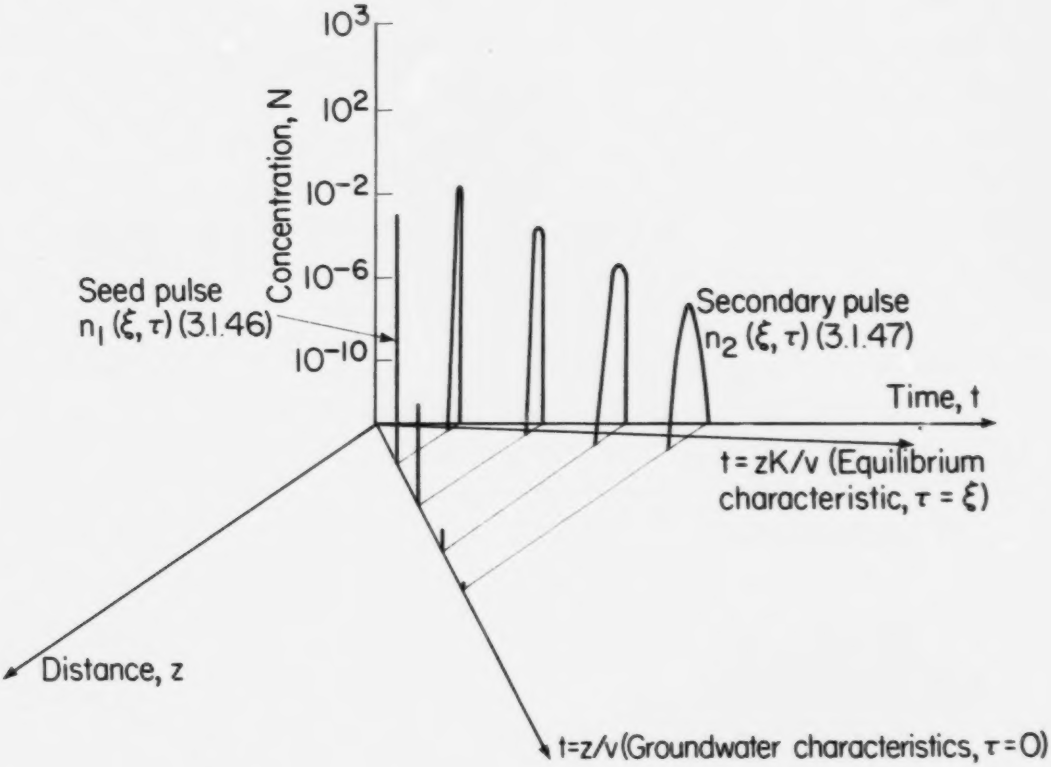
10^3
10^2
10^-2
10^-6
10^-10
Concentration, N
Seed pulse
n1 (ξ, τ) (3.1.46)
Secondary pulse
n2 (ξ, τ) (3.1.47)
Time, t
t = zK/v (Equilibrium characteristic, τ = ξ)
Distance, z
t=z/v(Groundwater characteristics, τ = 0)
XBL 812-203

Fig. 3.3.1 Conceptual view of the propagation of an impulse release, nonequilibrium adsorption.

]

There are two distinct regions: The first region is characterized by distances ξ small enough so that the seed pulse concentration has not decayed significantly. Therefore the solid phase concentration due to the passing of the seed pulse is still close to its maximum initial value (see Eq. (3.1.48)). This large mass transfer rate causes a sudden build up of the concentration in the solid phase and consequently a sudden build up of the secondary pulse concentration which at the origin was zero, i.e., $n_2(\xi,\tau \sim 0) = 0$ (see Eq. (3.1.49)).

At a given ξ in this first region the concentration in the solid phase is always larger than the concentration in the secondary pulse for any $\tau > 0$ resulting in a always negative mass transfer rate (i.e., the flux direction is from the solid phase to the liquid phase). In other words:

$$\text{in region 1:} \quad \begin{array}{lll} r(\tau = 0) > 0 & \text{any} & \xi < \xi^* \\ r(\tau > 0) < 0 & \text{any} & \xi < \xi^* \end{array}$$

where ξ^* determines the transition to region 2 (see Eq. (3.1.53) below).

This first region is illustrated by Figs. (3.1.2) and (3.1.3). One can also illustrate these processes by the following schematic representation: suppose the seed pulse n_1 is represented by a sphere, the solid phase by discrete squares and the secondary pulse n_2 following the seed pulse by triangles. The shadowed area would represent qualitatively the concentration and the arrows the direction of the mass transfer r:

1) At a very short distance (region 1)

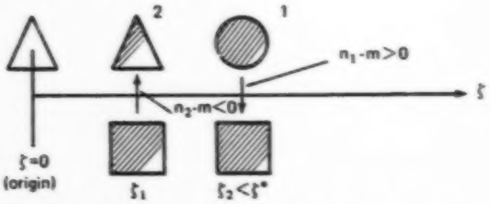

2) At a slightly larger distance (but still in region 1)

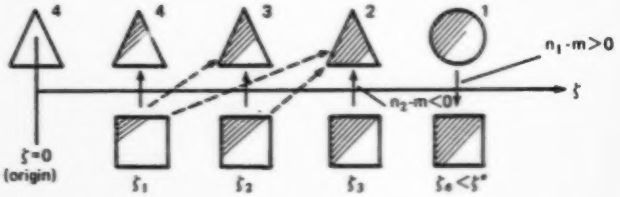

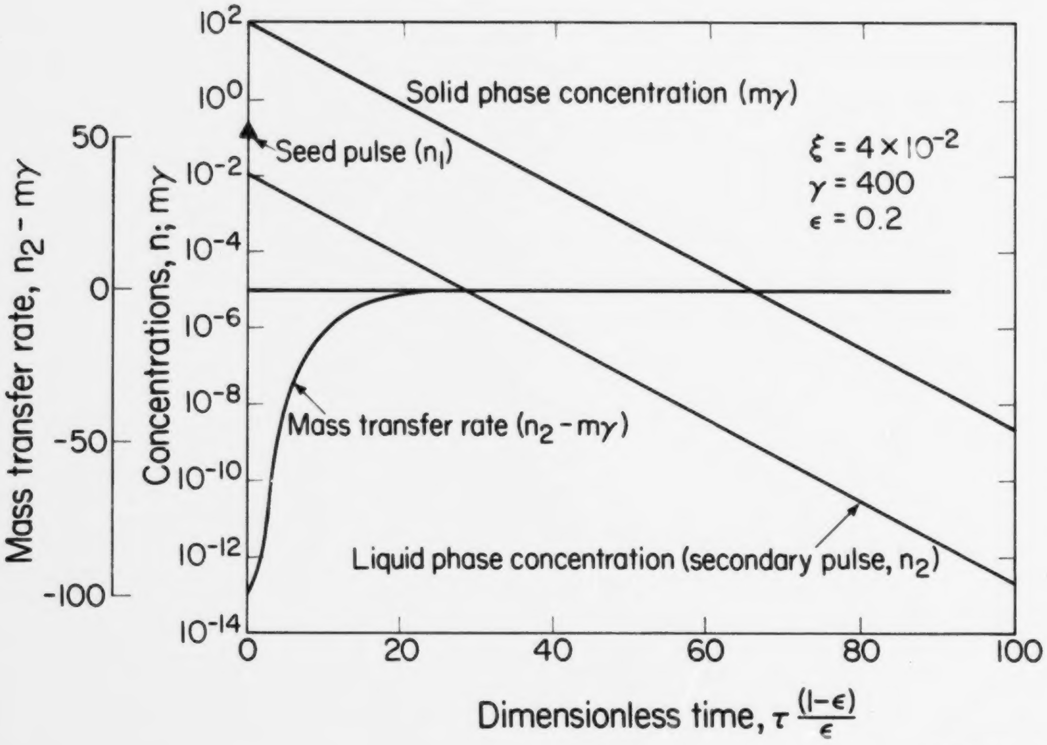

XBL 812-204

Fig. 3.1.2 Change in concentrations and mass transfer rate with time at $\xi = 4 \times 10^{-2}$.

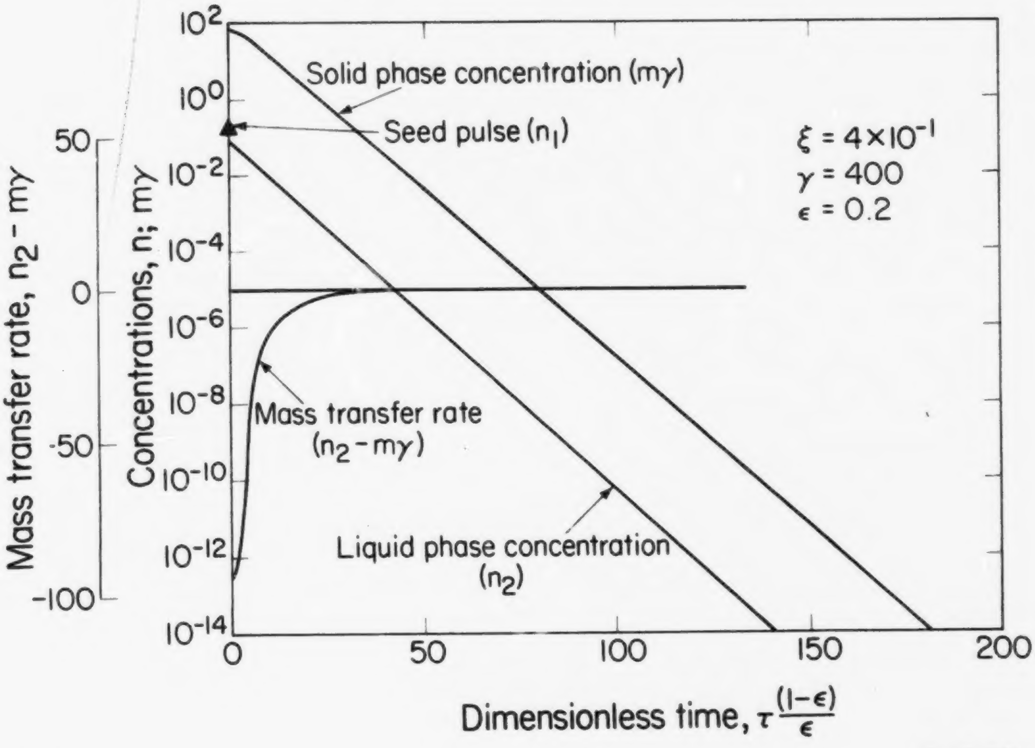

XBL 812-205

Fig. 3.1.3 Change in concentrations and reaction rate with time at $\xi = 4 \times 10^{-1}$.

3) at a distance near the end of region 1:

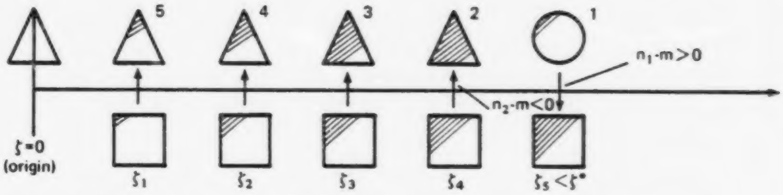

Note the following in the region 1:

--At the station where the seed pulse is (i.e., $\tau = 0$) the flux is always from liquid to solid ($r = n_1 - m > 0$)

--The seed pulse continuously decreases its concentration after going through stations ξ_1 through ξ_5

--The secondary pulse labeled by 2 continuously increases its concentration by receiving atoms in stations ξ_1 through ξ_4.

--The concentrations at the solid phase stations ξ_1 through ξ_5 continuously decreases their concentrations from an initial value determined when the seed pulse passed by.

The end of the first region and transition to the 2nd region is characterized by a very small concentration in the seed pulse.

The second region is initiated at a distance ξ^* where the seed pulse concentration is so small that the nuclides left at the solid phase results in a concentration smaller than that of the following secondary pulse.

This causes the flux at that position ξ for $\tau > 0$ to be initially positive (i.e., from liquid to solid). The flux decreases to zero and then becomes negative reaching a maximum negative value and then begins to increase again approaching asymptotically to zero.

In this second region, at a given position ξ, the concentrations in the solid phase and in the liquid phase increase with time ($r\ (\tau > 0) > 0$) reach a maximum ($r(\tau > 0) = 0$) and decrease towards zero ($r\ (\tau > 0) < 0$).

The position of maxima concentrations occurs along the characteristic

$$\tau = \xi \quad \text{where } r(\xi = \tau\ ,\ \tau > 0) = 0$$

This second region is illustrated by Figs. (3.1.4), (3.1.5) and (3.1.6). We can use again the discrete representation to show some characteristics of this second region:

BEST DOCUMENT AVAILABLE

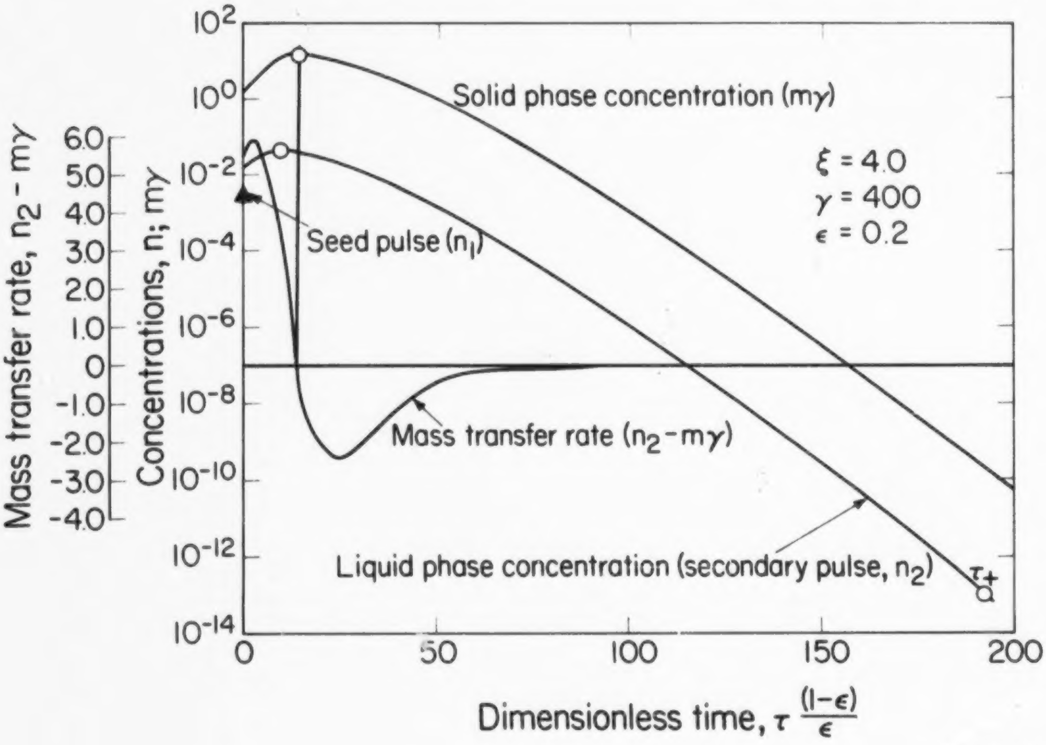

XBL 812-206

Fig. 3.1.4 Change in concentrations and reaction rate with time at a fixed $\xi = 4.0$.

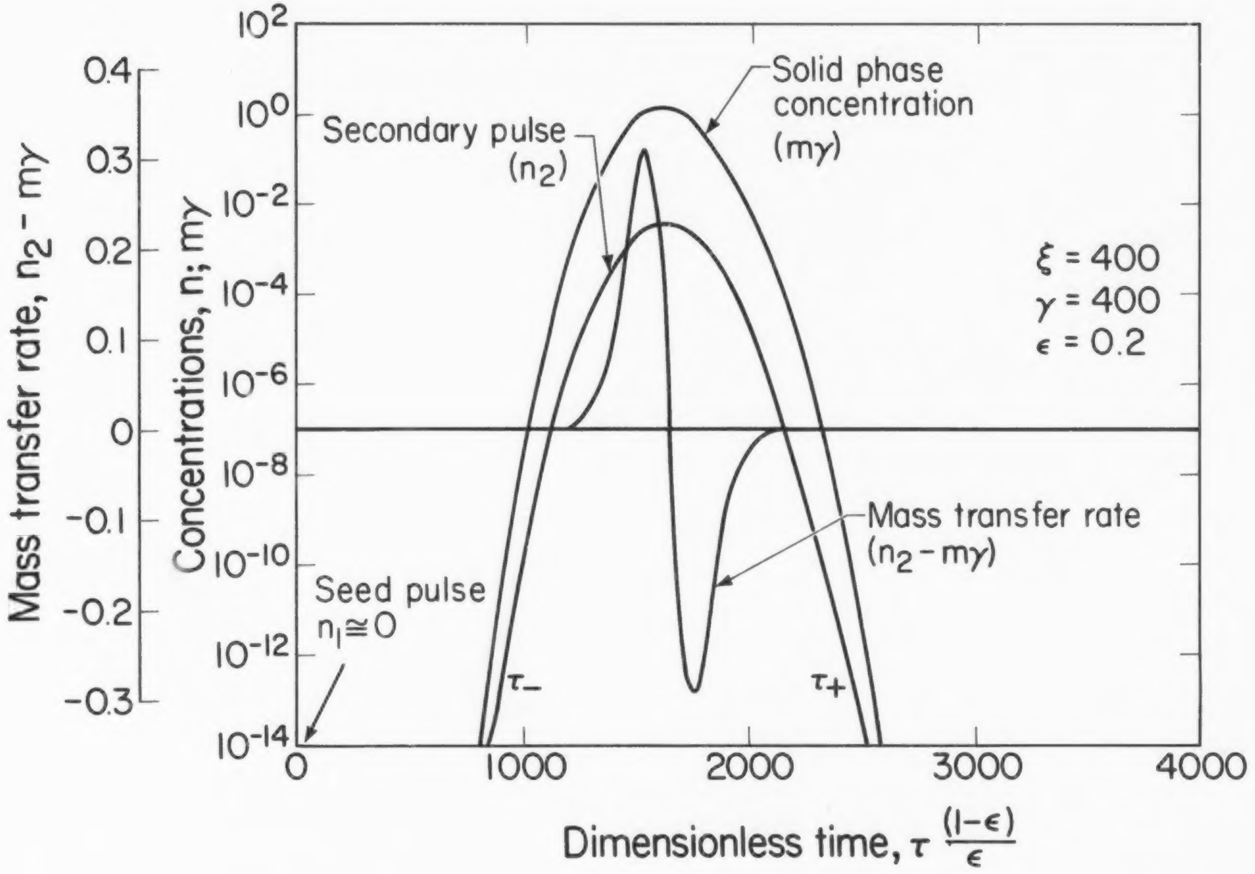

XBL 812-208

Fig. 3.1.5 Change in concentration and reaction rate with time at a fixed ξ = 40.

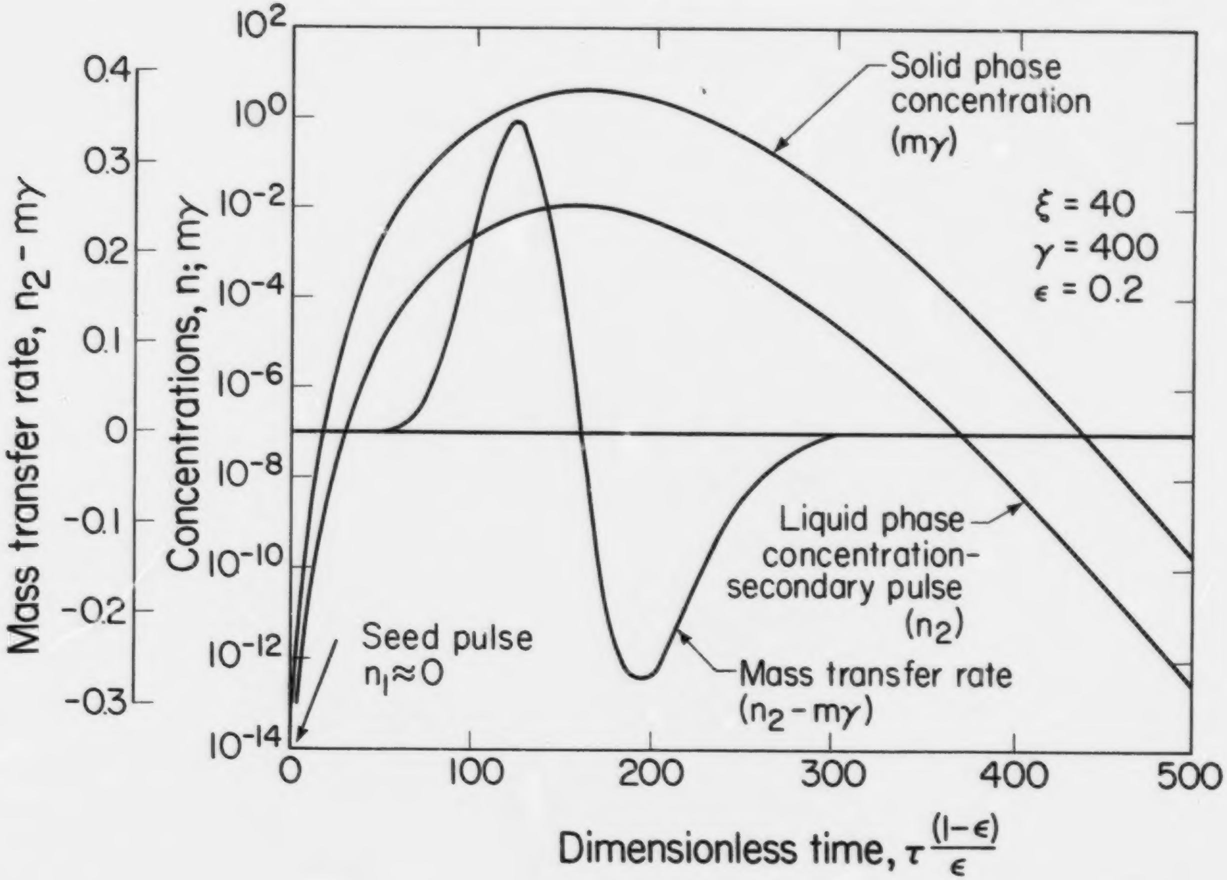

XBL 812-207

Fig. 3.1.6 Change in concentration and reaction rate with time at a fixed ξ = 400.

4) Near the point of transition from region 1 to region 2 (after)

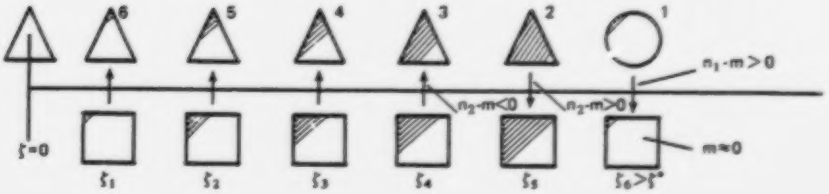
6
5
4
3
2
1
$n_1 - m > 0$
$n_2 - m < 0$
$n_2 - m > 0$
$\zeta = 0$
$m \approx 0$
ζ_1
ζ_2
ζ_3
ζ_4
ζ_5
$\zeta_6 > \zeta^*$

5) At a larger distance:

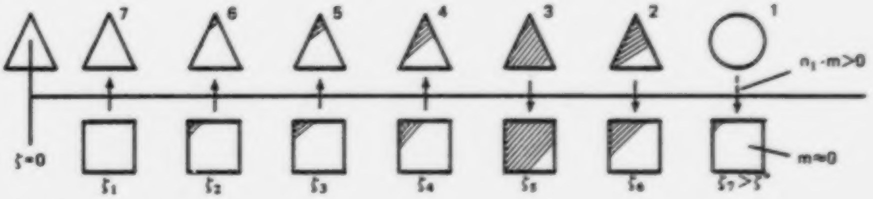
7
6
5
4
3
2
1
$n_1 - m > 0$
$\zeta = 0$
$m \approx 0$
ζ_1
ζ_2
ζ_3
ζ_4
ζ_5
ζ_6
$\zeta_7 > \zeta^*$

6) At farther downstream:

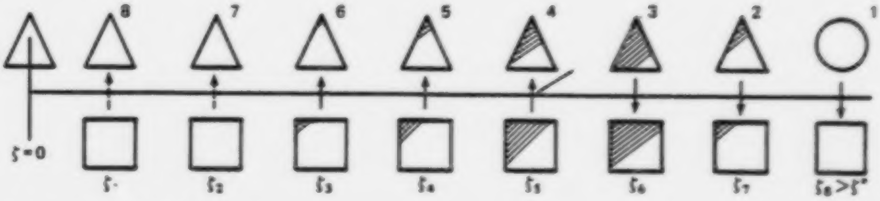
8
7
6
5
4
3
2
1
$\zeta = 0$
ζ_1
ζ_2
ζ_3
ζ_4
ζ_5
ζ_6
ζ_7
$\zeta_8 > \zeta^*$

One can note the following:

--The seed pulse concentration for distances $\xi > \xi^*$ is negligible and the solid phase station representing this position receives no nuclides ($m = 0$)

--The secondary pulse immediately following the seed pulse labeled by 2 which in region 1 always received atoms in region 2 is always giving atoms away because $r = n_2 - m > 0$.

--At the station ξ_5 which characterized the transition from region 1 to region 2 the solid phase receives atoms from pulse 2 but gives atoms to pulse 4 .

--One sees a "retardation" of the pulse with the largest concentration as one increases in distance. In other words: the seed pulse which had the largest concentration is gradually replaced by more and more delayed secondary pulses with large enough concentration to play the role that the seed pulse had previously.

This effect can be identified with the "retardation phenomena" existing in the equilibrium sorption solution.

3.1.4.2. Criteria to Determine the Equivalent "Zero" Concentration

Since in the non equilibrium solution the concentration distributions are represented by exponential functions and modified Bessel's functions of the first kind, the concentration will never reach absolute zero values.

To establish a lower "platform" for the concentration value (i.e., a value which one can assume the concentration to be negligible; this value can be very different from one radionuclide to another) one uses the concept of water dilution volume.

Let us define water dilution volume for contaminated groundwater by the following ratio:

$$I = \frac{\lambda N}{MPC} = \frac{[\text{curies/cm}^3 \text{ of contaminated groundwater}]}{[\text{curies/cm}^3 \text{ of clean water}]} \qquad (3.1.50)$$

The Maximum Permissible Concentrations (MPC) are defined in 10 CFR Part 20, Appendix B.

Therefore, the water dilution volume I is a measure of how many times more concentrated a given contaminated groundwater is compared to the maximum allowed concentration. Thus

$$I \equiv \frac{\text{cm}^3 \text{ of clean water}}{\text{cm}^3 \text{ of contaminated water}}$$

A way to define the "equivalent zero concentration is to set the water dilution volume equal to unity as the basic criteria, hence setting I = 1 in Eq. (3.1.50):

$$\lambda N_- = MPC$$

Let us denote the corresponding dimensionless concentration by $n_- = N_-/N_0$, thus:

$$n_- = \frac{(MPC)}{\lambda N_0} \qquad (3.1.51)$$

and n_- will be considered as the "equivalent zero concentration" in our next analyses.

This will be the dimensionless concentration corresponding to a water concentration of a particular radionuclide from which an average person can have its total daily intake of water without any harmful effect (B1).

And this dimensionless concentration can be used as our reference "zero concentration" in order to make comparisons between different radionuclides about the effects of non-equilibrium.

3.1.4.3. Comparison with the Equilibrium Solution

The solution to the governing equations (Eqs. (3.1.3) and (3.1.4)) when equilibrium sorption is assumed instead, can be easily obtained for the case of a impulse release boundary condition and reads:

$$n(\xi, \tau) = \delta(\tau - \xi) \tag{3.1.52}$$

The delta function can be interpreted as a pulse with constant magnitude traveling along the characteristic $\tau = \xi$ (same argument as in Eq. (3.1.46)).

By comparing above solution Eq. (3.1.52) with the non-equilibrium solution Eq. (3.1.32) and its graphical representation Fig. (3.1.1) one can recognize three major differences:

i) Along the characteristic $\tau = 0$ which represents the water traveling path we have the seed pulse in the non-equilibrium solution while in the equilibrium solution the concentration is zero.

ii) Let us define the contamination time as being the difference between the arrival time of the first nuclide and the departure time of the last radionuclide at a given position ξ. For the equilibrium solution this contamination time is a delta function (i.e., it is instantaneous) while for the non-equilibrium solution one might have in some instances large time intervals.

iii) The third major difference between the equilibrium and non equilibrium solution is that the equilibrium solution says that the pulse represented by Eq. (3.1.52) will be non-zero "ad infinitum" while the non-equilibrium solution says that both the seed pulse and the secondary pulse will tend to zero as τ or ξ tend to sufficiently large values.

It is proposed in this section to evaluate the range of τ and ξ in which these differences are significant in order to estimate the error that one introduces by assuming equilibrium sorption conditions.

i) The Seed Pulse Effect

As it was shown in Eq. (3.1.33) the seed pulse can be represented by:

$n_1 = e^{-\xi}$ when $\tau = 0$

This effect will be significant for short distances where the concentration predicted by the equilibrium solution will only happen in the form of a quick burst at the time $\tau = \xi$. But according to the non-equilibrium solution, the seed pulse which might still have a large concentration arrives at a much earlier time $\tau = 0$.

To evaluate how far the seed pulse goes before its concentration decays to a value smaller than the "equivalent zero concentration," Eq. (3.1.51) is used.

By setting $n_1 = n_-$

$$\frac{(MPC)}{\lambda N_o} = e^{-\xi} \quad , \quad \tau = 0$$

Therefore, the seed pulse has decayed to negligible concentrations at a position ξ^* given by:

$$\xi^* = \ln \frac{\lambda N_o}{(MPC)} \quad , \quad \text{for} \quad \tau = 0 \qquad (3.1\ 53)$$

ii) Contamination Time and Contaminated Region:

Let us rewrite the form of the solution for the secondary pulse Eq. (3.1.47):

$$n_2(\xi,\tau) = 2\xi e^{-(\tau+\xi)} \frac{I_1(\sqrt{4\xi\tau})}{\sqrt{4\xi\tau}} h(\tau) \qquad (3.1.47)$$

For each value of $n_2(\xi,\tau)$ we have two values of τ which satisfies Eq. (3.1.47) for each fixed value of the dimensionless position ξ. And conversely, for each fixed value of ξ we have two values of τ which satisfies Eq. (3.1.47) when we set $n_2(\xi,\tau)$ equal to a given value.

Let us set again the concentration to be equal to the "equivalent zero concentration" $n_- = (MPC)/\lambda N_o$, hence from Eq. (3.1.47)

$$\frac{(MPC)}{\lambda N_0} = 2\xi e^{-(\tau+\xi)} \frac{I_1(\sqrt{4\xi\tau})}{\sqrt{4\xi\tau}} \qquad (3.1.54)$$

Therefore if one considers a fixed position ξ; by solving Eq. (3.1.54) one obtains two values of time, say τ_- and τ_+. The contamination time at that position will be (referred to the "equivalent zero concentration"):

$$\theta(\xi) = \tau_+ - \tau_- \qquad (3.1.55)$$

Conversely, for a fixed time τ, we solve Eq. (3.1.54) to obtain ξ_- and ξ_+. With these values we can evaluate the contaminated region at time τ referred to the "equivalent zero concentration" as:

$$R(\tau) = \xi_+ - \xi_- \qquad (3.1.56)$$

Physically, the effect of non-equilibrium resulted in a pseudo-diffusion effect since the sharp pulse predicted by the equilibrium solution suffered a broadening in time and space. Such broadening can also be caused by dispersion which in the present case was not considered, leading us to attribute the broadening to non-equilibrium.

This effect can be seen in Fig. 3.1.5 and 3.1.6 where n_- was assumed arbitrarily to be 10^{-13}.

iii) Decay of the Secondary Pulse

The secondary pulse will decay towards zero even in absence of radioactive decay. The equilibrium solution predicts that if radioactive decay is not present, the original pulse will travel without decay throughout the media ad-infinitum.

But the non-equilibrium solution says that even in the absence of radioactive decay the secondary pulse dies away. Let us evaluate how the maxima concentration on the secondary pulse (denoted by $n_{2m}(\xi)$) will change as a function of ξ.

It was determined (see the graphs) that the maximum concentration on the secondary pulse travels along the characteristic $\tau = \xi$.

Substituting $\tau = \xi$ in Eq. (3.1.47) and expressing the modified Bessel's function by its assymptotic approximation for large arguments one has:

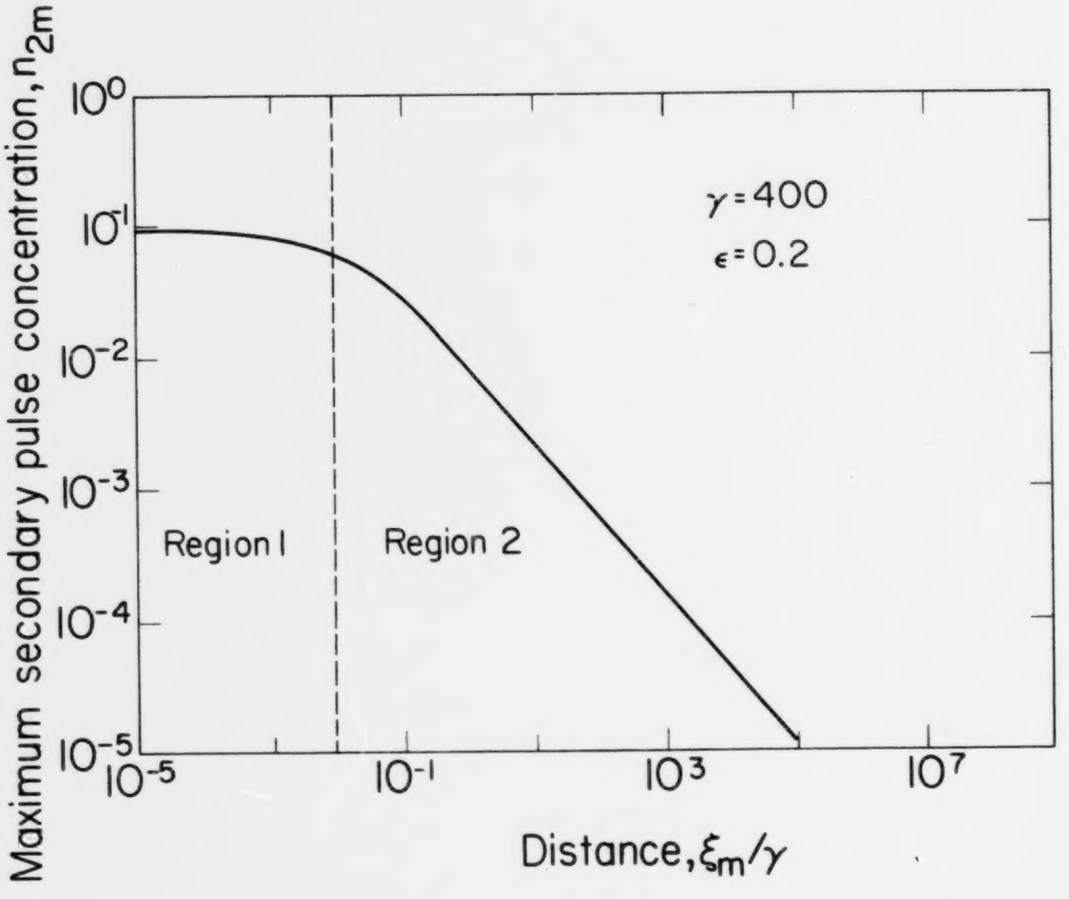

XBL 812-209

Fig. 3.1.7 The maximum concentration of the secondary pulse.

$$n_{2m}(\xi) = \frac{1}{2\sqrt{\pi}} \frac{1}{\sqrt{\xi}} \qquad (3.1.58)$$

One can conclude that the secondary pulse concentration decays proportionally to inverse square root of ξ.

This effect can be seen in Fig. (3.1.7) where $n_{2m}(\xi)$ was plotted.

3.1.5. Using the Analytical Solutions to Interpret Experimental Data

Seitz et al. (S1) have performed both batch and flowing sorption experiments with different types of rock and with solutions containing ^{237}Pu, ^{241}Am, ^{239}Np and ^{137}Cs. In this section the analytical solutions are fitted into their experimental data in order to verify the validity of the model as well as to obtain numerical estimates for the characteristic reaction time $(s\beta/\epsilon)^{-1}$ and for the equilibrium constant γ.

3.1.5.1. Batch Sorption Experiments

The contaminated solutions used in these batch experiments contained ^{237}Pu and ^{241}Am and they were expected to be in +4 and +3 valence states respectively. They were made in such a way as to represent natural groundwaters with leached nuclides.

This was done by reacting distilled water at ambient temperature with a fine aggregate of the rock to be studied. After the reaction is over the rock is filtered out leaving a solution called groundwater solution.

Well determined amounts of ^{237}Pu and ^{241}Am are then added to the groundwater solution.

Small tablets with rectangular shapes of the different rocks to be studied are then immersed in such solutions. The rock tablets are removed from time to time and the radionuclide concentration is determined by counting the radioactivity.

For all different types of rocks used, the resulting concentration profile with respect to time resulted in curves that can be fitted by exponentials functions.

This shows close agreement with the analytical solutions Eq. (3.1.44) and Eq. (3.1.45). When these experimental data are matched against the analytical solutions the parameters β and γ can be estimated. They are listed in Table 3.1.1.

3.1.5.2. Flowing Sorption Experiments

Seitz et al. (S1) also conducted several flowing sorption experiments to investigate the migration of plutonium, americium and neptunium through limestone, sandstone and tuff.

Cylindrical columns of the rock to be studied were fastened in polyethylene tubes. The rock column were wetted with groundwater solution, and nuclide solutions were added to the top surface of the columns in small volumes (1 cm^3). A pressure difference is then applied causing the contaminated groundwater solution to flow.

The solution collected at the bottom of the column was analyzed for the amount of nuclide that passed through the column.

The conditions of this experiment are very close to an impulse release boundary condition and our present solution is compared to the results of this experiment.

In Fig. 3.1.8, the cumulative amount of radionuclides (i.e., $\int_0^{\bar{\tau}} n(\xi,\tau)d\tau$) is plotted versus time τ.

The analytical solution is plotted using solid lines curves for fixed positions between $\xi/\gamma = 10^{-2}$ and $\xi/\gamma = 10^{-1}$.

Experimental results for the case of Pu^{4+} and Am^{3+} are then plotted.

The analytical solution has the following parameters: $\gamma = 400$, and $\epsilon = 0.2$.

From the batch experiments (Table 3.1.1), the resultant value of γ for Pu^{4+} in limestone is 370 while for Am^{3+} in limestone 385. They are both reasonably close to 400. The porosity of the limestone used is $\epsilon = 0.15$. Assuming that the parameters are in an agreement, from Fig. 3.1.8 one has that the resultant fitted curve for Pu^{4+} is associated to the dimensionless distance $\xi/\gamma = 2.5 \times 10^{-2}$. Recall the definition of ξ, Eq. (3.1.48)

$$\frac{\xi}{\gamma} = \frac{z}{V} \frac{1}{\left(\frac{s\beta}{\epsilon}\right)^{-1}}$$

Taking the height of the column to be about $z = 5$ cm while the estimated water velocity is $V = 0.6$ cm/hr one can use above values of ξ/γ for Pu^{4+} and limestone to estimate $(s\beta)$:

Table 3.1.1. Values for the reaction rate coefficient "β" and the equilibrium constant $\gamma = K_D \rho_S$ in static sorption experiments with groundwater solution at T = 25°C (S1).

Rock Type	β (cm/hr)		$\gamma \left(\frac{\text{cm}^3 \text{ liquid}}{\text{cm}^3 \text{ solid}}\right)$	
	Pu^{4+}	Am^{3+}	Pu^{4+}	Am^{3+}
Limestone	2.6×10^{-4}	1.0×10^{-3}	370	385
Granite	9.3×10^{-4}	6.3×10^{-4}	80	13
Basalt	1.5×10^{-3}	4.3×10^{-4}	620	860
Tuff	3.6×10^{-4}	1.7×10^{-3}	70	630
Schist	2.2×10^{-4}	3.2×10^{-2}	350	7
Magenta	9.3×10^{-3}	1.0×10^{-4}	100	120
Marble	3.5×10^{-3}	2.4×10^{-3}	270	470
Oolitic Limestone	1.4×10^{-3}	1.3×10^{-3}	480	530
Sandstone	2.9×10^{-3}	8.6×10^{-3}	20	20
Soapstone	1.1×10^{-2}	4.7×10^{-3}	60	180
Dolomite	2.7×10^{-2}	9.1×10^{-3}	40	150
Chalcopyrite	1.7×10^{-3}	7.9×10^{-3}	40	2

$s\beta = 3.7 \times 10^{-4}$ (1/hr) for the flowing system compared to $s\beta = 2.9 \times 10^{-4}$ (1/hr) for the batch system. Similarly for Am^{3+} with $\xi/\gamma = 3.0 \times 10^{-2}$ obtained from Fig. 3.1.8:

$s\beta = 4.5 \times 10^{-4}$ (1/hr) for the flowing system

$s\beta = 9.0 \times 10^{-4}$ (1/hr) for the batch system

3.2. Transport of Radionuclide Decay Chains with Nonequilibrium Reversible Reactions

3.2.1. Analytical Solution of the Three-States Model

Our preceding analyses (Section 2 and (H1)) of the transport of radionuclide decay chains through sorbing porous media have assumed local chemical equilibrium, except when a completely irreversible reaction removes a nuclide from the transport system. Here we consider the effect of non-

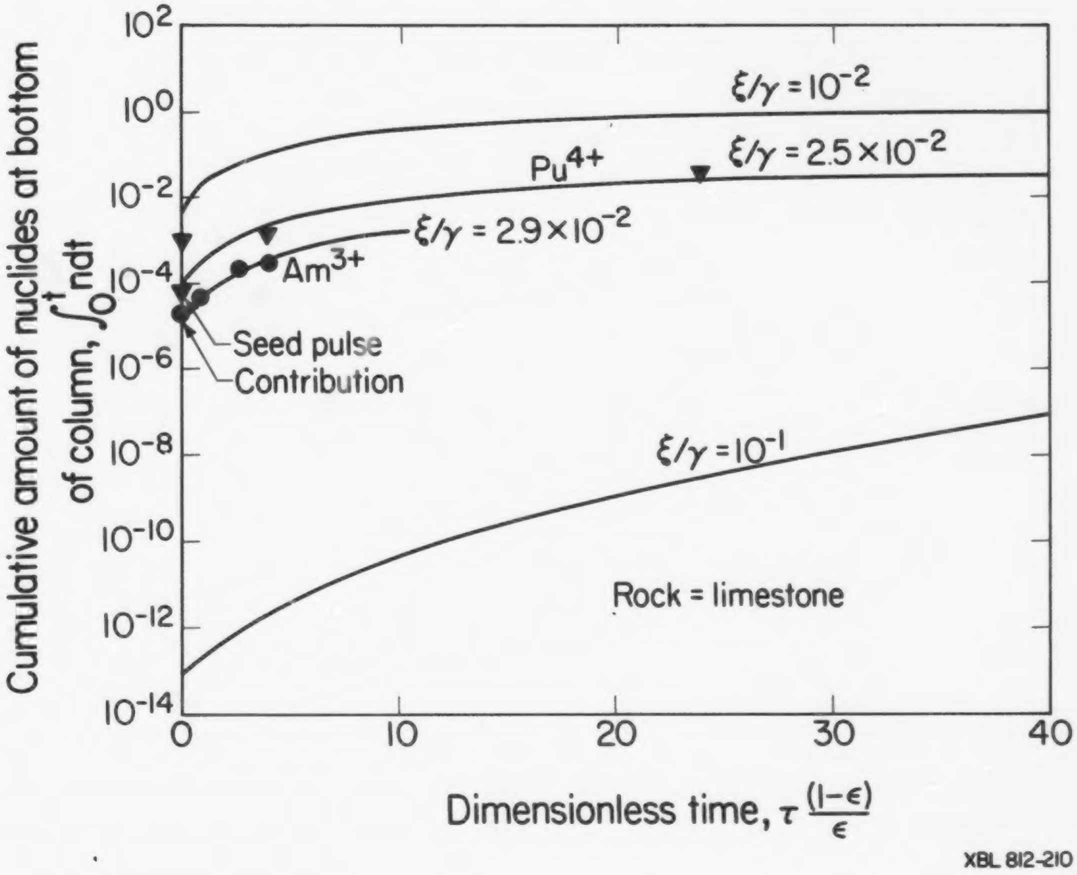

Fig. 3.1.8 Matching flowing experimental data with the analytical solution.

equilibrium reversible reactions on the migration features of the radionuclides in a decay chain. For example, the rate of mass transfer of sorbing species between liquid and solid may be so slow that sorption equilibrium is not established. This could change the effective migration speeds of the chromatographic bands. Or, a sorbed state in local equilibrium with the adjacent liquid may undergo a slow but reversible reaction to a more tightly bound "mineralized" state on the solid. If this mineralization reaction is reversible but does not reach equilibrium during the transport process, its reaction kinetics can affect the rate of migration of the chromatographic bands through the liquid.

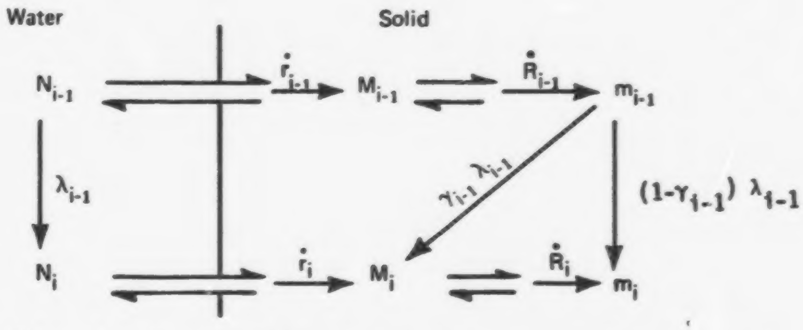

Fig. 3.2.1. Reaction scheme for three-states model.

This second example, referred to here as the "three-states model," is shown schematically in Fig. 3.2.1. In this diagram M represents the concentration of the sorbed species in equilibrium with the adjacent liquid, and m represents the concentration of the mineralized species. A fraction γ_{i-1} of the mineralized species of the nuclide i-1 decays to the nonmineralized sorbed species of nuclide i, and a fraction $1 - \gamma_{i-1}$ decays to the mineralized form of nuclide i. The net reaction rates from the first sorbed state to the mineralized state are denoted by $\dot{R}$.

In Section 3.2.3 the model of Fig. 3.2.1 is transformed to the case of non-equilibrium between the liquid and a single sorbed state by eliminating the intermediate state M. The reaction rates $\dot{R}$ then become net rates of mass transfer from liquid to solid.

Proceeding with the model of Fig. 3.2.1, local chemical equilibrium between the liquid and the non-mineralized sorbed state is expressed by:

$$M_i(z,t) = K_{D,i}N_i(z,t) \tag{3.2.1}$$

The overall sorption coefficient K_i (the "retardation coefficient" for an equilibrium two-state model) is:

$$K_i = 1 + \frac{1-\epsilon}{\epsilon} K_{D,i} \tag{3.2.2}$$

The rate of the mineralization reaction is assumed to be first order with respect to the sorbed and mineralized species:

$$\dot{R}_i = \vec{k}_i M_i - \overleftarrow{k}_i m_i \tag{3.2.3}$$

where $\vec{k}_i$ and $\overleftarrow{k}_i$ are the rate constants for the forward and reverse reactions, respectively.

When $\gamma_i = \overleftarrow{k}_i = 0$ for all i we have the case of irreversible mineralization already treated in Section 2.1. We give in Appendix E the explicit solutions for a three-member decay chain, assuming a step release with the source term given by Eq. (2.1.17), for the case with $R_i = 0$, but with γ_i retained as a finite quantity.

Assuming transport in a one-dimensional flow field and sources uniform over x and y, the conservation equations for the three species of nuclide i, valid for $-\infty < z < \infty$ and $t > 0$, are:

$$\frac{\partial N_i}{\partial t} = D \frac{\partial^2 N_i}{\partial z^2} - v \frac{\partial N_i}{\partial z} - \lambda_i N_i + \lambda_{i-1} N_{i-1} - \dot{r}_i + \phi_i'''(z,t) \tag{3.2.4}$$

$$\frac{\partial M_i}{\partial t} = -\lambda_i M_i + \lambda_{i-1} M_{i-1} + \gamma_{i-1} \lambda_{i-1} m_{i-1} + \frac{\epsilon}{1-\epsilon} \dot{r}_i - \dot{R}_i \tag{3.2.5}$$

$$\frac{\partial m_i}{\partial t} = -\lambda_i m_i + (1 - \gamma_{i-1}) \lambda_{i-1} m_{i-1} + \dot{R}_i \tag{3.2.6}$$

where $\phi_i'''(z,t)$ represents a general volumetric source term in the water phase. The concentration $N_i(z,t)$ is subject to the conditions given by Eqs. (2.1.7) and (2.1.8). Also,

$$M_i(z,0) = 0 \quad , \quad \text{for all } z \tag{3.2.7}$$

$$m_i(z,0) = 0 \quad , \quad \text{for all } z \tag{3.2.8}$$

Combining Eqs. (3.2.2) through (3.2.6), there results

$$\frac{\partial N_i}{\partial t} - \tilde{D}_i \frac{\partial^2 N_i}{\partial z^2} + v_i \frac{\partial N_i}{\partial z} + \lambda_i N_i + \overrightarrow{\sigma}_i N_i - \overleftarrow{\sigma}_i m_i = \tag{3.2.9}$$

$$= \frac{1}{K_i} \phi_i^{'''}(z,t) + \frac{K_{i-1}\lambda_{i-1}}{K_i} N_{i-1} + \frac{\gamma_{i-1}\lambda_{i-1}(1 - \epsilon)}{K_i \epsilon} m_{i-1} \equiv f_i(z,t)$$

and

$$\frac{\partial m_i}{\partial t} + X_i m_i - \overrightarrow{k}_i K_{Di} N_i - \lambda_{i-1}(1 - \gamma_{i-1})\, m_{i-1} = 0 \tag{3.2.10}$$

where

$$\tilde{D}_i \equiv D/K_i \tag{3.2.11}$$

$$X_i \equiv \lambda_i + \overleftarrow{k}_i \tag{3.2.12}$$

$$v_i \equiv v/K_i \tag{3.2.13}$$

$$\overleftarrow{\sigma}_i \equiv \frac{1 - \epsilon}{\epsilon} \overleftarrow{k}_i / K_i \tag{3.2.14}$$

$$\overrightarrow{\sigma}_i \equiv \frac{1 - \epsilon}{\epsilon} \overrightarrow{k}_i K_{D,i} / K_i \tag{3.2.15}$$

Equations (3.2.9) and (3.2.10) are subject to the conditions of Eqs. (2.1.7), (2.1.8) and (3.2.8).

The solution is obtained by an approach similar to that used by Lapidus and Amundson (L1), who analyzed the one-dimensional transport of a non-radioactive species with non-equilibrium sorption. The results (F1) are:

$$N_i(z,t) = \frac{e^{z v_i / 2\tilde{D}_i}}{2\tilde{D}_i} \int_{-\infty}^{\infty} e^{-z' v_i / 2\tilde{D}_i} \times \tag{3.2.16}$$

$$\times \int_0^t H_i(z - z',\tau)[F_i(z',t - \tau) + \tilde{F}_i(z',t - \tau)]\, d\tau\, dz'$$

$$M_i(z,t) = K_{D,i}N_i(z,t) \qquad (3.2.17)$$

$$m_i(z,t) = \overrightarrow{k}_i K_{D,i} e^{-\chi_i t}\int_0^t e^{\chi_i \tau} N_i(z,\tau)\,d\tau +$$

$$+ \lambda_{i-1}(1 - \gamma_{i-1})\, e^{-\chi_i t}\int_0^t e^{\chi_i \tau} m_{i-1}(z,\tau)\,d\tau \qquad (3.2.18)$$

where

$$f_i(z,t) = \frac{1}{K_i}\left[\phi_i'''(z,t) + K_{i-1}\lambda_{i-1}N_{i-1} + \gamma_{i-1}\lambda_{i-1}\,\frac{1-\epsilon}{\epsilon}\,m_{i-1}\right] \qquad (3.2.19)$$

$$\tilde{f}_i(z,t) = \overleftarrow{\sigma}_i\lambda_{i-1}(1 - \gamma_{i-1})\, e^{-\chi_i t}\int_0^t e^{\chi_i \theta} m_{i-1}(z,\theta)\,d\theta \qquad (3.2.20)$$

$$F_i(z,t-\tau) = \chi_i f_i(z,t-\tau) - \frac{\partial f_i(z,t-\tau)}{\partial \tau} \qquad (3.2.21)$$

$$\tilde{F}_i(z,t-\tau) = \chi_i \tilde{f}_i(z,t-\tau) - \frac{\partial \tilde{f}_i(z,t-\tau)}{\partial \tau} \qquad (3.2.22)$$

$$H_i(z,t) = \sqrt{\frac{\tilde{D}_i}{\pi}}\, e^{-\chi_i t}\int_0^t I_0[\xi_i(t,x)]\, G_i(z,x)\,dx \qquad (3.2.23)$$

$$G_i(z,x) = \frac{1}{\sqrt{x}}\exp\left(-\frac{z^2}{4x\tilde{D}_i} - d_i x\right) \qquad (3.2.24)$$

$$a_i = K_{D,i}\overleftarrow{\sigma}_i\overrightarrow{k}_i \qquad (3.2.25)$$

$$d_i = \lambda_i + \overrightarrow{\sigma}_i + \frac{v_i^2}{4\tilde{D}_i} - \chi_i \qquad (3.2.26)$$

$$\xi_i(t,x) = 2\sqrt{a_i x(t - x)} \qquad (3.2.27)$$

$I_o[\xi_i]$ = modified Bessel function of zero order.

3.2.2. Solutions for a Plane Source of Dissolving Nuclides at z = 0

Here we assume that the dissolving nuclides can be represented by an infinite plane source in the water at $z = 0$, characterized by:

$$\phi_i'''(z,t) = \phi_i''(t)\ \delta(z) \qquad (3.2.28)$$

where $\phi_i''(t)$ is the rate of dissolution of nuclide i per unit area of source in the water.

The function $f_i(z,t)$, defined by Eq. (3.2.19), is then:

$$f_i(z,t) = \frac{1}{K_i}\ \phi_i''(t)\ \delta(z) + f_i^P(z,t) \qquad (3.2.29)$$

where the contribution f_i^P from the precursor is given by:

$$f_i^P(z,t) = \frac{1}{K_i}\left[K_{i-1}\lambda_{i-1}N_{i-1}(z,t) + \gamma_{i-1}\lambda_{i-1}\ \frac{1-\varepsilon}{\varepsilon}\ m_{i-1}(z,t)\right] \qquad (3.2.30)$$

Substituting Eqs. (3.2.29) and (3.2.30) into (3.2.16), we obtain the following expression for N_i:

$$N_i(z,t) = \frac{e^{zv_i/2\tilde{D}_i}}{2K_i\sqrt{\pi\tilde{D}_i}} \int_0^t \phi_i''(t-\tau)\ e^{-X_i\tau}\ G_i(z,\tau)\ d\tau$$

$$+ \frac{e^{zv_i/2\tilde{D}_i}}{2\sqrt{\pi\tilde{D}_i}} \left\{ \int_{-\infty}^{\infty} e^{-z'v_i/2\tilde{D}_i} \left[\int_0^t \left(f_i^P(z',t-\tau) - \tilde{f}_i(z',t-\tau) \right) \times \right.\right.$$

$$\left.\left. \times\ e^{-X_i\tau}\ \tilde{G}_i(z-z',\tau)\ d\tau \right] dz' \right\} \qquad (3.2.31)$$

where

$$\tilde{G}_i(z,\tau) \equiv G_i(z,\tau) + \int_0^\tau I_1[\xi_i(\tau,x)]\, \frac{\xi_i(\tau,x)}{2(\tau - x)}\, G_i(z,x)\, dx \qquad (3.2.32)$$

$I_1(\xi)$ = modified Bessel function of first order.

M_i and m_i are still given by Eqs. (3.2.17) and (3.2.18).

3.2.3. Nonequilibrium between Liquid and Solid; Transport Limited by Rate of Mass Transfer

Here we consider the effects of slow mass transfer between liquid and solid, so that a radionuclide in the liquid is not in equilibrium with a sorbed state on the solid. Lapidus and Amundson (L1) analyzed the similar but simpler problem of the one-dimensional transport of a nonradioactive species with a constant distribution coefficient and with nonequilibrium between liquid and solid. Here we extend that analysis to the transport of nuclides in a radioactive decay chain, and more general sources and boundary conditions are introduced.

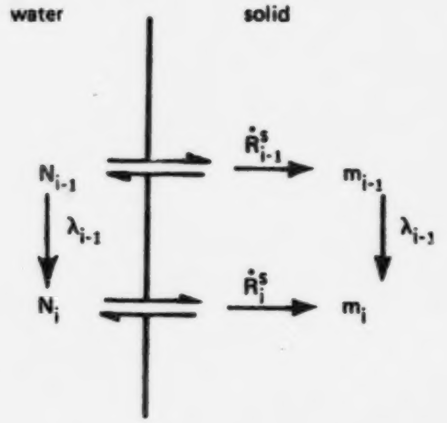

Fig. 3.2.2.
Reaction scheme for the nonequilibrium model.

The equations of Section 3.2.1 can be applied to this case by adopting the model shown in Fig. 3.2.2. Now the equilibrium sorbed state M is eliminated and the first-order rate process occurs between the radionuclides dissolved in the liquid and the sorbed state m, at a rate:

$$(1 - \epsilon)\, \dot{R}_i^S = \epsilon \overrightarrow{k}_i^S N_i - (1 - \epsilon)\, \overleftarrow{k}_i^S m_i \qquad (3.2.33)$$

$\dot{R}_i^S$ represents the net rate of sorption per cubic meter of solid and $\overrightarrow{k}_i^S$ and $\overleftarrow{k}_i^S$ are the rate constants for the forward and reverse sorption reactions, respectively. Equation (3.2.33) can be rewritten in terms of a mass-transfer coefficient $k_{m,i}$ as:

$$(1-\epsilon)\dot{R}_i^S = k_{m,i}S\left(N_i - \frac{m_i}{K_{D,i}^S}\right) \tag{3.2.34}$$

where

$$K_{D,i}^S = \frac{m_i}{N_i^*} = \frac{\epsilon \vec{k}_i^S}{(1-\epsilon)\,\overleftarrow{k}_i^S} \tag{3.2.35}$$

N_i^* is the concentration of nuclide i in the liquid that would be in equilibrium with a concentration m_i in the solid, with a sorption equilibrium constant $K_{D,i}^S$. S is the interfacial area for mass transfer, per unit volume of liquid plus solid, and

$$k_{m,i} = \frac{\epsilon \vec{k}_i^S}{S} \tag{3.2.36}$$

The one-dimensional transport equation for nuclide i now becomes:

$$\frac{\partial N_i}{\partial t} = D\frac{\partial^2 N_i}{\partial z^2} - v\frac{\partial N_i}{\partial z} - \lambda_i N_i + \lambda_{i-1}N_{i-1} - \left(\frac{1-\epsilon}{\epsilon}\right)\dot{R}_i^S + \phi_i'''(z,t) \tag{3.2.37}$$

with

$$\frac{\partial m_i}{\partial t} = -\lambda_i m_i + \lambda_{i-1}m_{i-1} + \dot{R}_i^S \tag{3.2.38}$$

Equations (3.2.37) and (3.2.38) are valid for $-\infty < z < \infty$ and $t > 0$ and are subject to Eqs. (2.1.7), (2.1.8) and (3.2.8). By substituting Eq. (3.2.34) we obtain:

$$\frac{\partial N_i}{\partial t} - D\frac{\partial^2 N_i}{\partial z^2} + v\frac{\partial N_i}{\partial z} + \lambda_i N_i + \frac{k_{m,i}S}{\epsilon}N_i - \frac{k_{m,i}S}{\epsilon K_{D,i}^S}m_i = \lambda_{i-1}N_{i-1} + \phi_i'''(z,t) \tag{3.2.39}$$

and

$$\frac{\partial m_i}{\partial t} + \lambda_i m_i - \lambda_{i-1} m_{i-1} - \frac{k_{m,i} S}{(1 - \epsilon)} N_i + \frac{k_{m,i} S}{(1 - \epsilon)\, K^S_{D,i}} m_i = 0 \qquad (3.2.40)$$

Comparing Eq. (3.2.39) with Eqs. (3.2.9) and (3.2.40) with Eq. (3.2.10), we find the same mathematical problem, with the correspondence given in Table 3.2.1. The solution to the present problem of non-equilibrium between the liquid and a single sorbed stated on the solid can therefore be obtained from Eqs. (3.2.16) and (3.2.27) by making the changes indicated above. The new parameters of the non-equilibrium sorption problem are contained in $k_{m,i}$, S, and $K^S_{D,i}$.

3.2.4. Comparison with the Cameron-Klute Model

Cameron and Klute (C1), analyzed the problem of the one-dimensional transport of a nonradioactive species, undergoing two different sorption mechanisms on the solid: a very fast one, for which the resulting sorbed species, M_i, in equilibrium with the adjacent liquid, with a sorption

Table 3.2.1. Correspondence between the three-state model and the mass-transfer-limited model, Eqs. (3.2.39) and (3.2.40).

Symbols in the Three State Model, Eqs. (3.2.9) and (3.2.10)	Replace by the Following for the Mass Transfer-Limited Model
K_i	1
γ_i	0
$K_{D,i}$	$\epsilon/(1 - \epsilon)$
$\overrightarrow{k}_i$	$\overrightarrow{k}^S_i = k_{m,i} S/\epsilon$
$\overleftarrow{k}_i$	$\overleftarrow{k}^S_i = k_{m,i} S[(1 - \epsilon)\, K^S_{D,i}]^{-1}$

equilibrium constant $K_{D,i}^{(1)}$; and a slower sorption mechanism, with an assumed rate of sorption given by:

$$(1 - \varepsilon)\, \dot{R}_i^s = \varepsilon \vec{k}_i^s N_i - (1 - \varepsilon)\, \overleftarrow{k}_i^s m_i \qquad (3.2.41)$$

As in Section 3.2.3, Eq. (3.2.41) can be written as:

$$(1 - \varepsilon)\, \dot{R}_i^s = k_{m,i} S \left[N_i - \frac{m_i}{K_{D,i}^s} \right] \qquad (3.2.42)$$

with

$$K_{D,i}^s = \frac{m_i}{N_i^*} = \frac{\varepsilon \vec{k}_i^s}{(1 - \varepsilon)\, \overleftarrow{k}_i^s} \qquad (3.2.43)$$

It is also assumed that the sorbed species characterized by M_i and m_i do not interact.

This model is shown schematically in Fig. 3.2.3:

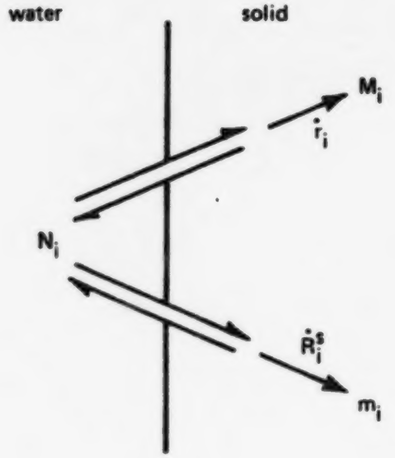

Fig. 3.2.3. Reaction scheme for the Cameron-Klute model.

The solution to this problem, extended to nuclides in a radioactive decay chain, with more general source and boundary conditions, can be obtained from the solutions presented in Section 3.2.1: $N_i(z,t)$ and $m_i(z,t)$ are obtained respectively by Eq. (3.2.18), by replacing:

K_i by $K_i^{(1)} = 1 + \frac{1 - \varepsilon}{\varepsilon} K_{D,i}^{(1)}$

γ_i by 0

$K_{D,i}$ by $\varepsilon/(1 - \varepsilon)$

$\vec{k}_i$ by $k_i^s = k_{m,i} S/\varepsilon$

$\overleftarrow{k}_i$ by $k_i^s = k_{m,i} S[(1 - \varepsilon)\, K_{D,i}^s]^{-1}$

while $M_i(z,t)$ is given by:

$$M_i(z,t) = K_{D,i}^{(1)} N_i(z,t) \qquad (3.2.44)$$

3.2.5. Non-Equilibrium Transport of ^{234}U

The equations in Sections 3.2.3 and 3.2.4 are used here to illustrate the nonequilibrium transport of ^{234}U, which is assumed to be present in the waste with no precursors. Figure 3.2.4 shows concentrations as a function of distance at a time of 10^5 yr after the beginning of waste dissolution. A band release is assumed, with a leach time T of 3 x 10^4 yr. The assumed transport properties are:

$D = 10^3$ m^2/yr

$v = 100$ m/yr

$K_U = 10^4$

$\varepsilon = 0.5$

Curve (a) is the familiar band for local equilibrium, with no mineralization ($\vec{k} = \overleftarrow{k} = 0$). The sharp edges of the bands in earlier illustrations do not appear here because dispersion has been included.

Curve (b) shows the effect of nonequilibrium reversible mineralization, with $\vec{k} = \overleftarrow{k} = 10^{-4}$/yr. The peak concentration is attenuated by mineralization, and the effective migration speed of the peak is decreased. The band broadens considerably due to the delayed demineralization and desorption.

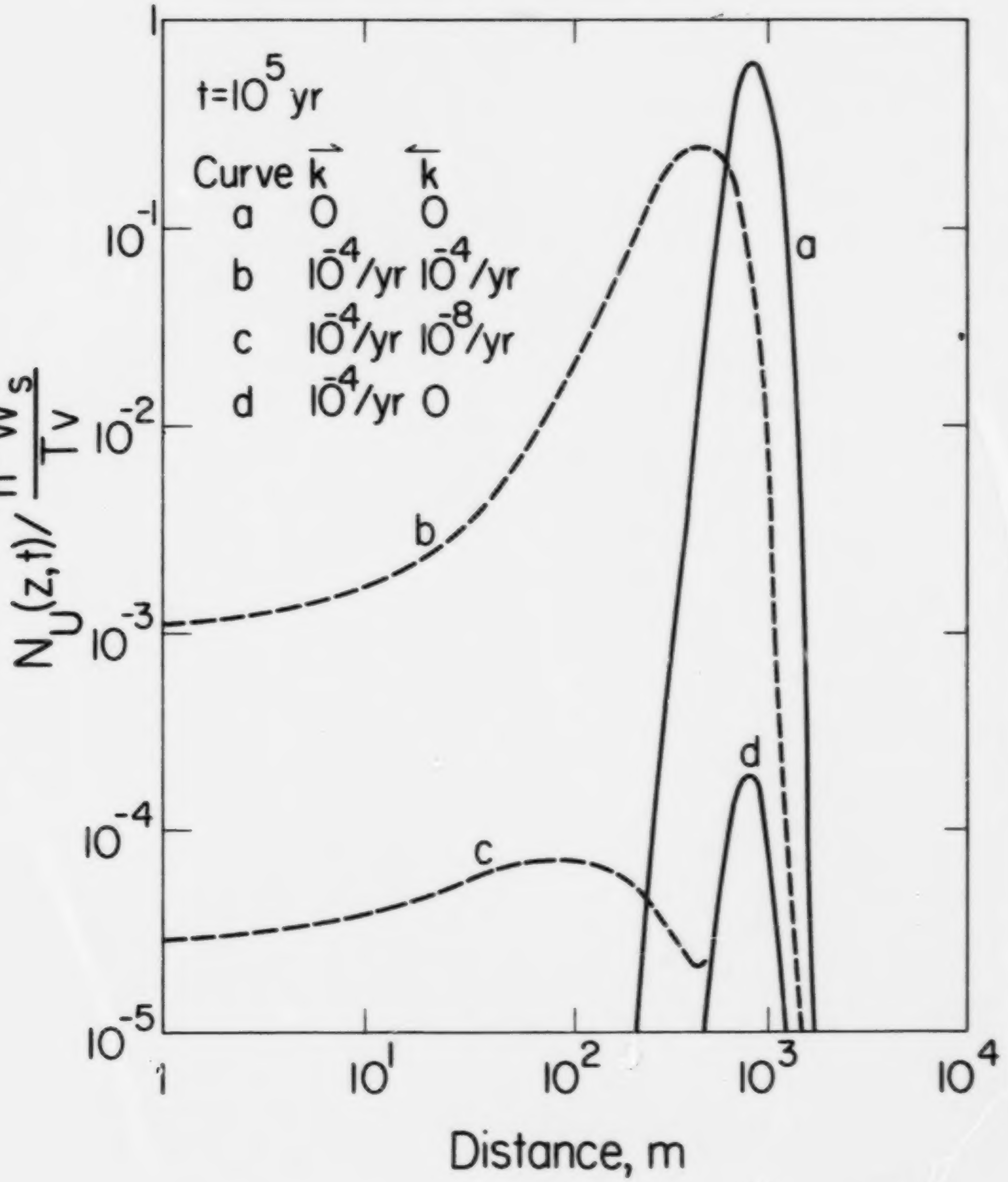

XBL 812-211

Fig. 3.2.4. Effect of mineralization on ^{234}U, three-states model, $N_U(z,t)$ = atoms/m^3 of ^{234}U, D = 10^3 m^2/yr, v = 100 m/yr, T = 3 x 10^4 yr, $K_U = 10^4$, ε = 0.5.

In curve (c) a more stable mineralized species is assumed, with $\vec{k} = 10^{-4}$/yr and $\overleftarrow{k} = 10^{-8}$/yr. The magnitude of the peak concentration is greatly decreased, because in the earlier times of the band front mineralization removes uranium from the liquid. The smaller rate constant for demineralization delays the appearance of the broadened band, and a second but smaller peak concentration appears behind the first peak.

Curve (d) shows the effect of irreversible mineralization, with $\vec{k} = 10^{-4}$/yr and $\overleftarrow{k} = 0$. The attenuation of the first peak is identical to that of curve (c). However, because there is no demineralization, the broadened band and second peak do not appear.

Figure 3.2.5 shows concentration profiles as a function of distance at a time of 10^4 yr after the beginning of waste dissolution. The assumed transport properties are:

$D = 10^3$ m^2/yr
$v = 1$ m/yr
$\epsilon = 0.5$
$T = 100$ yr

The sorption equilibrium constant $K^s_{D,U}$, given by Eq. (3.2.35) is assumed to have the constant value of 10^4.

The relatively high concentrations at short distances, appearing in curves (a) through (g), are caused by dispersion and by the assumed low water velocity.

Curve (a) is the band for the case without mineralization or local equilibrium ($k_{m,U}S = 0$).

Curve (b) shows the effect of non-equilibrium reversible mineralization, with $k_{m,U}S = 5 \times 10^{-5}$ yr^{-1}. The peak concentration is attenuated by mineralization.

In curve (c) a greater rate of mass transfer is assumed, $k_{m,U}S = 5 \times 10^{-4}$ yr^{-1}. The magnitude of the peak concentration is greatly decreased, because in the earlier times of the band front, mineralization removes uranium from the liquid.

Curves (d) to (f) show the effect of increasing k_mS values. The uranium concentration in water increases due to the increasing de-mineralization rate, but the front of the band is delayed. As $k_{m,U}S$ increases, the concentration

BEST DOCUMENT AVAILABLE

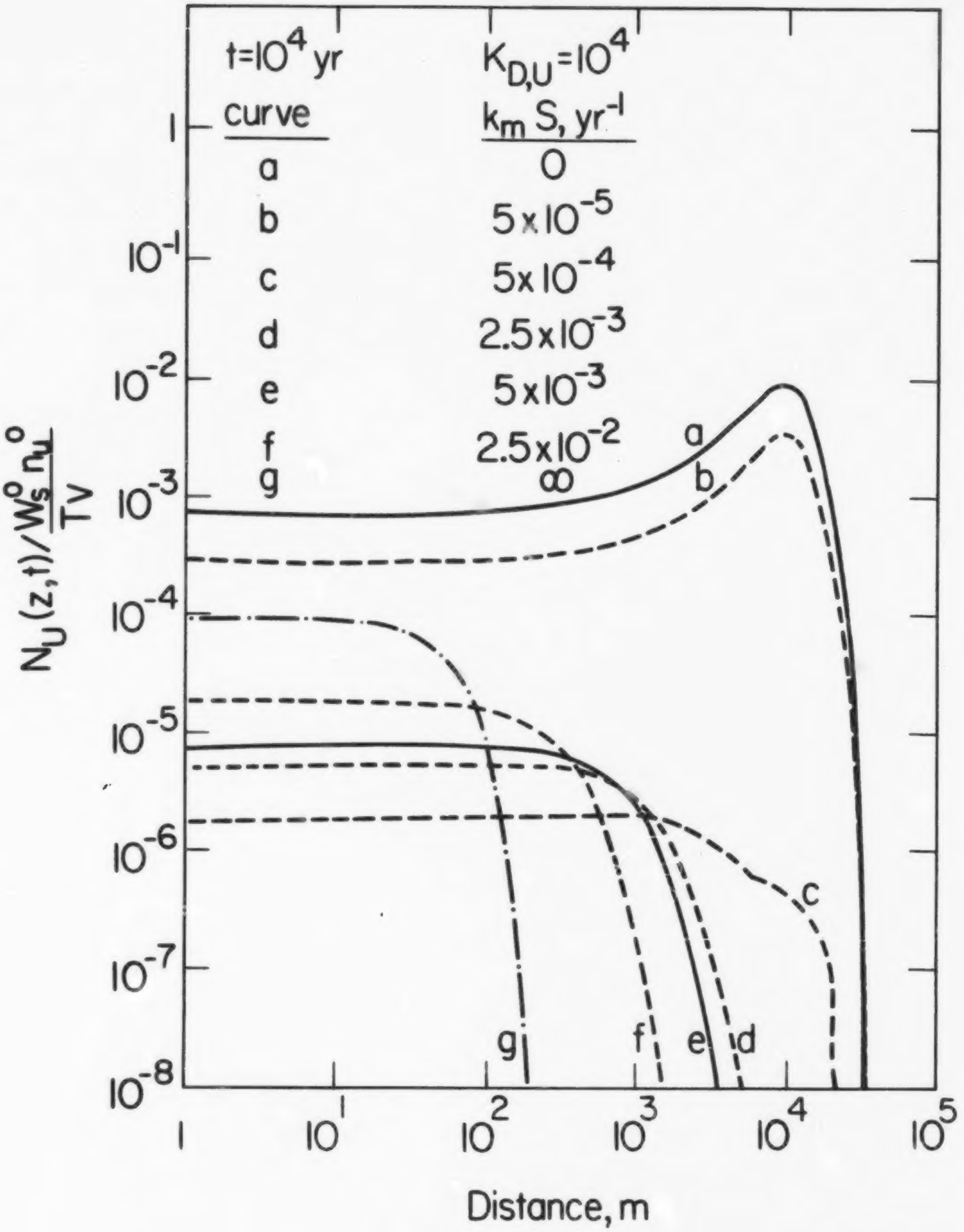

XBL 812-212

Fig. 3.2.5. Effect of rate of mass transfer on ^{234}U, $N_U(z,t)$ = atoms/m^3 of ^{234}U, $D = 10^3$ m^2/yr, $v = 1$ m/yr, $T = 100$ yr, $\varepsilon = 0.5$, for curve (g), $K_U = 1000/$.

profiles approach the local equilibrium profile, which results when the mass transfer coefficient becomes infinite.

Curve (g) shows the local equilibrium profile, calculated from the solutions presented in Section 2.1, Eqs. (2.1.20), (2.1.35) and (2.1.18). The retardation coefficient K_u, equal to 1001, is obtained from Eq. (2.1.3), together with the values for ϵ and $K_{D,u}^S$ assumed for Fig. 3.2.5.

3.3. Two Chemical Species in Liquid Nonequilibrium

In mathematical modeling the migration of radionuclides through sorbing media, the effects of nonequilibrium in chemical reactions among species of different valences, compounds, complexes, and sorption processes are usually neglected from the consideration that the time required to establish local equilibrium is very short compared with the time scale of interest in nuclide migration. The concept of local equilibrium, which simplifies the migration problem, may be a suitable approximation for long-lived radionuclides. For short-lived radio-nuclides, assumption of local equilibrium may introduce significant error in estimating time-space dependent concentration. Also, in the time scale of laboratory experiments, the effects of nonequilibrium become more important.

In this section we formulate the transport equation for two chemical species of a radionuclide which undergo chemical reaction. We present analytical solutions for a radionuclide with no precursor, and we provide a numerical demonstration of the effect of nonequilibrium on the transport of the radionuclide.

3.3.1. Mathematical Model

Let N_i^m and M_i^m be the concentrations of the mth chemical species of the ith nuclide in water and in solid, respectively, and assume that the ground-water flows in the z direction. For the case of dispersion free, the nuclide conservation equations are:

$$\frac{\partial}{\partial t}(\epsilon N_i^m) + v\frac{\partial}{\partial z}(\epsilon N_i^m) + k_m s\left(N_i^m - \frac{1}{K_{Di}^m} M_1^m\right) + \epsilon\left(k_{fi}^{ml} N_i^m - k_{fi}^{lm} N_i^l\right)$$

$$+ \epsilon(\lambda_i N_i^m - \lambda_{i-1} N_{i-1}^m) = 0 \qquad (3.3.1)$$

$$\frac{\partial}{\partial t}\left[(1-\varepsilon)\,M_1^m\right] - k_m s\left(N_i^m - \frac{1}{K_{Di}^m}M_i^m\right) + (1-\varepsilon)\,(k_{si}^{ml}M_i^m - k_{si}^{lm}M_i^l)$$

$$+ (1-\varepsilon)(\lambda_i M_i^m - \lambda_{i-1}M_i^m) = 0 \qquad (3.3.2)$$

$i = 1,2,3,\ldots\,, \quad m,l = 1,2\,, \quad \lambda_0 = 0$

$t \geq 0\,, \quad \infty \geq z \geq 0$

where v is the water velocity, k_m is the mass transfer coefficient at the interface between water and solid phases, s is the interfacial area per unit volume of water plus solid, $k_{fi}^{m\ell}$ and $k_{si}^{m\ell}$ are rate constants for chemical reactions from mth to ℓth species in water and solid, λ_i is the decay constant of the ith nuclide, K_{Di}^m is the distribution coefficient of species m, and ε is the porosity of the geologic medium.

The initial conditions for $N_i^m(z,t)$ and $M_i^m(z,t)$ are

$$N_i^m(z,0) = 0\,, \quad \infty \geq z \geq 0 \qquad (3.3.3)$$

$$M_i^m(z,0) = 0\,, \quad \infty \geq z \geq 0 \qquad (3.3.4)$$

$i = 1,2,3,\ldots \quad m = 1,2$

The concentration boundary condition is

$$N_i^m(0,t) = \begin{cases} B_i^m(t) & t \geq 0 \\ 0 & t < 0 \end{cases} \qquad (3.3.5)$$

The functions $B_i^m(t)$ should generally be given by solutions of the following equation:

$$\frac{\partial B_i^m}{\partial t} + k_{fi}^{ml}B_i^m - k_{fi}^{lm}B_i^l + \lambda_i B_i^m - \lambda_{i-1}B_i^m = 0\,, \quad m,l = 1,2 \qquad (3.3.6)$$

The initial condition is

$$B_i^m(0) = N_{i0}^m \qquad (3.3.7)$$

where N^m_{i0} (i = 1,2,3, . . . , m = 1,2) is the initial concentration of the mth species of the ith nuclide.

When there is no precusor, Eqs. (3.3.1) and (3.3.2) can be written down in simple form as

$$\frac{\partial N^1_1}{\partial t} + v\,\frac{\partial N^1_1}{\partial z} + \frac{k_m s}{\varepsilon}\left(N^1_1 - \frac{1}{K^1_{D1}}\,M^1_1\right) + k^{12}_{f1}N^1_1 - k^{21}_{f1}N^2_1 + \lambda_1 N^1_1 = 0 \tag{3.3.8}$$

$$\frac{\partial N^2_1}{\partial t} + v\,\frac{\partial N^2_1}{\partial z} + \frac{k_m s}{\varepsilon}\left(N^2_1 - \frac{1}{K^2_{D1}}\,M^2_1\right) - k^{12}_{f1}N^1_1 + k^{21}_{f1}N^2_1 + \lambda_1 N^2_1 = 0 \tag{3.3.9}$$

$$\frac{\partial M^1_1}{\partial t} - \frac{k_m s}{1 - \varepsilon}\left(N^1_1 - \frac{1}{K^2_{D1}}\,M^1_1\right) + k^{12}_{s1}M^1_1 - k^{21}_{s1}M^2_1 + \lambda_1 M^1_1 = 0 \tag{3.3.10}$$

$$\frac{\partial M^2_1}{\partial t} - \frac{k_m s}{1 - \varepsilon}\left(N^2_1 - \frac{1}{K^2_{D1}}\,M^2_1\right) - k^{12}_{s1}M^1_1 + k^{21}_{s1}M^2_1 + \lambda_1 M^2_1 = 0 \tag{3.3.11}$$

Solving Eq. (3.3.6) subject to Eq. (3.3.7), we have $B^m_1(t)$ for the first nuclide

$$B^1_1(t) = \frac{(k^{12}_{f1}N^1_{10} - k^{21}_{f1}N^2_{10})\,e^{-(\lambda_1 + k^{21}_{f1} + k^{12}_{f1})t} + k^{21}_{f1}(N^1_{10} + N^2_{10})\,e^{-\lambda_1 t}}{K^{12}_{f1} + k^{21}_{f1}} \tag{3.3.12}$$

$$B^2_1(t) = \frac{(k^{21}_{f1}N^2_{10} - k^{12}_{f1}N^1_{10})\,e^{-(\lambda_1 + k^{21}_{f1} + k^{12}_{f1})t} + k^{12}_{f1}(N^1_{10} + N^2_{10})\,e^{-\lambda_1 t}}{k^{12}_{f1} + k^{21}_{f1}} \tag{3.3.13}$$

For a single species Eqs. (3.3.12) and (3.3.13) reduce to

$$B_1(t) = B^1_1(t) + B^2_1(t) = N^0_1 e^{-\lambda_1 t} \tag{3.3.14}$$

where N_1^0 is the initial total concentration of the nuclide at the waste repository. This is just the Bateman equation for first nuclide.

3.3.2. Local Reaction Equilibrium

We first consider the case where the rates of chemical reactions in solid and in water are much more rapid than those of sorption processes. In this particular case, the chemical reactions are assumed to be equilibrated at any location and holds the relation:

$$\frac{N_1^2}{N_1^1} = K_{e1}^f \tag{3.3.15}$$

$$\frac{M_1^2}{M_1^1} = K_{e1}^s \tag{3.3.16}$$

where K_{e1}^f and K_{e1}^s are chemical equilibrium constants between two species in water and solid phases, respectively.

Introducing Eqs. (3.3.15) and (3.3.16) into the set of equations, Eqs. (3.3.8) ~ (3.3.11), we can eliminate the chemical reaction terms and concentrations in water and solid of the second species. Then the transport equations become

$$\frac{\partial N_1^1}{\partial t} + v\,\frac{\partial N_1^1}{\partial t} + \Lambda_1^f N_1^1 - K_m^f M_1^1 = 0 \tag{3.3.17}$$

$$\frac{\partial M_1^1}{\partial t} + \Lambda_1^s M_1^1 - K_m^s N_1^1 = 0 \tag{3.3.18}$$

where

$$\Lambda_1^f = \lambda_1 + \frac{k_m s}{\varepsilon} \tag{3.3.19}$$

$$\Lambda_1^s = \lambda_1 + \frac{k_m s}{1 - \varepsilon} \cdot \frac{K_{D1}^2 + K_{e1}^s K_{D1}^1}{K_{D1}^1 K_{D1}^2 (1 + K_{e1}^s)} \tag{3.3.20}$$

$$K_m^f = \frac{k_m s}{\varepsilon} \cdot \frac{K_{D1}^2 + K_{e1}^s K_{D1}^1}{K_{D1}^1 K_{D1}^2 (1 + K_{e1}^f)} \tag{3.3.21}$$

$$K_m^s = \frac{K_m s}{1 - \varepsilon} \; \frac{1 + K_{e1}^f}{1 + K_{e1}^s} \tag{3.3.22}$$

This couple of equations has the same form as that for transport of single species with the exception of constant parameters.

The initial and boundary conditions for $N_1^1(z,t)$ and $M_1^1(z,t)$ are given by Eqs. (3.3.3), (3.3.4) and (3.3.5) with the function $B_1^1(t)$ given by

$$B_1^1(t) = b_{11}^1 N_1^0 e^{-\lambda_1 t} \tag{3.2.23}$$

where

$$b_{11}^1 = 1/(1 + K_{e1}^f) \tag{3.3.24}$$

The couple of equations, Eqs. (3.3.17) and (3.3.18) can be solved by the Laplace transform technique. The solutions for $N_1^1(z,t)$ and $M_1^1(z,t)$ are

$$N_1^1(z,t) = \exp\left(-\frac{\Lambda_1^f}{v} z\right) \psi_N(z,t) * B_1^1(t) + \exp\left(-\frac{\Lambda_1^f}{v} z\right) B_1^1\left(t - \frac{z}{v}\right) \tag{3.3.25}$$

$$M_1^1(z,t) = K_m^s \cdot \exp\left(-\frac{\Lambda_1^f}{v} z\right) \psi_M(z,t) * B_1^1(t) \tag{3.3.26}$$

where

$$\psi_N(z,t) = \begin{cases} \sqrt{\dfrac{K_m^f K_m^s z}{v(t - z/v)}} \, e^{-\Lambda_1^s\left(t - \frac{z}{v}\right)} I_1\left[2\sqrt{\dfrac{K_m^f K_m^s z}{v}\left(t - \dfrac{z}{v}\right)}\right] & \text{for } vt \geq z \\ 0 & \text{for } vt < z \end{cases} \tag{3.3.27}$$

$$\psi_M(z,t) = \begin{cases} e^{-\Lambda_1^s\left(t - \frac{z}{v}\right)} I_0\left[2\sqrt{\dfrac{K_m^f K_m^s z}{v}\left(t - \dfrac{z}{v}\right)}\right] & \text{for } vt \geq z \\ 0 & \text{for } vt < z \end{cases} \tag{3.3.28}$$

The concentration profiles of the second species in water and in solid, $N_1^2(z,t)$ and $M_1^2(z,t)$, are obtained directly from the relation given by Eqs. (3.3.15) and (3.3.16).

3.3.3. Local Sorption Equilibrium, Nonequilibrium Reactions

Consider the case where the rate of sorption is much faster than the rate of chemical reactions, so that local equilibrium is established for the sorption but not for the chemical reactions in each phase. In this particular case we can express the concentration of mth chemical species in the solid phase in term of the concentration of mth species in the water phase, thus

$$M_1^m = K_{D1}^m N_1^m \quad , \quad m = 1,2 \tag{3.3.29}$$

Substituting Eq. (3.3.29) into Eqs. (3.3.8) to (3.3.11) and summing up the resultant equations for respective concentrations of mth species in the water and solid phases, we have the following couple of equations:

$$K_1^1 \frac{\partial N_1^1}{\partial t} + v \frac{\partial N_1^1}{\partial z} + k_1^{12} N_1^1 - k_1^{21} N_1^2 + \lambda_1 K_1^1 N_1^1 = 0 \tag{3.3.30}$$

$$K_1^2 \frac{\partial N_1^2}{\partial t} + v \frac{\partial N_1^2}{\partial z} - k_1^{12} N_1^1 + k_1^{21} N_1^2 + \lambda_1 K_1^2 N_1^2 = 0 \tag{3.3.31}$$

where

$$K_1^1 = 1 + (1 - \epsilon)\, K_{D1}^1/\epsilon \tag{3.3.32}$$

$$K_1^2 = 1 + (1 - \epsilon)\, K_{D1}^2/\epsilon \tag{3.3.33}$$

$$k_1^{12} = k_{f1}^{12} + (1 - \epsilon)\, k_{s1}^{12} K_{D1}^1/\epsilon \tag{3.3.34}$$

$$k_1^{21} = k_{f1}^{21} + (1 - \epsilon)\, k_{s1}^{21} K_{D1}^2/\epsilon \tag{3.3.35}$$

Dividing Eq. (3.3.30) by K_1^1 and Eq. (3.3.31) by K_1^2 and arranging the resultant equations, we have

$$\frac{\partial N_1^1}{\partial t} + v_1^1 \frac{\partial N_1^1}{\partial z} + \left(\frac{k_1^{12}}{K_1^1} + \lambda_1 \right) N_1^1 - \frac{k_1^{21}}{K_1^1} N_1^2 = 0 \qquad (3.3.36)$$

$$\frac{\partial N_1^2}{\partial t} + v_1^2 \frac{\partial N_1^2}{\partial z} + \left(\frac{k_1^{21}}{K_1^2} + \lambda_1 \right) N_1^2 - \frac{k_1^{12}}{K_1^2} N_1^1 = 0 \qquad (3.3.37)$$

where

$$v_1^1 = \frac{v}{K_1^1} \quad , \quad v_1^2 = \frac{v}{K_1^2} \quad , \quad \text{but} \quad v_1^2 > v_1^1 \qquad (3.3.38)$$

The assumption of inequality $v_1^2 > v_1^1$ does not spoil the generality of the problem.

Let introduce r_{ij} constants:

$$\begin{aligned} r_{11} &= \frac{k_1^{12}}{K_1^1} + \lambda_1 \quad , \quad r_{12} = - \frac{k_1^{21}}{K_1^1} \\ r_{21} &= - \frac{k_1^{12}}{K_1^2} \quad , \quad r_{22} = \frac{k_1^{21}}{K_1^2} + \lambda_1 \end{aligned} \qquad (3.3.39)$$

then we have

$$\frac{\partial N_1^1}{\partial t} + v_1^1 \frac{\partial N_1^2}{\partial z} + r_{11} N_1^1 + r_{12} N_1^2 = 0 \qquad (3.3.40)$$

$$\frac{\partial N_1^2}{\partial t} + v_1^2 \frac{\partial N_1^2}{\partial z} + r_{21} N_1^1 + r_{22} N_1^2 = 0 \qquad (3.3.41)$$

The initial conditions for $N_1^1(z,t)$ and $N_1^2(z,t)$ are given by Eq. (3.3.3) and the boundary conditions are given by Eq. (3.3.5) with Eqs. (3.3.12) and (3.3.13).

A. Solution for Irreversible Reaction

When the chemical reaction is irreversible, namely $k_{f1}^{21} = k_{s1}^{21} = 0$, the set of equations reduces to

$$\frac{\partial N_1^1}{\partial t} + v_1^1 \frac{\partial N_1^1}{\partial z} + r_{11} N_1^1 = 0 \tag{3.3.42}$$

$$\frac{\partial N_1^2}{\partial t} + v_1^2 \frac{\partial N_1^2}{\partial z} + r_{21} N_1^1 + r_{22} N_1^2 = 0 \tag{3.3.43}$$

and the functions $B_1^1(t)$ and $B_1^2(t)$ are given by

$$B_1^1(t) = N_{10}^1 e^{-(\lambda_1 + k_{f1}^{12})t} \tag{3.3.44}$$

$$B_1^2(t) = -N_{10}^1 e^{-(\lambda_1 + k_{f1}^{12})t} + (N_{10}^1 + N_{10}^2)\, e^{-\lambda_1 t} \tag{3.3.45}$$

The solutions for $N_1^1(z,t)$ and $N_1^2(z,t)$ are given by

$$N_1^1(z,t) = N_1^{1,1}(z,t) \tag{3.3.46}$$

$$N_1^2(z,t) = N_1^{2,1}(z,t) + N_1^{2,2}(z,t) \tag{3.3.47}$$

where

$$N_1^{1,1}(z,t) = N_{10}^1\, e^{-\frac{r_{11}}{v_1^1} z}\, e^{-(\lambda_1 + k_{f1}^{12})\left(t - \frac{z}{v_1^1}\right)} h\left(t - \frac{z}{v_1^1}\right) \tag{3.3.48}$$

$$N_1^{2,2}(z,t) = \left[-N_{10}^1\, e^{-(\lambda_1 + k_{f1}^{12})\left(t - \frac{z}{v_1^2}\right)} + \left(N_{10}^1 + N_{10}^2\right) e^{-\lambda_1\left(t - \frac{z}{v_1^2}\right)}\right] \cdot e^{-\frac{r_{22}}{v_1^2} z}\, h\left(t - \frac{z}{v_1^2}\right) \tag{3.3.49}$$

$$N_1^{2,1}(z,t) = \frac{r_{21} N_{10}^1}{v_1^2 \left[\Lambda_1^{12} - (\lambda_1 + k_{f1}^{12})\, \Gamma_1^{12}\right]}$$

$$\cdot \left\{ e^{-\frac{r_{22}}{v_1^2} z} \left[e^{-\frac{\Lambda_1^{12}}{\Gamma_1^{12}}\left(t - \frac{z}{v_1^2}\right)} - e^{-(\lambda_1 + k_{f1}^{12})\left(t - \frac{z}{v_1^2}\right)} \right] h\left(t - \frac{z}{v_1^2}\right)\right.$$

$$\left. - e^{-\frac{r_{11}}{v_1^1} z} \left[e^{-\frac{\Lambda_1^{12}}{\Gamma_1^{12}}\left(t - \frac{z}{v_1^1}\right)} - e^{-(\lambda_1 + k_{f1}^{12})\left(t - \frac{z}{v_1^1}\right)} \right] h\left(t - \frac{z}{v_1^1}\right) \right\} \qquad (3.3.50)$$

$$\Gamma_1^{12} = \frac{1}{v_1^1} - \frac{1}{v_1^2} \qquad (3.3.51)$$

$$\Lambda_1^{12} = \frac{r_{11}}{v_1^1} - \frac{r_{22}}{v_1^2} \qquad (3.3.52)$$

B. Solution for Reversible Reaction

The solutions of the couple of equations, Eqs. (3.3.36) and (3.3.37) subject to the initial condition, Eq. (3.3.3) and boundary condition, Eq. (3.3.5) with Eqs. (3.3.12) and (3.3.13) are given by

$$N_1^1(z,t) = e^{-\frac{r_{11}}{v_1^1} z}\, B_1^1\left(t - \frac{z}{v_1^1}\right) h\left(t - \frac{z}{v_1^1}\right) + v_1^1 \int_0^t H_{11}(z,t-\tau)\, B_1^1(\tau)\, d\tau$$

$$- r_{12} v_1^2 \int_0^t H_{12}(z,t-\tau)\, B_1^2(\tau)\, d\tau \qquad (3.3.53)$$

$$N_1^2(z,t) = e^{-\frac{r_{22}}{v_1^2} z} B_1^2\left(t - \frac{z}{v_1^2}\right) h\left(t - \frac{z}{v_1^2}\right) + v_1^2 \int_0^t H_{22}(z,t-\tau)\, B_1^2(\tau)\, d\tau$$

$$- r_{21} v_1^1 \int_0^t H_{21}(z,t-\tau)\, B_1^1(\tau)\, d\tau \qquad (3.3.54)$$

where

$$H_{11}(z,t) = \begin{cases} \dfrac{1}{\left|v_1^2 - v_1^1\right|} \sqrt{r_{12} r_{21} \dfrac{v_1^2 t - z}{z - v_1^1 t}} \exp\left[\dfrac{(v_1^1 r_{22} - v_1^2 r_{11}) t + (r_{11} - r_{22})\, z}{(v_1^2 - v_1^1)}\right] \\ \cdot I_1\left[\dfrac{2}{v_1^2 - v_1^1} \sqrt{r_{12} r_{21} (v_1^2 t - z)(z - v_1^1 t)}\right], \quad \text{for} \quad v_1^2 t > z > v_1^1 t \\ 0, \quad \text{for} \quad z < v_1^1 t \quad \text{or} \quad z > v_1^2 t \end{cases} \qquad (3.3.55)$$

$$H_{12}(z,t) = \begin{cases} \dfrac{1}{\left|v_1^2 - v_1^1\right|} \exp\left[\dfrac{(v_1^1 r_{22} - v_1^2 r_{11})\, t + (r_{11} - r_{22})\, z}{\left(v_1^2 - v_1^1\right)}\right] \\ \cdot I_0\left[\dfrac{2}{v_1^2 - v_1^1} \sqrt{r_{12} r_{21} (v_1^2 t - z)(z - v_1^1 t)}\right], \quad \text{for} \quad v_1^2 t > z > v_1^1 t \\ 0, \quad \text{for} \quad z < v_1^1 t \quad \text{or} \quad z > v_1^2 t \end{cases} \qquad (3.3.56)$$

The functions $H_{2,j}(z,t)$ $(j = 1,2)$ are given by the expressions similar to $H_{1,j}(z,t)$ but with the superscript of v_1^m and subscript of r_{ij} interchanged. In a particular case of $v_1 = v_2 = v$, the solutions are given by

BEST DOCUMENT AVAILABLE

$$N_1^1(z,t) = e^{-\left(\frac{r_{11}+r_{22}}{2v}\right)z}\left[\cosh\left(\frac{\sqrt{b}}{v} z\right) B_1^1\left(t - \frac{z}{v}\right)\right.$$

$$+ \frac{r_{22}-r_{11}}{2\sqrt{b}} B_1^1\left(t - \frac{z}{v}\right) \sinh\left(\frac{\sqrt{b}}{v} z\right)$$

$$\left.- \frac{r_{12}}{\sqrt{b}} B_1^2\left(t - \frac{z}{v}\right) \sinh\left(\frac{\sqrt{b}}{v} z\right)\right] \qquad (3.3.57)$$

$$N_1^2(z,t) = e^{-\left(\frac{r_{11}+r_{22}}{2v}\right)z}\left[\cosh\left(\frac{\sqrt{b}}{v} z\right) B_1^2\left(t - \frac{z}{v}\right)\right.$$

$$+ \frac{r_{11}-r_{22}}{2\sqrt{b}} B_1^2\left(t - \frac{z}{v}\right) \sinh\left(\frac{\sqrt{b}}{v} z\right)$$

$$\left.- \frac{r_{21}}{\sqrt{b}} B_1^1\left(t - \frac{z}{v}\right) \sinh\left(\frac{\sqrt{b}}{v} z\right)\right] \qquad (3.3.58)$$

where

$$b = \frac{1}{4}(r_{11} - r_{22})^2 + r_{12}r_{21} \qquad (3.3.59)$$

3.3.4. Nonequilibrium Sorption

The detailed discussion on the effects of nonequilibrium sorption has been given in the foregoing section for single species. The only important difference between the solutions for two chemical species of a nuclide and a single species is that the migration path is elongated or shrunk by the existence of a second species which has a different sorption equilibrium constant.

[redacted]

3.3.5. Two Species, Irreversible Reaction

Figure 3.3.1 shows the concentration profiles of two assumed chemical species of ^{237}Np which have assumed sorption equilibrium constants, K_1^1 = 10,000 for the first chemical species and K_1^2 = 100 for the second chemical species. These concentrations are calculated from the solutions of irreversible linear reaction, for a step release with none of the second species initially present. The assumed values of physicochemical parameters used in the calculations are listed in the figure caption. The solid lines in the figure show the concentration profiles of two chemical species at nonequilibrium and the dashed line shows the total concentration of two species at nonequilibrium, namely $N_1 = N_1^1 + N_1^2$. Since the chemical reaction is assumed to be irreversible, when the reaction reaches the equilibrium there remains only the second more mobile species. The one dot broken line shows the concentration profile of the second chemical species after the reaction having been equilibrated. This flat profile with the leading edge at z = 50,000 m also shows the total concentration of the nuclide.

If there is no chemical reaction from the first species initially present to second species, the leading edge of neptunium band reaches a smaller distance of z = 500 m at a time of 50,000 yr, with none of the more mobile species, N_1^2 found in this region. If there occurs the irreversible chemical reaction from the first to second species, the feature of the migration behavior is much changed by the existence of the second species. Because of the high mobility, the second species can run over the locus of the leading edge of the first species and migrate farther to reach z = 50,000 m. Moreover, in the path ranging from the waste to z = 500 m, the second species is incessantly generated by the chemical reaction until the chemical equilibrium is established, and it, due to the higher convective transport, shows the maximum in concentration at the locus of the leading edge of the first species. The total concentration of two species at nonequilibrium, namely the concentration of the nuclide also shows the maximum concentration at z = 500 m, which is never found in the concentration profile of the nuclide (with single species) at equilibrium.

Shown in Fig. 3.3.2 are the concentration profiles of two species at nonequilibrium at t = 50,000 yr, but with a lower sorption constant, K_1^1 = 100, for the first species and a higher sorption constant, K_1^2 = 10,000, for the second species. When there is no chemical reaction, the nuclide can

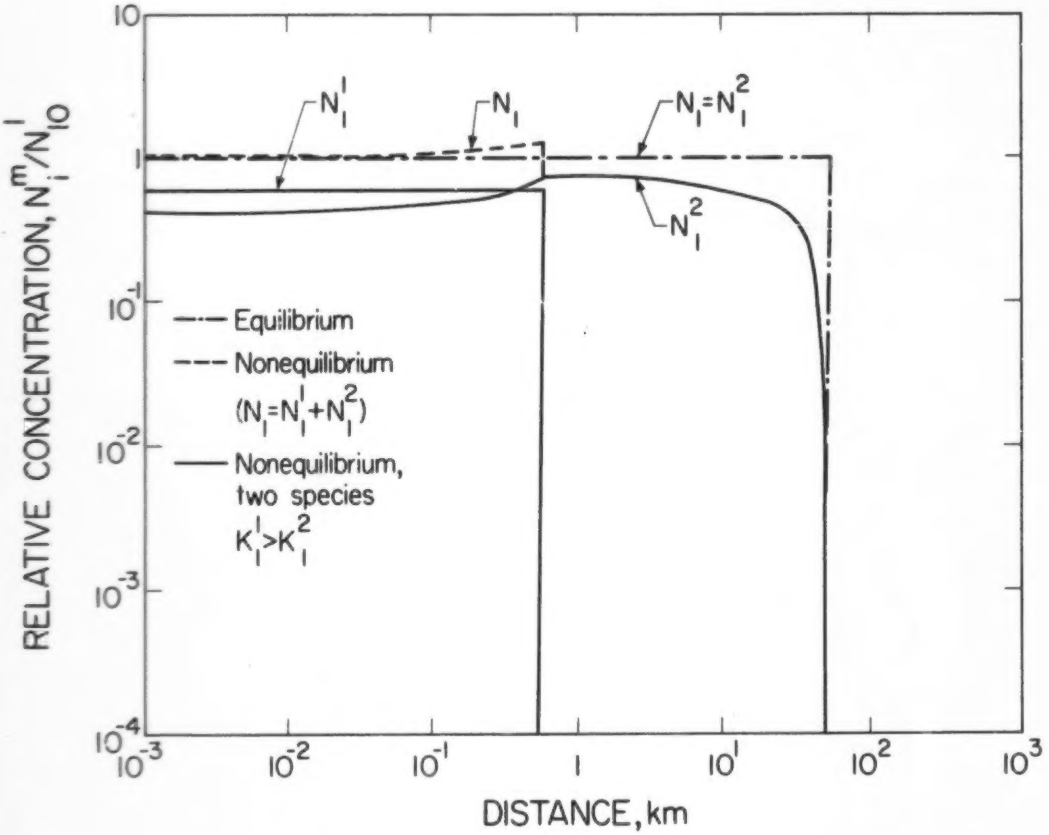

XBL 812-213

Fig. 3.3.1. Comparison of concentration profile of two-species nuclide at nonequilibrium with that of single-species nuclide at equilibrium: ^{237}Np, step release, irreversible kinetics, $t = 50{,}000$ yr, $v = 100$ m/yr, $K_{f1}^{12} = 10^{-5}$ yr^{-1}, $k_{f1}^{21} = 0$, $K_1^1 = 10{,}000$, $K_1^2 = 100$.

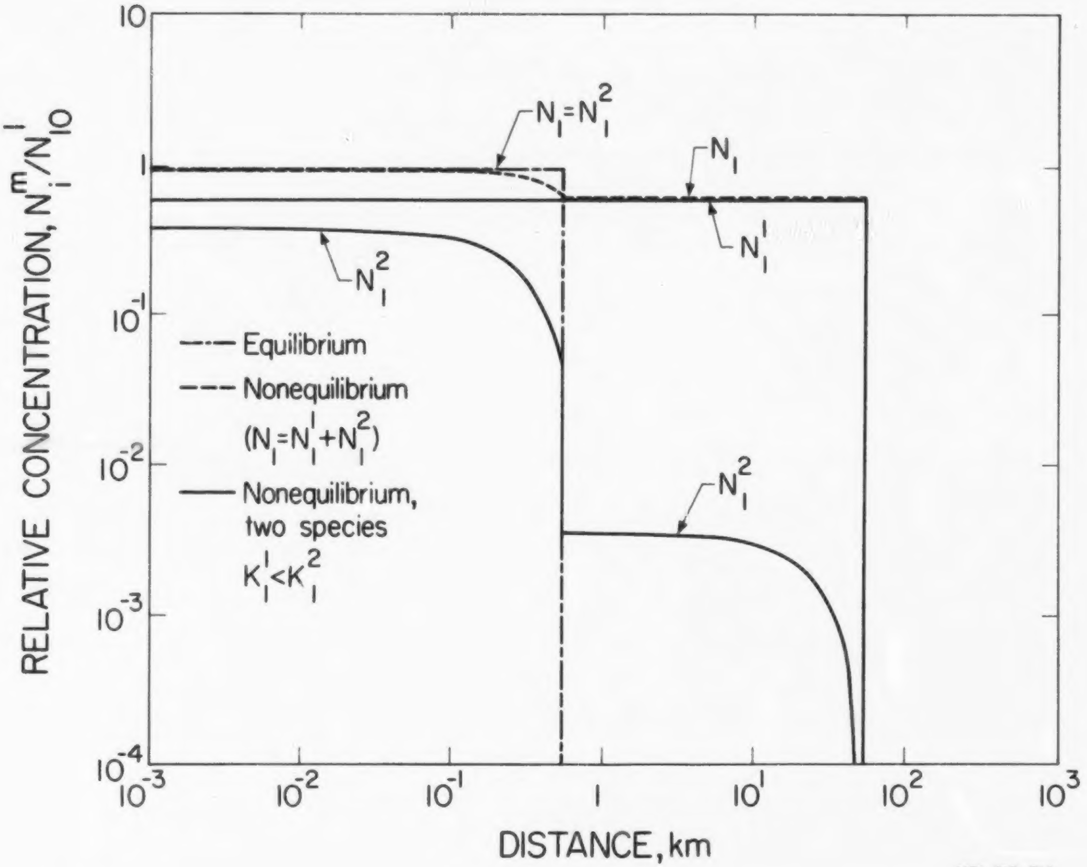

XBL 812-214

Fig. 3.3.2. Comparison of concentration profile of two-species nuclide at nonequilibrium with that of single-species nuclide at equilibrium; ^{237}Np, step release, irreversible kinetics, $t = 50{,}000$ yr, $v = 100$ m/yr, $k_{f1}^{12} = 10^{-5}$ yr^{-1}, $k_{f1}^{21} = 0$, $K_1^1 = 100$, $K_1^2 = 10{,}000$.

[redacted]

exist only as the first, more mobile species in aquifer and can migrate farther to the locus at $z = 50{,}000$ m. In the case of nonequilibrium, the chemical reaction causes to reduce the concentration of the first, mobile species, which results in reduction of the convective transport of the nuclide. The total concentration of two species at nonequilibrium is shown by the dashed line. In this case of $K_1^1 < K_1^2$, the concentration profile of the nuclide has a wide plateau but does not show the maximum concentration. When the irreversible reaction has been performed, there exists only the second species which migrates at lower velocity, and the path contaminated is much shrunk as shown as the one dot broken line.

From a comparison of the concentration profile of nuclide at nonequilibrium shown as dashed line and with that at equilibrium shown as one dot broken line, given in these two figures, we find that the nuclide which forms two more and less mobile species at nonequilibrium shows the concentration profile quiet different from that predicted from the solution for single species at equilibrium.

3.3.6. Two Species, Reversible Reactions, Nonequilibrium

In Fig. 3.3.3 are shown the concentration profiles of two assumed neptunium chemical species at nonequilibrium which have different sorption equilibrium constants, for a step release and with none of the second species initially present. The reaction rate constants are assumed to be $k_{f1}^{12} = 10^{-5}\ \mathrm{yr}^{-1}$ and $k_{f1}^{21} = 10^{-4}\ \mathrm{yr}^{-1}$, corresponding to an equilibrium constant $K_{e1}^1 = 0.1$. the other assumed physicochemical parameters are given in the figure caption. The solid lines show the concentration profiles of two chemical species at nonequilibrium and the dashed line shows the total concentration of the two species, namely the concentration of the nuclide, whereas the one dot broken line shows the concentration profiles of the two species calculated from the solution for equilibrium condition and the two dots broken line shows the total concentration of two species at equilibrium. In the absence of chemical reaction and there exists only the first, strongly sorbed species, the concentration profile of the nuclide is flat with its leading edge at $z = z_1 = v_1^1 t$ (= 500 m). If there are two chemical species in equilibrium, the concentration profile of each species is still flat. The leading edge occurs at $z = (1 + K_{e1}^1)\, vt/(K_1^1 + K_{e1}^1 K_1^2)$ (= 549 m). With nonequilibrium chemical reaction the first species, which is released as such from the waste, decreases in concentration gradually with the distance from the repository due to chemical reaction to the second species. It decreases discontinuously at $z = z_1$ (= 500 m), but the first species continues to migrate farther to reach the leading edge of the second species. The second species, which does not exist initially in the waste is generated from the first species by chemical reaction during migration, increases in concentration with increasing distance, and reaches a maximum in concentration at $z = 500$ m. Beyond this point, the concentration of the second species decreases with distance and vanishes at $z = v_1^2 t$ (= 50,000 m). As seen from the figure the migration behavior of a mother nuclide which forms two chemical species is predominantly governed by the migration of the more mobile, weakly sorbed chemical species.

Figure 3.3.4 shows a comparison of the concentration profiles of two species at nonequilibrium, for a step release, with rate constants assumed to be $k_{f1}^{12} = 10^{-5}$ yr^{-1} and $k_{f1}^{21} = 10^{-6}$ yr^{-1}, corresponding to an equilibrium constant $K_{e1}^{1} = 10$. Each of the chemical species, if at equilibrium, will show a flat concentration profile with its leading edge at $z = 5{,}000$ m. For non-equilibrium, the first, strongly sorbed species shows an almost flat profile at a distance less than $z = z_1 = 500$ m, but with a relatively wide plateau of smaller concentration at $z > z_1$, resulting from the chemical reaction of the second to the first species. The second, weakly sorbed species, generated by chemical reaction, increases in concentration with increasing distance, shows a maximum concentration at $z > z_1$, and then decreases gradually to its sharp leading edge at $z = z_2$ (= 50,000 m). the total concentration of neptunium, the sum of the concentration of the two species, reaches a maximum at $z = z_1$. This maximum is not found in the concentration profile of equilibrium neptunium. In this case of $k_{f1}^{12} > k_{f1}^{21}$, the migration behavior of the mother nuclide is again governed predominantly by the weakly sorbed, more mobile chemical species.

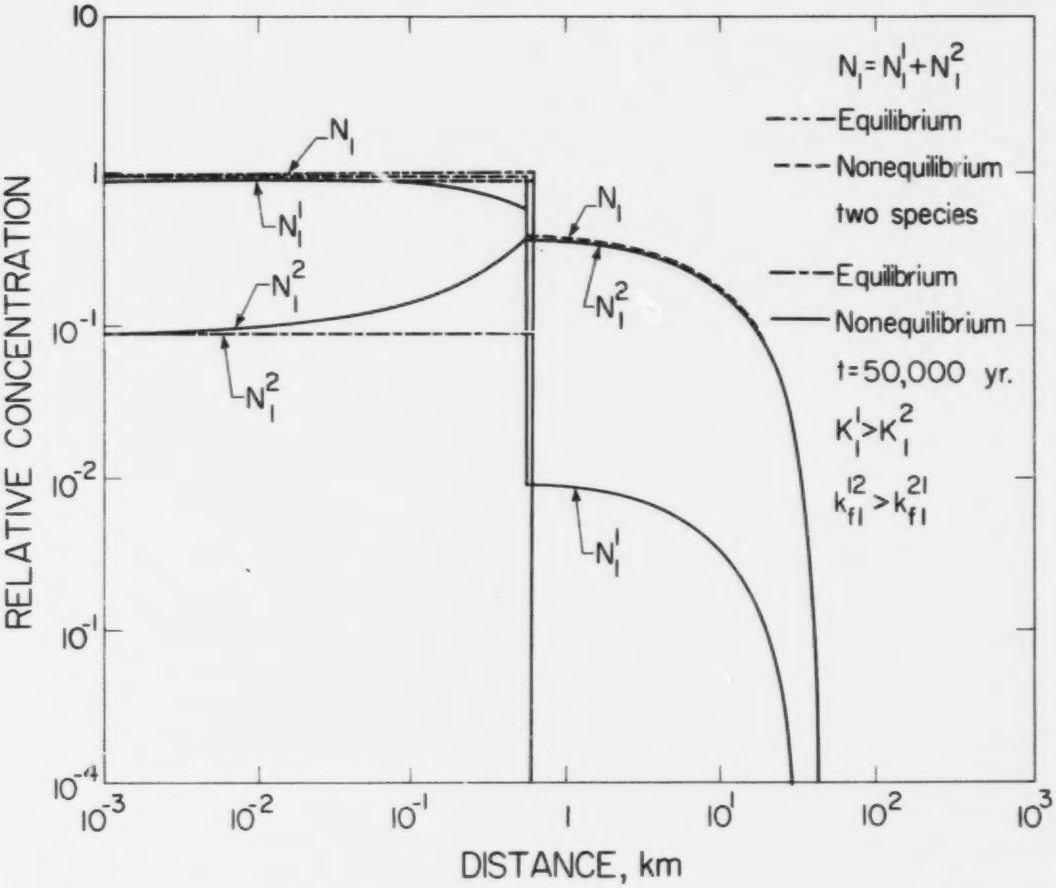

XBL 812-215

Fig. 3.3.3. Comparison of concentration profiles of two chemical species at nonequilibrium with those of two species at equilibrium; ^{237}Np, step release, reversible kinetics, t = 50,000 yr, v = 100 m/yr, $k_{f1}^{12} = 10^{-5}$ yr^{-1}, $k_{f1}^{21} = 10^{-4}$ yr^{-1}, $k_1^1 = 10{,}000$, $K_1^2 = 100$.

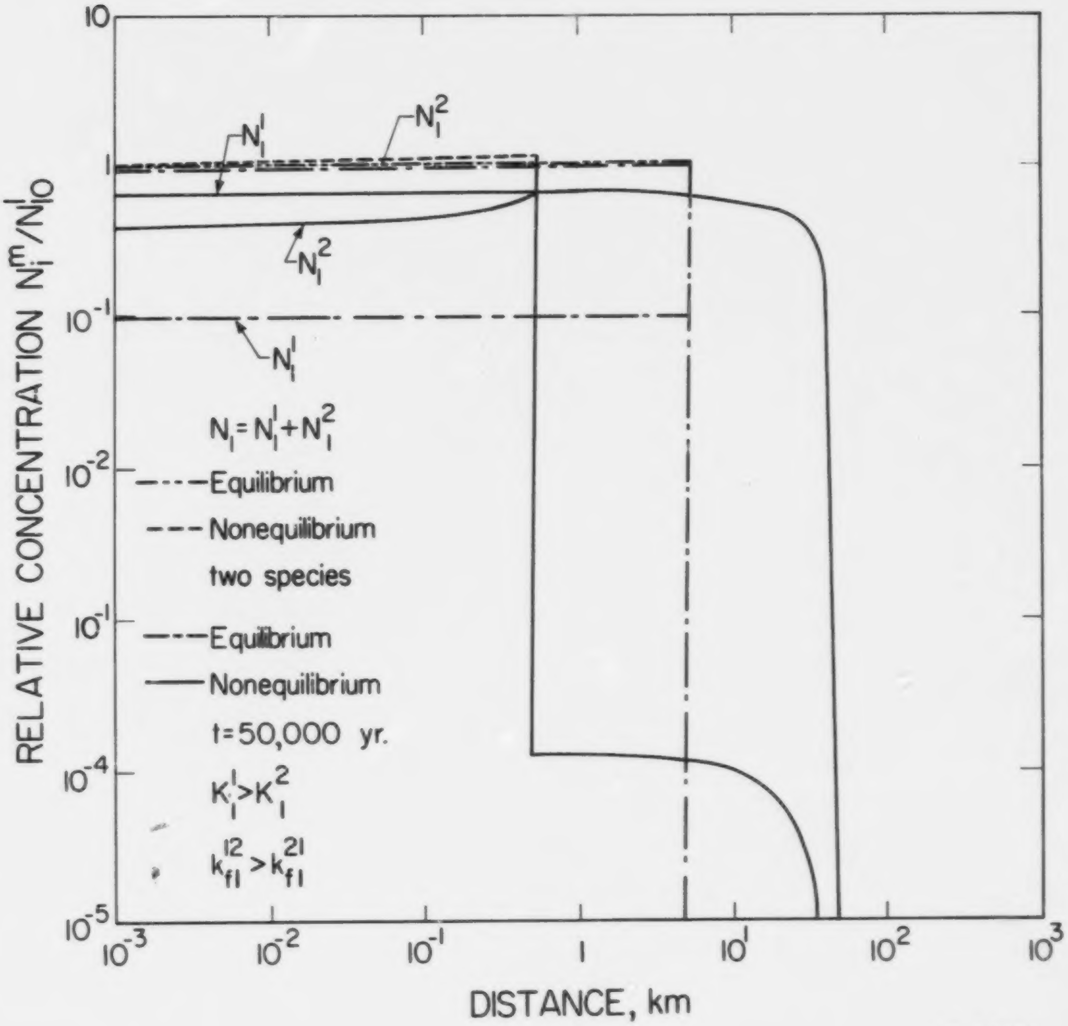

XBL 812-216

Fig. 3.3.4. Comparison of concentration profiles of two chemical species at nonequilibrium with those of two species at equilibrium; ^{237}Np, step release, reversible kinetics, $t = 50{,}000$ yr, $v = 100$ m/yr, $k_{f1}^{12} = 10^{-5}$ yr^{-1}, $k_{f1}^{21} = 10^{-6}$ yr^{-1}, $K_1^1 = 10{,}000$, $K_1^2 = 100$.

NOMENCLATURE

a_i	defined by Eq. (3.2.25)
b_{11}^m	fraction of concentration of mth chemical species at equilibrium
$B_i^m(t)$	time dependent concentration of the mth chemical species of the ith nuclide at repository
d_i	defined by Eq. (3.2.26)
D	axial dispersion coefficient, m^2/yr
$\tilde{D}_i$	D/K_i
$E(i,j,k)$	defined in Appendix C
$f_1(z,t),\tilde{f}_1(z,t)$	defined by Eqs. (3.2.19) and (3.2.20)
$f_1^p(z,t)$	defined by Eq. (3.2.30)
$F(z,t),\tilde{F}_1(z,t)$	defined by Eqs. (3.2.21) and (3.2.22)
$g_i(z,t)$	defined by Eq. (3.2.32)
$G_i(z,t)$	defined by Eq. (3.2.24)
$H_i(z,t)$	defined by Eq. (3.2.23)
$H_{i,j}(z,t)$	defined by Eqs. (3.3.55) and (3.3.56)
I_o,I_1	modified Bessel function of zero (first) order
k_m	mass transfer coefficient at interfacial area between water and solid phases.
$k_{m,i}$	mass transfer coefficient defined by Eq. (3.2.36)
k_{fi}^{ml}	rate constant for chemical reaction from mth to lth chemical species in the water phase, 1/yr
k_{si}^{ml}	rate constant for chemical reaction from mth to lth chemical species in the solid phase, 1/yr
$\vec{k}_i$	rate constant for the forward mineralization reaction, 1/yr

$\overrightarrow{k}_i^s$	rate constant for the forward sorption reaction, 1/yr
$\overleftarrow{k}_i$	rate constant for the reverse mineralization reaction, 1/yr
$\overleftarrow{k}_i^s$	rate constant for the reverse sorption reaction, 1/yr
$K_{D,i}, K_{D,i}^s, K_{D,i}^m$	Distribution coefficient (of the mth chemical species of the ith nuclide)
K_{ei}^f, K_{ei}^s	equilibrium constants between two species in water and solid phases
K_i, K_i^m	sorption retardation coefficient (of the mth chemical species)
K_i^{ml}	constant defined by Eq. (3.3.34) or Eq. (3.3.35)
K_m^f	constant defined by Eq. (3.3.21)
K_m^s	constant defined by Eq. (3.3.22)
$m_i(z,t)$	concentration of mineralized species
$M_i(z,t)$	concentration of sorbed species in equilibrium with the adjacent liquid
$M_i^m(z,t)$	concentration of the mth chemical species of the ith nuclide in the solid phase
$N_i(z,t)$	concentration of nuclide i in the water phase
$N_i^m(z,t)$	concentration of the mth chemical species of the ith nuclide in the water phase
N_i^0	initial total concentration of nuclide i
$N_i^{\cdot}$	introduced in Section 3.2.3
N_{i0}^m	initial concentration of mth, chemical species of ith nuclide in the water phase
$N_i^{lm}(z,t)$	function used in Eq. (3.3.46) or Eq. (3.3.47)
r_{lm}	constant defined by Eq. (3.3.39)

$\dot{r}_i$	adsorption reaction rate
$\dot{R}_i$	mineralization reaction rate, atoms/(yr)(m^3)
$\dot{R}_i^s$	net rate of sorption, atoms/(yr)(m^3 solid)
s	interfacial area per unit volume of sorbing medium, m^2
t	time after beginning of leach, yr
v	water velocity, m/yr
v_i, v_i^m	migration velocity $\equiv v/K_i$ (of the mth, chemical species of the ith nuclide $\equiv v/K_i^m$), m/yr
W_s^0	initial density of total waste material in the plane source in the water phase, atoms/m^2
α	longitudinal dispersivity factor $\equiv D/v$,m
γ_{i-1}	fraction of mineralized i-1 species decaying to nonmineralized sorbed i species
Γ_1^{lm}	constant defined by Eq. (3.3.51)
$\delta(z)$	Dirac delta function, 1/m
ϵ	porosity
η_i	defined by Eq. (2.1.4)
λ_i	decay constant, 1/yr
Λ_1^f	constant defined by Eq. (3.3.19)
Λ_1^s	constant defined by Eq. (3.3.20)
$\Lambda_1^{\ell m}$	constant defined by Eq. (3.3.52)
$\xi_i(t,x)$	defined by Eq. (3.2.27)
χ_i	$\equiv \gamma_i + \overleftarrow{k}_i$
$\vec{\sigma}_i$	defined by Eq. (3.2.15)
$\overleftarrow{\sigma}_i$	defined by Eq. (3.2.14)

$\psi_N(z,t)$	function defined by Eq. (3.3.27)
$\psi_M(z,t)$	function defined by Eq. (3.3.28)

Subscripts

b	bed (fluid + solid)
f	fluid
i	nuclide
s	solid

Superscripts

l,m	chemical species

LITERATURE REFERENCES

B1 M. Benedict, T. H. Pigford and H. W. Levi, "Nuclear Chemical Engineering," 2nd ed., McGraw Hill, NY, in publication.

C1 D. R. Cameron and A. Klute, "Convective-Dispersive Solute Transport with a Combined Equilibrium and Kinetic Adsorption Model," Water Resonance Res. 13: 183-188, 1977.

F1 M. Foglia, Ph. D. Dissertation, University of California, Berkeley, 1980.

H1 M. Harada, P. L. Chambre', M. Foglia, K. Higashi, F. Iwamoto, D. Leung, T. H. Pigford, D. Ting, "Migration of Radionuclides through Sorbing Media, Analytical Solutions--I," LBL-10500, 1980.

H2 O. A. Hougen and K. M. Watson, "Chemical Process Principles--Part III: Kinetics and Catalysis," J. Wiley and Sons, NY, 1947.

L1 L. Lapidus and N. Amundson, "Mathematics of Adsorption in Beds VI. The Effect of Longitudinal Diffusion in Ion Exchange and Chromatographic Columns," J. Phys. Chem. 56, 984, 1952.

S1 M. G. Seitz, P. G. Rickert, S. Fried, A. M. Friedman and M. I. Steindler, "Migratory Properties of Some Nuclear Waste Elements in Geologic Media," Nuclear Technology 44: 284-296, July, 1979.

*USGPO: 1982 — 559-099/5351

This report was done with support from the Department of Energy. Any conclusions or opinions expressed in this report represent solely those of the author(s) and not necessarily those of The Regents of the University of California, the Lawrence Berkeley Laboratory or the Department of Energy.

Reference to a company or product name does not imply approval or recommendation of the product by the University of California or the U.S. Department of Energy to the exclusion of others that may be suitable.

225